BioMed Research International

Impact of Nutritional and Environmental Factors on Inflammation, Oxidative Stress, and the Microbiome 2020

Lead Guest Editor: Gang Liu
Guest Editors: Lei Sun, Hengjia Ni, Deguang Song, and Yan Huang

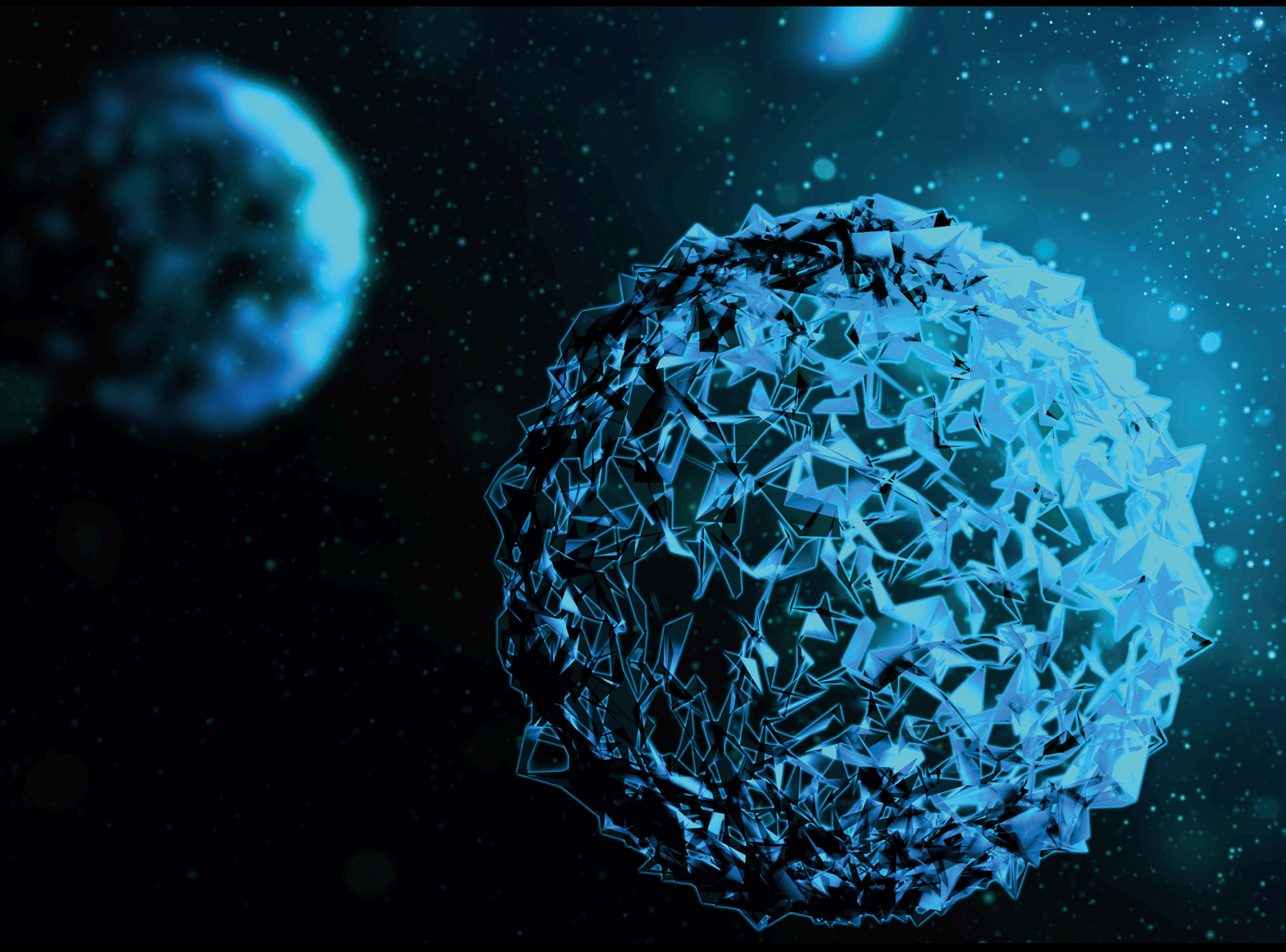

Impact of Nutritional and Environmental Factors on Inflammation, Oxidative Stress, and the Microbiome 2020

BioMed Research International

Impact of Nutritional and Environmental Factors on Inflammation, Oxidative Stress, and the Microbiome 2020

Lead Guest Editor: Gang Liu
Guest Editors: Lei Sun, Hengjia Ni, Deguang Song, and Yan Huang

Section Editors

Academic Editors

Biochemistry

Contents

Retracted: MicroRNA-205-5p Targets HMGB1 to Suppress Inflammatory Responses during Lung Injury after Hip Fracture
BioMed Research International
Retraction (1 page), Article ID 9836273, Volume 2024 (2024)

Retracted: Component-Resolved Diagnostic Study of Egg Allergy in Northern Chinese Children
BioMed Research International
Retraction (1 page), Article ID 9820370, Volume 2024 (2024)

Retracted: Protective Effects of Hydrogen on Myocardial Mitochondrial Functions in Septic Mice
BioMed Research International
Retraction (1 page), Article ID 9794810, Volume 2024 (2024)

Retracted: Glucosamine Supplementation in Premating Drinking Water Improves Within-Litter Birth Weight Uniformity of Rats Partly through Modulating Hormone Metabolism and Genes Involved in Implantation
BioMed Research International
Retraction (1 page), Article ID 9791359, Volume 2024 (2024)

Retracted: Association between Rosacea and Cardiovascular Diseases and Related Risk Factors: A Systematic Review and Meta-Analysis
BioMed Research International
Retraction (1 page), Article ID 9762194, Volume 2024 (2024)

Retracted: Bone Marrow Plasma Cytokine Signature Profiles in Severe Aplastic Anemia
BioMed Research International
Retraction (1 page), Article ID 9753242, Volume 2024 (2024)

Antioxidant Function and Metabolomics Study in Mice after Dietary Supplementation with Methionine
Manrong Yu, Hui Chen, Pan Liu, Mei Yang, Leqin Zou, and Dingfu Xiao
Research Article (6 pages), Article ID 9494528, Volume 2020 (2020)

[Retracted] Association between Rosacea and Cardiovascular Diseases and Related Risk Factors: A Systematic Review and Meta-Analysis
Yanmei Li, Linghong Guo, Dan Hao, Xiaoxue Li, Yujia Wang, and Xian Jiang
Research Article (11 pages), Article ID 7015249, Volume 2020 (2020)

Preventive Effects of Kaempferol on High-Fat Diet-Induced Obesity Complications in C57BL/6 Mice
Tieqiao Wang, Qiaomin Wu, and Tingqi Zhao
Research Article (9 pages), Article ID 4532482, Volume 2020 (2020)

Antioxidant and Anti-Inflammatory Effects of Different Zinc Sources on Diquat-Induced Oxidant Stress in a Piglet Model
Jieping Guo, Liuqin He, Tiejun Li, Jie Yin, Yulong Yin, and Guiping Guan
Research Article (10 pages), Article ID 3464068, Volume 2020 (2020)

Alterations of the Predominant Fecal Microbiota and Disruption of the Gut Mucosal Barrier in Patients with Early-Stage Colorectal Cancer
Xia Liu, Yiwen Cheng, Li Shao, and Zongxin Ling
Research Article (8 pages), Article ID 2948282, Volume 2020 (2020)

[Retracted] Component-Resolved Diagnostic Study of Egg Allergy in Northern Chinese Children
Jiayi Zhang, Yongming Shen, Junpu Li, Huiqiang Li, and Ping Si
Research Article (9 pages), Article ID 3831087, Volume 2020 (2020)

The Antitumor Efficacy of β-Elemene by Changing Tumor Inflammatory Environment and Tumor Microenvironment
Qiang Xie, Fengzhou Li, Lei Fang, Wenzhi Liu, and Chundong Gu
Review Article (13 pages), Article ID 6892961, Volume 2020 (2020)

[Retracted] Bone Marrow Plasma Cytokine Signature Profiles in Severe Aplastic Anemia
Bingnan Liu, Yuanyuan Shao, Zixuan Liu, Chunyan Liu, Tian Zhang, and Rong Fu
Research Article (11 pages), Article ID 8789275, Volume 2020 (2020)

[Retracted] Protective Effects of Hydrogen on Myocardial Mitochondrial Functions in Septic Mice
Yuanyuan Zhang, Aili Dong, Keliang Xie, and Yonghao Yu
Research Article (7 pages), Article ID 1568209, Volume 2020 (2020)

[Retracted] Glucosamine Supplementation in Premating Drinking Water Improves Within-Litter Birth Weight Uniformity of Rats Partly through Modulating Hormone Metabolism and Genes Involved in Implantation
Cuiping Feng, Taolin Yuan, Shilan Wang, Ting Liu, Shiyu Tao, Dandan Han, and Junjun Wang
Research Article (9 pages), Article ID 1630890, Volume 2020 (2020)

What Is the Impact of Diet on Nutritional Diarrhea Associated with Gut Microbiota in Weaning Piglets: A System Review
Jing Gao, Jie Yin, Kang Xu, Tiejun Li, and Yulong Yin
Review Article (14 pages), Article ID 6916189, Volume 2019 (2019)

The Protective Effect of Bosentan against Atherosclerosis in Apolipoprotein E-Deficient Mice Is Mediated by miRNA-21
Xiaona Xu, Zhiqiang Zhao, and Guangping Li
Research Article (8 pages), Article ID 8348430, Volume 2019 (2019)

[Retracted] MicroRNA-205-5p Targets HMGB1 to Suppress Inflammatory Responses during Lung Injury after Hip Fracture
Xiaojie Yu, Xiaobin Chen, and Tiansheng Sun
Research Article (13 pages), Article ID 7304895, Volume 2019 (2019)

Hindawi
BioMed Research International
Volume 2024, Article ID 9836273, 1 page
https://doi.org/10.1155/2024/9836273

Retraction

Retracted: MicroRNA-205-5p Targets HMGB1 to Suppress Inflammatory Responses during Lung Injury after Hip Fracture

BioMed Research International

Received 12 March 2024; Accepted 12 March 2024; Published 20 March 2024

This article has been retracted by Hindawi following an investigation undertaken by the publisher [1]. This investigation has uncovered evidence of one or more of the following indicators of systematic manipulation of the publication process:

(1) Discrepancies in scope

(2) Discrepancies in the description of the research reported

(3) Discrepancies between the availability of data and the research described

(4) Inappropriate citations

(5) Incoherent, meaningless and/or irrelevant content included in the article

(6) Manipulated or compromised peer review

The presence of these indicators undermines our confidence in the integrity of the article's content and we cannot, therefore, vouch for its reliability. Please note that this notice is intended solely to alert readers that the content of this article is unreliable. We have not investigated whether authors were aware of or involved in the systematic manipulation of the publication process.

Wiley and Hindawi regrets that the usual quality checks did not identify these issues before publication and have since put additional measures in place to safeguard research integrity.

We wish to credit our own Research Integrity and Research Publishing teams and anonymous and named external researchers and research integrity experts for contributing to this investigation.

The corresponding author, as the representative of all authors, has been given the opportunity to register their agreement or disagreement to this retraction. We have kept a record of any response received.

References

[1] X. Yu, X. Chen, and T. Sun, "MicroRNA-205-5p Targets HMGB1 to Suppress Inflammatory Responses during Lung Injury after Hip Fracture," *BioMed Research International*, vol. 2019, Article ID 7304895, 13 pages, 2019.

Hindawi
BioMed Research International
Volume 2024, Article ID 9820370, 1 page
https://doi.org/10.1155/2024/9820370

Retraction

Retracted: Component-Resolved Diagnostic Study of Egg Allergy in Northern Chinese Children

BioMed Research International

Received 12 March 2024; Accepted 12 March 2024; Published 20 March 2024

This article has been retracted by Hindawi following an investigation undertaken by the publisher [1]. This investigation has uncovered evidence of one or more of the following indicators of systematic manipulation of the publication process:

(1) Discrepancies in scope

(2) Discrepancies in the description of the research reported

(3) Discrepancies between the availability of data and the research described

(4) Inappropriate citations

(5) Incoherent, meaningless and/or irrelevant content included in the article

(6) Manipulated or compromised peer review

The presence of these indicators undermines our confidence in the integrity of the article's content and we cannot, therefore, vouch for its reliability. Please note that this notice is intended solely to alert readers that the content of this article is unreliable. We have not investigated whether authors were aware of or involved in the systematic manipulation of the publication process.

Wiley and Hindawi regrets that the usual quality checks did not identify these issues before publication and have since put additional measures in place to safeguard research integrity.

We wish to credit our own Research Integrity and Research Publishing teams and anonymous and named external researchers and research integrity experts for contributing to this investigation.

The corresponding author, as the representative of all authors, has been given the opportunity to register their agreement or disagreement to this retraction. We have kept a record of any response received.

References

[1] J. Zhang, Y. Shen, J. Li, H. Li, and P. Si, "Component-Resolved Diagnostic Study of Egg Allergy in Northern Chinese Children," *BioMed Research International*, vol. 2020, Article ID 3831087, 9 pages, 2020.

Hindawi
BioMed Research International
Volume 2024, Article ID 9794810, 1 page
https://doi.org/10.1155/2024/9794810

Retraction

Retracted: Protective Effects of Hydrogen on Myocardial Mitochondrial Functions in Septic Mice

BioMed Research International

Received 12 March 2024; Accepted 12 March 2024; Published 20 March 2024

This article has been retracted by Hindawi following an investigation undertaken by the publisher [1]. This investigation has uncovered evidence of one or more of the following indicators of systematic manipulation of the publication process:

(1) Discrepancies in scope

(2) Discrepancies in the description of the research reported

(3) Discrepancies between the availability of data and the research described

(4) Inappropriate citations

(5) Incoherent, meaningless and/or irrelevant content included in the article

(6) Manipulated or compromised peer review

The presence of these indicators undermines our confidence in the integrity of the article's content and we cannot, therefore, vouch for its reliability. Please note that this notice is intended solely to alert readers that the content of this article is unreliable. We have not investigated whether authors were aware of or involved in the systematic manipulation of the publication process.

Wiley and Hindawi regrets that the usual quality checks did not identify these issues before publication and have since put additional measures in place to safeguard research integrity.

We wish to credit our own Research Integrity and Research Publishing teams and anonymous and named external researchers and research integrity experts for contributing to this investigation.

The corresponding author, as the representative of all authors, has been given the opportunity to register their agreement or disagreement to this retraction. We have kept a record of any response received.

References

[1] Y. Zhang, A. Dong, K. Xie, and Y. Yu, "Protective Effects of Hydrogen on Myocardial Mitochondrial Functions in Septic Mice," *BioMed Research International*, vol. 2020, Article ID 1568209, 7 pages, 2020.

Hindawi
BioMed Research International
Volume 2024, Article ID 9791359, 1 page
https://doi.org/10.1155/2024/9791359

Retraction

Retracted: Glucosamine Supplementation in Premating Drinking Water Improves Within-Litter Birth Weight Uniformity of Rats Partly through Modulating Hormone Metabolism and Genes Involved in Implantation

BioMed Research International

Received 12 March 2024; Accepted 12 March 2024; Published 20 March 2024

This article has been retracted by Hindawi following an investigation undertaken by the publisher [1]. This investigation has uncovered evidence of one or more of the following indicators of systematic manipulation of the publication process:

(1) Discrepancies in scope

(2) Discrepancies in the description of the research reported

(3) Discrepancies between the availability of data and the research described

(4) Inappropriate citations

(5) Incoherent, meaningless and/or irrelevant content included in the article

(6) Manipulated or compromised peer review

The presence of these indicators undermines our confidence in the integrity of the article's content and we cannot, therefore, vouch for its reliability. Please note that this notice is intended solely to alert readers that the content of this article is unreliable. We have not investigated whether authors were aware of or involved in the systematic manipulation of the publication process.

Wiley and Hindawi regrets that the usual quality checks did not identify these issues before publication and have since put additional measures in place to safeguard research integrity.

We wish to credit our own Research Integrity and Research Publishing teams and anonymous and named external researchers and research integrity experts for contributing to this investigation.

The corresponding author, as the representative of all authors, has been given the opportunity to register their agreement or disagreement to this retraction. We have kept a record of any response received.

References

[1] C. Feng, T. Yuan, S. Wang et al., "Glucosamine Supplementation in Premating Drinking Water Improves Within-Litter Birth Weight Uniformity of Rats Partly through Modulating Hormone Metabolism and Genes Involved in Implantation," *BioMed Research International*, vol. 2020, Article ID 1630890, 9 pages, 2020.

Hindawi
BioMed Research International
Volume 2024, Article ID 9762194, 1 page
https://doi.org/10.1155/2024/9762194

Retraction

Retracted: Association between Rosacea and Cardiovascular Diseases and Related Risk Factors: A Systematic Review and Meta-Analysis

BioMed Research International

Received 12 March 2024; Accepted 12 March 2024; Published 20 March 2024

This article has been retracted by Hindawi following an investigation undertaken by the publisher [1]. This investigation has uncovered evidence of one or more of the following indicators of systematic manipulation of the publication process:

(1) Discrepancies in scope

(2) Discrepancies in the description of the research reported

(3) Discrepancies between the availability of data and the research described

(4) Inappropriate citations

(5) Incoherent, meaningless and/or irrelevant content included in the article

(6) Manipulated or compromised peer review

The presence of these indicators undermines our confidence in the integrity of the article's content and we cannot, therefore, vouch for its reliability. Please note that this notice is intended solely to alert readers that the content of this article is unreliable. We have not investigated whether authors were aware of or involved in the systematic manipulation of the publication process.

Wiley and Hindawi regrets that the usual quality checks did not identify these issues before publication and have since put additional measures in place to safeguard research integrity.

We wish to credit our own Research Integrity and Research Publishing teams and anonymous and named external researchers and research integrity experts for contributing to this investigation.

The corresponding author, as the representative of all authors, has been given the opportunity to register their agreement or disagreement to this retraction. We have kept a record of any response received.

References

[1] Y. Li, L. Guo, D. Hao, X. Li, Y. Wang, and X. Jiang, "Association between Rosacea and Cardiovascular Diseases and Related Risk Factors: A Systematic Review and Meta-Analysis," *BioMed Research International*, vol. 2020, Article ID 7015249, 11 pages, 2020.

Hindawi
BioMed Research International
Volume 2024, Article ID 9753242, 1 page
https://doi.org/10.1155/2024/9753242

Retraction

Retracted: Bone Marrow Plasma Cytokine Signature Profiles in Severe Aplastic Anemia

BioMed Research International

Received 12 March 2024; Accepted 12 March 2024; Published 20 March 2024

This article has been retracted by Hindawi following an investigation undertaken by the publisher [1]. This investigation has uncovered evidence of one or more of the following indicators of systematic manipulation of the publication process:

(1) Discrepancies in scope

(2) Discrepancies in the description of the research reported

(3) Discrepancies between the availability of data and the research described

(4) Inappropriate citations

(5) Incoherent, meaningless and/or irrelevant content included in the article

(6) Manipulated or compromised peer review

The presence of these indicators undermines our confidence in the integrity of the article's content and we cannot, therefore, vouch for its reliability. Please note that this notice is intended solely to alert readers that the content of this article is unreliable. We have not investigated whether authors were aware of or involved in the systematic manipulation of the publication process.

Wiley and Hindawi regrets that the usual quality checks did not identify these issues before publication and have since put additional measures in place to safeguard research integrity.

We wish to credit our own Research Integrity and Research Publishing teams and anonymous and named external researchers and research integrity experts for contributing to this investigation.

The corresponding author, as the representative of all authors, has been given the opportunity to register their agreement or disagreement to this retraction. We have kept a record of any response received.

References

[1] B. Liu, Y. Shao, Z. Liu, C. Liu, T. Zhang, and R. Fu, "Bone Marrow Plasma Cytokine Signature Profiles in Severe Aplastic Anemia," *BioMed Research International*, vol. 2020, Article ID 8789275, 11 pages, 2020.

Hindawi
BioMed Research International
Volume 2020, Article ID 9494528, 6 pages
https://doi.org/10.1155/2020/9494528

Research Article

Antioxidant Function and Metabolomics Study in Mice after Dietary Supplementation with Methionine

Manrong Yu,[1] Hui Chen,[1] Pan Liu,[1] Mei Yang,[1] Leqin Zou,[1] and Dingfu Xiao[1,2]

[1]*College of Animal Science and Technology, Hunan Agricultural University, Changsha Hunan 410128, China*
[2]*Hunan Collaborative Innovation Center of Animal Production Safety, Changsha Hunan 410128, China*

Correspondence should be addressed to Dingfu Xiao; xiaodingfu2001@163.com

Received 18 February 2020; Accepted 15 May 2020; Published 21 October 2020

Guest Editor: Lei Sun

The antioxidant function and metabolic profiles in mice after dietary supplementation with methionine were investigated. The results showed that methionine supplementation enhanced liver GSH-Px activity and upregulated Gpx1 expression in the liver and SOD1 and Gpx4 expressions in the jejunum. Nrf2/Keap1 is involved in oxidative stress, and the western blotting data exhibited that dietary methionine markedly increased Keap1 abundance, while failed to influence the Nrf2 signal. Metabolomics investigation showed that methionine administration increased 2-hydroxypyridine, salicin, and asparagine and reduced D-Talose, maltose, aminoisobutyric acid, and inosine 5'-monophosphate in the liver, which are widely reported to involve in oxidative stress, lipid metabolism, and nucleotides generation. In conclusion, our study provides insights into antioxidant function and liver metabolic profiles in response to dietary supplementation with methionine.

1. Introduction

Methionine is an essential amino acid and mainly contributes to protein and S-adenosylmethionine (SAM) synthesis in the liver. SAM serves as a versatile methyl donor for nucleic acids and proteins, and the methylation of DNA and proteins is a major regulating mechanism for various physiological functions, including heat shock response [1, 2], regulation of intestinal barrier integrity [3], development [4], and gene expression [5]. Meanwhile, methionine has been widely demonstrated to involve in oxidative stress via the transsulfuration pathway for cysteine generation [6]. Cysteine further corresponds for glutathione (GSH) production [6], which is a major thiol group and contributes to antioxidant function against free radical species [7–10].

Here, we found that methionine enhanced antioxidant function via increasing antioxidant enzyme activity and expression. In addition, gas chromatography-mass spectrometry (GC-MS) was performed to investigate the liver metabolic profile after dietary methionine, and the results showed that 7 metabolites (i.e., hydroxypyridine, salicin, asparagine, D-talose, maltose, aminoisobutyric acid, and inosine 5'-monophosphate) were altered and these metabolites are involved in oxidative stress, lipid metabolism, and nucleotides generation.

2. Methods and Materials

2.1. Animal and Group. Twenty female ICR mice weighting 22.75 ± 0.43 g were assigned into two experimental groups: a control group in which mice received a normal diet (containing 0.43% methionine) and a Met group in which mice received an additional 0.5% DL-methionine [11]. Body weight and feed intake were recorded. After three weeks, blood was collected from the eyes, liver, and jejuna, and ilea samples were collected. This study involving animal subjects was approved by the College of Animal Science and Technology, Hunan Agricultural University.

2.2. Antioxidant Function. Serum samples were separated and stored for further analyses. Liver samples were homogenized; then, the supernatant was collected for further analyses. Antioxidant indexes (i.e., superoxide dismutase (SOD),

Table 1: PCR primer sequences: the forward primers (F) and the reverse primers (R) used in this study.

Gene	Accession no.	Nucleotide sequence of primers (5′–3′)	Size (bp)
β-Actin	NM_007393.3	F:GTCCACCTTCCAGCAGATGT R:GAAAGGGTGTAAAACGCAGC	117
CAT	XM_006498624.1	F:AATATCGTGGGTGACCTCAA R:CAGATGAAGCAGTGGAAGGA	243
ZnCuSOD	NM_011434.1	F:CCACTGCAGGACCTCATTTT R:CACCTTTGCCCAAGTCATCT	216
Gpx1	NM_008160.6	F:GGTTCGAGCCCAATTTTACA R:CCCACCAGGAACTTCTCAAA	199
Gpx4	NM_001037741.3	F:CTCCATGCACGAATTCTCAG R:ACGTCAGTTTTGCCTCATTG	117
UCP2	NM_011671.5	F:TAGTGCGCACCGCAGCC R:AGCTCATCTGGCGCTGCAG	126

Table 2: Growth performance after dietary supplementation with methionine. IBD: initial body weight; FBW: final body weight; AFI: average feed intake; ABWG: average body weight gain; F : G: the ratio of feed intake to weight gain.

Item	IBW	FBW	AFI	ABWG	F : G
Cont	22.26 ± 0.37	28.27 ± 0.53	5.65 ± 0.05	0.30 ± 0.01	19.36 ± 0.88
Met	23.24 ± 0.50	26.84 ± 0.47	5.76 ± 0.02	0.27 ± 0.02	21.85 ± 1.26

glutathione peroxidase (GSH-Px), and catalase (CAT)) were tested (Nanjing Jiancheng, China) [12].

2.3. RT-PCR. RNA isolation and cDNA synthesis were conducted according to previous studies [13]. Primer 5.0 was used to design the primer (Table 1). RT-PCR was performed according to previous studies [14–18].

2.4. Western Blot. Liver proteins were extracted by the Thermo Fisher kits (Waltham, MA, USA) and separated by SDS-PAGE electrophoresis [14, 19, 20]. Then, the separated proteins were transferred onto PVDF membranes (Millipore, MA, USA) for the incubation of antibodies, including taste receptor type 1 member 1 (T1R1), taste receptor type 1 member 3 (T1R3), Kelch-like ECH-associating protein 1 (Keap1), nuclear factor erythroid *2*-related factor *2* (Nrf2), and uncoupling protein 2 (Ucp2) (Abcam Bio).

2.5. Gas Chromatography-Mass Spectrometry (GC-MS) Analysis. Metabolomics study of liver samples was investigated (Agilent 7890A, Agilent, USA), and data were analyzed by the Chroma TOF 4.3X software (LECO Corporation, USA) and LECO-Fiehn Rtx5 database [21–25].

2.6. Statistical Analysis. All data were analyzed using the Students' *T* test (SPSS 17.0 software). Data are expressed as the mean ± sem. Values in the same row with different superscripts are significant ($P < 0.05$).

3. Results

3.1. Growth Performance. Dietary 0.5% methionine had no effect on the body weight gain, average feed intake, and the ratio of feed intake to body weight gain ($P < 0.05$) (Table 2).

Table 3: GSH-Px, SOD, and CAT activities in the serum and liver after dietary supplementation with methionine. The * means the difference is significant between the two groups ($P < 0.05$).

Item	GSH-Px	SOD	CAT
Serum (U/ml)			
Cont	17.89 ± 1.22	116.74 ± 20.48	366.52 ± 135.33
Met	28.95 ± 7.78	131.06 ± 12.51	216.77 ± 34.27
Liver (U/mgprot)			
Cont	26.80 ± 2.35	2342.63 ± 50.94	188.12 ± 15.24
Met	152.88 ± 30.01*	2398.21 ± 70.69	116.08 ± 20.47*

3.2. Antioxidant Function. Serum and liver GSH-Px, SOD, and CAT were measured to evaluate the antioxidant function after dietary supplementation with methionine (Table 3). In the serum, we did not find any significant difference on GSH-Px, SOD, and CAT activities ($P > 0.05$). In addition, methionine supplementation markedly enhanced liver GSH-Px activity ($P < 0.05$), while liver CAT activity was inhibited in the Met group ($P < 0.05$).

We further determined the expression of antioxidant genes (CAT, SOD1, Gpx, Gpx4, and UCP2) in the liver, jejunum, and ileum (Figure 1). In the liver, methionine markedly upregulated the Gpx1 expression ($P < 0.05$). In the jejunum, methionine markedly increased SOD1 and Gpx4 mRNA abundances ($P < 0.05$).

3.3. T1R1 and T1R3. Intestinal T1R1 and T1R3 were determined via western blot (Figure 2). In the jejunum and ileum,

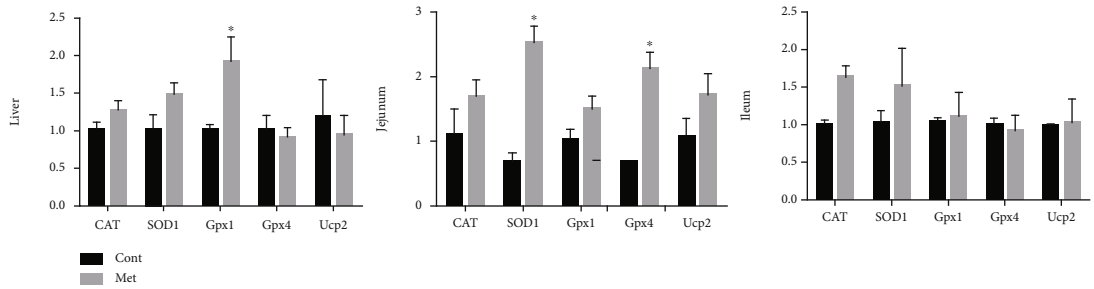

Figure 1: The expression of antioxidant genes (CAT, SOD1, Gpx, Gpx4, and UCP2) in the liver, jejunum, and ileum.

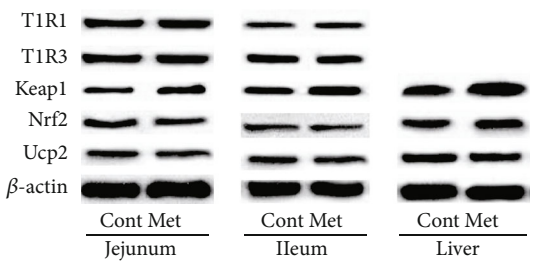

Figure 2: Western blot: T1R1 and T1R3 of jejunum, ileum, and liver.

dietary supplementation failed to influence T1R1 and T1R3 abundance ($P > 0.05$).

3.4. Nrf2/Keap1 Signal. In this study, dietary supplementation significantly enhanced the liver and ileal Keap1 expression ($P < 0.05$), but Nrf2 expression was not changed ($P > 0.05$).

3.5. Metabolic Profiles Analyzed by GC-MS. Metabolites in the liver were analyzed from 534 peaks (Figure 3(a)). PLS-DA score plots exhibited that dietary supplementation with methionine leaded distinctive metabolic profiles in mice compared with the control mice (Figure 3(b) and 3(c)).

The identified potential markers after dietary supplementation with methionine are listed in Table 4. Dietary methionine significantly increased liver 2-hydroxypyridine, salicin, and asparagine concentrations. Meanwhile, liver D-talose, maltose, aminoisobutyric acid, and inosine 5'-monophosphate were markedly reduced after dietary methionine.

4. Discussion

Methionine is a limiting AA in most cereal soybean-based diets for growing pigs [26]. Recently, methionine has been reported to involve in lipid metabolism [27], translational capacity [28], autophagy [29], and maintenance and differentiation of pluripotent stem cells [30]. Meanwhile, dietary methionine or methionine restriction has been demonstrated to influence growing performance [31, 32], while the current study did not observed any significant difference in the growth performance in mice. In addition, we found that dietary supplementation with methionine enhanced antioxidant function and upregulated liver Keap1 expression. Meanwhile, 7 metabolites were found related to dietary methionine based on GC-MS-based metabolomics investigation.

Methionine can sustain cellular redox homeostasis via the generation of cysteine, which is a substance for GSH synthesis [6, 33]. In this study, we found that dietary methionine increased antioxidant function evidenced by the enhanced serum GSH-Px activity and upregulation of Gpx1, Gpx4, and SOD1. Methionine can form cysteine via the transsulfuration pathway to serve as a precursor for GSH, hydrogen sulfide, and taurine [6]. These metabolites have been demonstrated to mediate oxidative stress via scavenging hydroxyl radical and superoxide directly and serving as a cofactor for the antioxidant enzymes, including GSH peroxidase (Gpx) [6]. Meanwhile, Campbell et al. reported that methionine affects the oxidative branch of the pentose phosphate pathway and increased abundance of the NADPH producing enzyme 6PGDH, which further plays a protective role against oxidative stress [34].

Nrf2/keap1 signaling pathway is widely involved in oxidative stress and regulates the expression of antioxidant genes [12, 14, 15]. Normally, Nrf2 protein is sequestered in the cytosol via targeting Keap1 and soon be degraded under cellular homeostasis [35]. Although Keap1 was upregulated after dietary methionine, liver, jejunal, and ileal Nrf2 expression was not changed in this study. Nrf2 activation was observed under methionine restriction [36, 37], which further regulated antioxidant genes and oxidative stress.

Metabolomics investigation revealed 7 metabolites after dietary methionine, including hydroxypyridine, salicin, asparagine, D-Talose, maltose, aminoisobutyric acid, and inosine 5'-monophosphate. Salicin has been studied as a potent anti-inflammatory agent and exhibits an anti-inflammatory and antioxidant functions in various inflammation-related diseases [38, 39]. Asparagine is a metabolic product of the aspartate, which has been demonstrated to alleviate diquat-induced oxidative injury in piglets [40]. Thus, the increased contents of salicin and asparagine in the Met group may indicate methionine mediates inflammation and oxidative stress via indirectly affecting salicin and asparagine concentrations. Aminoisobutyric acid, a low molecular myokine, contributes to the conversion of white adipose tissue into brown fat, accelerating the breakdown of lipids into heat, water, and CO_2 [41]. Previous reports also demonstrated that methionine regulates lipid metabolism via increasing metabolic flexibility and overall insulin sensitivity [42]. Inosine 5'-monophosphate is an intermediate of purine metabolism and serves as a

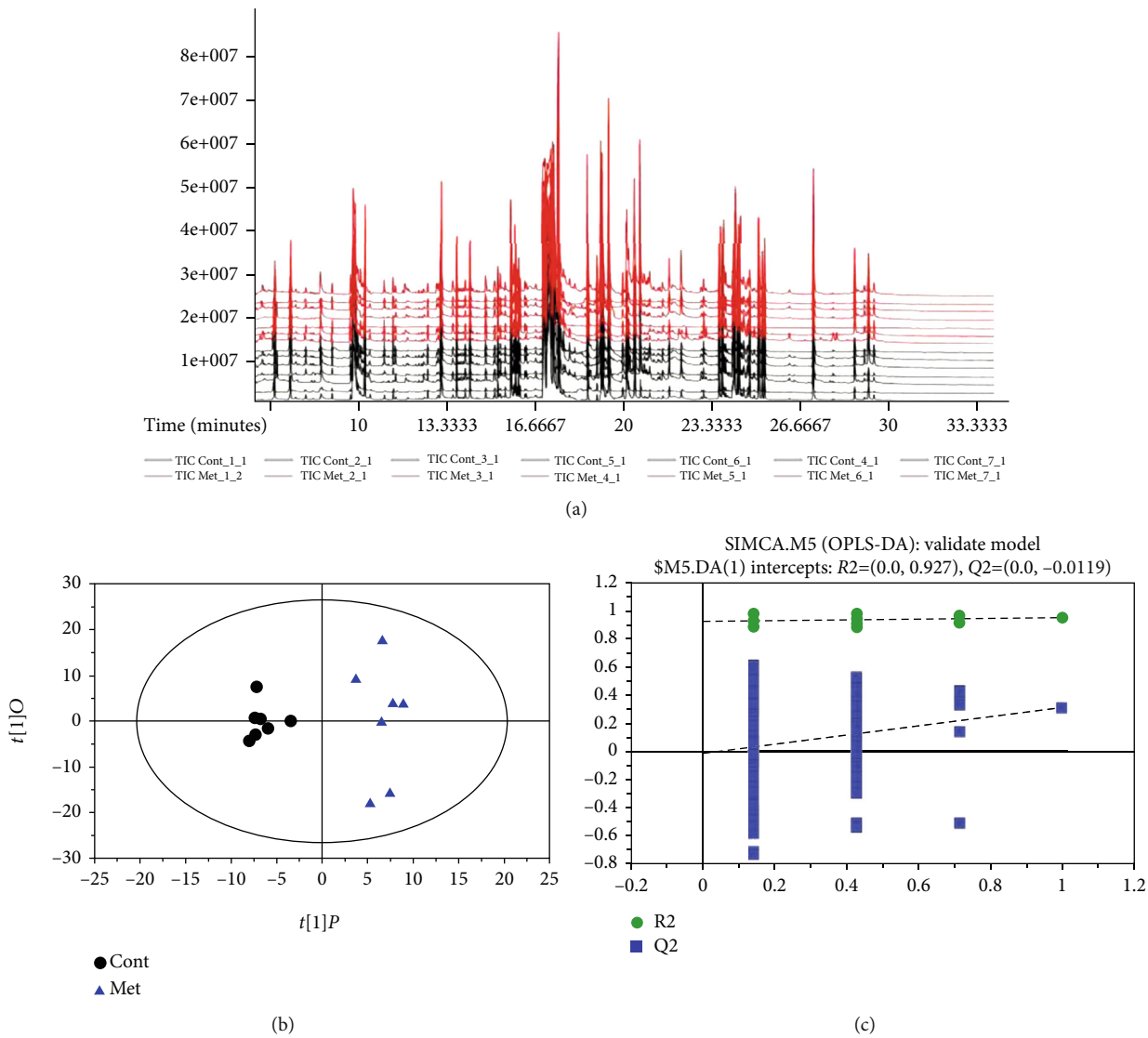

Figure 3: Metabolites identified from 534 peaks in the chromatograms and PLS-DA score plots.

Table 4: List of differential metabolites between the control and Met groups.

ID	Peak	R.T.	Count	Mass	Cont	Met	VIP	*P* value	Fold change
13	2-hydroxypyridine	6.61	29	152	0.64	1.32	1.94	0.03	2.05
421	D-Talose	17.38	16	235	0.25	0.00	1.92	0.04	0.00
662	Maltose	24.22	17	361	4.39	1.10	1.96	0.03	0.25
204	Aminoisobutyric acid	12.31	23	174	0.11	0.04	2.04	0.04	0.36
597	Salicin	22.42	29	169	0.02	0.03	1.99	0.04	2.08
711	Inosine 5'-monophosphate	25.87	19	169	0.01	0.00	1.94	<0.01	0.09
300	Asparagine	14.37	19	229	0.00	0.01	2.69	<0.01	3980383.06

precursor for other nucleotides used for metabolic functions [43, 44]. Thus, we speculated that dietary methionine serves as a regulator in nucleotide metabolism, which was further demonstrated by Benjamin P. Tu who reported that methionine regulates translational capacity through modulation of tRNA thiolation [28].

In conclusion, dietary supplementation with methionine enhanced antioxidant function. Meanwhile, metabolomics investigation revealed that methionine influenced 7 metabolites, including hydroxypyridine, salicin, asparagine, D-Talose, maltose, aminoisobutyric acid, and inosine 5'-monophosphate.

Data Availability

The data used to support the findings of this study are available from the corresponding author upon request.

Conflicts of Interest

The authors have declared no conflict of interest.

Authors' Contributions

D.F., Xiao designed the experiment. M.R Yu, D.F. Xiao, H. Chen, P. Liu, L.Q. Zou, and M. Yang conducted the experiment. H. Chen performed the data analysis. D.F. Xiao wrote the manuscript.

Acknowledgments

This study was jointly supported by the National Natural Science Foundation of China (No.31872991) and the "double first Class" Construction Project of Hunan Agricultural University (kxk201801004).

References

[1] J. Zhou, J. Wan, X. Gao, X. Zhang, S. R. Jaffrey, and S. B. Qian, "Dynamic m(6)A mRNA methylation directs translational control of heat shock response," *Nature*, vol. 526, no. 7574, pp. 591–594, 2015.

[2] A. Bhattacharya, M. Sharma, C. Packianathan, B. P. Rosen, P. Leprohon, and M. Ouellette, "Genomewide Analysis of Mode of Action of the S-Adenosylmethionine Analogue Sinefungin in Leishmania infantum," *Msystems*, vol. 4, p. e00416, 2019.

[3] P. G. Thomes, N. A. Osna, S. M. Bligh, D. J. Tuma, and K. K. Kharbanda, "Role of defective methylation reactions in ethanol-induced dysregulation of intestinal barrier integrity," *Biochemical Pharmacology*, vol. 96, no. 1, pp. 30–38, 2015.

[4] C. Li, S. Guo, M. Zhang, J. Gao, and Y. Guo, "DNA methylation and histone modification patterns during the late embryonic and early postnatal development of chickens," *Poultry Science*, vol. 94, no. 4, pp. 706–721, 2015.

[5] J. Dunn, H. Qiu, S. Kim et al., "Flow-dependent epigenetic DNA methylation regulates endothelial gene expression and atherosclerosis," *The Journal of Clinical Investigation*, vol. 124, no. 7, pp. 3187–3199, 2014.

[6] J. Yin, W. Ren, G. Yang et al., "l-Cysteine metabolism and its nutritional implications," *Molecular Nutrition & Food Research*, vol. 60, no. 1, pp. 134–146, 2016.

[7] H. A. El Hendy and H. A. Al-Gemeai, "Effect of broccoli intake on antioxidant in the liver and kidney tissues of hyperglycemic rats," *Integrative food, nutrition and metabolism*, vol. 1, pp. 83–86, 2014.

[8] M. J. McCann, J. E. Dalziel, R. Bibiloni, and M. P. G. Barnett, "An integrated approach to assessing the bio-activity of nutrients in vitro: the anti-oxidant effects of catechin and chlorogenic acid as an example," *Integrative food, nutrition and metabolism*, vol. 2, pp. 197–204, 2015.

[9] A. B. Shori and A. S. Baba, "Fermented milk derives bioactive peptides with antihypertensive effects," *Integrative food, nutrition and metabolism*, vol. 2, pp. 178–181, 2015.

[10] S. Mileva, B. Galunska, M. Gospodinova, D. Gerova, and D. Svinarov, "Vitamin D3 status in children with acute diarrhea," *Integrative food, nutrition and metabolism*, vol. 1, pp. 1–6, 2014.

[11] W. Ren, S. Chen, J. Yin et al., "Dietary arginine supplementation of mice alters the microbial population and activates intestinal innate immunity," *The Journal of Nutrition*, vol. 144, no. 6, pp. 988–995, 2014.

[12] J. Yin, J. Duan, Z. Cui, W. Ren, T. Li, and Y. Yin, "Hydrogen peroxide-induced oxidative stress activates NF-κB and Nrf2/Keap1 signals and triggers autophagy in piglets," *RSC Advances*, vol. 5, no. 20, pp. 15479–15486, 2015.

[13] D. Xiao, Z. Tang, Y. Yin et al., "Effects of dietary administering chitosan on growth performance, jejunal morphology, jejunal mucosal sIgA, occludin, claudin-1 and TLR4 expression in weaned piglets challenged by enterotoxigenic Escherichia coli," *International Immunopharmacology*, vol. 17, no. 3, pp. 670–676, 2013.

[14] J. Yin, W. Ren, G. Liu et al., "Birth oxidative stress and the development of an antioxidant system in newborn piglets," *Free Radical Research*, vol. 47, no. 12, pp. 1027–1035, 2013.

[15] J. Yin, M. M. Wu, H. Xiao et al., "Development of an antioxidant system after early weaning in piglets," *Journal of Animal Science*, vol. 92, no. 2, pp. 612–619, 2014.

[16] J. Yin, Y. Li, H. Han et al., "Melatonin reprogramming of gut microbiota improves lipid dysmetabolism in high-fat diet-fed mice," *Journal of Pineal Research*, vol. 65, no. 4, article e12524, 2018.

[17] Y. Duan, Y. Zhong, H. Xiao et al., "Gut microbiota mediates the protective effects of dietary β-hydroxy-β-methylbutyrate (HMB) against obesity induced by high-fat diets," *The FASEB Journal*, vol. 33, no. 9, pp. 10019–10033, 2019.

[18] I. Chouikha, D. E. Sturdevant, C. Jarrett, Y. C. Sun, and B. J. Hinnebusch, "Differential Gene Expression Patterns ofYersinia pestisandYersinia pseudotuberculosisduring Infection and Biofilm Formation in the Flea Digestive Tract," *Msystems*, vol. 4, no. 1, 2019.

[19] J. Yin, Y. Li, H. Han et al., "Effects of lysine deficiency and Lys-Lys dipeptide on cellular apoptosis and amino acids metabolism," *Molecular Nutrition & Food Research*, vol. 61, no. 9, 2017.

[20] J. Yin, Y. Li, X. Zhu et al., "Effects of long-term protein restriction on meat quality, muscle amino acids, and amino acid transporters in pigs," *Journal of Agricultural and Food Chemistry*, vol. 65, no. 42, pp. 9297–9304, 2017.

[21] J. Yin, F. Li, X. Kong et al., "Dietary xylo-oligosaccharide improves intestinal functions in weaned piglets," *Food & Function*, vol. 10, no. 5, pp. 2701–2709, 2019.

[22] J. Yin, Y. Li, H. Han et al., "Long-term effects of lysine concentration on growth performance, intestinal microbiome, and metabolic profiles in a pig model," *Food & Function*, vol. 9, no. 8, pp. 4153–4163, 2018.

[23] M. L. Han, Y. Zhu, D. J. Creek et al., "Comparative metabolomics and transcriptomics reveal multiple pathways associated with polymyxin killing in Pseudomonas aeruginosa," *Msystems*, vol. 4, no. 1, 2019.

[24] M. A. Henson, G. Orazi, P. Phalak, and G. A. O'Toole, "Metabolic Modeling of Cystic Fibrosis Airway Communities Predicts Mechanisms of Pathogen Dominance," *Msystems*, vol. 4, 2019.

[25] Y. Zhu, J. X. Zhao, M. H. M. Maifiah, T. Velkov, F. Schreiber, and J. Li, "Metabolic responses to polymyxin treatment in

Acinetobacter baumannii ATCC 19606: integrating transcriptomics and metabolomics with genome-scale metabolic modeling," *Msystems*, vol. 4, no. 1, 2019.

[26] S. Metayer, I. Seiliez, A. Collin et al., "Mechanisms through which sulfur amino acids control protein metabolism and oxidative status," *The Journal of Nutritional Biochemistry*, vol. 19, no. 4, pp. 207–215, 2008.

[27] P. Jha, A. Knopf, H. Koefeler et al., "Role of adipose tissue in methionine-choline-deficient model of non-alcoholic steatohepatitis (NASH)," *Biochimica et Biophysica Acta*, vol. 1842, no. 7, pp. 959–970, 2014.

[28] S. Laxman, B. M. Sutter, X. Wu et al., "Sulfur amino acids regulate translational capacity and metabolic homeostasis through modulation of tRNA thiolation," *Cell*, vol. 154, no. 2, pp. 416–429, 2013.

[29] B. M. Sutter, X. Wu, S. Laxman, and B. P. Tu, "Methionine inhibits autophagy and promotes growth by inducing the SAM-responsive methylation of PP2A," *Cell*, vol. 154, no. 2, pp. 403–415, 2013.

[30] N. Shiraki, Y. Shiraki, T. Tsuyama et al., "Methionine metabolism regulates maintenance and differentiation of human pluripotent stem cells," *Cell Metabolism*, vol. 19, no. 5, pp. 780–794, 2014.

[31] F. Hirai and T. Matsui, "Status of food intake and elemental nutrition in patients with Crohn's disease," *Integrative food, nutrition and metabolism*, vol. 2, pp. 148–150, 2015.

[32] J. Eastep and G. Chen, "The relationships of high-fat diet and metabolism of lipophilic vitamins," *Integrative food, nutrition and metabolism*, vol. 2, pp. 174–179, 2015.

[33] S. Eriksson, J. R. Prigge, E. A. Talago, E. S. J. Arner, and E. E. Schmidt, "Dietary methionine can sustain cytosolic redox homeostasis in the mouse liver," *Nature communications*, vol. 6, 2015.

[34] K. Campbell, J. Vowinckel, M. A. Keller, and M. Ralser, "Methionine metabolism alters oxidative stress resistance via the pentose phosphate pathway," *Antioxidants & Redox Signaling*, vol. 24, no. 10, pp. 543–547, 2016.

[35] J. Yin, W. K. Ren, X. S. Wu et al., "Oxidative stress-mediated signaling pathways: a review," *Journal of Food, Agriculture and Environment*, vol. 11, pp. 132–139, 2013.

[36] Y. K. Zhang, R. L. Yeager, Y. Tanaka, and C. D. Klaassen, "Enhanced expression of Nrf2 in mice attenuates the fatty liver produced by a methionine- and choline-deficient diet," *Toxicology and Applied Pharmacology*, vol. 245, no. 3, pp. 326–334, 2010.

[37] A. H. Lin, H. W. Chen, C. T. Liu, C. W. Tsai, and C. K. Lii, "Activation of Nrf2 Is Required for Up-Regulation of the π Class of GlutathioneS-Transferase in Rat Primary Hepatocytes withl-MethionineStarvation," *Journal of agricultural and food chemistry*, vol. 60, no. 26, pp. 6537–6545, 2012.

[38] Y. Li, Q. Wu, Y. Deng et al., "D(-)-Salicin inhibits the LPS-induced inflammation in RAW264.7 cells and mouse models," *International immunopharmacology*, vol. 26, no. 2, pp. 286–294, 2015.

[39] N. Verma, R. Verma, R. Kumari, R. Ranjha, and J. Paul, "Effect of salicin on gut inflammation and on selected groups of gut microbiota in dextran sodium sulfate induced mouse model of colitis," *Inflammation Research*, vol. 63, no. 2, pp. 161–169, 2014.

[40] J. Yin, M. Liu, W. Ren et al., "Effects of dietary supplementation with glutamate and aspartate on diquat-induced oxidative stress in piglets," *PLoS One*, vol. 10, no. 4, article e0122893, 2015.

[41] E. Ginter and V. Simko, "Recent data on obesity research: β-aminoisobutyric acid," *Bratislavske lekarske listy*, vol. 115, no. 8, pp. 492-493, 2014.

[42] M. L. Orgeron, K. P. Stone, D. Wanders, C. C. Cortez, N. T. Van, and T. W. Gettys, "The Impact of Dietary Methionine Restriction on Biomarkers of Metabolic Health," *Progress in molecular biology and translational science*, vol. 121, pp. 351–376, 2014.

[43] H. H. Stein and D. Y. Kil, "Reduced use of antibiotic growth promoters in diets fed to weanling pigs: dietary tools, part 2," *Animal Biotechnology*, vol. 17, no. 2, pp. 217–231, 2006.

[44] T. Ma, L. Xu, H. Wang et al., "Mining the key regulatory genes of chicken inosine 5'-monophosphate metabolism based on time series microarray data," *Journal of Animal Science and Biotechnology*, vol. 6, no. 1, p. 21, 2015.

Hindawi
BioMed Research International
Volume 2024, Article ID 9762194, 1 page
https://doi.org/10.1155/2024/9762194

Retraction

Retracted: Association between Rosacea and Cardiovascular Diseases and Related Risk Factors: A Systematic Review and Meta-Analysis

BioMed Research International

Received 12 March 2024; Accepted 12 March 2024; Published 20 March 2024

This article has been retracted by Hindawi following an investigation undertaken by the publisher [1]. This investigation has uncovered evidence of one or more of the following indicators of systematic manipulation of the publication process:

(1) Discrepancies in scope

(2) Discrepancies in the description of the research reported

(3) Discrepancies between the availability of data and the research described

(4) Inappropriate citations

(5) Incoherent, meaningless and/or irrelevant content included in the article

(6) Manipulated or compromised peer review

The presence of these indicators undermines our confidence in the integrity of the article's content and we cannot, therefore, vouch for its reliability. Please note that this notice is intended solely to alert readers that the content of this article is unreliable. We have not investigated whether authors were aware of or involved in the systematic manipulation of the publication process.

Wiley and Hindawi regrets that the usual quality checks did not identify these issues before publication and have since put additional measures in place to safeguard research integrity.

We wish to credit our own Research Integrity and Research Publishing teams and anonymous and named external researchers and research integrity experts for contributing to this investigation.

The corresponding author, as the representative of all authors, has been given the opportunity to register their agreement or disagreement to this retraction. We have kept a record of any response received.

References

[1] Y. Li, L. Guo, D. Hao, X. Li, Y. Wang, and X. Jiang, "Association between Rosacea and Cardiovascular Diseases and Related Risk Factors: A Systematic Review and Meta-Analysis," *BioMed Research International*, vol. 2020, Article ID 7015249, 11 pages, 2020.

Hindawi
BioMed Research International
Volume 2020, Article ID 7015249, 11 pages
https://doi.org/10.1155/2020/7015249

Research Article

Association between Rosacea and Cardiovascular Diseases and Related Risk Factors: A Systematic Review and Meta-Analysis

Yanmei Li, Linghong Guo, Dan Hao, Xiaoxue Li, Yujia Wang, and Xian Jiang

Department of Dermatology, West China Hospital, Sichuan University, Chengdu 610041, China

Correspondence should be addressed to Xian Jiang; jennyxianj@163.com

Received 25 February 2020; Revised 2 June 2020; Accepted 3 June 2020; Published 18 June 2020

Guest Editor: Deguang Song

Background. Rosacea is a common inflammatory skin disorder. Several studies, but not all, have suggested a high prevalence of cardiovascular diseases (CVDs) in rosacea patients. This study is aimed at investigating the association between rosacea and CVDs and related risk factors. *Methods*. We performed a literature search through PubMed, Embase, and Web of Science databases, from their respective inception to December 21, 2019. Two reviewers independently screened the articles, extracted data, and performed analysis, following the PRISMA guidelines. Odds ratios (OR) or standardized mean differences (SMD) and 95% confidence intervals (CI) were calculated for outcomes. The included studies' quality was evaluated using the Newcastle Ottawa Scale (NOS). *Results*. The final meta-analysis included ten studies. The pooled analysis found no association between rosacea prevalence and the incidence of CVDs (OR 0.97; 95% CI 0.86-1.10). Rosacea was found to be significantly associated with several risk factors for CVDs (OR 1.17; 95% CI 1.05-1.31), including hypertension (OR 1.17; 95% CI 1.02-1.35), dyslipidemia (OR 1.34; 95% CI 1.00-1.79), and metabolic syndrome (OR 1.72; 95% CI 1.09-2.72). However, no association was found between rosacea and diabetes mellitus (OR 0.98; 95% CI 0.82-1.16). Among the biological parameters, a significant association was found between rosacea and total cholesterol (SMD = 0.40; 95% CI = −0.00, 0.81; $p < 0.05$), low-density lipoprotein cholesterol (SMD = 0.28; 95% CI = 0.01, 0.56; $p < 0.05$), and C-reactive protein (CRP) (SMD = 0.25; 95% CI = 0.10, 0.41; $p < 0.05$). We found no association between rosacea and high-density lipoprotein cholesterol (SMD = 0.00; 95% CI = −0.18, 0.18; $p = 0.968$) or triglycerides (SMD = 0.10; 95% CI = −0.04, 0.24; $p = 0.171$). *Conclusions*. Although no significant association was found between rosacea and CVDs, rosacea was found to be associated with several of related risk factors. Patients with rosacea should pay more attention to identifiable CVD risk factors, especially those related to inflammatory and metabolic disorders.

1. Introduction

Rosacea is a common, chronic inflammatory skin disease. It is characterized by flushing, persistent erythema, papules, pustules, telangiectasia, and phymatous changes affecting mainly the convexities of the face, with ocular involvement [1]. According to published data [2], the global adult prevalence of rosacea is about 5.46%. There is no significant sex difference in rosacea incidence. People between the ages of 45-60 are more susceptible. The complex pathomechanism of rosacea involves the interplay of genetic factors; dysregulation of the immune, vascular, and nervous systems; and environmental factors such as ultraviolet radiation, alcohol, and microorganisms [3]. Studies have shown that rosacea starts with an inappropriate innate immune response due to external stimuli. This response eventually leads to worsened inflammation and abnormal blood vessels. Upregulation of inflammation-related genes and infiltration of inflammatory cells are found in all rosacea subtypes, even in those with transient erythema [4]. The sebaceous glands, abundant in the centrofacial region, were also suggested to participate in the inflammatory process of rosacea, which is consistent with the clinical manifestation of centrofacial distribution [5].

Cardiovascular diseases (CVDs), especially coronary heart disease and stroke, are together the number one global death cause [6]. Risk assessment is a critical step in the current approach aimed at preventing CVDs. The main risk factors include diabetes mellitus (DM), hypertension,

dyslipidemia, and metabolic syndrome (MS). The disrupted metabolism of lipids plays a crucial role in the development of CVDs. It affects not only the heart's circulation but also the peripheral and cerebral arteries. Accumulation of lipids or fibrous material in the intima of arteries causes atherosclerosis. Serum lipids are prone to form plaques on the affected intima. When such plaques detach, they might block important arteries, leading to ischemic events [6]. In some guidelines, biomarkers of inflammation, notably C-reactive protein (CRP), were added to traditional risk factors as potential predictors of CVDs, especially in patients at intermediate risk [7].

Accumulating evidence has shown that rosacea is a systemic disease. The association between rosacea and multiple comorbidities, including depression, migraines, gastrointestinal disorders, and autoimmune conditions, has been demonstrated [8]. Several investigators have suggested that rosacea might increase the prevalence of CVDs and related risk factors [9–14]. However, the evidence is limited and still controversial [15–18]. This discrepancy might be because the available evidence comes from studies with a small sample size and inadequate statistical power, using different study methods, and with publication bias. Mechanistically, vascular endothelial growth factor (VEGF)+405C/G polymorphism was reported to be significantly associated with rosacea and is also a risk factor for abnormal coronary microvasculature [19]. Moreover, the same pathways were previously shown to be active in rosacea and atherosclerosis, including increased cathelicidins, proinflammatory cytokines, and endoplasmic reticulum stress [18, 20, 21]. Considering that rosacea and CVDs are both chronic diseases involving an interplay between genetic and inflammatory elements, we thought it is necessary to perform a meta-analysis to explore the relationship between them and the CVD-associated risk factors.

2. Materials and Methods

This systematic review and meta-analysis was conducted in accordance with PRISMA guidelines.

2.1. Search Strategy. We searched PubMed, Embase, and Web of Science databases from their inception dates to December 21, 2019. Keywords for this search were as follows: ("rosacea") and ("cardiovascular" or "metabolic syndrome" or "diabetes" or "hypertension" or "dyslipidemia" or "cholesterol" or "C-reactive protein"). In addition, we screened references in all retrieved articles to identify potentially eligible studies and evaluated them based on the inclusion and exclusion criteria. Only studies in English were included for assessment.

2.2. Inclusion and Exclusion Criteria. Studies were selected for the final analysis according to the following inclusion criteria: (i) studies evaluating the association between rosacea and CVDs and risk factors, (ii) case-control studies, and (iii) studies directly providing odds ratios (OR) for major CVDs and risk factors, or mean and standard deviation (SD) for biochemical factors, or giving original and sufficient data to calculate OR. The exclusion criteria were (i) studies of reviews, abstracts, case reports, or conference publications; (ii) studies of the repeated report of same research subjects or repeated publications; and (iii) studies not reporting relevant data or data not available.

2.3. Data Extraction. Two investigators (Y.L. and L.G.) independently reviewed literature, extracted data from each eligible study, and cross-checked, with disagreements resolved by consensus discussion with the third investigator (D.H.). The missing data were obtained by contacting the study author. The following clinical and demographic characteristics of included studies were extracted: (i) study characteristics including lead author, year of publication, and country; (ii) participant characteristics encompassing age, sample size, and diagnostic criteria for rosacea; and (iii) main outcomes including OR and 95% confidence interval for CVDs, including cardiovascular death (CD), CVD, major adverse cardiovascular events (MACE), peripheral atherosclerotic occlusive disease (PAOD), ischemic heart disease (IHD), myocardial infarction (MI), stroke, coronary artery disease (CAD) and heart failure (HF), and CVD risk factors (hypertension, DM, dyslipidemia, and MS). Mean and SD for biochemical indicators include high-density lipoprotein cholesterol (HDL-C), low-density lipoprotein cholesterol (LDL-C), total cholesterol (TC), triglycerides (TG), and CRP. In this study, the primary outcome was the association between rosacea and overall cardiovascular disease, while the secondary outcome was the relationship between rosacea and CVD-related risk diseases and the association of rosacea with biochemical indicators related to cardiovascular diseases.

2.4. Quality Assessment. The quality assessment was based on the Newcastle-Ottawa Quality Assessment Scale (NOS) for case-control studies [22]. Each article was judged based on eight items that consider the representativeness of study population, the comparability of cases and controls, and ascertainment of the exposure. High-quality articles can earn up to 9 points (the comparability question gets up to two points). The studies given more than 7 points were considered high quality. More than 5 points were included in the meta-analysis.

2.5. Statistical Analysis. Quantitative meta-analyses were performed using the software Stata 12.0 (Stata Corporation, College Station, TX, USA). OR and 95% CI were meta-analyzed to assess the strength of the association between rosacea and CVDs and susceptibility to major risk factors. For biochemical indicators, the mean and SD were pooled and analyzed for comparison. Heterogeneity was tested based on Cochrane's Q statistic (significant at $p < 0.10$) and the I^2 test (significant at $I^2 > 50\%$). All meta-analyses were performed using a random effects model. To assess the impact of individual studies and to explain heterogeneity, we conducted a one-study removed sensitivity analysis. The risk of publication was assessed using Egger's test. p value of less than 0.05 was considered statistically significant.

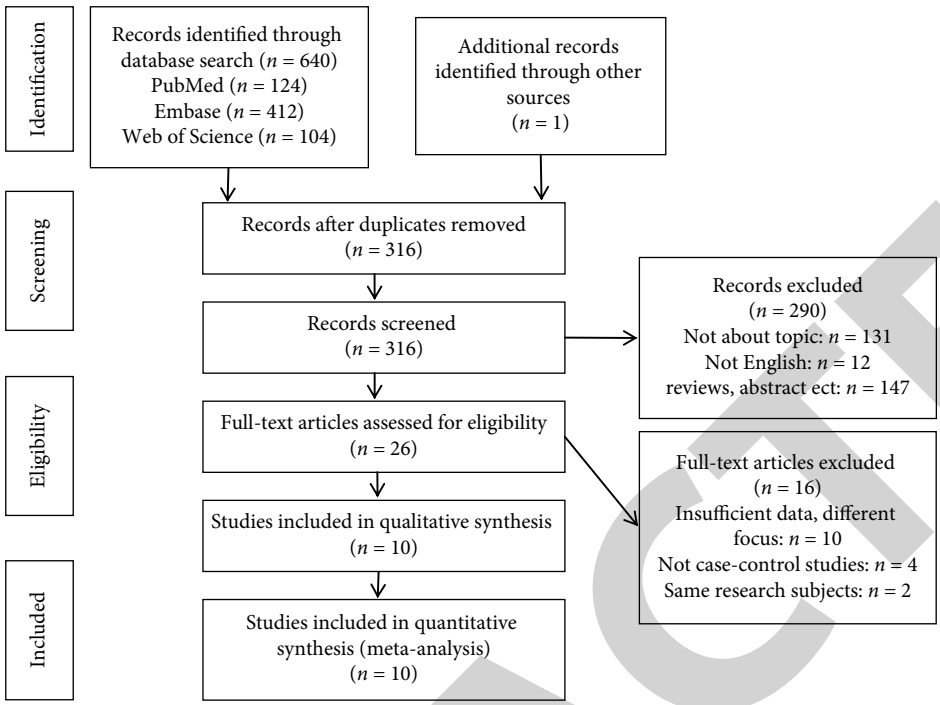

Figure 1: Flow diagram of the literature search and selection process.

3. Results

3.1. Search Results. A total of 641 studies were identified after the initial search. After removing duplicates, 316 potentially eligible records remained. Titles and abstracts of these articles were further screened, resulting in the selection of 26 potential publications. After reviewing the full text of these 26 studies, we selected for the final analysis, ten case-control studies that met the inclusion criteria, with a combined sample size of 97,456 patients (Figure 1).

3.2. Study Characteristics and Quality Assessment. The basic characteristics of the ten studies are shown in Table 1. The studies were published between 2014 and 2019. Four studies were conducted in European countries, two in the United States, and four in Asia. The mean age, which was reported in nine studies, ranged between 44 and 50.63 years. The sample size ranged between 46 and 53,927 patients. The quality assessment of the included studies is summarized in Table 2. Seven of the studies were considered as being of high quality, with a quality score of ≥7 points. Two studies were of moderate quality (7 > score ≥ 5 points).

3.3. Assessment of the Association between Rosacea and CVDs. Five studies, with 97,054 rosacea and 1,546,111 control cases, were included to assess the association between rosacea and the susceptibility for CVDs. The pooled analysis found no association between rosacea prevalence and the susceptibility for overall CVDs (OR 0.97; 95% CI 0.86-1.10) (Figure 2).

3.4. Meta-Analysis of Association between Rosacea and Diseases That Increase the Risk for CVDs. Seven studies, with 95,160 rosacea and 1,542,042 control cases, were included to assess the association between rosacea and the susceptibility to present with risk factors for CVDs. The pooled analysis found a significant association between rosacea and diseases that increase the risk for CVDs (OR 1.17; 95% CI 1.05-1.31). Our results show that for individual risk factors, the prevalence of hypertension (OR 1.17; 95% CI 1.02-1.35), dyslipidemia (OR 1.34; 95% CI 1.00-1.79), and MS (OR 1.72; 95% CI 1.09-2.72) is higher in rosacea patients than in the control group. However, there was no association between rosacea and DM (OR 0.98; 95% CI 0.82-1.16) (Figure 3).

3.5. Meta-Analysis of Association between Rosacea and Biological Indicators for CVD Risk. Four studies, with 337 rosacea cases and 457 controls, were included to assess the association between rosacea and biological indicators for CVD risk. Our results show that the levels of TC (SMD = 0.40; 95% CI = −0.00, 0.81; $p < 0.05$) and LDL-C (SMD = 0.28; 95% CI = 0.01, 0.56; $p < 0.05$) in rosacea patients were higher than those in the control group. However, no differences were found in HDL-C (SMD = 0.00; 95% CI = −0.18, 0.18; $p = 0.968$) and TG (SMD = 0.10; 95% CI = −0.04, 0.24; $p = 0.171$) between the two groups (Figure 4). The pooled results for CRP and hs-CRP showed that both were higher in rosacea patients (SMD = 0.25; 95% CI = 0.10, 0.41; $p < 0.05$), for CRP (MD = 0.37; 95% CI = 0.07, 0.67; $p < 0.05$) and hs-CRP (MD = 0.21; 95% CI = 0.03, 0.40; $p < 0.05$), respectively (Figure 5).

3.6. Sensitivity Analysis and Publication Bias. The result of sensitivity analysis by emitting a single study in each turn showed that there is no substantial change in the results, indicating good robustness of meta-analysis results (Figure 6).

Table 1: Basic characteristics of included studies.

First author, year	Country	Age (mean ± SD)	Rosacea (no.)	Control (no.)	Match factors	Rosacea subtype	Rosacea diagnosis	CVDs and related risk diseases	Reference
Sinikumpu, 2019	Finland	46	146	278	Gender, BMI, and tobacco use	Erythematotelangiectatic, papulopustular, phymatous, and ocular rosacea	ICD-10	N/A	13
Marius, 2019	Romania	47.87 ± 15.11	46	39	Age and gender	Erythematotelangiectatic and papulopustular rosacea	National Rosacea Society criteria	MS, HBP	14
Son, 2018	Korea	47.21 ± 15.01	2,536	1,396,992	N/A	N/A	ICD-10	IS, PAOD, IHD, DLP, DM, HBP	12
Belli, 2017	Turkey	50.63 ± 8.45	85	90	Age, gender, and BMI	Erythematotelangiectatic and papulopustular rosacea	N/A	MS	18
Egeberg, 2016	Denmark	49.2 ± 14.5	4,948	23,823	Age, gender, and calendar time	N/A	ICD-10	CD, MACE, IS, MI, HS, DM, HBP	16
Marshall, 2016	USA	49.1 ± 9.0	2,090	4,263	Age and gender	N/A	ICD-9	CVD,DM,	17
Rainer, 2015	USA	50.6 ± 14.1	65	65	Age, gender, and race	Erythematotelangiectatic, papulopustular, phymatous, and ocular rosacea	National Rosacea Society criteria	MS, HBP	11
Hua, 2015	China, Taiwan	44	33,553	67,106	Age and gender	N/A	ICD-9	IS, PAOD, CAD, DLP, DM, HBP	10
Duman, 2014	Turkey	44.65 ± 12.9	60	50	Age and gender	Erythematotelangiectatic, papulopustular, phymatous, and ocular rosacea	National Rosacea Society criteria	N/A	9
Spoendlin, 2014	UK	N/A	53,927	53,927	Age, gender, general practice, and calendar time	N/A	N/A	IS/TIA, MI, IHD, HF, DLP, DM, HBP	15

BMI: body mass index; N/A: not applicable; CD: cardiovascular death; CVDs: cardiovascular diseases; MACE: major adverse cardiovascular events; IS: ischemic stroke; TIA: transient ischemic attack; PAOD: peripheral atherosclerotic occlusive disease; MI: myocardial infarction; IHD: ischemic heart disease; CAD: coronary artery disease; HS: hemorrhagic stroke; HF: heart failure; HBP: hypertension; DM: diabetes mellitus; DLP: dyslipidemia; MS: metabolic syndrome.

Table 2: Quality assessment of the included studies.

Study	Selection				Comparability	Exposure			Total score
	Adequate definition of the cases	Representativeness of the cases	Selection of controls	Definition of controls	Control of important factors	Ascertainment of exposure	Same method of ascertainment for cases and controls	Nonresponse rate	
Duman, 2014	*	—	—	*	*	*	*	—	5
Belli, 2017	*	*	—	*	**	*	*	—	7
Sinikumpu, 2019	*	*	—	*	**	*	*	—	7
Rainer, 2015	*	*	*	*	**	*	*	—	8
Spoendlin, 2014	*	*	*	*	**	*	*	—	8
Egeberg, 2016	*	*	*	*	**	*	*	—	8
Hua, 2015	*	*	*	*	**	*	*	—	8
Marshall, 2016	*	*	*	*	**	*	*	—	8
Son, 2018	*	*	—	*	—	*	*	—	5
Marius, 2019	*	*	—	*	*	*	*	—	6

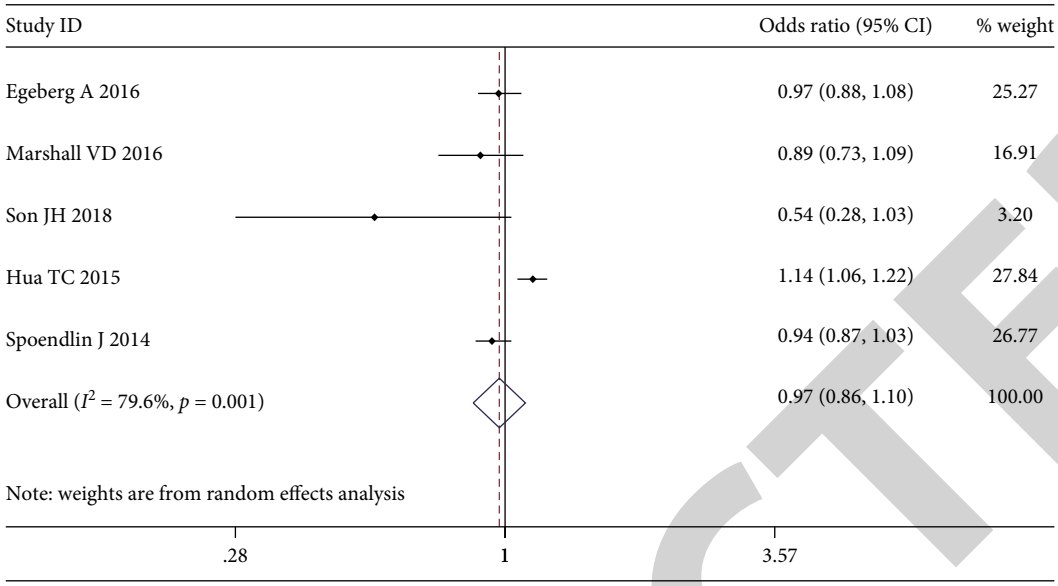

Figure 2: Forest plot of the association between rosacea and overall cardiovascular diseases (CVDs) in case-control studies.

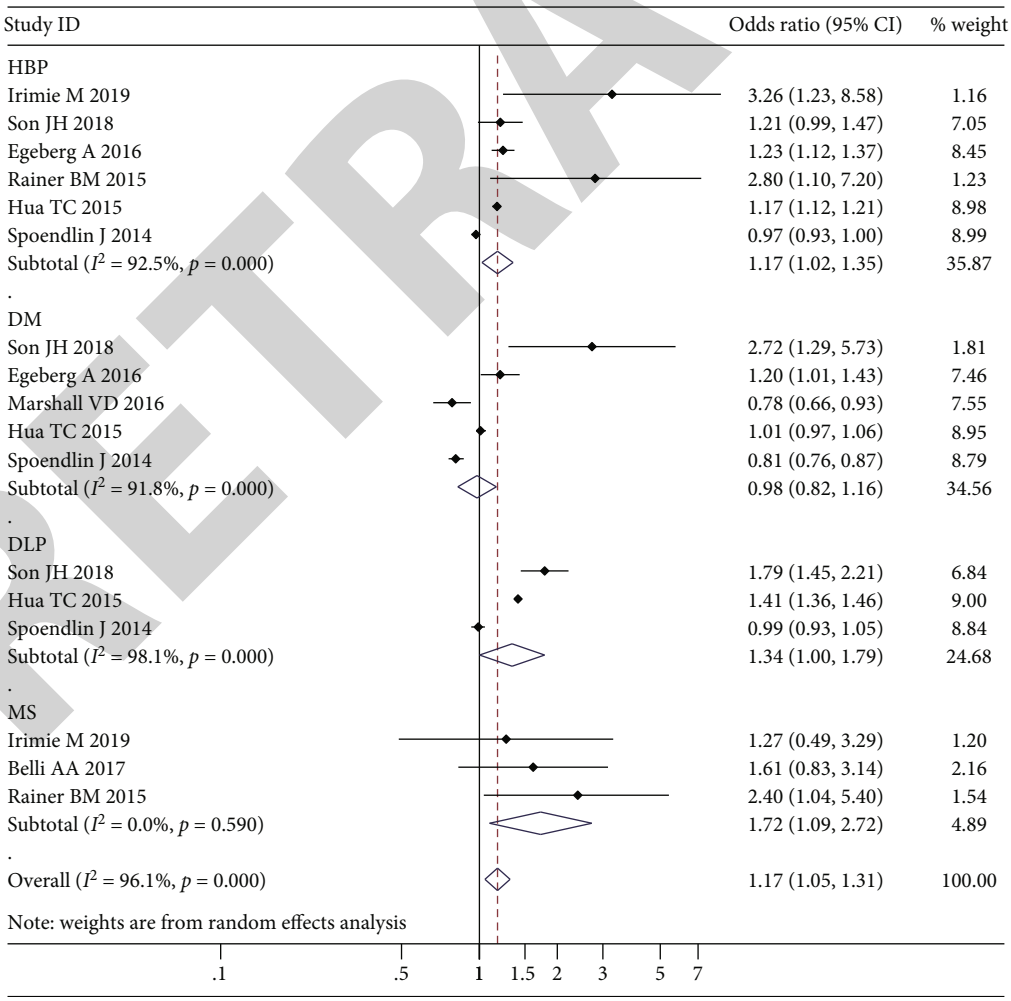

Figure 3: Forest plot of the association between rosacea and cardiovascular disease (CVD) risk factors in case-control studies.

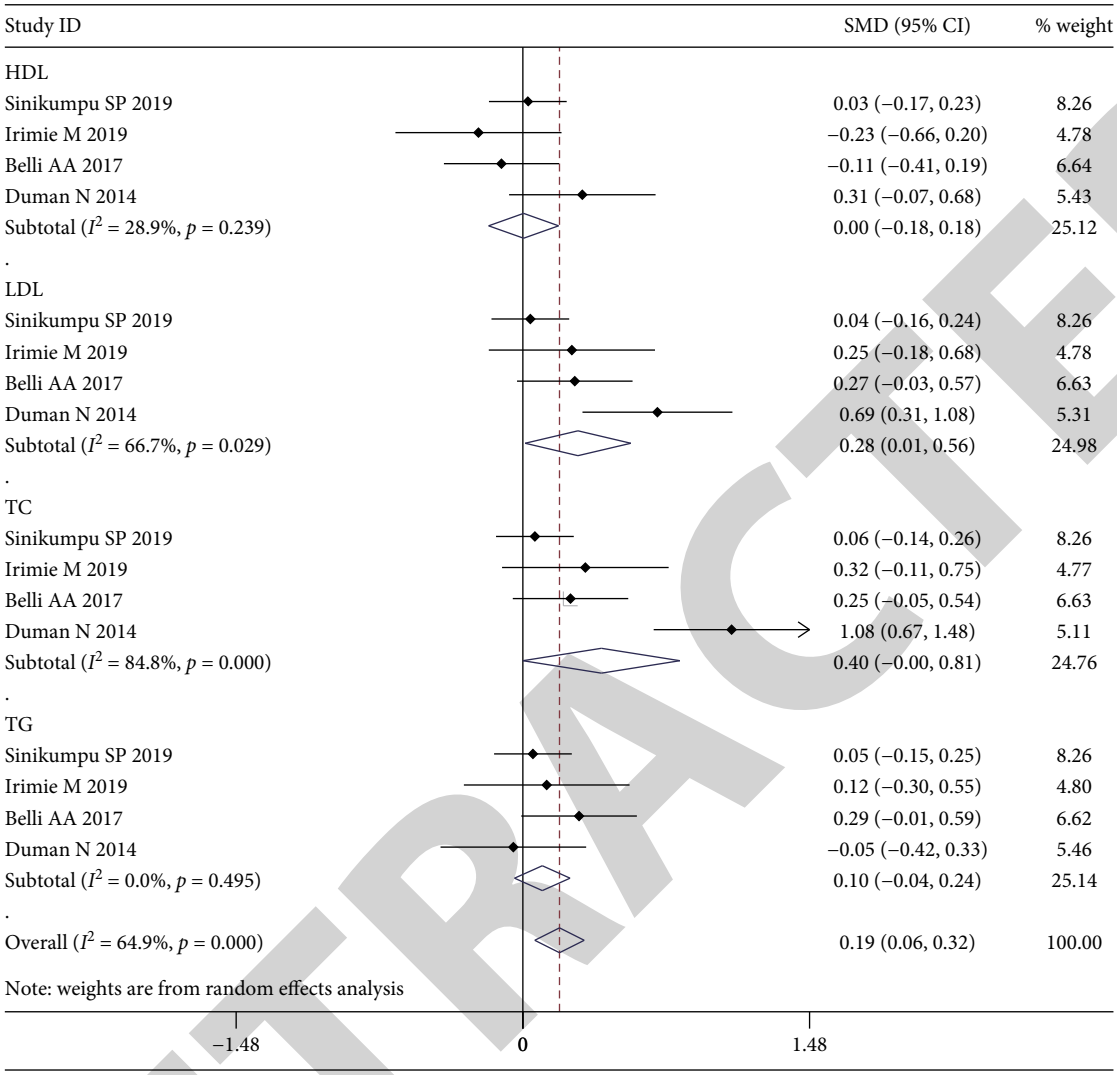

Figure 4: Forest plot of the association between rosacea and lipid metabolism indicators in case-control studies.

No significant publication bias was found ($p = 0.200$) (Figure 7).

4. Discussion

In this meta-analysis study, we found no significant association between rosacea prevalence and the incidence of CVDs (OR 0.97; 95% CI 0.86-1.10). Similarly, a large Danish cohort study of 5,993 rosacea patients found no association between rosacea and CVDs (HR 0.93; 95% CI 0.77-1.12) [23]. Several specific reasons apply to the interpretation of the current results. First, except that one study described a minimum follow-up time of 1 year [17], the remaining four studies [10, 12, 15, 16] did not provide the minimum follow-up time. Therefore, the follow-up period in the included studies may be too short to detect a rise in CVDs, especially for younger patients. Second, the severity levels of rosacea might affect CVD clinical outcomes. A study found that the CVD risk of moderate to severe rosacea was significantly higher than mild rosacea [11]. Furthermore, a meta-analysis study showed that the incidence of CVDs increased only in individuals with severe psoriasis [24]. This association might also be found in rosacea patients. However, few enrolled studies in our meta-analysis provided detailed information on the severity of rosacea in patients. Third, the lack of association might be related to drug intervention. Recently published studies have shown that tetracycline reduces the risk for vascular diseases in patients with rosacea. It is speculated that, as an inhibitor of metalloproteinases, the beneficial effect of tetracycline might be due to its anti-inflammatory properties [25]. Due to the above reasons and the limitations of available data, we believe that this result needs to be interpreted with caution.

We found significantly higher prevalence rates of hypertension, dyslipidemia, and MS among patients with rosacea. It might be related to the chronic inflammation in rosacea. MS is a group of classical cardiovascular risk factors, including central obesity, hypertension, dyslipidemia, and glucose intolerance/type 2 diabetes. Systemic inflammation is assumed to promote the development of MS [26]. Underlying inflammation and dysfunction of the arterial wall in rosacea might explain the development of hypertension [27].

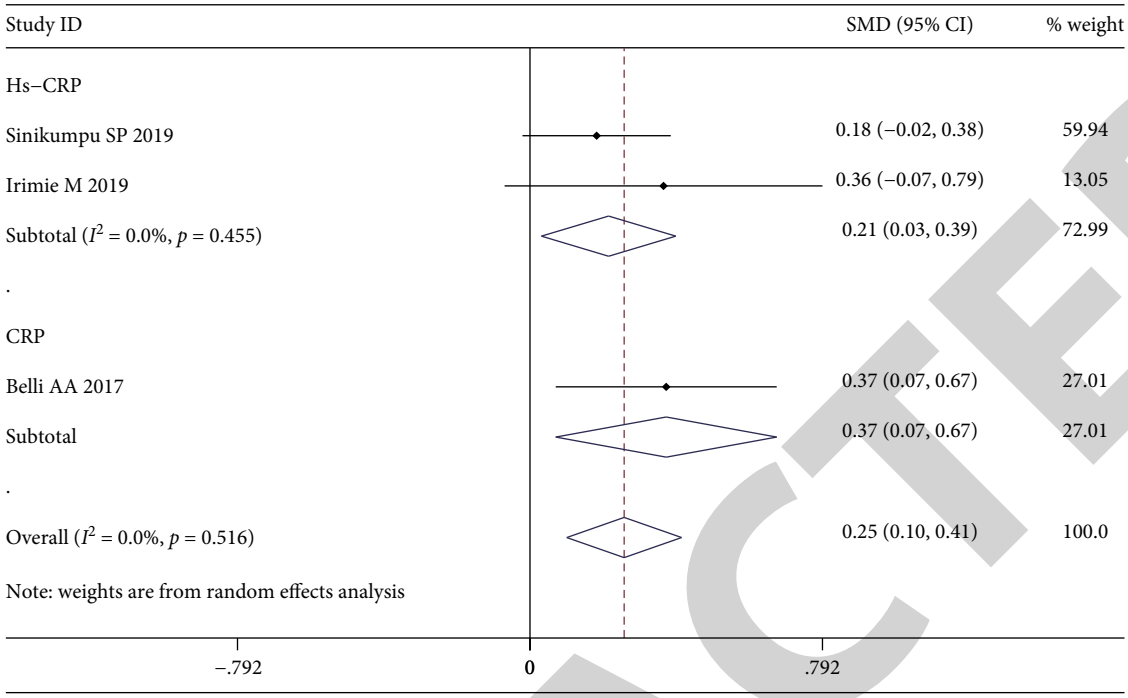

Figure 5: Forest plot of the association between rosacea and C-reactive protein (CRP) in case-control studies.

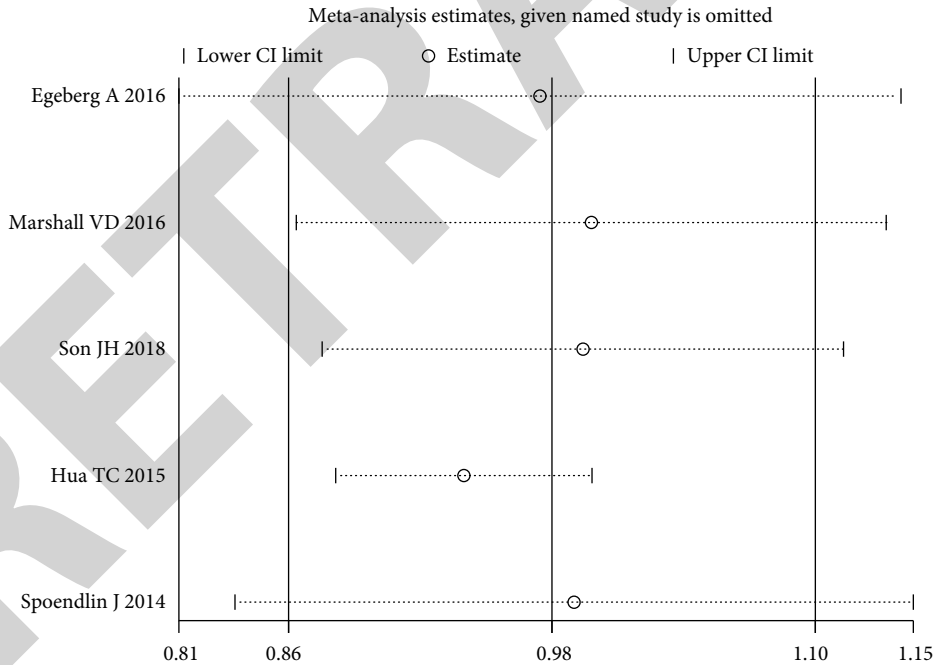

Figure 6: Sensitivity analysis for primary outcome.

From a different perspective, it was hypothesized that calcium channel blockers (CCBs) trigger rosacea. This assumption was based on the fact that CCB triggers the flushing reaction. However, a large observational case-control study found no association between either ACEIs or ARBs and the risk for rosacea [15]. The effect of antihypertensive drugs on rosacea needs further research. As for dyslipidemia, it is known that systemic inflammation can cause structural changes in lipoproteins, which negatively affect their ability to eliminate cholesterol [28]. Another cause might be associated with the decrease in paraoxonase-1 (PON1) level, an HDL-associated antioxidant enzyme. Lower serum PON1 activity has been demonstrated in both dyslipidemic patients and rosacea patients [29]. However, we did not find a significant association between DM and rosacea. A previous study suggested that patients with advanced DM have a reduced

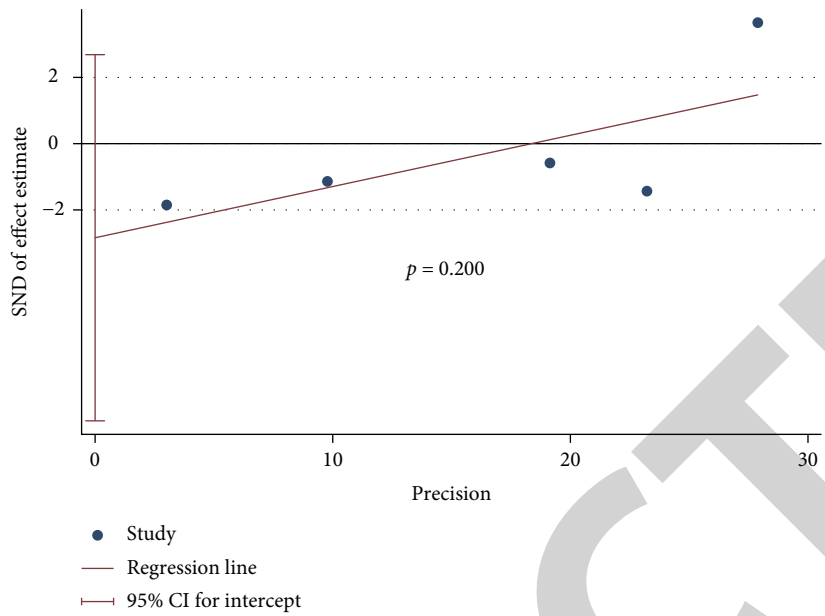

Figure 7: Publication bias based on Egger's test.

risk for rosacea because advanced DM is often accompanied by impaired vasodilation, whereas one of rosacea's key characteristics is vasodilation [30].

Furthermore, we found a significant association between rosacea and both CPR and hs-CRP. A test for hs-CRP is usually used to measure low-grade inflammation. Such inflammation is a chronic, subclinical, and systemic condition that contributes to the pathogenesis of many noncommunicable diseases like atherosclerosis. Both clinical and experimental studies have confirmed the important role of inflammation in the pathogenesis of rosacea [31]. A cross-sectional study found that hs-CRP was higher in patients with rosacea than in those with no skin disease ($p = 0.001$) [32]. All these indicate that, in analogy to psoriasis [33], the low-grade inflammation in rosacea might be systemic.

Recently, much attention has been paid to studying the role of lipid metabolism in rosacea patients. Transcriptome analysis of rosacea patients demonstrated significant upregulation of genes related to alcohol and lipid metabolism and sebaceous gland regulation [4]. We found a significant association between rosacea and the levels of TC and LDL-C, but no association with HDL-C or TG. In the bloodstream, cholesterol is transported as various lipoproteins, primarily LDLs. LDL-C is a generally acknowledged risk factor for atherosclerotic cardiovascular disease (ASCVD) [6]. One study found that a decrease in LDL-C was directly associated with a decrease in the risk for major vascular diseases. Such a proportional reduction was noted irrespective of the baseline LDL-C concentration [34]. Therefore, monitoring and controlling total cholesterol levels in patients with rosacea, especially the concentration of LDL-C, are likely to have cardiovascular benefits. HDL-C was once considered to be beneficial because of its ability to transport cholesterol to the liver for metabolism and its inverse relationship with the risk for developing CVDs. However, given that no benefit has been observed following clinical applications, the functional quality of HDL-C needs further study [35]. Taken together, we found that there may be a correlation between rosacea and abnormal lipid metabolism, although the cause-effect relationship is unclear. This prompts us to be alert to lipid metabolic disorder and related complications in patients with rosacea.

Our study has some limitations. First, heterogeneity and other confounding factors might have affected our findings. The results should, therefore, be interpreted with caution. Second, it would have been interesting to evaluate the association between different severity levels of rosacea or its different phenotypes and CVDs and related risk factors. This, however, was not possible due to the limited data. Third, the case-control design of the included studies makes it impossible to fully evaluate the cause-effect relationships.

5. Conclusion

The present meta-analysis indicates that although no significant association was found between rosacea and CVDs, rosacea was found to be associated with several CVD risk factors. Patients with rosacea need to pay more attention to identifiable risk factors, especially those related to inflammatory and metabolic disorders. A comprehensive understanding of the incidence of risk factors for CVDs in rosacea patients can inform future preventive practices and treatment recommendations. Therefore, it is necessary to conduct prospective studies to determine whether patients with rosacea should more closely monitor the known CVD risk factors.

Data Availability

All the underlying data in the article are available online.

Conflicts of Interest

The authors declare no conflicts of interest.

Authors' Contributions

Yanmei Li and Linghong Guo contributed equally to this work.

References

[1] J. Tan, L. M. C. Almeida, A. Bewley et al., "Updating the diagnosis, classification and assessment of rosacea: recommendations from the global ROS acea CO nsensus (ROSCO) panel," *The British Journal of Dermatology*, vol. 176, no. 2, pp. 431–438, 2017.

[2] L. Gether, L. K. Overgaard, A. Egeberg, and J. P. Thyssen, "Incidence and prevalence of rosacea: a systematic review and meta-analysis," *The British Journal of Dermatology*, vol. 179, no. 2, pp. 282–289, 2018.

[3] A. D. Holmes, J. Spoendlin, A. L. Chien, H. Baldwin, and A. L. S. Chang, "Evidence-based update on rosacea comorbidities and their common physiologic pathways," *Journal of the American Academy of Dermatology*, vol. 78, no. 1, pp. 156–166, 2018.

[4] M. Steinhoff, J. Schauber, and J. J. Leyden, "New insights into rosacea pathophysiology: a review of recent findings," *Journal of the American Academy of Dermatology*, vol. 69, no. 6, pp. S15–S26, 2013.

[5] S. H. Lee, S. B. Lee, J. H. Heo et al., "Sebaceous glands participate in the inflammation of rosacea," *Journal of the European Academy of Dermatology and Venereology*, vol. 34, no. 3, 2019.

[6] P. Libby, J. E. Buring, L. Badimon et al., "Atherosclerosis," *Nature reviews Disease primers*, vol. 5, no. 1, 2019.

[7] F. Mach, C. Baigent, A. L. Catapano et al., "2019 Esc/Eas guidelines for the management of dyslipidaemias: lipid modification to reduce cardiovascular risk: The Task Force for the management of dyslipidaemias of the European Society of Cardiology (ESC) and European Atherosclerosis Society (EAS)," *European Heart Journal*, vol. 41, no. 1, pp. 111–188, 2020.

[8] R. Haber and M. El Gemayel, "Comorbidities in rosacea: a systematic review and update," *Journal of the American Academy of Dermatology*, vol. 78, no. 4, pp. 786–792.e8, 2018.

[9] N. Duman, S. Ersoy Evans, and N. Atakan, "Rosacea and cardiovascular risk factors: a case control study," *Journal of the European Academy of Dermatology and Venereology*, vol. 28, no. 9, pp. 1165–1169, 2014.

[10] T.-C. Hua, P.-I. Chung, Y.-J. Chen et al., "Cardiovascular comorbidities in patients with rosacea: A nationwide case-control study from Taiwan," *Journal of the American Academy of Dermatology*, vol. 73, no. 2, pp. 249–254, 2015.

[11] B. M. Rainer, A. H. Fischer, D. Luz Felipe da Silva, S. Kang, and A. L. Chien, "Rosacea is associated with chronic systemic diseases in a skin severity- dependent manner: Results of a case-control study," *Journal of the American Academy of Dermatology*, vol. 73, no. 4, pp. 604–608, 2015.

[12] J. H. Son, B. Y. Chung, M. J. Jung, Y. W. Choi, H. O. Kim, and C. W. Park, "The risk of rosacea according to chronic diseases and medications: a 5-year retrospective, multi-institutional case-control study," *Annals of Dermatology*, vol. 30, no. 6, pp. 676–687, 2018.

[13] S. Sinikumpu, J. Jokelainen, J. Auvinen et al., "Increased risk of cardiovascular diseases in female rosacea patients: a nested case-control study," *Acta Dermato Venereologica*, vol. 99, no. 7, pp. 705-706, 2019.

[14] I. Marius, "Rosacea and cardiovascular risk factors," *Dermatovenoerologia*, vol. 64, no. 2, pp. 7–14, 2019.

[15] J. Spoendlin, J. J. Voegel, S. S. Jick, and C. R. Meier, "Antihypertensive drugs and the risk of incident rosacea," *British Journal of Dermatology*, vol. 171, no. 1, pp. 130–136, 2014.

[16] A. Egeberg, P. R. Hansen, G. H. Gislason, and J. P. Thyssen, "Assessment of the risk of cardiovascular disease in patients with rosacea," *Journal of the American Academy of Dermatology*, vol. 75, no. 2, pp. 336–339, 2016.

[17] V. D. Marshall, F. Moustafa, S. D. Hawkins, R. Balkrishnan, and S. R. Feldman, "Cardiovascular disease outcomes associated with three major inflammatory dermatologic diseases: a propensity-matched case control study," *Dermatology and Therapy*, vol. 6, no. 4, pp. 649–658, 2016.

[18] A. A. Belli and I. Altun, "Assessment of Framingham risk score and systemic coronary risk evaluation in rosacea patients," *Dermatologica Sinica*, vol. 35, no. 3, pp. 127–130, 2017.

[19] Y. Hayran, I. Lay, M. C. Mocan, T. Bozduman, and S. Ersoy-Evans, "Vascular endothelial growth factor gene polymorphisms in patients with rosacea: a case-control study," *Journal of the American Academy of Dermatology*, vol. 81, no. 2, pp. 348–354, 2019.

[20] K. Edfeldt, B. Agerberth, M. E. Rottenberg et al., "Involvement of the antimicrobial peptide Ll-37 in human atherosclerosis," *Arteriosclerosis, Thrombosis, and Vascular Biology*, vol. 26, no. 7, pp. 1551–1557, 2006.

[21] B. C. Melnik, "Endoplasmic reticulum stress: key promoter of rosacea pathogenesis," *Experimental Dermatology*, vol. 23, no. 12, pp. 868–873, 2014.

[22] G. A. Wells, B. Shea, D. O'Connell et al., *The Newcastle-Ottawa Scale (Nos) for assessing the quality of nonrandomised studies in meta-analysis*, 2006, http://www.ohri.ca/programs/clinical_epidemiology/oxford.asp.

[23] A. Egeberg, J. F. Fowler Jr., G. H. Gislason, and J. P. Thyssen, "Nationwide assessment of cause-specific mortality in patients with rosacea: a cohort study in Denmark," *American Journal of Clinical Dermatology*, vol. 17, no. 6, pp. 673–679, 2016.

[24] E. J. Samarasekera, J. M. Neilson, R. B. Warren, J. Parnham, and C. H. Smith, "Incidence of cardiovascular disease in individuals with psoriasis: a systematic review and meta-analysis," *The Journal of Investigative Dermatology*, vol. 133, no. 10, pp. 2340–2346, 2013.

[25] J. R. Dosal, G. L. Rodriguez, C. F. Pezon, H. Li, and J. E. Keri, "Effect of tetracyclines on the development of vascular disease in veterans with acne or rosacea: a retrospective cohort study," *The Journal of Investigative Dermatology*, vol. 134, no. 8, pp. 2267–2269, 2014.

[26] K. G. Alberti, K. G. M. M. Alberti, P. Zimmet, and J. Shaw, "The metabolic syndrome–a new worldwide definition," *The Lancet*, vol. 366, no. 9491, pp. 1059–1062, 2005.

[27] N. Idris-Khodja, M. O. R. Mian, P. Paradis, and E. L. Schiffrin, "Dual opposing roles of adaptive immunity in hypertension," *European Heart Journal*, vol. 35, no. 19, pp. 1238–1244, 2014.

[28] P. Libby, P. M. Ridker, and A. Maseri, "Inflammation and atherosclerosis," *Circulation*, vol. 105, no. 9, pp. 1135–1143, 2002.

[29] S. K. Kota, S. K. Kota, S. V. S. Krishna, L. K. Meher, K. D. Modi, and S. Jammula, "Implications of serum paraoxonase activity

Hindawi
BioMed Research International
Volume 2020, Article ID 4532482, 9 pages
https://doi.org/10.1155/2020/4532482

Research Article

Preventive Effects of Kaempferol on High-Fat Diet-Induced Obesity Complications in C57BL/6 Mice

Tieqiao Wang,[1] **Qiaomin Wu**,[2] **and Tingqi Zhao**[1]

[1]*The Affiliated Hospital of Medical School, Ningbo University, Ningbo, Zhejiang, China*
[2]*Endocrinology Department, First Affiliated Hospital of Zhejiang Chinese Medical University, Hangzhou, Zhejiang, China*

Correspondence should be addressed to Tieqiao Wang; fywangtieqiao@nbu.edu.cn

Received 22 February 2020; Accepted 16 March 2020; Published 7 April 2020

Academic Editor: Gang Liu

Kaempferol is a dietary flavanol that regulates cellular lipid and glucose metabolism. Its mechanism of action in preventing hepatic steatosis and obesity-related disorders has yet to be clarified. The purpose of this research was to examine kaempferol's antiobesity effects in high-fat diet- (HFD-) fed mice and to investigate its impact on their gut microbiota. Using a completely randomized design, 30 mice were equally assigned to a control group, receiving a low-fat diet, an HFD group, receiving a high-fat diet, and an HFD+kaempferol group, receiving a high-fat diet and kaempferol doses of 200 mg/kg in the diet. After eight weeks, the HFD mice displayed substantial body and liver weight gain and high blood glucose and serum cholesterol levels. However, treatment with kaempferol moderated body and liver weight gain and elevation of blood glucose and serum cholesterol and triglyceride levels. Examination of 16S ribosomal RNA showed that HFD mice exhibited decreased microbial diversity, but kaempferol treatment maintained it to nearly the same levels as those in the control group. In conclusion, kaempferol can protect against obesity and insulin resistance in mice on a high-fat diet, partly through regulating their gut microbiota and moderating the decrease in insulin resistance.

1. Introduction

Obesity is the result of the accumulation of excessive amounts of fat in adipose tissue. Obesity is linked to many risk factors, including cardiovascular diseases, hypertension, hepatic steatosis, insulin resistance, and dyslipidemia [1, 2]. The prevalence of obesity and associated metabolic disorders (e.g., type 2 diabetes mellitus and cardiovascular diseases) has increased considerably in the last century, not only in developed but also in developing countries [3]. Rat studies indicate that long-term intake of a high-fat diet (HFD) can lead to impaired lipid metabolism, as indicated by elevated total cholesterol (TC), triglyceride (TG), and low-density lipoprotein (LDL) levels [4]. In addition to the disruption of lipid metabolism, low-grade chronic inflammation has been identified as a potential mechanism of obesity-related conditions [5].

It has been hypothesized that excessive accumulation of adipose tissue is a precursor to the production of proinflammatory cytokines, which can lead to hypertension and insulin resistance [6]. Moreover, data from both human and animal studies suggest a close connection between the emergence of an obese phenotype and the gut microbiome. The microbiota of obese mice is marked by an increase in the relative abundance of Firmicutes and a decrease in Bacteroidetes [7]. The literature suggests that substantial changes occur in the composition of the gut microbiota within 24 h of a switch to an HFD [8]. Presently, various medications are administered to prevent, treat, and manage obesity. However, pharmacological agents of this kind are associated with adverse side effects and are not always effective [9]. In view of this, many scholars have focused their efforts on developing novel therapeutic agents for obesity-related complications.

Polyphenols have attracted considerable interest in recent years owing to their potential use in the management of diabetes [10, 11]. As secondary plant metabolites, polyphenolic compounds are the principal source of dietary antioxidants for humans, in whom the normal intake of polyphenols is approximately 1 g per day [12]. Noteworthily, robust

research findings indicate that dietary polyphenols mitigate HFD-induced obesity by regulating the gut microbiota [13, 14].

Kaempferol (3,5,7-trihydroxy-2-(4-hydroxyphenyl)-4H-1-benzopyran-4-one) is a flavanol that has been identified in a variety of edible plants and traditional medicines. Studies suggest that it may be an effective agent against obesity [15, 16]. In a study involving HFD obese mice, the administration of kaempferol in daily doses of 50 mg/kg was associated with significant improvements in blood glucose control, which were in turn attributed to reduced hepatic glucose production and enhanced whole-body insulin sensitivity [16]. Significantly, no alterations were observed in terms of body weight gain, adiposity, or food consumption. However, the mechanism of action that underpins the antiobesity activity of this flavanol is not yet understood.

With the above considerations in mind, the purpose of this study was to identify notable metabolites and to investigate the potential preventive mechanism of action associated with kaempferol in HFD-induced obesity in C57BL/6 mice.

2. Materials and Methods

2.1. Animal Care and Experimental Design. Approval was obtained from Zhejiang Traditional Chinese Hospital's Animal Use and Welfare Committee. Thirty C57BL/6 mice aged nine weeks were procured from Nanjing University's Model Animal Research Center, stored in standard, pathogen-free conditions (temperature: 22 ± 2°C; relative humidity: 50 ± 5 %; and 12 h light/dark cycles), and provided with water and food *ad libitum*.

Using a completely randomized design, each mouse was assigned to one of the following three groups ($n = 10$ each): a control group, receiving a low-fat diet; an HFD group, receiving a high-fat diet; and an HFD+kaempferol group, receiving a high-fat diet and 200 mg/kg kaempferol in the diet. The low-fat diet consisted of 10% (kcal%) fat, 20% protein, and 70% carbohydrate, whereas the HFD consisted of 45% fat, 20% protein, and 35% carbohydrate (Research Diets, Inc., New Brunswick, NJ, USA). The experimental period was eight weeks.

Upon completion of the experiment, the mice were subjected to fasting for 4 h, after which blood samples were taken from the retro-orbital sinus. After cervical dislocation, the inguinal white adipose tissue (iWAT), perirenal white adipose tissue (pWAT), epididymal white adipose tissue (eWAT), and finally the liver were weighed.

2.2. Biochemical Analysis. The blood samples were centrifuged at 3,000 rpm at 4°C for 10 min to obtain serum. A Beckman CX4 biochemical analyzer (Beckman Coulter, Brea, CA, USA) and kits manufactured by Roche (Basel, Switzerland) were used to measure serum triglyceride (TG), glucose, high-density lipoprotein (HDL), low-density lipoprotein (LDL), and total cholesterol (TC) levels.

2.3. Glucose and Insulin Tolerance Measurements. A Glucometer Elite (Bayer, Leverkusen, Germany) was used to measure blood glucose levels in blood obtained from the tail vein. For the glucose tolerance tests (GTT), blood glucose was measured 0, 15, 30, 60, and 120 min after administration of bolus intraperitoneal glucose in a dose of 2 g/kg to mice subjected to overnight fasting (12 h). For the insulin tolerance tests (ITT), blood glucose was measured 0, 15, 30, 60, and 90 min after administration of an intraperitoneal injection of regular human insulin in a dose of 0.80 U/kg to mice subjected to fasting for 6 h. The homeostasis model assessment of the insulin resistance index was calculated according to the following standard formula: basal glucose (mM) and basal insulin (mU/L)/22.5.

2.4. Gut Microbiota Analysis. A QIAamp DNA Stool Mini Kit (Qiagen, Duesseldorf, Germany) was used to extract total DNA from fecal samples according to the manufacturer's instructions (QIAamp DNA Stool Handbook, 04/2010). A MiSeq instrument (Illumina Inc., San Diego, CA, USA) was used by Majorbio (Shanghai, China) to perform 16S ribosomal RNA (rRNA) high-throughput sequencing. Amplification of the variable regions V3-V4 of the 16S rRNA genes was performed with barcode-indexed primers 338F and 806R. The forward and reverse primer sequences were 5′-ACTC CTACGGGAGGCAGCA-3′ and 5′-GGACTACHVGGGT WTCTAAT-3′, respectively. A 2% gel extraction kit (AxyPrep DNA Gel Extraction Kit; Axygen Biosciences, Union City, CA, USA) was used to purify the amplicons according to the manufacturer's instructions. Polymerase chain reaction (PCR) product concentrations were assessed with a QuantiFluor™-ST (Promega, Madison, WI, USA), and product normalization was performed at equimolar concentrations with paired-end sequencing (2 × 250) using the MiSeq platform (Illumina Inc.) according to standard protocols. After sequencing, raw data splicing and filtration were performed to obtain cleaned data. Operational taxonomic unit (OTU) clustering and species classification were performed to acquire information about the species present and their abundance distribution.

2.5. Statistical Analysis. One-way analysis of variance (ANOVA) using SAS 8.2 for Windows (SAS Inc., Cary, NC, USA) was applied for the statistical tests. Differences between the means of each group were comparatively examined with the Duncan multiple comparison test and unpaired t-tests. The values were expressed as mean ± standard deviation. A value of $P < 0.05$ was considered the cutoff of statistical significance.

3. Results

3.1. Kaempferol Moderated Adipose Accumulation in HFD Mice. Measurements of the body weight, liver, iWAT, eWAT, and pWAT were performed to assess the impact of kaempferol on HFD mice. As shown in Figures 1(a) and 1(b), the body and liver weight gain of HFD mice was higher than that of the control group ($P < 0.05$). However, it was lower in the HFD+kaempferol group than in the HFD group ($P < 0.05$). As shown in Figures 1(c)–1(h), the iWAT, eWAT, and pWAT were significantly

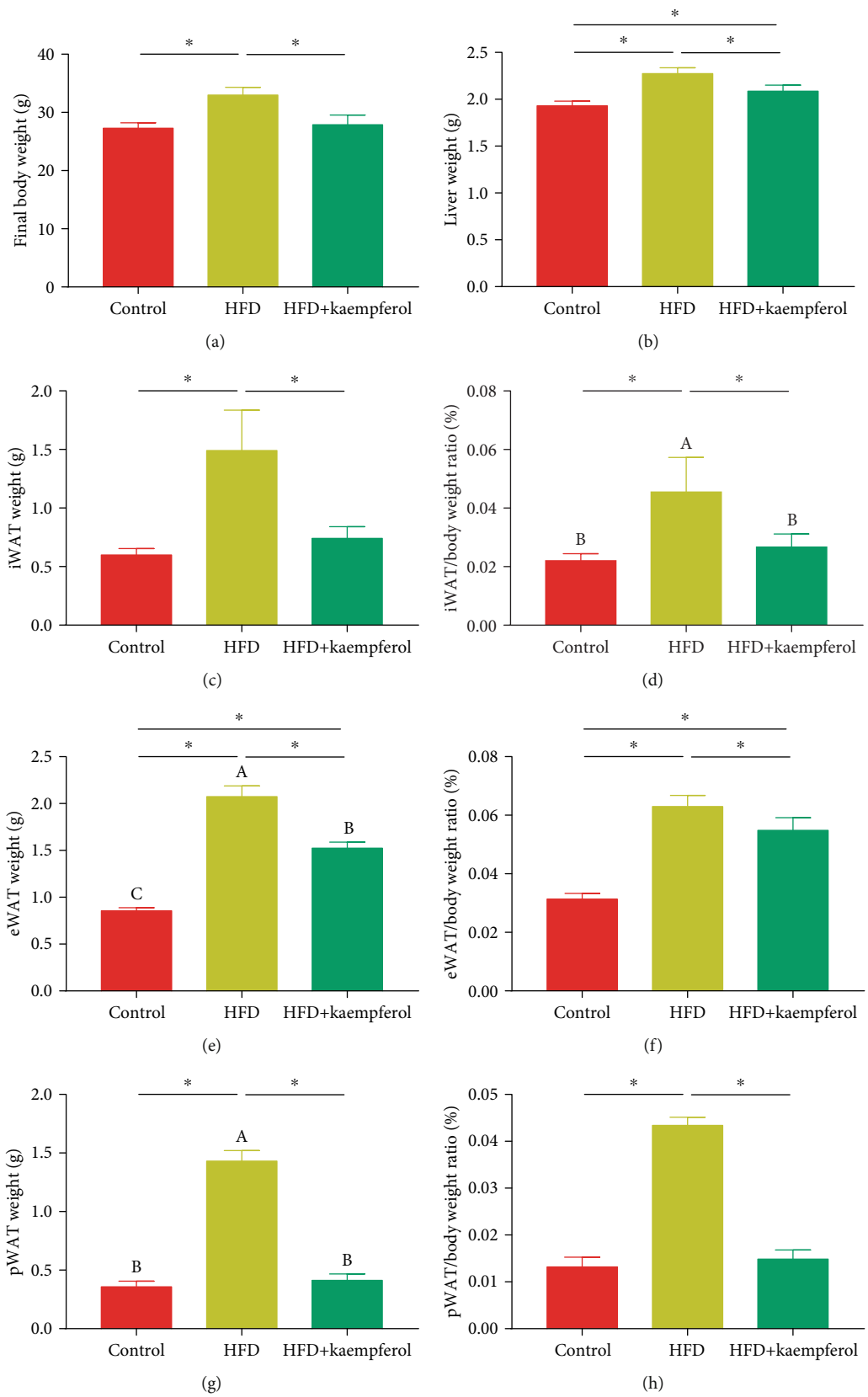

Figure 1: Body, liver, and adipose tissue weight measurements in the control, HFD, and HFD+kaempferol groups. The mice were randomly assigned to a control group, receiving a low-fat diet, an HFD group, receiving an HFD, and an HFD+kaempferol group, receiving an HFD and 200 mg/kg kaempferol ($n = 10$ each). (a) Body weight, (b) liver weight, (c) iWAT weight, (d) iWAT/body weight ratio, (e) eWAT weight, (f) eWAT/body weight ratio, (g) pWAT weight, and (h) pWAT/body weight ratio. Values are expressed as mean ± standard deviation. $^{*}P < 0.05$.

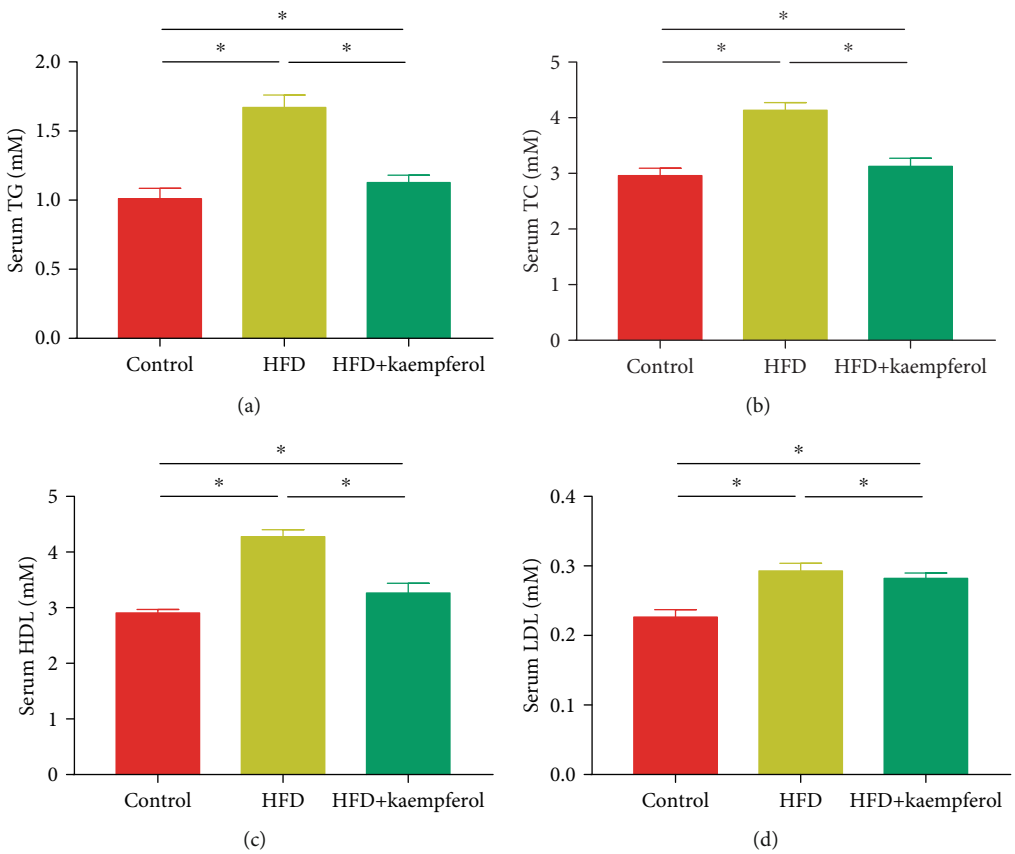

Figure 2: Serum concentrations of (a) total cholesterol (TC), (b) triglycerides (TG), (c) high-density lipoprotein (HDL), and (d) low-density lipoprotein (LDL) in the control, HFD, and HFD+kaempferol groups. Values are expressed as mean ± standard deviation (SD). $^{*}P < 0.05$.

heavier in the HFD mice compared to the control group ($P < 0.05$) but weighed less in the HFD+kaempferol group than in the HFD group ($P < 0.05$).

3.2. Kaempferol Ameliorated Hyperlipidemia in HFD Mice. To examine the effect of kaempferol on the amelioration of hyperlipidemia, the concentrations of serum parameters were measured. Figure 2 shows that serum TC, TG, HDL, and LDL concentrations were higher in the HFD mice compared to the control group ($P < 0.05$). However, kaempferol treatment led to significantly lower serum TC, TG, HDL, and LDL concentrations in the HFD+kaempferol group compared to the HFD group ($P < 0.05$).

3.3. Kaempferol Improved Glucose Tolerance and Insulin Resistance in HFD Mice. Given that obesity is linked to insulin resistance and glucose tolerance, an analysis of the concentrations of fasting blood glucose was performed. Figure 3 shows that kaempferol supplementation kept fasting blood glucose to near-normal levels. Furthermore, intravenous glucose and insulin tolerance tests, paired with the corresponding values associated with the area under the curve, demonstrated that kaempferol led to less severe impairment of glucose tolerance and insulin resistance in the HFD +kaempferol group than in the HFD group.

3.4. Kaempferol Maintained Microbial Diversity and Altered Microbial Communities in HFD Mice. The impact of kaempferol on gut microbiota compositions was assessed by sequencing the bacterial 16S rRNA V3-V4 region. Figure 4 shows that gut microbiota diversity was lower in the HFD group than in the control group, as demonstrated by the higher Shannon indices in the latter ($P < 0.05$). Interestingly, the Shannon index in the HFD+kaempferol group was at the same level as that in the control group ($P < 0.05$). The total microbial compositions in the experimental groups at the phylum and genus levels are shown in Figures 4(b)–4(e) and 4(f)–4(k), respectively. The four main phyla in the three groups were Bacteroidetes, Firmicutes, Proteobacteria, and Verrucomicrobia (Figure 4(b)). Firmicutes were more abundant in the HFD group than in the control group ($P < 0.05$) and significantly less abundant in the HFD+kaempferol group than in the HFD group ($P < 0.05$). Conversely, Bacteroidetes and Proteobacteria were less abundant in the HFD group than in the control group ($P < 0.05$) and significantly more abundant in the HFD+kaempferol group than in the HFD group ($P < 0.05$). Moreover, Proteobacteria were significantly more abundant in the HFD+kaempferol group than in the control group ($P < 0.05$). Comparisons at the genus level revealed that *Akkermansia*, *Bacteroides*, and *Lactobacillus* were less abundant in the HFD group than in the control group

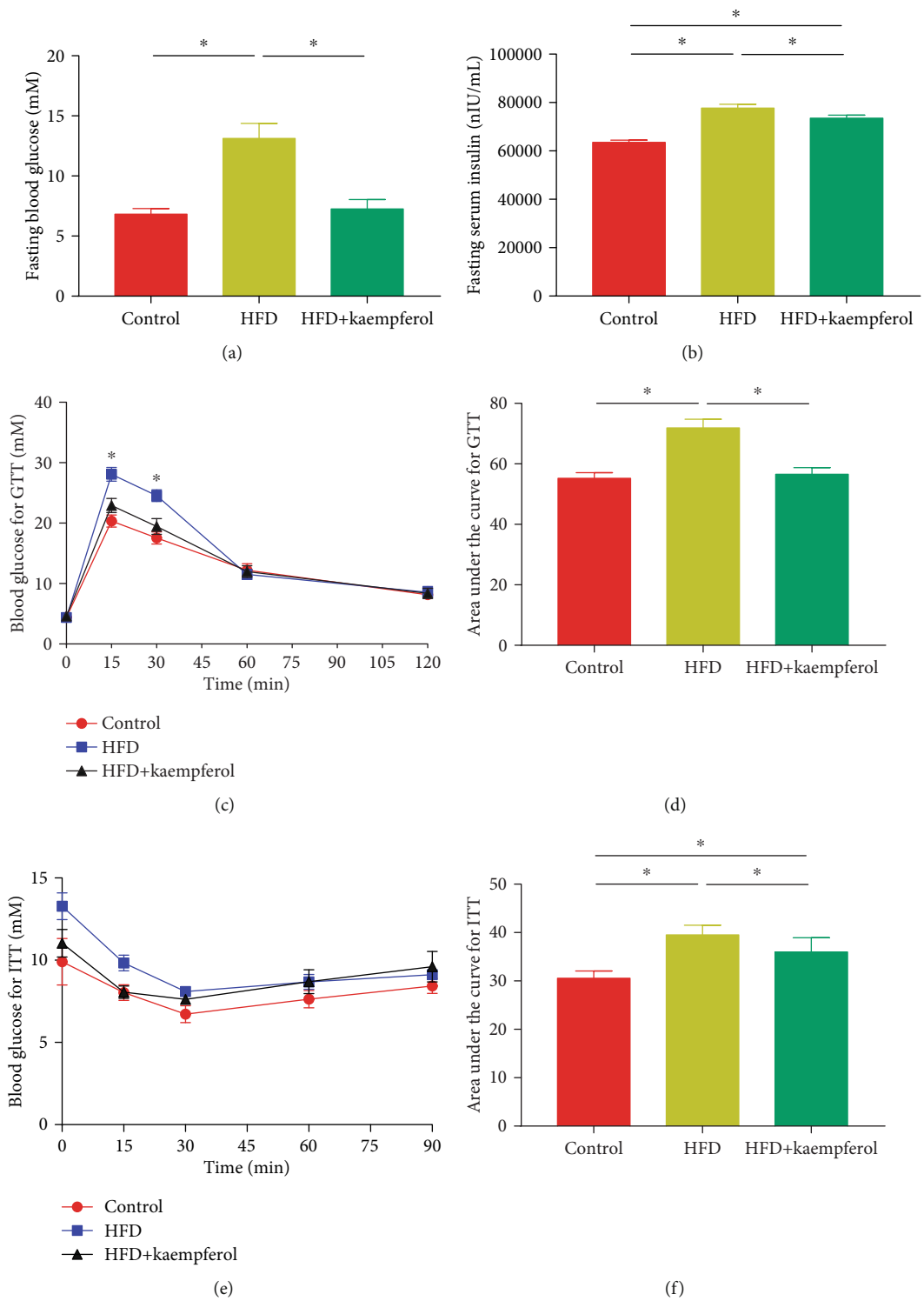

FIGURE 3: Serum concentrations of (a) blood glucose and (b) insulin, (c) curves of blood glucose levels, (d) calculated area under the curve for intravenous glucose tolerance tests (IGTT), (e) curves of blood glucose levels, and (f) calculated area under the curve for insulin tolerance tests in the control, HFD, and HFD+kaempferol groups. Values are expressed as mean ± standard deviation. $^{*}P < 0.05$.

($P < 0.05$) and significantly more abundant in the HFD +kaempferol group than in the HFD group ($P < 0.05$). In addition, *Akkermansia* was more abundant in the HFD +kaempferol group than in the control group ($P < 0.05$). Unclassified genera were more abundant in the HFD group than in the control group ($P < 0.05$) and significantly less abundant in the HFD+kaempferol group than in the HFD group ($P < 0.05$).

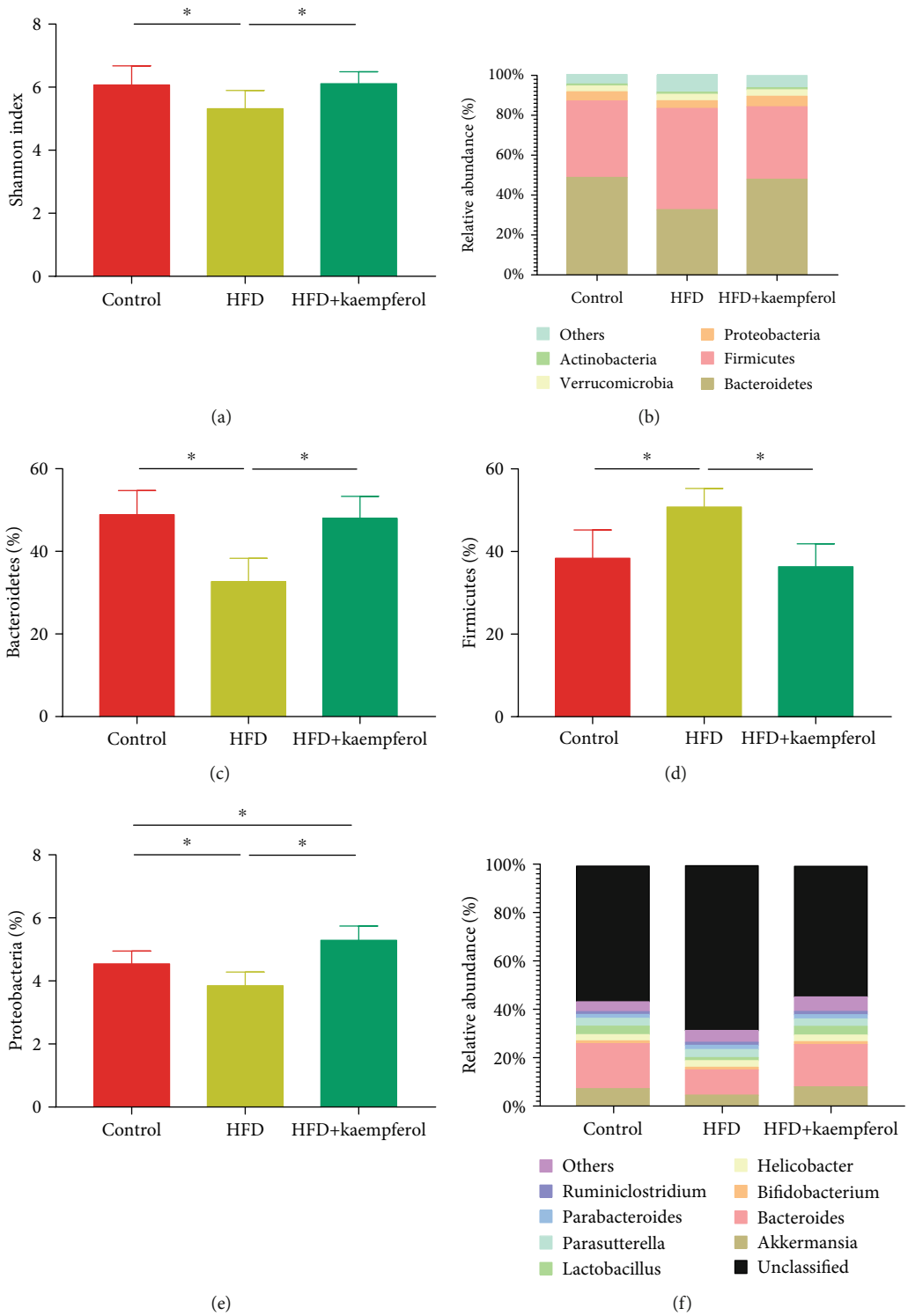

Figure 4: Continued.

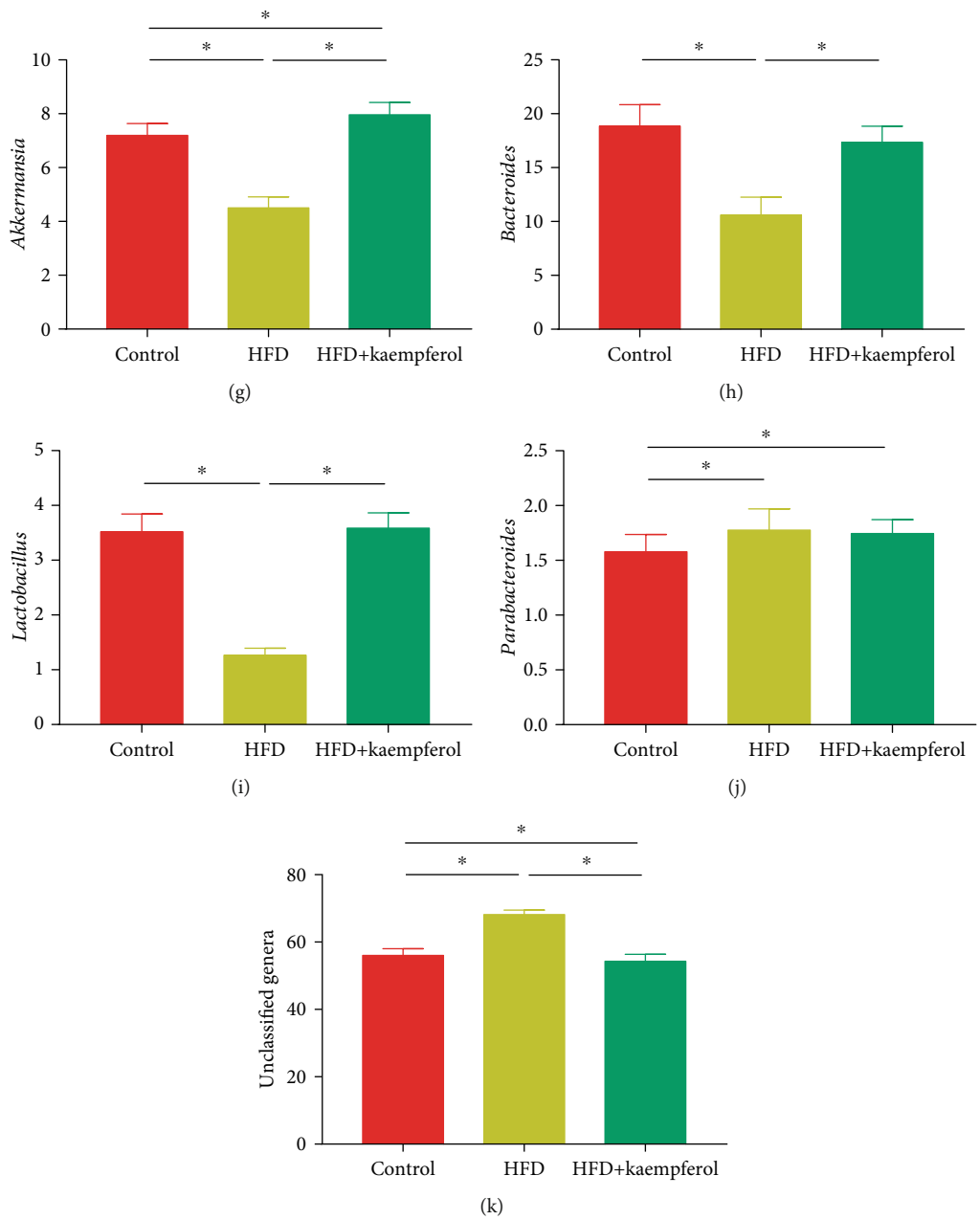

Figure 4: Gut microbiota analyses in the control, HFD, and HFD+kaempferol groups. (a) Shannon index in α-diversity analysis, (b) relative abundance of microbiota at the phylum level, (c) Bacteroidetes, (d) Firmicutes, and (e) Proteobacteria levels, (f) microbiota compositions at the genus level, (g) *Akkermansia*, (h) *Bacteroides*, (i) *Helicobacter*, (j) *Parabacteroides*, and (k) unclassified genus levels. Values are expressed as mean ± standard deviation. $^{*}P < 0.05$.

4. Discussion

Pharmacological research indicates that kaempferol, a natural flavonoid found in various plant-based foods, is beneficial to human health. Antidiabetic activity is associated with kaempferol administration, including anti-inflammatory, antioxidative, and antihyperlipidemic effects, as well as protection of pancreatic β-cells [17]. However, findings regarding kaempferol's impact on gut microbiota and insulin resistance are scarce. Therefore, it is significant that in this study, kaempferol treatment was associated with fewer obesity-related complications in HFD mice. A statistically significant difference in body weight gain was observed between the HFD+kaempferol group and the HFD group. When treating obesity-related complications, reduction of fat storage and body weight is critical. Therefore, this study's results indicate that this natural flavonoid can be exploited as a cost-effective and safe compound for the treatment and prevention of HFD-induced obesity and insulin resistance.

In this study, kaempferol treatment led to differences in the epidermal white adipose tissue mass between the HFD +kaempferol group and the HFD group. Additionally,

dietary kaempferol was associated with significantly less liver weight gain and enlargement compared to the HFD group. Moreover, in the HFD+kaempferol group, kaempferol kept body weight gain and elevation of blood glucose, serum cholesterol, and triglyceride levels lower than in the HFD group. It also resulted in lower hepatic lipid accumulation compared to the HFD group. One way to account for the increase in lipid metabolism associated with dietary kaempferol is by observing its impact on the regulation of hepatic expression of peroxisome proliferator-activated receptor α target genes [18]. Kaempferol may promote programmed cell death, thereby exerting an antitoxicological effect in various cancer cell types (e.g., pancreatic β-cells) [19]. Importantly, this effect is associated with concentrations of at least 30 μmol/L, which is significant because dietary kaempferol levels are typically lower than 1 μmol/L [20].

This study's data indicate that kaempferol administration improved insulin sensitivity and glucose tolerance in HFD mouse livers. *In vivo* experiments show that transcriptional regulation of lipogenesis genes (e.g., *Srebp-1c*, *Fas*, and *Scd*) is affected by insulin sensitivity changes in the liver [21]. Several *in vivo* studies indicate that obesity can be prevented by inhibiting hepatic lipogenesis and suppressing hepatic adipogenesis [22–24]. Thus, the preventive effect of kaempferol on obesity-related complications is possibly attributable to the weakened pathological processes of insulin resistance and inflammation [25].

The key to understanding obesity may be related to changes in the gut microbiota and its function in response to diet [26]. Several studies confirm that in both human and rat models, the gut microbiota in obesity exhibits greater relative abundance of Firmicutes and decreased levels of Bacteroidetes [27–29]. In line with these findings, this study found relative changes in the gut microbiota of HFD mice, showing that kaempferol supplementation led to lower levels of Firmicutes and higher levels of Bacteroidetes. However, the way in which kaempferol exerts these effects on the gut microbiota remains unclear. Its impact, particularly on Bacteroidetes, might be related to a consequent increase in the production of propionic acid, thereby mediating HFD-induced lipid metabolic dysfunction. These results are consistent with studies showing that an increase in propionate can attenuate weight gain in overweight human adults [30]. This mechanism may be linked to an increase in the secretion of gut hormones, including peptide YY and glucagon-like peptide-1 [30].

Overall, this study found that kaempferol administration in HFD mice moderated body and liver weight gain, hepatic lipid accumulation, and elevation of serum cholesterol, blood glucose, and triglyceride levels. The results also indicate that dietary kaempferol mediates the regulation of the gut microbiota, particularly by reversing the relative abundances of Firmicutes and Bacteroidetes to the levels observed in organisms with a healthy weight. This suggests that the gut microbiota may be implicated in the positive effect of kaempferol in HFD-induced lipid dysmetabolism. This study demonstrates that kaempferol supplementation has protective effects against insulin resistance and obesity in HFD mice, partly through mitigating insulin resistance deterioration and regulating the gut microbiota.

Data Availability

All the data to support this study are available at the correspondence author upon request.

Conflicts of Interest

The authors declare that there are no conflicts of interest.

Acknowledgments

This study was supported by the Zhejiang Provincial Medicine and Healthcare Scientific Project (2016KYB214).

References

[1] V. Ormazabal, S. Nair, O. Elfeky, C. Aguayo, C. Salomon, and F. A. Zuniga, "Association between insulin resistance and the development of cardiovascular disease," *Cardiovascular Diabetology*, vol. 17, no. 1, p. 122, 2018.

[2] L. Lee and R. A. Sanders, "Metabolic syndrome," *Pediatrics in Review*, vol. 33, no. 10, pp. 459–468, 2012.

[3] P. Zimmet, K. G. Alberti, D. J. Magliano, and P. H. Bennett, "Diabetes mellitus statistics on prevalence and mortality: facts and fallacies," *Nature Reviews Endocrinology*, vol. 12, no. 10, pp. 616–622, 2016.

[4] D. Yang, C. Hu, X. Deng et al., "Therapeutic effect of chitooligosaccharide tablets on lipids in high-fat diets induced hyperlipidemic rats," *Molecules*, vol. 24, no. 3, p. 514, 2019.

[5] P. Ahechu, G. Zozaya, P. Martí et al., "NLRP3 inflammasome: a possible link between obesity-associated low-grade chronic inflammation and colorectal cancer development," *Frontiers in Immunology*, vol. 9, p. 2918, 2018.

[6] P. Jiang, D. Ma, X. Wang et al., "Astragaloside IV prevents obesity-associated hypertension by improving pro-inflammatory reaction and leptin resistance," *Molecules and Cells*, vol. 41, no. 3, pp. 244–255, 2018.

[7] U. D. Wankhade, Y. Zhong, P. Kang et al., "Maternal high-fat diet programs offspring liver steatosis in a sexually dimorphic manner in association with changes in gut microbial ecology in mice," *Scientific Reports*, vol. 8, no. 1, article 16502, 2018.

[8] C. He, D. Cheng, C. Peng, Y. Li, Y. Zhu, and N. Lu, "High-Fat diet induces dysbiosis of gastric microbiota prior to gut microbiota in association with metabolic disorders in mice," *Frontiers in Microbiology*, vol. 9, p. 639, 2018.

[9] A. Hussain, M. K. Yadav, S. Bose et al., "Daesiho-Tang is an effective herbal formulation in attenuation of obesity in mice through alteration of gene expression and modulation of intestinal microbiota," *PLoS One*, vol. 11, no. 11, article e0165483, 2016.

[10] J. Y. Kim, Y. H. Cheon, H. M. Oh et al., "Oleanolic acid acetate inhibits osteoclast differentiation by downregulating PLCγ2–Ca^{2+}-NFATc1 signaling, and suppresses bone loss in mice," *Bone*, vol. 60, pp. 104–111, 2014.

[11] S. Ding, H. Jiang, and J. Fang, "Regulation of immune function by polyphenols," *Journal of Immunology Research*, vol. 2018, Article ID 1264074, 8 pages, 2018.

[12] R. Zamora-Ros, V. Knaze, I. Romieu et al., "Impact of thearubigins on the estimation of total dietary flavonoids in the European Prospective Investigation into Cancer and Nutrition (EPIC) study," *European Journal of Clinical Nutrition*, vol. 67, no. 7, pp. 779–782, 2013.

[13] A. Kumar Singh, C. Cabral, R. Kumar et al., "Beneficial effects of dietary polyphenols on gut microbiota and strategies to improve delivery efficiency," *Nutrients*, vol. 11, no. 9, p. 2216, 2019.

[14] E. A. Murphy, K. T. Velazquez, and K. M. Herbert, "Influence of high-fat diet on gut microbiota: a driving force for chronic disease risk," *Current Opinion in Clinical Nutrition and Metabolic Care*, vol. 18, no. 5, pp. 515–520, 2015.

[15] G. Zheng, C. Fan, S. Di et al., "Ectopic expression of tea *MYB* genes alter spatial flavonoid accumulation in alfalfa (*Medicago sativa*)," *PLoS One*, vol. 14, no. 7, article e0218336, 2019.

[16] H. Alkhalidy, W. Moore, A. Wang et al., "Kaempferol ameliorates hyperglycemia through suppressing hepatic gluconeogenesis and enhancing hepatic insulin sensitivity in diet-induced obese mice," *The Journal of Nutritional Biochemistry*, vol. 58, pp. 90–101, 2018.

[17] Y. Zhang and D. Liu, "Flavonol kaempferol improves chronic hyperglycemia-impaired pancreatic beta- cell viability and insulin secretory function," *European Journal of Pharmacology*, vol. 670, no. 1, pp. 325–332, 2011.

[18] C. J. Chang, T. F. Tzeng, S. S. Liou, Y. S. Chang, and I. M. Liu, "Kaempferol regulates the lipid-profile in high-fat diet-fed rats through an increase in hepatic PPARα Levels," *Planta Medica*, vol. 77, no. 17, pp. 1876–1882, 2011.

[19] Q. Dang, W. Song, D. Xu et al., "Kaempferol suppresses bladder cancer tumor growth by inhibiting cell proliferation and inducing apoptosis," *Molecular Carcinogenesis*, vol. 54, no. 9, pp. 831–840, 2014.

[20] A. Barve, C. Chen, V. Hebbar, J. Desiderio, C. L.-L. Saw, and A.-N. Kong, "Metabolism, oral bioavailability and pharmacokinetics of chemopreventive kaempferol in rats," *Biopharmaceutics & Drug Disposition*, vol. 30, no. 7, pp. 356–365, 2009.

[21] F. W. B. Sanders and J. L. Griffin, "*De novo* lipogenesis in the liver in health and disease: more than just a shunting yard for glucose," *Biological Reviews of the Cambridge Philosophical Society*, vol. 91, no. 2, pp. 452–468, 2016.

[22] S. F. Xing, L. H. Liu, M. L. Zu et al., "The inhibitory effect of gypenoside stereoisomers, gypenoside L and gypenoside LI, isolated from *Gynostemma pentaphyllum* on the growth of human lung cancer A549 cells," *Journal of Ethnopharmacology*, vol. 219, pp. 161–172, 2018.

[23] E. S. Kao, M. Y. Yang, C. H. Hung, C. N. Huang, and C. J. Wang, "Polyphenolic extract from *Hibiscus sabdariffa* reduces body fat by inhibiting hepatic lipogenesis and preadipocyte adipogenesis," *Food & Function*, vol. 7, no. 1, pp. 171–182, 2016.

[24] H. Liu, M. Liu, Z. Jin et al., "Ginsenoside Rg2 inhibits adipogenesis in 3T3-L1 preadipocytes and suppresses obesity in high-fat-diet-induced obese mice through the AMPK pathway," *Food & Function*, vol. 10, no. 6, pp. 3603–3614, 2019.

[25] C. Luo, H. Yang, C. Tang et al., "Kaempferol alleviates insulin resistance via hepatic IKK/NF-κB signal in type 2 diabetic rats," *International Immunopharmacology*, vol. 28, no. 1, pp. 744–750, 2015.

[26] A. Federico, M. Dallio, R. di Sarno, V. Giorgio, and L. Miele, "Gut microbiota, obesity and metabolic disorders," *Minerva Gastroenterologica e Dietologica*, vol. 63, no. 4, pp. 337–344, 2017.

[27] Y. Duan, Y. Zhong, H. Xiao et al., "Gut microbiota mediates the protective effects of dietary β-hydroxy-β-methylbutyrate (HMB) against obesity induced by high-fat diets," *The FASEB Journal*, vol. 33, no. 9, pp. 10019–10033, 2019.

[28] C. J. Chang, C. S. Lin, C. C. Lu et al., "Correction: Corrigendum: *Ganoderma lucidum* reduces obesity in mice by modulating the composition of the gut microbiota," *Nature Communications*, vol. 8, no. 1, article 16130, 2017.

[29] C. J. Chang, C. S. Lin, C. C. Lu et al., "*Ganoderma lucidum* reduces obesity in mice by modulating the composition of the gut microbiota," *Nature Communications*, vol. 6, no. 1, article 7489, 2015.

[30] E. S. Chambers, A. Viardot, A. Psichas et al., "Effects of targeted delivery of propionate to the human colon on appetite regulation, body weight maintenance and adiposity in overweight adults," *Gut*, vol. 64, no. 11, pp. 1744–1754, 2015.

Hindawi
BioMed Research International
Volume 2020, Article ID 3464068, 10 pages
https://doi.org/10.1155/2020/3464068

Research Article

Antioxidant and Anti-Inflammatory Effects of Different Zinc Sources on Diquat-Induced Oxidant Stress in a Piglet Model

Jieping Guo,[1] **Liuqin He**,[2,3] **Tiejun Li**,[2] **Jie Yin**,[1] **Yulong Yin**,[1,2] **and Guiping Guan**[1,2]

[1]*College of Animal Science and Technology, Hunan Agricultural University, Changsha, 410128 Hunan, China*
[2]*Scientific Observing and Experimental Station of Animal Nutrition and Feed Science in South-Central, Ministry of Agriculture, Hunan Provincial Engineering Research Center of Healthy Livestock, Key Laboratory of Agro-ecological Processes in Subtropical Region, Institute of Subtropical Agriculture, Chinese Academy of Sciences, Changsha, Hunan 410125, China*
[3]*Hunan International Joint Laboratory of Animal Intestinal Ecology and Health, Laboratory of Animal Nutrition and Human Health, College of Life Sciences, Hunan Normal University, Changsha 410081, China*

Correspondence should be addressed to Yulong Yin; yinyulong@isa.ac.cn and Guiping Guan; guanguiping@hunau.edu.cn

Received 19 January 2020; Revised 21 February 2020; Accepted 10 March 2020; Published 21 March 2020

Guest Editor: Deguang Song

Zinc (Zn) plays a crucial role in reducing oxidative stress and diarrhea in postweanling piglets. This study is aimed at comparing the effects of zinc chelate of 2-hydroxy-4 methyl-thio butanoic acid (HMZn) and $ZnSO_4$ on the oxidative stress in weaned piglets. A total of 32 piglets were randomly divided into 4 treatments: CON: basal diet+80 mg/kg Zn as $ZnSO_4$; DIQ: basal diet+80 mg/kg Zn as $ZnSO_4$; HMZn: basal diet+200 mg/kg Zn as HMZn; and $ZnSO_4$: basal diet+200 mg/kg Zn as $ZnSO_4$. On day 15, the DIQ, HMZn, and $ZnSO_4$ groups were injected intraperitoneally with diquat except for the CON group. The trial lasted 21 days. The results showed that zinc sources did not influence the growth performance during the first 14 days. But HMZn increased activities of superoxide dismutase (SOD), glutathione peroxidase (GPX), and total antioxidant capacity (T-AOC) in serum ($P < 0.05$). After diquat injection, the fecal score was decreased in the HMZn group. Both HMZn and $ZnSO_4$ increased the activities of GPX and T-AOC in serum and the relative mRNA expressions of hepatic and renal Nrf2, SOD1, and GPX compared with the DIQ group ($P < 0.05$). Moreover, the relative mRNA expression of inflammatory factors in the small intestine, liver, and kidney was downregulated; the phosphorylation of NF-κB protein was inhibited in the HMZn group compared with the DIQ and $ZnSO_4$ groups ($P < 0.05$). In general, HMZn showed notable advantage over $ZnSO_4$ in reducing diarrhea and improving antioxidant and anti-inflammatory ability in piglets challenged with diquat.

1. Introduction

Zinc (Zn), as an essential constituent of more than 200 enzymes involving antioxidant enzymes, plays important roles in their biochemical and pathophysiological functions [1]. An increasing amount of evidence suggests that Zn is one of the redox-active trace minerals and participates in the modulation of intracellular and extracellular redox state [2]. Zinc supplementation was demonstrated to significantly improve growth performance, antioxidant ability, and immune function of weanling pigs [3]. Although weaning piglets are highly susceptible to weaned syndrome, including growth retardation, diarrhea, metabolic disorders, and even death, dietary Zn supplementation could improve growth performance in the weaning stress conditions [4–7]. Many forms of inorganic Zn (i.e., $ZnSO_4$, ZnO) have been used in weanling piglets' diets to improve growth performance in the last decades; for example, a pharmacological level of ZnO (1500~3000 mg Zn/kg diet) is commonly used to prevent diarrhea and deemed as an alternative for antibiotics in weaning piglets [8–10]. While there is certain disputation on bioavailability of Zn from different sources, an increasing number of reports show that megadose of in-feed inorganic Zn with low absorption efficiency has been the source of environmental pollution [4, 11, 12].

HMZn, chelated by the hydroxy analogue of methionine (HMA) and Zn, is chemically stable and could be decomposed to HMA and Zn in the acid gastrointestinal tract. Diffusion and monocarboxylate transporters are the main transport pathways for HMA absorption; thus, HMA avoids competitions from amino acid transporter-dependent amino acids (Martin-Venegas et al. 2007; Fang et al. 2010b). The absorbed HMA is subsequently converted to methionine and acts as an endogenous antioxidant in cells. Some recent reports indicate that organic Zn in pigs is more conducive to mediate the adaptive response to piglets' oxidative stress compared with inorganic Zn [13, 14]. However, the effect of HMZn on regulating antioxidant and anti-inflammatory ability has not been well studied, especially on comparative effect of HMZn and $ZnSO_4$ in piglet nursery diets and evaluated potential benefits of organic HMZn on the intestinal antioxidant capacity of piglets in oxidative stress conditions. Considering its stable structure and potential supply of methionine, we hypothesized that HMZn might be advanced in antioxidative and anti-inflammatory capacity compared with $ZnSO_4$. To test the hypothesis, diquat-challenged piglets were used as oxidative stress models to investigate effects of HMZn and $ZnSO_4$ on antioxidant capacity and anti-inflammatory gene expression in the intestine.

2. Materials and Methods

2.1. Animal Experiment. This study was approved by the Laboratory Animal Welfare Commission of the Institute of Subtropical Agriculture, Chinese Academy of Sciences.

A total of 32 (35-day-old) health piglets (Duroc × Landrace × Yorkshire, 9.41 ± 0.11 kg BW) were allotted randomly to the following treatments: (1) control group (C): basal diet+80 mg/kg Zn as $ZnSO_4$; (2) negative control (NC): basal diet+diquat+80 mg/kg Zn as $ZnSO_4$; (3) HMZn group (HMZn): basal diet+diquat+200 mg/kg Zn as HMZn; and (4) $ZnSO_4$ group ($ZnSO_4$): basal diet+diquat+200 mg/kg Zn as $ZnSO_4$. Basal diet was formulated to meet the nutrient requirements recommended by the National Research Council (2012) and is shown in Table 1. Animals were housed in individual pens and had free access to water and feed. On day 15, the 2 to 4 groups were injected intraperitoneally (i.p.) with 10 mg/kg BW diquat (Diquat Dibromide Monohydrate, PS365; Sigma Co.) to induce oxidative stress, while the control group was intraperitoneally injected with the sterile saline. On day 21, all pigs were anaesthetized according to our previous methods; then, the blood and small intestine were sampled [15].

2.2. The Determination of Growth Performance and Diarrhea Index. The daily feed intake and the body weight per piglet were recorded during the whole experimental period in order to calculate the average daily gain (ADG), average daily feed intake (ADFI), and food conversion rate (FCR). The fecal consistency was daily observed and scored for individual piglets according to the following criterion. Diarrhea index was calculated according to a previous study [16].

2.3. Intestinal Histomorphology. The duodenum, jejunum, ileum, and colon samples were fixed with neutral formalin solution and then embedded in paraffin. After being cut into approximately 5 μm thicknesses, the paraffin sections were stained with hematoxylin and eosin. The intestinal villus height and crypt depth were measured using a light microscope equipped with a calibrated eyepiece graticule (BioScan Optimetric, BioScan Inc., Edmonds, WA, USA) [17]. Quantitative analysis of the digitally acquired images was performed by ImageJ software. The ratio of villi and crypt was calculated.

Table 1: Composition and nutrient level of the basal diets.

Items	Basal diet
Ingredient (%)	
Corn meal	60
Extruded soybean	10
Soybean meal	15
Fish powder	9.5
Whey powder	3
Premix*	2.5
Composition	
Metabolism energy (MJ)	13.23
Crude protein (%)	18.95
Met (%)	0.27
Zn (mg/kg)	19.65

*Premix (per kg of diet): vitamin A, 30 mg; cholecalciferol, 0.5 mg; vitamin C, 120 mg; vitamin E, 250 mg; menadione, 52 mg; vitamin B_1, 18 mg; vitamin B_2, 150 mg; vitamin B_6, 5.5 mg; vitamin B_{12}, 0.33 mg; nicotinic acid, 300 mg; folic acid, 4.2 mg; $CuSO_4{\cdot}5H_2O$, 400 mg; $MnSO_4{\cdot}H_2O$, 120 mg; $Fe[C_2H_4O_2N]HSO_4$, 595 mg; KI, 0.24 mg; Na_2SeO_3, 0.24 mg; $CaHPO_4$, 1. 2 g.

2.4. The Determination of Serum Antioxidant Enzymes. On days 7, 14, 17, and 21, blood samples were collected from jugular vein puncture, and the serum was obtained after centrifugation (3000 × g, 10 min, 4°C). The prepared serum samples were stored at −20°C for further analysis. The activities of total superoxide dismutase (T-SOD), glutathione peroxidase (GPX), total antioxidant capacity (T-AOC), catalase [18], and concentrations of malondialdehyde (MDA) were determined by commercial ELISA kits according to the instruction (Nanjing Jiancheng Bioengineering Institute, China).

2.5. Quantitative Real-Time PCR. Total RNA of the liver, kidney, and intestinal samples was isolated using TRIzol reagent (Invitrogen, China), and the quality of RNA was further checked on 1% agarose gel electrophoresis. Then, the cDNA was synthesized by a PrimeScript™ RT Reagent Kit (Takara, China) according to the instructions. Real-time PCR was performed to determine the relative mRNA expression of copper-zinc-superoxide dismutase (CuZnSOD, SOD1), glutathione peroxidase 1 (GPX1), catalase (CAT), NF-E2-related factor 2 (Nrf2), tumor necrosis factor-α (TNFα), interleukin-1β (IL-1β), IL-6, IL-8, and IL-10. β-Actin was used as a reference gene to normalize target gene transcript levels. Primers used in this study are shown in Table 2. The cDNA and primers were used to perform real-time PCR according to a previous study [16]. In brief, real-time PCR

Table 2: Primers used for quantitative reverse transcription-PCR.

Genes	Primers	Product length (bp)
β-Actin	F: CTGCGGCATCCACGAAACT R: AGGGCCGTGATCTCCTTCTG	147
SOD1	F: TCCATGTCCATCAGTTTGGA R: CTGCCCAAGTCATCTGGTTT	250
GPX1	F: CTTCGAGAAGTTCCTGGTGG R: CCTGGACATCAGGTGTTCCT	232
CAT	F: CCACTAATGTCCAGCGTCT R: CAGCCTTATTCACCACTACCTG	159
Nrf2	F: AGTGCAAGGCGGAGGTGA R: AGCCCGTTGGTGAACATAG	235
TNFα	F: ACCACGCTCTTCTGCCT R:GGCTTATCTGAGGTTTG	128
IL-1β	F: CAGCTGCAAATCTCTCACCA R: TCTTCATCGGCTTCTCCACT	85
IL-6	F: TTCACCTCTCCGGACAAAC R: TCTGCCAGTACCTCCTTGCT	122
IL-8	F: ACTTCCAAACTGGCTGTTGC R: GGAATGCGTATTTATGCACTGG	120
IL-10	F: TAATGCCGAAGGCAGAGT R: GGCCTTGCTCTTGTTTTCAC	134

was performed in a total volume of 25 μl, which consists of 1 μg of cDNA template, 1 μmol/l of forward and reverse primers, and 12.5 μl SYBR Green Mix. The result was expressed as a ratio of the target gene to the reference gene using the formula $2^{-(\Delta\Delta Ct)}$.

2.6. Western Blot. Antibodies against NF-κB (Bioss, China), p-NF-κB (Bioss, China), and β-actin (Proteintech, USA) were used in this study. Briefly, frozen intestinal samples were homogenized and subsequently determined for protein concentration using the bicinchoninic acid (BCA) protein assay kit (Wellbio, China). Equal quantity of protein samples was separated on SDS-PAGE and then transferred to polyvinylidene difluoride (PVDF) membranes. After being blocked with 5% skim milk for 1 h at room temperature, the membranes were incubated with the indicated primary antibodies at 4°C overnight. Then, blots were stripped, followed by the incubation with HRP-conjugated secondary antibody (Proteintech, USA) for 1 h. The chemiluminescence signals were obtained using ECL Plus kits (Thermo, USA). The band density was normalized to β-actin and expressed as a relative level to control value.

2.7. Statistical Analysis. Data were analyzed by one-way ANOVA followed by Duncan's test using the SPSS statistical software. $P < 0.05$ was considered to be statistically significant. $0.05 < P < 0.10$ was considered a tendency. All data are presented as mean ± SEM.

3. Results

3.1. Effect of Different Zn Sources on Growth Performance in Piglets under Oxidative Stress. The results of growth performance are presented in Table 3. During the 14 days of the prestarter period, dietary HMZn or $ZnSO_4$ supplementations did not affect FCR or fecal sore in piglets ($P > 0.05$). Compared with the control group, diquat injection reduced ADG and increased FCR and fecal score ($P < 0.05$) during the 7 days of the starter period. HMZn and $ZnSO_4$ both failed to exert notable protective effect on growth performance, while HMZn supplementation notably decreased fecal score.

3.2. Effect of Different Zn Sources on Intestinal Morphology in Piglets under Oxidative Stress. As shown in Figure 1, diquat exposure significantly decreased villus depth in the jejunum, while exerted no effect on the ratio of villi and crypt. Dietary HMZn supplementation tended to increase jejunal villus depth compared with NC groups ($P > 0.05$).

3.3. Effect of Different Zn Sources on Serum Antioxidant Capacity in Piglets under Oxidative Stress. As shown in Figure 2, serum MDA content was not affected by different sources of Zn supplementation during the prestarter period but was notably increased by diquat 3 days and 7 days after injection ($P < 0.05$), suggesting that the oxidative stress model was well established. Compared with the Con group, the activities of serum SOD, GPX, and T-AOC in the HMZn group were increased on day 14 ($P < 0.05$), while CAT remained unaffected. The serum antioxidant capacity of postinjection is illustrated in Figure 3. On day 17 (3 days post injection), the MDA content in serum was notably increased by diquat injection ($P < 0.05$), and the tendency was remained on day 21. The activities of serum GPX and T-AOC were notably decreased on days 17 and 21 ($P < 0.05$). It is noteworthy that both HMZn and $ZnSO_4$ effectively attenuated the diquat-induced suppression of GPX activity. The relative mRNA expressions of antioxidant pathway-related genes in the small intestine, liver, and kidney are illustrated in Figure 4. Diquat exposure decreased the relative mRNA level of Nrf2 in the liver and CAT in the jejunum and ileum compared with the CON group ($P < 0.05$). While both HMZn and $ZnSO_4$ showed notable effect on attenuating the diquat-induced suppression of mRNA expression of Nrf2, SOD1, and CAT, HMZn was proved to be more effective.

3.4. Effect of Different Zn Sources on Proinflammatory Cytokines in the Small Intestine of Piglets under Oxidative Stress. Diquat injection significantly increased the relative mRNA levels of TNFα and IL-1β compared with the control group ($P < 0.05$). Both HMZn and $ZnSO_4$ supplementations alleviate the proinflammatory effect of diquat (Figure 5), and HMZn exhibited notable advantage over $ZnSO_4$. Western blot results showed diquat challenge remarkably upregulated phosphorylation of NF-κB protein ($P < 0.05$) (Figure 6). HMZn effectively lowered the NF-κB phosphorylation while $ZnSO_4$ showed little alleviating effect.

Table 3: Effects of different dietary Zn sources on growth performance in diquat-challenged piglets.

Items	CON	DIQ	HMZn	$ZnSO_4$	*P* value
Prestarter (0~14 days)					
ADG (kg/d)	0.23 ± 0.01	0.21 ± 0.02	0.23 ± 0.03	0.24 ± 0.02	0.931
ADFI (kg/d)	0.42 ± 0.01	0.39 ± 0.01	0.4 ± 0.03	0.45 ± 0.02	0.279
FCR	1.87 ± 0.09	1.96 ± 0.09	1.83 ± 0.13	1.93 ± 0.08	0.787
Fecal score	2.15 ± 0.2	2.05 ± 0.15	1.72 ± 0.13	1.79 ± 0.14	0.236
Starter (15~21 days)					
ADG (kg)	0.39 ± 0.05^{a}	0.21 ± 0.03^{b}	0.33 ± 0.03^{ab}	0.27 ± 0.04^{ab}	0.042
ADFI (kg)	0.84 ± 0.15	0.64 ± 0.11	0.79 ± 0.2	0.71 ± 0.13	0.805
FCR	2.15 ± 0.19^{b}	3.05 ± 0.21^{a}	2.42 ± 0.20^{ab}	2.63 ± 0.23^{ab}	0.049
Fecal score	2.36 ± 0.08^{b}	3.54 ± 0.25^{a}	2.55 ± 0.18^{b}	3.18 ± 0.23^{a}	<0.01

ADG = average daily gain; ADFI = average daily feed intake; FCR = food conversion rate. Values are expressed as mean ± SEM, $n = 8$. [a,b]Means within a row with different letters were significantly different compared to the other groups ($P < 0.05$).

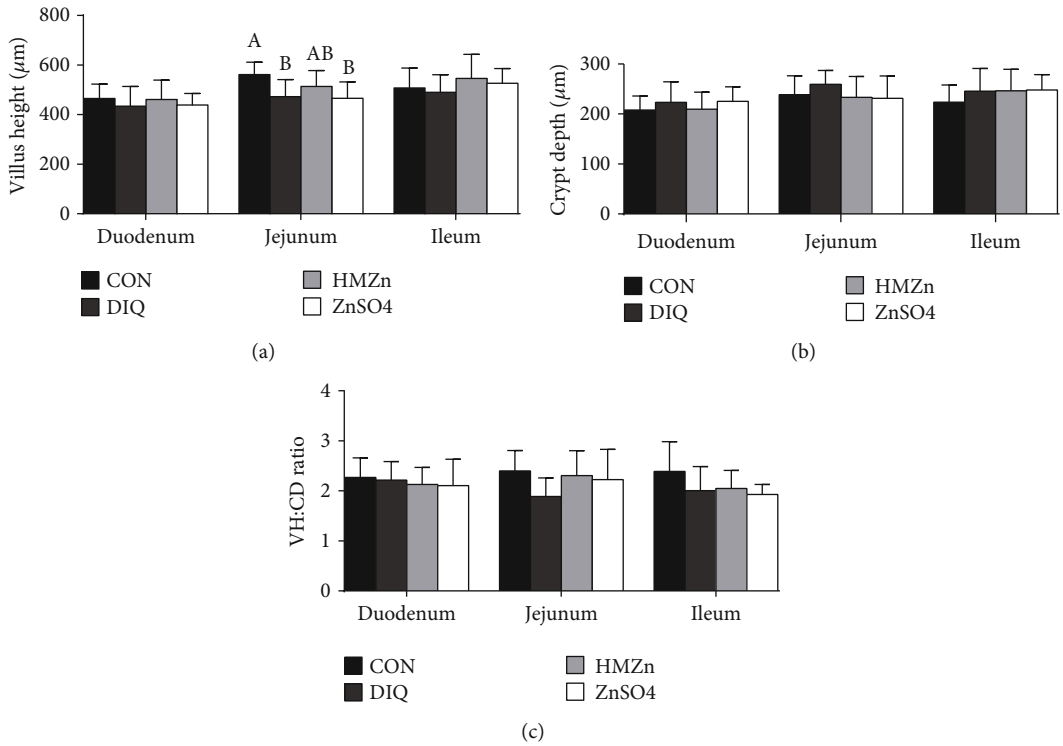

Figure 1: Effects of different dietary Zn sources on the small intestinal morphology in piglets under oxidative stress. Values are expressed as mean ± SEM, $n = 6$. [a,b]Means of the bars with different letters were significantly different compared to the other groups ($P < 0.05$).

4. Discussion

Zinc, as a component of some antioxidant enzymes and proteins (i.e., SOD, glutathione) involved in the subsequent scavenge progress, participates in antioxidant defense by activating the activity of several enzymes [19]. Previous studies in humans and mice revealed that Zn deficiency from marginal to moderate led to growth retardation, immunity disorder, gastrointestinal impairment, and aggravated oxidative stress [20, 21].

In our study, the basal diet in the current experiment contained 80 mg/kg of Zn to meet the suggested NRC (2012) requirement. Zn supplementations did not have an impact on growth performance and diarrhea rate during the prestarter period. But after diquat injection, the effect of additional Zn supplementation on growth performance and diarrhea rate became significant. It can be explained that additional Zn supplementation facilitated the synthesis of Zn-containing antioxidant enzymes, thus improving the defense ability against oxygen-free radicals, which is helpful in maintaining the intestinal health and reducing inflammatory processes after diquat challenge, and finally improving growth performance. The data also suggested that HMZn had better effect than $ZnSO_4$ on decreasing

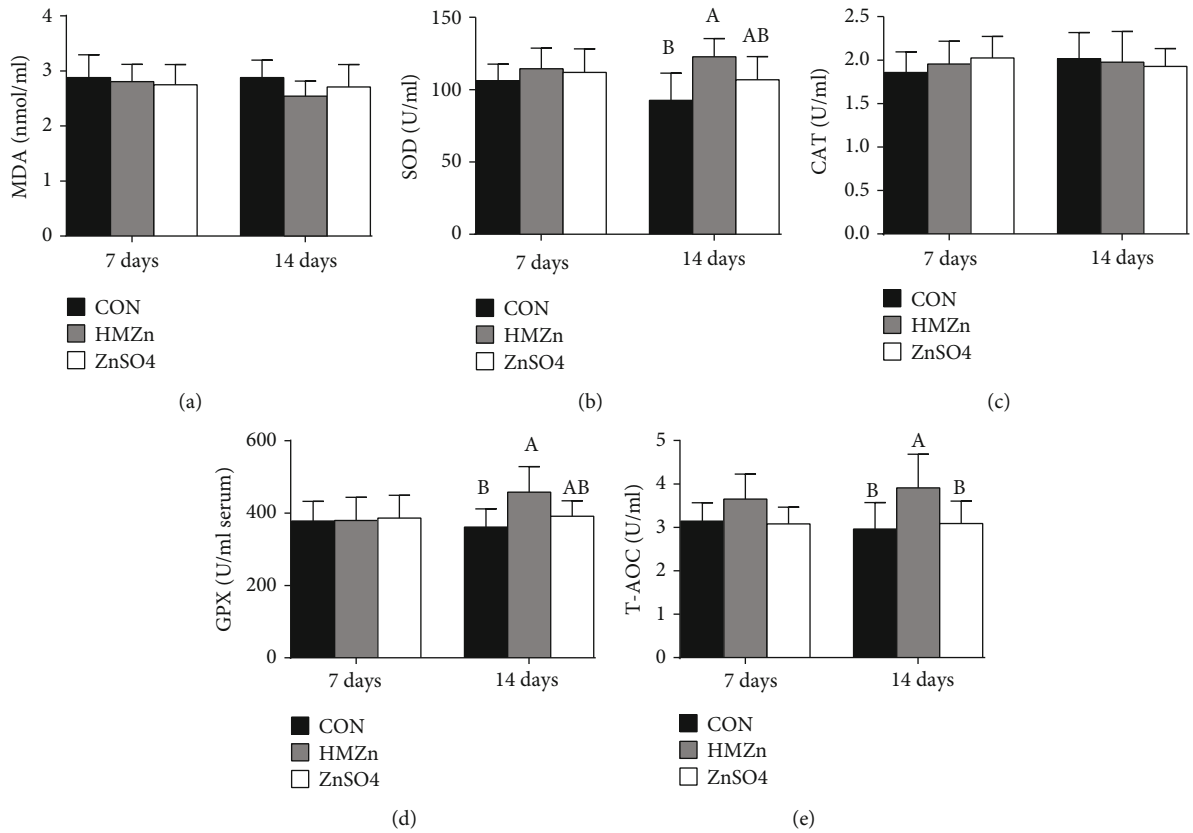

Figure 2: Effects of different dietary Zn sources on antioxidant capacity of piglets before diquat challenge. Values are expressed as mean ± SEM, $n = 6$. [a,b]Means of the bars with different letters were significantly different compared to the other groups ($P < 0.05$).

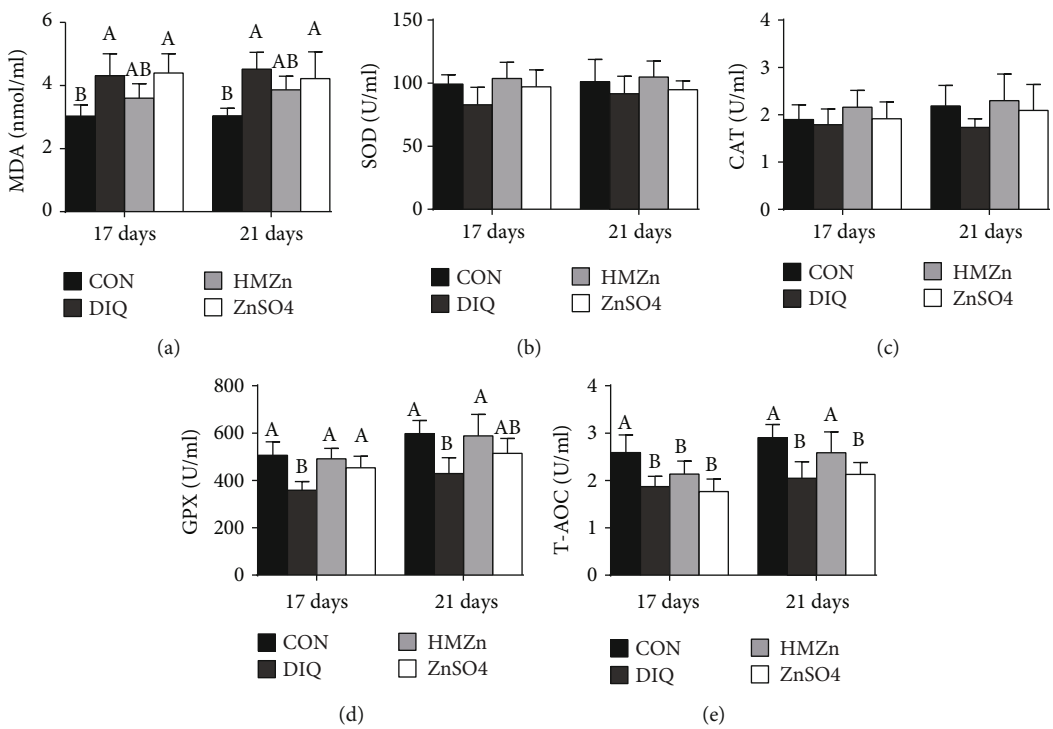

Figure 3: Effects of different dietary Zn sources on serum antioxidant capacity in piglets under oxidant stress. Values are expressed as mean ± SEM, $n = 6$. [a,b]Means of the bars with different letters were significantly different compared to the other groups ($P < 0.05$).

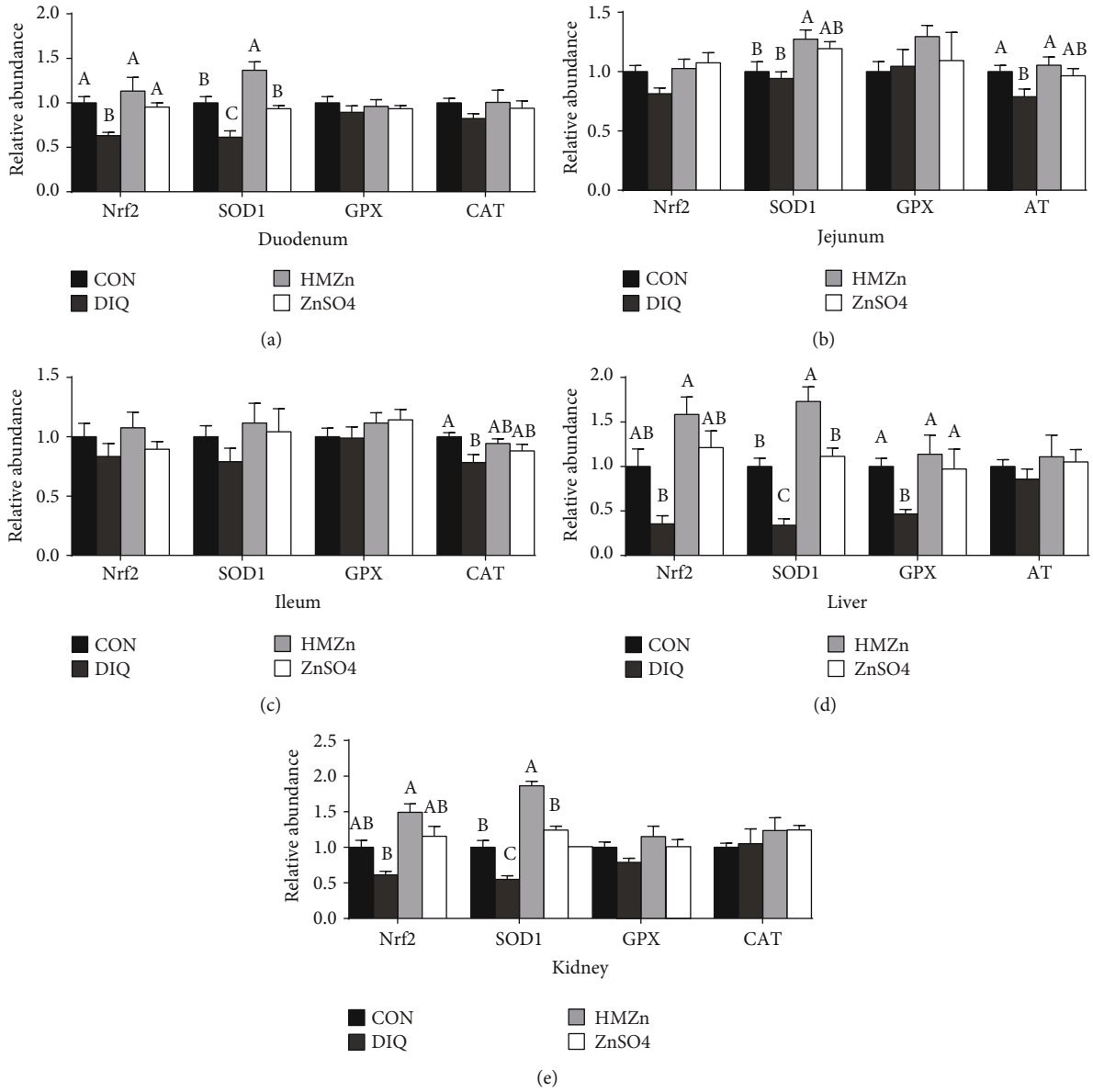

Figure 4: Effects of different dietary Zn sources on mRNA expression of antioxidant-related genes in piglets under oxidative stress. Values are expressed as mean ± SEM, $n = 6$. [a,b]Means of the bars with different letters were significantly different compared to the other groups ($P < 0.05$).

diarrhea, which is consistent with another study conducted in broiler chicks [22].

Villus height, crypt depth, and the ratio of villi and crypt are commonly used as important indicators for estimating intestinal integrity, which play critical roles in nutrient absorption [23]. Weaning stress often leads to villus impairment and malabsorption, finally resulting in diarrhea and retarded growth in weaned piglets [24]. Yin et al. (2015) reported that diquat challenge caused intestinal morphological injury [25]. Similarly, the present study showed that diquat challenge significantly decreased jejunal villus height but showed no negative effect on the rest of the recorded indices in intestinal morphology. Furthermore, villus height and the ratio of villi and crypt did not change in response to difference sources of Zn supplementation, except a compensatory increase in jejunal villus height in HMZn-supplemented pigs. These were supported by the findings that Zn enhanced the integrity of the intestinal epithelial barrier and promoted villus growth and intestinal absorption.

Malondialdehyde (MDA) is a metabolite produced by lipid peroxidation and widely used as an indicator of oxidative stress [9, 26, 27]. In the present study, regardless of sources, Zn supplementation showed no positive effect on serum MDA concentration during the prestarter period. The serum MDA concentration was then significantly increased during the postinjection period, indicating that the oxidative stress model induced by diquat was successful.

There is a dynamic equilibrium between the antioxidant capacity of the body and the production of reactive oxygen

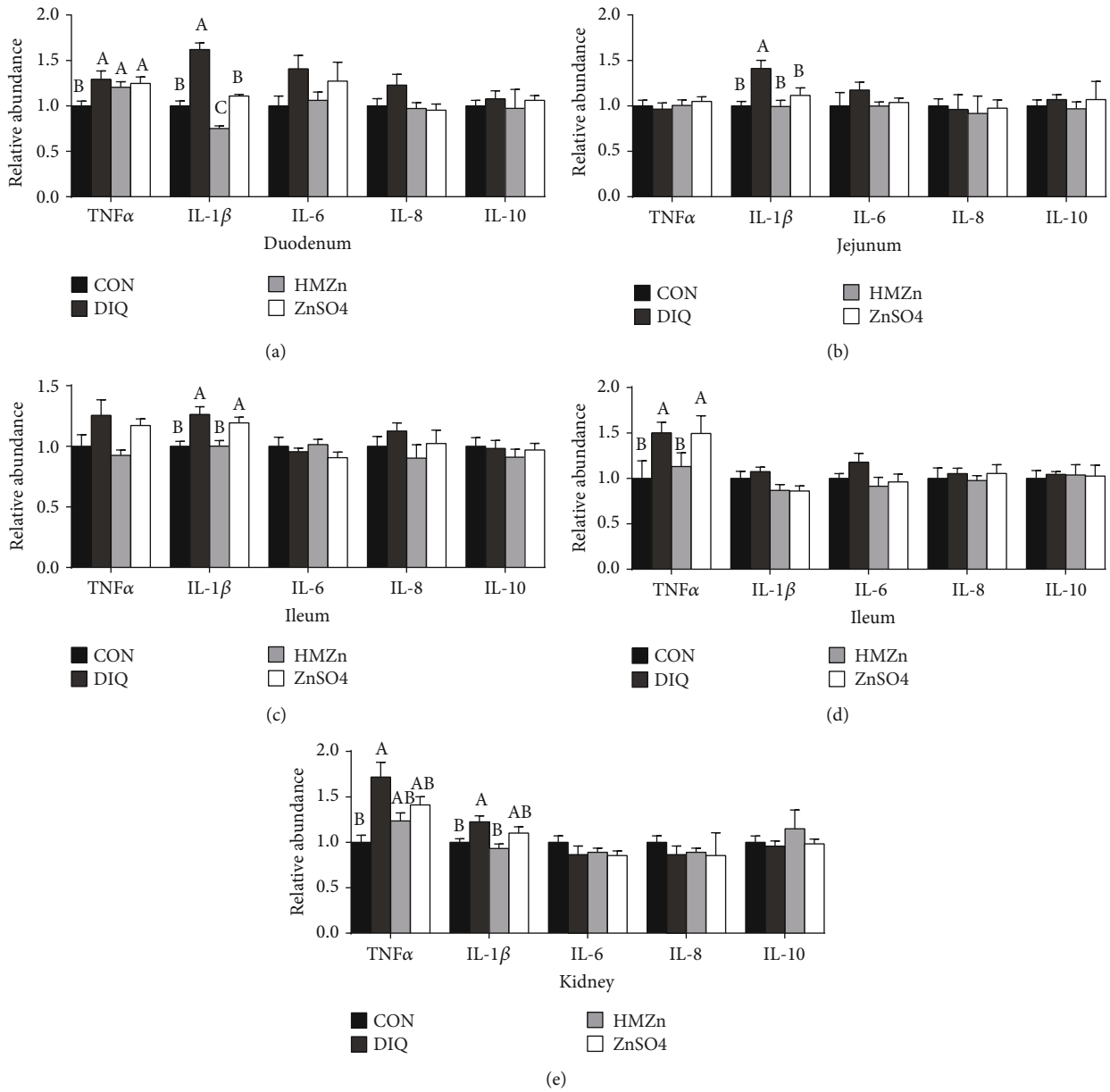

Figure 5: Effects of different dietary Zn sources on mRNA expression of proinflammatory cytokines in piglets under oxidative stress.

species (ROS); however, excessive ROS caused by oxidative stress may impair the antioxidant defense system, thus further resulting in cellular damage, death, and even tissue injury [28–30]. Enzymatic antioxidants, including SOD, CAT, and GPX, and nonenzymatic antioxidants can eliminate ROS or inhibit their generation and have important function on maintaining redox homeostasis [26]. Our results suggested that before diquat injection, HMZn supplementation improved the activity of serum SOD1, GPX, and T-AOC during the prestarter period. During the starter period (17 d, 21 d), the activity of GPX and T-AOC was significantly inhibited. It is evident that CAT and GPX provide vital antioxidant defenses against the excess of cellular ROS by decomposing hydrogen peroxide (H_2O_2) (Cui et al. 2016; Jarosz et al. 2017). Comparison of the different Zn treatments revealed that HMZn supplementation was efficacious in enhancing serum antioxidative enzyme activities and decreasing serum MDA concentration, while $ZnSO_4$ showed little effects in decreasing serum MDA concentration. Nrf2 can bind to the promoter region of genes of endogenous antioxidant enzymes and facilitate the gene transcription of these enzymes [31]. Scientific evidence showed that Zn has the potential to activate the Nrf2 signaling pathway and Nrf2 target antioxidant enzyme genes and in turn to enhance the expression of several antioxidative and cytoprotective genes (i.e., SOD, GPX1, CAT, and Nrf2) in mice [32, 33]. Our study further showed that diquat challenge downregulated the relative mRNA expression of Nrf2 and its target antioxidant enzymes in the liver, kidney, and intestine.

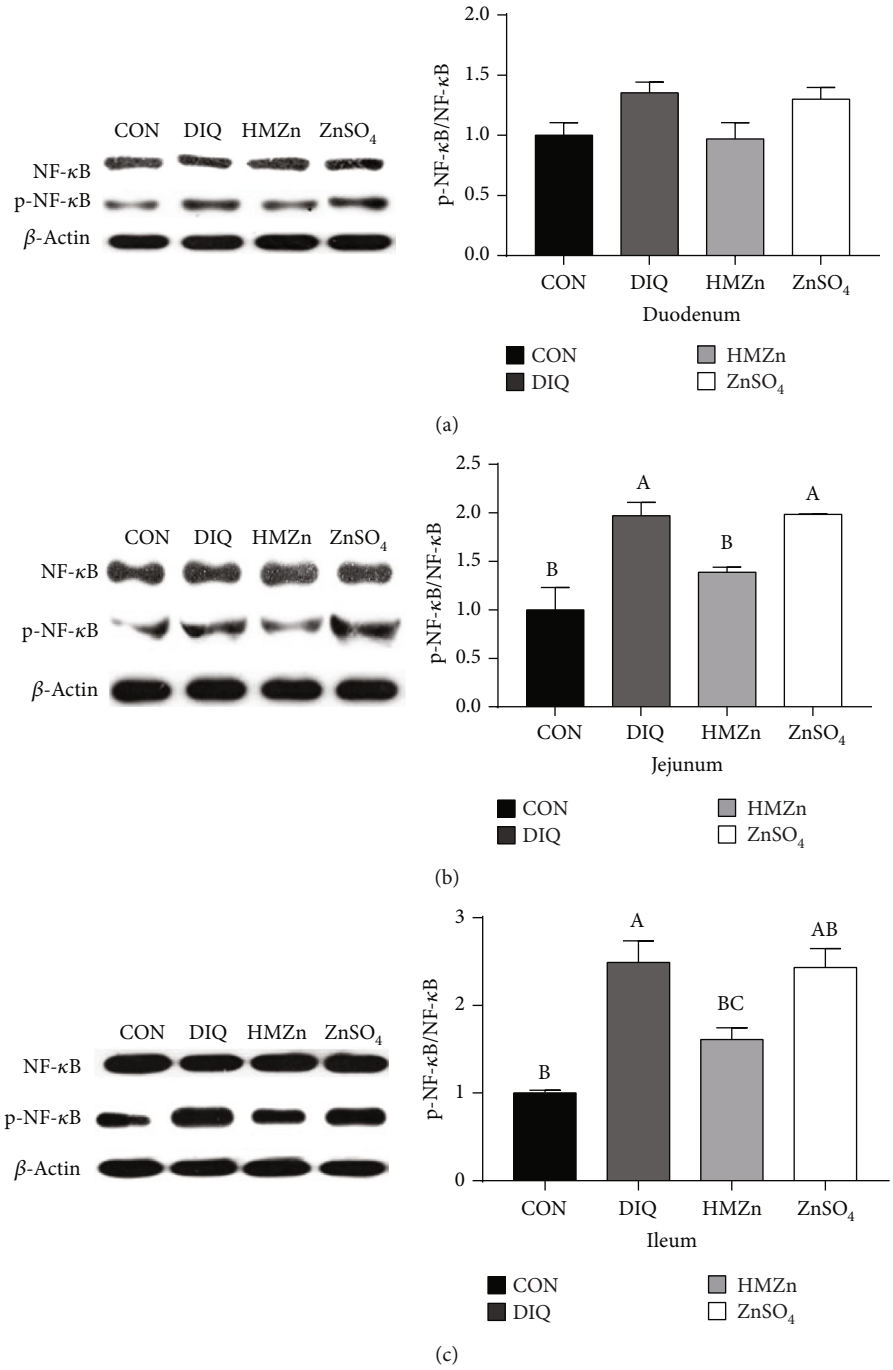

Figure 6: Effects of different dietary Zn sources on phosphorylation of NF-κB in piglets under oxidative stress.

The NF-κB signaling pathway plays an important role in the regulation of inflammation, immune responses, and many cellular stress responses [26]. In the present study, phosphorylations of NF-κB in the jejunum and ileum were significantly enhanced by diquat injection, as well as the elevation of relative mRNA expression of inflammatory factors in the duodenum, jejunum, ileum, liver, and kidney. HMZn supplementation exhibited notable alleviating effect on the diquat-induced inflammatory response, and the results suggested that HMZn may work through NF-κB pathways.

5. Conclusion

Our results indicated that 80 mg/kg of Zn in the basal diet is not sufficient for adequate antioxidant enzyme activities in pigs, and addition of 200 mg/kg Zn was effective in protecting weanling piglet from oxidative stress by improving antioxidant systems. Dietary supplementation with 200 mg/kg Zn as HMZn provided more potent protection compared with the equal level of Zn as $ZnSO_4$. However, more studies are required to explore long-term effects of HMZn in pigs and

further investigate its underlying mechanisms of the antioxidant property.

Data Availability

The data used to support the findings of this study are available from the corresponding author upon request.

Conflicts of Interest

All authors declare no competing financial, professional, or personal interests that might have influenced the performance or presentation of this work.

Acknowledgments

This work was supported by the National Key Research and Development Program of China (2018YFD0500405); the National Natural Science Foundation of China (31872371 and 31702125); the key research and development programs of Hunan Province (2017NK2321); the Open Fund of Key Laboratory of Agro-ecological Processes in Subtropical Region, Chinese Academy of Sciences (ISA2018204); the project of "Innovation Platform and Talents Program" of Hunan Provincial Science and Technology Department (2018RS3105); and the Hunan Province Key Laboratory of Animal Nutritional Physiology and Metabolic Process (2018TP1031).

References

[1] X. X. Chien, S. Zafra-Stone, M. Bagchi, and D. Bagchi, "Bioavailability, antioxidant and immune-enhancing properties of zinc methionine," *BioFactors*, vol. 27, no. 1-4, pp. 231–244, 2006.

[2] J. D. Richards, J. Zhao, R. J. Harrell, C. A. Atwell, and J. J. Dibner, "Trace mineral nutrition in poultry and swine," *Asian-Australasian Journal of Animal Sciences*, vol. 23, no. 11, pp. 1527–1534, 2010.

[3] K. Xiao, Y. Liu, T. Qi et al., "A highly pi-stacked organic semiconductor for field-effect transistors based on linearly condensed pentathienoacene," *Journal of the American Chemical Society*, vol. 127, no. 38, pp. 13281–13286, 2005.

[4] L. I. Chiba and L. I. Chiba, *Sustainable Swine Nutrition*, Wiley, 2012.

[5] J. P. Lallès, "Nutrition and gut health of the young pig around weaning: what news?," *Archiva Zootechnica*, vol. 11, pp. 5–15, 2008.

[6] M. S. Hedemann, B. B. Jensen, and H. D. Poulsen, "Influence of dietary zinc and copper on digestive enzyme activity and intestinal morphology in weaned pigs," *Journal of Animal Science*, vol. 84, no. 12, pp. 3310–3320, 2006.

[7] G. M. Hill, D. C. Mahan, S. D. Carter et al., "Effect of pharmacological concentrations of zinc oxide with or without the inclusion of an antibacterial agent on nursery pig performance," *Journal of Animal Science*, vol. 79, no. 4, pp. 934–941, 2001.

[8] C. Wang, J. Lu, L. Zhou et al., "Effects of long-term exposure to zinc oxide nanoparticles on development, zinc metabolism and biodistribution of minerals (Zn, Fe, Cu, Mn) in mice," *PLoS One*, vol. 11, no. 10, article e0164434, 2016.

[9] C. Zhu, H. Lv, Z. Chen et al., "Dietary zinc oxide modulates antioxidant capacity, small intestine development, and jejunal gene expression in weaned piglets," *Biological Trace Element Research*, vol. 175, no. 2, pp. 331–338, 2017.

[10] P. S. Swain, S. B. N. Rao, D. Rajendran, G. Dominic, and S. Selvaraju, "Nano zinc, an alternative to conventional zinc as animal feed supplement: a review," *Animal Nutrition*, vol. 2, no. 3, pp. 134–141, 2016.

[11] M. M. Martínez, J. E. Link, and G. M. Hill, "Dietary pharmacological or excess zinc and phytase effects on tissue mineral concentrations, metallothionein, and apparent mineral retention in the newly weaned pig," *Biological Trace Element Research*, vol. 105, no. 1-3, pp. 097–116, 2005.

[12] G. M. Hill, *Minerals and Mineral Utilization in Swine*, Blackwell Publishing Ltd, 2015.

[13] J. W. Swinkels, E. T. Kornegay, W. Zhou, M. D. Lindemann, Webb KE Jr, and M. W. Verstegen, "Effectiveness of a zinc amino acid chelate and zinc sulfate in restoring serum and soft tissue zinc concentrations when fed to zinc-depleted pigs," *Journal of Animal Science*, vol. 74, no. 10, pp. 2420–2430, 1996.

[14] Y. Ma, Q. Huang, M. Lv et al., "Chitosan-Zn chelate increases antioxidant enzyme activity and improves immune function in weaned piglets," *Biological Trace Element Research*, vol. 158, no. 1, pp. 45–50, 2014.

[15] L. He, H. Li, N. Huang et al., "Effects of alpha-ketoglutarate on glutamine metabolism in piglet enterocytes in vivo and in vitro," *Journal of Agricultural and Food Chemistry*, vol. 64, no. 13, pp. 2668–2673, 2016.

[16] L. He, N. Huang, H. Li et al., "AMPK/α-ketoglutarate axis regulates intestinal water and ion homeostasis in young pigs," *Journal of Agricultural and Food Chemistry*, vol. 65, no. 11, pp. 2287–2298, 2017.

[17] L. He, L. Wu, Z. Xu et al., "Low-protein diets affect ileal amino acid digestibility and gene expression of digestive enzymes in growing and finishing pigs," *Amino Acids*, vol. 48, no. 1, pp. 21–30, 2016.

[18] W. J. Bettger, P. G. Reeves, E. A. Moscatelli, G. Reynolds, and B. L. O'Dell, "Interaction of zinc and essential fatty acids in the rat," *Journal of Nutrition*, vol. 109, no. 3, pp. 480–488, 1979.

[19] L. H. Ho, R. E. Ruffin, C. Murgia, L. Li, S. A. Krilis, and P. D. Zalewski, "Labile zinc and zinc transporter ZnT4in mast cell granules: role in regulation of caspase activation and NF-κB translocation," *Journal of Immunology*, vol. 172, no. 12, pp. 7750–7760, 2004.

[20] A. S. Prasad, "Zinc is an antioxidant and anti-inflammatory agent: its role in human health," *Frontiers in Nutrition*, vol. 1, p. 14, 2014.

[21] Y. Zhao, Y. Tan, J. Dai et al., "Exacerbation of diabetes-induced testicular apoptosis by zinc deficiency is most likely associated with oxidative stress, p38 MAPK activation, and p53 activation in mice," *Toxicology Letters*, vol. 200, no. 1-2, pp. 100–106, 2011.

[22] J. Zhao, R. B. Shirley, J. J. Dibner et al., "Superior growth performance in broiler chicks fed chelated compared to inorganic zinc in presence of elevated dietary copper," *Journal of Animal Science and Biotechnology*, vol. 7, no. 1, pp. 561–569, 2016.

[23] M. J. A. Nabuurs, "Weaning piglets as a model for studying pathophysiology of diarrhea," *Veterinary Quarterly*, vol. 20, Supplement 3, pp. 42–45, 1998.

[24] M. S. Hedemann, S. Højsgaard, and B. B. Jensen, "Small intestinal morphology and activity of intestinal peptidases in piglets

around weaning," *Journal of Animal Physiology and Animal Nutrition*, vol. 87, no. 1-2, pp. 32–41, 2003.

[25] J. Yin, M. Liu, W. Ren et al., "Effects of dietary supplementation with glutamate and aspartate on diquat-induced oxidative stress in piglets," *PLoS One*, vol. 10, no. 4, article e0122893, 2015.

[26] M. Jarosz, M. Olbert, G. Wyszogrodzka, K. Młyniec, and T. Librowski, "Antioxidant and anti-inflammatory effects of zinc. Zinc-dependent NF-κB signaling," *Inflammopharmacology*, vol. 25, no. 1, pp. 11–24, 2017.

[27] F. Nielsen, B. B. Mikkelsen, J. B. Nielsen, H. R. Andersen, and P. Grandjean, "Plasma malondialdehyde as biomarker for oxidative stress: reference interval and effects of life-style factors," *Clinical Chemistry*, vol. 43, no. 7, pp. 1209–1214, 1997.

[28] J. M. Gutteridge, "Lipid peroxidation and antioxidants as biomarkers of tissue damage," *Clinical Chemistry*, vol. 41, no. 12, pp. 1819–1828, 1995.

[29] S. Dzięgielewska-Gęsiak, E. Wysocka, S. Michalak, E. Nowakowska-Zajdel, T. Kokot, and M. Muc-Wierzgoń, "Role of lipid peroxidation products, plasma total antioxidant status, and Cu-, Zn-superoxide dismutase activity as biomarkers of oxidative stress in elderly prediabetics," *Oxidative Medicine and Cellular Longevity*, vol. 2014, Article ID 987303, 8 pages, 2014.

[30] Y. S. Ho, J. L. Magnenat, M. Gargano, and J. Cao, "The nature of antioxidant defense mechanisms: a lesson from transgenic studies," *Environmental Health Perspectives*, vol. 106, Supplement 5, pp. 1219–1228, 1998.

[31] T. W. Kensler, N. Wakabayashi, and S. Biswal, "Cell survival responses to environmental stresses via the Keap1-Nrf2-ARE pathway," *Annual Review of Pharmacology and Toxicology*, vol. 47, no. 1, pp. 89–116, 2007.

[32] F. Wang, Y. Li, Y. Cao, and C. Li, "Zinc might prevent heat-induced hepatic injury by activating the Nrf2-Antioxidant in mice," *Biological Trace Element Research*, vol. 165, no. 1, pp. 86–95, 2015.

[33] Y. Cao, Y. S. Li, Z. J. Li, F. Wang, and C. M. Li, "Dietary zinc may attenuate heat-induced testicular oxidative stress in mice via up-regulation of Cu-Zn SOD," *Genetics and Molecular Research*, vol. 14, no. 4, pp. 16616–16626, 2015.

Hindawi
BioMed Research International
Volume 2020, Article ID 2948282, 8 pages
https://doi.org/10.1155/2020/2948282

Research Article

Alterations of the Predominant Fecal Microbiota and Disruption of the Gut Mucosal Barrier in Patients with Early-Stage Colorectal Cancer

Xia Liu,[1] **Yiwen Cheng**,[2] **Li Shao**,[3,4] **and Zongxin Ling**[2]

[1]*Department of Intensive Care Unit, The First Affiliated Hospital, School of Medicine, Zhejiang University, Hangzhou, Zhejiang 310003, China*
[2]*Collaborative Innovation Center for Diagnosis and Treatment of Infectious Diseases, State Key Laboratory for Diagnosis and Treatment of Infectious Diseases, National Clinical Research Center for Infectious Diseases, The First Affiliated Hospital, School of Medicine, Zhejiang University, Hangzhou, Zhejiang 310003, China*
[3]*Hangzhou Normal University, Hangzhou, Zhejiang 311121, China*
[4]*Institute of Translational Medicine, The Affiliated Hospital of Hangzhou Normal University, Hangzhou, Zhejiang 310015, China*

Correspondence should be addressed to Li Shao; 0011334@zju.edu.cn and Zongxin Ling; lingzongxin@zju.edu.cn

Received 17 January 2020; Revised 18 February 2020; Accepted 9 March 2020; Published 21 March 2020

Guest Editor: Yan Huang

Growing evidence indicated that the gut microbiota was the intrinsic and essential component of the cancer microenvironment, which played vital roles in the development and progression of colorectal cancer (CRC). In our present study, we investigated the alterations of fecal abundant microbiota with real-time quantitative PCR and the changes of indicators of gut mucosal barrier from 53 early-stage CRC patients and 45 matched healthy controls. We found that the traditional beneficial bacteria such as *Lactobacillus* and *Bifidobacterium* decreased significantly and the carcinogenic bacteria such as Enterobacteriaceae and *Fusobacterium nucleatum* were significantly increased in CRC patients. We also found gut mucosal barrier dysfunction in CRC patients with increased levels of endotoxin (LPS), D-lactate, and diamine oxidase (DAO). With Pearson's correlation analysis, D-lactate, LPS, and DAO were correlated negatively with *Lactobacillus* and *Bifidobacterium* and positively with Enterobacteriaceae and *F. nucleatum*. Our present study found dysbiosis of the fecal microbiota and dysfunction of the gut mucosal barrier in patients with early-stage CRC, which implicated that fecal abundant bacteria and gut mucosal barrier indicators could be used as targets to monitor the development and progression of CRC in a noninvasive and dynamic manner.

1. Introduction

Colorectal cancer (CRC) is one of the leading causes of cancer-related mortality, accounting for the fifth most commonly diagnosed cancer and the fifth most common cause of death by cancer in China [1]. The overall decline or stabilization in the incidence of CRC was noted in several high-income countries [2]; however, the incidence and mortality rates of CRC in China still showed an increasing trend in the past decades, with approximately 376,300 new cases and 191,000 deaths per year [3]. Recently, many previous studies have verified that the human intestinal microbiota, including microbiome, mycobiome, and virome, was one of the important factors associated with CRC [4–10]. Intestinal microbiota, one part of the tumor microenvironment, has attracted increasing attention, as it can affect CRC growth and spread in many ways. A variety of intestinal commensal bacteria and their metabolites are known for triggering inflammatory cascades and oncogenic signaling, thereby promoting genetic and epigenetic alterations in CRC development [11].

Increasing evidence indicated that intestinal dysbiosis plays vital roles in CRC initiation, progression, and metastasis. Our previous study has found that the structures of the intestinal microbiota altered significantly in CRC patients compared to healthy individuals, which found that *Fusobacterium*, *Porphyromonas*, *Peptostreptococcus*, and

Mogibacterium increased in CRC patients significantly [4]. These bacteria might influence CRC risk via cometabolism or metabolic exchange with the host. Wei et al. demonstrated that *Ruminococcus obeum* and *Allobaculum*-like bacteria were enriched in the feces of 1,2-dimethyl hydrazine treated rats developing precancerous mucosal lesions [12]. Wang et al. also found that an increase of opportunistic pathogens and a reduction of butyrate-producing bacteria may constitute a major structural imbalance of gut microbiota in these CRC patients [13]. Several bacterial species, such as *Fusobacterium nucleatum*, *Peptostreptococcus anaerobius*, and *Bacteroides clarus* [6, 14–16], have been implicated in the development of CRC, which could promote carcinogenesis upon invasion of host cells. In addition, Coker et al. also revealed CRC-associated mycobiome dysbiosis characterized by altered fungal composition and ecology, signifying that the gut mycobiome might also play a role in CRC development [5]. Recently, an international panel of experts from International Cancer Microbiome Consortium delivered a consensus statement on the role of the human microbiome in carcinogenesis [17], which emphasized that future studies should provide direct evidence to demonstrate the roles of the human commensal microbiome in the aetiopathogenesis of cancer including CRC.

Our present study, enrolling confirmed early-stage CRC subjects and matched healthy controls, aimed at assessing the abundant bacteria in the fecal microbiota with quantitative PCR and evaluating the functions of the gut mucosal barrier, which would demonstrate the altered composition of the fecal microbiota in early-stage CRC patients and host response in an easy and rapid way. These results might be helpful for CRC precise diagnosis and personalized treatment targeting on human microbiota.

2. Methods

2.1. Subjects' Selection. A total of 53 patients who were diagnosed with primary early-stage CRC (aged 46-75 years old) between January 2011 and March 2012 were consecutively recruited from the First Affiliated Hospital, School of Medicine, Zhejiang University, Zhejiang, China. The diagnosis and stages of CRC were based on NCCN clinical practice guidelines in oncology (2010 edition) [18]. None of the patients were on any medications before sample collection. 45 sex-, age-, and body mass index- (BMI-) matched healthy subjects were selected as controls from the same cohorts during a routine physical examination, which were also confirmed by screening colonoscopy and pathology later. The following exclusion criteria were established: obesity (BMI > 30); diabetes; hypertension; family history of CRC; previous colon or rectal surgery; gastrointestinal disorders such as irritable bowel syndrome (IBS) and inflammatory bowel disease (IBD); emergency colonoscopy; known active bacterial, fungal, and viral infections; and the use of probiotics, prebiotics, synbiotics, or antibiotics in the previous month. The study protocol was approved by the Ethics Committee of the First Affiliated Hospital, School of Medicine, Zhejiang University (Zhejiang, China). Written informed consent was obtained from all participants prior to the enrollment.

2.2. Sampling. Prior to bowel cleansing for scheduled colonoscopy, fecal samples and blood samples were collected from these participants. We collected approximately 2 g of fresh feces into a sterile plastic cup from these participants and kept these samples in an icebox. Samples for bacterial genomic DNA extraction were transferred immediately to the laboratory and stored at -80°C after preparation within 15 min until use. In addition, blood samples were also collected simultaneously from these participants for intestinal mucosal barrier function analysis. Plasma was also stored at -80°C after preparation within 15 min (Table 1 shows the details of the samples).

2.3. Bacterial Genomic DNA Extraction. Fecal genomic DNA was extracted using a QIAamp® DNA Stool Mini Kit (QIAGEN, Hilden, Germany) according to our previous studies [4, 19]. The amount of bacterial genomic DNA was analyzed using a NanoDrop ND-1000 spectrophotometer; the integrity and size of bacterial genomic DNA were checked by electrophoresis. All bacterial genomic DNA was stored at -80°C for further use.

2.4. Fecal Abundant Bacteria Analysis. For fecal abundant bacteria analysis, real-time quantitative PCR (qPCR) was performed on ABI Prism 7900HT real-time PCR system (Applied Biosystems, Carlsbad, CA) with a Power SYBR Green PCR Master Mix (Takara, Dalian, China) according to the manufacturer's instructions. The bacterial primer sets and the reaction conditions are shown in Table 2 [19, 20]. SDS 2.4 was used for the data analysis. Triplicate repeats were carried out for all reactions in every analysis with a nontemplate included. The quantity of these bacteria was presented as log10 bacteria per gram of feces (wet weight).

2.5. Intestinal Mucosal Barrier Function Analysis. The plasma from each participants was collected for intestinal mucosal barrier function analysis. The parameters of gut mucosal barrier function such as endotoxin (LPS), D-lactate, and diamine oxidase (DAO) were detected by a dry chemical method using the Intestinal Mucosal Barrier Biochemical Index Analysis System (JY-DLT, Beijing Zhongsheng Jinyu Diagnostic Technology Co., Ltd., China) [19, 21, 22]. The experiments were undergone according to the protocols suggested by the manufacturer and conducted within 4 h after plasma extraction.

2.6. Statistical Analysis. The quantitative data of fecal abundant bacteria and other parameters in our study are presented as the mean ± standard deviation (SD), the differences between the two groups were evaluated by Student's t test, and the correlations between variables were tested by Pearson correlation using SPSS version 20.0 (SPSS Inc., Chicago, IL.), respectively. $p < 0.05$ was considered statistically significant for all analyses.

3. Results

3.1. Characteristics of the Early-Stage CRC Patients. In our present study, these participants were all newly diagnosed early-stage CRC patients in our hospital, who were not

Table 1: Summary information of the samples.

	CRC	Control
Sample size	53	45
Age (years): mean ± SD	52.4 ± 18.8	53.7 ± 16.7
Gender (male/female)	33/20	25/20
BMI	24.8 ± 3.58	23.7 ± 3.67

treated with antibiotics, prebiotics, probiotics, and synbiotics in the previous month. Before sampling, these participants have been performed a complete physical examination such as colonoscopy and pathology, serological markers detection, and radiological examination. Most of the CRC patients (50/53) were found to be positive in fecal occult blood testing, while several patients (8/53) occurred severe diarrhoea. In our study, the BMI values and the serum liver function, kidney function, lipid levels, blood sugar, and blood pressure in the CRC patients were not different from healthy controls significantly ($p > 0.05$). However, the serological marker such as carcinoembryonic antigen (CEA) was increased significantly in CRC patients when compared with healthy controls ($p < 0.05$). Our study demonstrated that no any CRC patients were found to be positive in tumor metastasis.

3.2. Abnormal Fecal Microbiota in CRC Patients. In our present study, we investigated the abundant bacteria in the fecal microbiota by real-time quantitative PCR (Figure 1). The abundant bacteria represented the higher relative abundance of bacteria in the fecal microbiota, which would determine the overall structure and composition of the fecal microbiota. Ten abundant bacteria, which accounted for more than 90% of the total bacteria, were selected to explore the alterations of fecal microbiota in these CRC patients. We found that the copy numbers of the total bacteria were not significantly different between healthy controls and CRC patients. However, the traditional beneficial bacteria such as *Lactobacillus* and *Bifidobacterium* decreased significantly in CRC patients. In addition, the gut-indigenous *Clostridium* included several different clusters, including abundant clusters such as *Clostridium* cluster I, cluster XI, and cluster XIVb. Our data indicated that *Clostridium* cluster I was significantly decreased in CRC patients when compared with healthy controls, while *Clostridium* cluster XI and cluster XIVb were not significantly different between healthy controls and CRC patients. Another bacterium, Enterobacteriaceae, was considered as gut harmful bacteria, which could produce lipopolysaccharide into peripheral blood. We observed that Enterobacteriaceae was significantly increased in CRC patients when compared with healthy controls. *F. nucleatum* was the confirmed carcinogenic bacterium that associated with CRC development. Consistent with the previous studies, our results demonstrated that *F. nucleatum* was significantly increased in CRC patients when compared with healthy controls. Our data indicated that dysbiosis of fecal microbiota was found in CRC patients, which might be contributed to CRC initiation, progression, and metastasis.

3.3. Changed Intestinal Mucosal Barrier Function. The three parameters such as LPS, D-lactate, and DAO could be used to evaluate the integrity of the gut mucosal barrier. The increased permeability of the gut mucosal barrier was associated with increased systemic and local inflammation, which was closely correlated with the initiation and development of CRC. In our present study, we found obviously disturbed gut mucosal barrier in CRC patients when compared with healthy controls. Our data indicated that plasma D-lactate, a byproduct of bacterial metabolism, increased significantly in CRC patients when compared with healthy controls ($p < 0.01$; Figure 2(a)). LPS, a structural component of the cell wall of Gram-negative bacteria, was a potent inducer of proinflammatory cytokines that activate a systemic inflammatory response syndrome. Elevated LPS level has been reported to be an early marker of impaired mucosal barrier function. In our study, we also observed that the levels of LPS were significantly higher in the CRC patients than that in the healthy controls ($p < 0.01$; Figure 2(b)). In addition, DAO, an enzyme which deaminates histamine and polyamines, has its highest activity in the intestinal mucosa in most mammalian species, including humans. DAO activity has been shown to reflect changes associated with the gut mucosal barrier. Our data indicated that significant differences of DAO levels were observed between CRC patients and healthy controls ($p < 0.01$; Figure 2(c)). Taken together, our results showed that the loss of gut mucosal barrier integrity and function was found in CRC patients, which indicated that the impairment of gut mucosal barrier function might be one of the important factors for the initiation and development of CRC.

3.4. Correlations between Differential Bacteria and Indicators of Gut Mucosal Barrier. In our present study, Pearson correlation was used to examine the relationship between differential fecal bacteria and indicators of the gut mucosal barrier (Table 3). We found that the differential fecal bacteria such as *Lactobacillus*, *Bifidobacterium*, and *Clostridium* cluster I correlated with D-Lactate and endotoxin negatively ($p < 0.05$), while *Lactobacillus*, but not *Bifidobacterium* and *Clostridium* cluster I, correlated with DAO negatively ($p < 0.05$). In addition, we also found that *Fusobacterium nucleatum* and Enterobacteriaceae correlated positively with D-Lactate, DAO, and endotoxin ($p < 0.05$). Among these indicators of gut mucosal barrier, strong correlations (Pearson's $r \geq 0.50$) were observed between *Bifidobacterium* and endotoxin ($r = -0.752$, $p < 0.000$), between *Clostridium* cluster I and endotoxin ($r = -0.630$, $p < 0.000$), between *Fusobacterium nucleatum* and D-Lactate ($r = 0.809$, $p < 0.000$), and between Enterobacteriaceae and endotoxin ($r = 0.802$, $p < 0.000$).

4. Discussion

The development of human CRC is influenced by various risk factors, such as diets, genetic, epigenetic, environmental, and metabolic factors, while environmental factors are the predominant trigger for CRC [23]. A growing body of evidence has indicated that human gut microbiota may be an important environmental factor that promotes CRC development [15, 24]. With the advent of high-throughput

Table 2: Bacterial-specific primer sets for detection of fecal microbiota by qPCR.

PCR specificity	Primer	Sequence (5′→3′)	Annealing temperature (°C)	Amplicon size (bp)
Total bacteria	Uni331F	TCCTACGGGAGGCAGCAGT	58	466
	Uni797R	GGACTACCAGGGTATCTATCCTGTT		
Bacteroides-Prevotella group	Bac303F	GAAGGTCCCCCACATTG	56	418
	Bac708R	CAATCGGAGTTCTTCG		
Lactobacillus spp.	Lac-F	AGCAGTAGGGAATCTTCCA	58	341
	Lac-R	CACCGCTACACATGGAG		
Bifidobacterium spp.	Bifid-F	CTCCTGGAAACGGGTGG	55	550
	Bifid-R	GGTGTTCTTCCCGATATCTACA		
Clostridium cluster I	CG1-F	TACCHRAGGAGGAAGCCAC	63	700
	CG1-R	GTTCTTCCTAATCTCTACGCAT		
Clostridium cluster XI	CG2-F	ACGCTACTTGAGGAGGA	58	141
	CG2-R	GAGCCGTAGCCTTTCACT		
Clostridium cluster XIVab	CG3-F	GAWGAAGTATYTCGGTATGT	52	152
	CG3-R	CTACGCWCCCTTTACAC		
Faecalibacterium prausnitzii	Fpra-F	GATGGCCTCGCGTCCGATTAG	58	199
	Fpra-R	CCGAAGACCTTCTTCCTCC		
Fusobacterium nucleatum	Fn-F	CAACCATTACTTTAACTCTACCATGTTCA	60	112
	Fn-R	GTTGACTTTACAGAAGGAGATTATGTAAA AATC		
Enterobacteriaceae	Eco-F	CATTGACGTTACCCGCGAGAAGAAGC	63	195
	Eco-R	CTCTACGAGCTCAAGCTTGC		
Enterococcus spp.	ENco-F	CCCTTATTGTTAGTTGCCATCATT	61	144
	ENco-R	ACTCGTTGTACTTCCCATTGT		

sequencing platforms "omics" technologies and advanced bioinformatics approaches, the changes of the composition and function of the gut microbiota have been identified in the last decades, and the suspected causative roles and molecular mechanisms of gut microbiota in CRC development have been established by many previous studies. Recently, several bacterial species such as *Fusobacterium nucleatum* and *Peptostreptococcus anaerobius* have been confirmed in the CRC development and progression [14, 25]. These fecal bacteria have been considered as one of the most important elements of the tumor microenvironment. Now, fecal candidate bacteria can be used as novel biomarkers with existing methods, such as real-time qPCR and fecal immunochemical test, for noninvasive diagnosis of CRC [7].

With real-time qPCR, we found that the abundant fecal bacteria changed significantly in these early-stage CRC patients, which indicated that the dysbiosis of fecal microbiota might participate in CRC development and progression. In our present study, ten abundant bacteria were investigated to illustrate the alterations of fecal microbiota in CRC patients. In our present study, the two traditional beneficial bacteria such as *Lactobacillus* and *Bifidobacterium* (belonged to the lactic acid bacteria category) decreased significantly in these CRC patients, which were consistent with previous study [26]. Mendes et al. has found that the abundance of the genera *Lactobacillus* and *Bifidobacterium* increased significantly after microbiota modification by probiotic supplementation [27]. Increasing reports in recent years have shown that these bacteria have demonstrated a host of properties in preventing CRC development by inhibiting initiation or progression through multiple pathways, such as apoptosis, antioxidant DNA damages, immune responses, and epigenetics [28–30]. Although *Lactobacillus* and *Bifidobacterium* may only act before carcinogenesis and have little inhibitory impact on established cancer, these two beneficial bacteria were the most frequently used as probiotics to prevent colon carcinogenesis in animal models or patients, which might help regulate the CRC-related tumor microenvironment. Different from *Lactobacillus* and *Bifidobacterium*, Enterobacteriaceae was often considered as harmful bacteria in the fecal microbiota, which could induce inflammation in the host gut epithelium [31]. As inflammation has been a well-documented risk factor for various form of cancer [32], it was implicated that Enterobacteriaceae participated actively in the development and progression of CRC. Previous studies showed that the actions of Enterobacteriaceae are similar to the prolonged inflammatory response induced by enterotoxigenic *Bacteroides fragilis* [33, 34]. Sun et al. has showed significant enrichment of Enterobacteriaceae in the DMH-induced CRC animal model [35]. They also found that Enterobacteriaceae showed higher relative abundance in the early stages of tumor formation, while it was gradually replaced with other bacteria such as Rikenellaceae, Lachnospiraceae, Ruminococcaceae, and Streptococcaceae

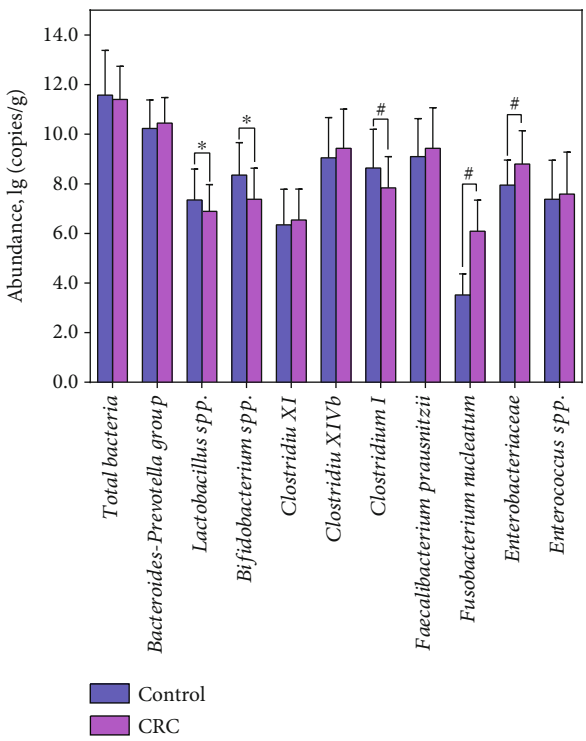

Figure 1: Quantitative real-time PCR analysis of the fecal abundant bacteria in patients with colorectal cancer (log10 copies per gram of fresh feces). $^{*}p < 0.05$; $^{\#}p < 0.01$.

[35]. Another potential cancer-promoting bacterium, *F. nucleatum*, was associated with CRC. Previous studies found that *F. nucleatum* is enriched in both the feces and colonic mucosa of CRC patients [4, 36, 37] and plays important roles in colorectal carcinogenesis [38, 39]. *F. nucleatum* may promote colorectal tumor growth and inhibit T cell-mediated immune responses against colorectal tumors [40]. Rubinstein et al. also found that *F. nucleatum* binds E-cadherin on epithelial cells and activates β-catenin signaling, driving epithelial cell proliferation [39]. With quantitative PCR and fecal immunochemical test, Liang and their colleagues found that *F. nucleatum* alone can discriminate CRC from controls with a sensitivity of 77.7%, and specificity of 79.5%, which can serve as a novel noninvasive diagnostic method for patients with CRC [7]. Mima et al. also found that the amount of *F. nucleatum* in CRC tissue is associated with shorter survival and may potentially serve as a prognostic biomarker [40]. Bullman et al. observed that treatment of mice bearing a CRC xenograft with the antibiotic metronidazole reduced *F. nucleatum* load, cancer cell proliferation, and overall tumor growth, which indicated that microbiota modulation as a potential treatment for *Fusobacterium*-associated colorectal carcinomas [41]. In addition, we also found that *Clostridium* cluster I decreased significantly in CRC patients when compared with healthy controls. Kostic et al. found that CRC tissues have decreased microbial diversity, including a reduction of certain bacterial genera like *Clostridium* and *Bacteroides* [42]. However, the genus *Clostridium* includes a diverse group of Gram-positive, spore-forming anaerobes [43]. In general, clostridial fermentative metabolism functions by the conversion of hexose sugars to butyrate, acetate, and CO_2 [44]. Our study firstly found that *Clostridium* cluster I was negatively correlated with CRC development. The present study indicated that the abundant bacteria in fecal microbiota participated actively in the development and progression of CRC.

The gut mucosal barrier is a functional unit organized as a multilayer system, and its multiple functions are crucial for maintaining gut homeostasis. The inherent property of the gut to act as a semipermeable barrier is crucial for the maintenance of health. Dysfunction of the gut mucosal barrier leads to increased translocation of commensal bacteria and their metabolites locally and systemically, triggering the inflammatory response. Gut inflammation results in excess production of proinflammatory cytokines that can in turn increase mucosal permeability by altering intercellular tight junction structure and induce apoptosis of intestinal epithelial cells. Numerous scientific evidences showed a significant association between impaired gut mucosal barrier and gastrointestinal/extraintestinal diseases [45–48]. Previous study has found that progression of colorectal neoplasia has been linked to alterations of tumor microenvironment and gut mucosal barrier function, which facilitate the interaction of microbial products with host pathways [11]. D-lactate, LPS, and DAO were three accepted and convenient indicators to evaluate the integrity of the gut mucosal barrier. The increased permeability of the gut mucosal barrier would lead to bacterial translocation that was accompanied by increasing levels of D-lactate, LPS, and DAO, which finally contribute to a number of intestinal diseases such as CRC. D-lactate, a bydroxycarboxylic acid produced by bacterial fermentation, is a useful indicator of increased gut permeability and gut barrier dysfunction. Our present study found that the level of D-lactate was increased significantly in CRC patients, which was correlated with *Lactobacillus*, *Bifidobacterium*, and *Clostridium* cluster I negatively and with *F. nucleatum* and Enterobacteriaceae positively, confirming the existence of gut mucosal barrier dysfunction. LPS is large molecules found in the outer membrane of Gram-negative bacteria. The increase in LPS is associated with bacterial translocation due to the impairment of intestinal epithelial cell [49]. Previous study has found that gut microbiota dysbiosis alters the intestinal barrier function, increases plasma LPS levels, which promotes endotoxemia, and contributes to the onset and development of CRC [50]. Our study also found that the concentration of LPS increased significantly in CRC patients, which was correlated with *Lactobacillus*, *Bifidobacterium*, and *Clostridium* cluster I negatively and with *F. nucleatum* and Enterobacteriaceae positively. The results suggest that there was an increased intestinal permeability in these CRC patients. DAO is an enzyme mainly produced in the small intestine involved in the histamine metabolism [51]. Yee et al. has found that an established first-line treatment for patients in T2DM, metformin, inhibits DAO activity [52]. Previous study also found that serum DAO activity decreased step-by-step significantly during anticancer drug therapy in human, which may be to serve as a useful predictor of gastrointestinal toxicity due to anticancer drug [53]. Our present data found that the levels of DAO also increased significantly

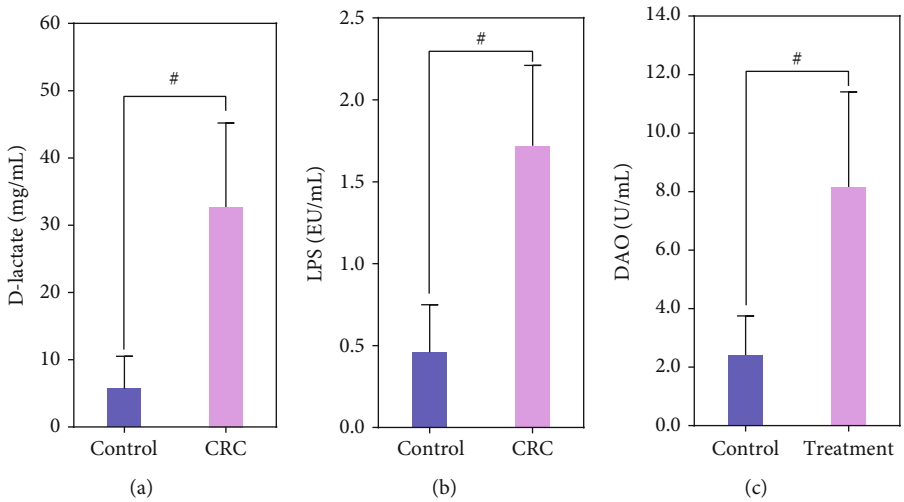

Figure 2: The alterations of the indicators of the gut mucosal barrier in patients with colorectal cancer. (a) D-lactate; (b) LPS; (c) DAO. $^{\#}p < 0.01$.

Table 3: Pearson's correlation coefficients between differential abundant bacteria and indicators of gut mucosal barrier.

	D-lactate (mg/ml)		DAO (U/ml)		LPS (EU/ml)	
	r	*p*	*r*	*p*	*r*	*p*
Lactobacillus	-0.314	0.043	-0.411	0.006	-0.456	0.002
Bifidobacterium	-0.385	0.011	-0.149	0.341	-0.752	0.000
Clostridium cluster I	-0.332	0.030	-0.252	0.103	-0.630	0.000
Fusobacterium nucleatum	0.809	0.000	0.339	0.026	0.456	0.002
Enterobacteriaceae	0.402	0.007	0.342	0.025	0.802	0.000

in CRC patients, which was correlated with *Lactobacillus*, *Bifidobacterium*, and *Clostridium* cluster I negatively and with *F. nucleatum* and Enterobacteriaceae positively. Taken together, the low levels of D-lactate, LPS, and DAO in normal conditions increased significantly in CRC patients, suggesting a breakdown of the gut mucosal barrier.

In summary, dysbiosis of the fecal microbiota, which was featured by altered abundant fecal bacteria, and dysfunction of the gut mucosal barrier, which was characterized by increased levels of D-lactate, LPS, and DAO, occurred in patients with early-stage CRC. The abundant bacteria in the feces and the indicators of the gut mucosal barrier in the plasma could be used as targets to monitor the development and progression of CRC in the future.

Data Availability

The data used to support the findings of this study are available from the corresponding author upon request.

Ethical Approval

All research conformed to the Helsinki Declaration and was approved by the Ethics Committee of the First Affiliated Hospital, School of Medicine, Zhejiang University (China), and was implemented in accordance with the approved guidelines.

Consent

Informed written consent was obtained from each of the patients before enrollment.

Conflicts of Interest

The authors declare that the research was conducted in the absence of any commercial or financial relationships that could be construed as a potential conflict of interest.

Authors' Contributions

XL and ZXL conceived and designed the experiments. XL, YWC, LS, and ZXL performed the experiments and analyzed the data. XL and ZXL wrote the paper and edited the manuscript. The final manuscript was read and approved by all authors. Xia Liu and Yiwen Cheng contributed equally to this work.

Acknowledgments

The authors thank all of the participants who recruited patients in this study. This present work was funded by the grants from the National Natural Science Foundation of China under Grant Nos. 31700800, 81771724, 81790631, and 31870839 and National S&T Major Project of China

under Grant No. 2018YFC2000500 and the Nutrition and Care of Maternal & Child Research Fund Project of Guangzhou Biostime Institute of Nutrition & Care (2019BINCMCF045).

References

[1] W. Chen, K. Sun, R. Zheng et al., "Cancer incidence and mortality in China, 2014," *Chinese Journal of Cancer Research*, vol. 30, no. 1, pp. 1–12, 2018.

[2] M. Araghi, I. Soerjomataram, A. Bardot et al., "Changes in colorectal cancer incidence in seven high-income countries: a population-based study," *Lancet Gastroenterol Hepatol*, vol. 4, no. 7, pp. 511–518, 2019.

[3] W. Chen, R. Zheng, P. D. Baade et al., "Cancer statistics in China, 2015," *CA: a Cancer Journal for Clinicians*, vol. 66, no. 2, pp. 115–132, 2016.

[4] W. Chen, F. Liu, Z. Ling, X. Tong, and C. Xiang, "Human intestinal lumen and mucosa-associated microbiota in patients with colorectal cancer," *PLoS One*, vol. 7, no. 6, article e39743, 2012.

[5] O. O. Coker, G. Nakatsu, R. Z. Dai et al., "Enteric fungal microbiota dysbiosis and ecological alterations in colorectal cancer," *Gut*, vol. 68, no. 4, pp. 654–662, 2019.

[6] S. H. Wong, L. Zhao, X. Zhang et al., "Gavage of fecal samples from patients with colorectal cancer promotes intestinal carcinogenesis in germ-free and conventional mice," *Gastroenterology*, vol. 153, no. 6, pp. 1621–1633.e6, 2017.

[7] Q. Liang, J. Chiu, Y. Chen et al., "Fecal bacteria act as novel biomarkers for noninvasive diagnosis of colorectal cancer," *Clinical Cancer Research*, vol. 23, no. 8, pp. 2061–2070, 2017.

[8] G. Nakatsu, X. Li, H. Zhou et al., "Gut mucosal microbiome across stages of colorectal carcinogenesis," *Nat Commun*, vol. 6, no. 1, 2015.

[9] J. Yu, Q. Feng, S. H. Wong et al., "Metagenomic analysis of faecal microbiome as a tool towards targeted non-invasive biomarkers for colorectal cancer," *Gut*, vol. 66, no. 1, pp. 70–78, 2016.

[10] G. Nakatsu, H. Zhou, W. K. K. Wu et al., "Alterations in enteric virome are associated with colorectal cancer and survival outcomes," *Gastroenterology*, vol. 155, no. 2, pp. 529–541.e5, 2018.

[11] T. Irrazabal, A. Belcheva, S. E. Girardin, A. Martin, and D. J. Philpott, "The multifaceted role of the intestinal microbiota in colon cancer," *Molecular Cell*, vol. 54, no. 2, pp. 309–320, 2014.

[12] H. Wei, L. Dong, T. Wang et al., "Structural shifts of gut microbiota as surrogate endpoints for monitoring host health changes induced by carcinogen exposure," *FEMS Microbiology Ecology*, vol. 73, no. 3, pp. 577–586, 2010.

[13] T. Wang, G. Cai, Y. Qiu et al., "Structural segregation of gut microbiota between colorectal cancer patients and healthy volunteers," *The ISME Journal*, vol. 6, no. 2, pp. 320–329, 2012.

[14] H. Tsoi, E. S. H. Chu, X. Zhang et al., "*Peptostreptococcus anaerobius* Induces Intracellular Cholesterol Biosynthesis in Colon Cells to Induce Proliferation and Causes Dysplasia in Mice," *Gastroenterology*, vol. 152, no. 6, pp. 1419–1433.e5, 2017.

[15] G. Zeller, J. Tap, A. Y. Voigt et al., "Potential of fecal microbiota for early-stage detection of colorectal cancer," *Molecular Systems Biology*, vol. 10, no. 11, p. 766, 2014.

[16] T. N. Y. Kwong, X. Wang, G. Nakatsu et al., "Association between bacteremia from specific microbes and subsequent diagnosis of colorectal cancer," *Gastroenterology*, vol. 155, no. 2, pp. 383–390.e8, 2018.

[17] A. J. Scott, J. L. Alexander, C. A. Merrifield et al., "International Cancer Microbiome Consortium consensus statement on the role of the human microbiome in carcinogenesis," *Gut*, vol. 68, no. 9, pp. 1624–1632, 2019.

[18] R. W. Burt, J. S. Barthel, K. B. Dunn et al., "NCCN clinical practice guidelines in oncology. Colorectal cancer screening," *Journal of the National Comprehensive Cancer Network*, vol. 8, no. 1, pp. 8–61, 2010.

[19] X. Xia, J. Chen, J. Xia et al., "Role of probiotics in the treatment of minimal hepatic encephalopathy in patients with HBV-induced liver cirrhosis," *Journal of International Medical Research*, vol. 46, no. 9, pp. 3596–3604, 2018.

[20] C. Tan, Z. Ling, Y. Huang et al., "Dysbiosis of intestinal microbiota associated with inflammation involved in the progression of acute pancreatitis," *Pancreas*, vol. 44, no. 6, pp. 868–875, 2015.

[21] Z. Ling, X. Liu, S. Guo et al., "Role of probiotics in mycoplasma pneumoniae pneumonia in children: a short-term pilot project," *Frontiers in Microbiology*, vol. 9, 2019.

[22] L. Shen, L. Ao, H. Xu et al., "Poor short-term glycemic control in patients with type 2 diabetes impairs the intestinal mucosal barrier: a prospective, single-center, observational study," *BMC Endocrine Disorders*, vol. 19, no. 1, p. 29, 2019.

[23] E. Nistal, N. Fernández-Fernández, S. Vivas, and J. L. Olcoz, "Factors determining colorectal cancer: the role of the intestinal microbiota," *Frontiers in Oncology*, vol. 5, p. 220, 2015.

[24] I. Sobhani, J. Tap, F. Roudot-Thoraval et al., "Microbial dysbiosis in colorectal cancer (CRC) patients," *PLoS One*, vol. 6, no. 1, article e16393, 2011.

[25] T. Yu, F. Guo, Y. Yu et al., "*Fusobacterium nucleatum* Promotes Chemoresistance to Colorectal Cancer by Modulating Autophagy," *Cell*, vol. 170, no. 3, pp. 548–563.e16, 2017.

[26] S. J. D. O'Keefe, "Diet, microorganisms and their metabolites, and colon cancer," *Nature Reviews Gastroenterology & Hepatology*, vol. 13, no. 12, pp. 691–706, 2016.

[27] M. C. S. Mendes, D. S. Paulino, S. R. Brambilla, J. A. Camargo, G. F. Persinoti, and J. B. C. Carvalheira, "Microbiota modification by probiotic supplementation reduces colitis associated colon cancer in mice," *World Journal of Gastroenterology*, vol. 24, no. 18, pp. 1995–2008, 2018.

[28] L. Zhong, X. Zhang, and M. Covasa, "Emerging roles of lactic acid bacteria in protection against colorectal cancer," *World Journal of Gastroenterology*, vol. 20, no. 24, pp. 7878–7886, 2014.

[29] S. Danese, "Inflammatory bowel disease and inflammation-associated colon cancer: partners in crime," *Current Drug Targets*, vol. 9, no. 5, p. 360, 2008.

[30] A. Nowak, A. Paliwoda, and J. Blasiak, "Anti-proliferative, pro-apoptotic and anti-oxidative activity of *Lactobacillus* and *Bifidobacterium* strains: a review of mechanisms and therapeutic perspectives," *Critical Reviews in Food Science and Nutrition*, vol. 59, no. 21, pp. 3456–3467, 2019.

[31] C. Lupp, M. L. Robertson, M. E. Wickham et al., "Host-mediated inflammation disrupts the intestinal microbiota and promotes the overgrowth of Enterobacteriaceae," *Cell Host & Microbe*, vol. 2, no. 2, pp. 119–129, 2007.

[32] E. Elinav, R. Nowarski, C. A. Thaiss, B. Hu, C. Jin, and R. A. Flavell, "Inflammation-induced cancer: crosstalk between

tumours, immune cells and microorganisms," *Nature Reviews Cancer*, vol. 13, no. 11, pp. 759–771, 2013.

[33] F. Housseau and C. L. Sears, "Enterotoxigenic *Bacteroides fragilis* (ETBF)-mediated colitis in Min (*Apc*+/-) mice: a human commensal-based murine model of colon carcinogenesis," *Cell Cycle*, vol. 9, no. 1, pp. 3–5, 2010.

[34] P. R. Mangan, L. E. Harrington, D. B. O'Quinn et al., "Transforming growth factor-β induces development of the T_H17 lineage," *Nature*, vol. 441, no. 7090, pp. 231–234, 2006.

[35] T. Sun, S. Liu, Y. Zhou et al., "Evolutionary biologic changes of gut microbiota in an 'adenoma-carcinoma sequence' mouse colorectal cancer model induced by 1, 2-dimethylhydrazine," *Oncotarget*, vol. 8, no. 1, pp. 444–457, 2017.

[36] J. Ahn, R. Sinha, Z. Pei et al., "Human gut microbiome and risk for colorectal cancer," *JNCI: Journal of the National Cancer Institute*, vol. 105, no. 24, pp. 1907–1911, 2013.

[37] M. Castellarin, R. L. Warren, J. D. Freeman et al., "Fusobacterium nucleatum infection is prevalent in human colorectal carcinoma," *Genome Research*, vol. 22, no. 2, pp. 299–306, 2012.

[38] A. D. Kostic, E. Chun, L. Robertson et al., "*Fusobacterium nucleatum* Potentiates Intestinal Tumorigenesis and Modulates the Tumor-Immune Microenvironment," *Cell Host & Microbe*, vol. 14, no. 2, pp. 207–215, 2013.

[39] M. R. Rubinstein, X. Wang, W. Liu, Y. Hao, G. Cai, and Y. W. Han, "*Fusobacterium nucleatum* Promotes Colorectal Carcinogenesis by Modulating E-Cadherin/ β-Catenin Signaling via its FadA Adhesin," *Cell Host & Microbe*, vol. 14, no. 2, pp. 195–206, 2013.

[40] K. Mima, R. Nishihara, Z. R. Qian et al., "Fusobacterium nucleatum in colorectal carcinoma tissue and patient prognosis," *Gut*, vol. 65, no. 12, pp. 1973–1980, 2016.

[41] S. Bullman, C. S. Pedamallu, E. Sicinska et al., "Analysis ofFusobacteriumpersistence and antibiotic response in colorectal cancer," *Science*, vol. 358, no. 6369, pp. 1443–1448, 2017.

[42] A. D. Kostic, D. Gevers, C. S. Pedamallu et al., "Genomic analysis identifies association of Fusobacterium with colorectal carcinoma," *Genome Research*, vol. 22, no. 2, pp. 292–298, 2012.

[43] P. Patakova, M. Linhova, M. Rychtera, L. Paulova, and K. Melzoch, "Novel and neglected issues of acetone-butanol-ethanol (ABE) fermentation by clostridia: *Clostridium* metabolic diversity, tools for process mapping and continuous fermentation systems," *Biotechnol Adv*, vol. 31, no. 1, pp. 58–67, 2013.

[44] J. B. Therien, J. H. Artz, S. Poudel et al., "The physiological functions and structural determinants of catalytic bias in the [FeFe]-hydrogenases CpI and CpII of Clostridium pasteurianum strain W5," *Frontiers in Microbiology*, vol. 8, p. 1305, 2017.

[45] F. Scaldaferri, M. Pizzoferrato, V. Gerardi, L. Lopetuso, and A. Gasbarrini, "The gut barrier: new acquisitions and therapeutic approaches," *Journal of Clinical Gastroenterology*, vol. 46, pp. S12–S17, 2012.

[46] C. R. Weber and J. R. Turner, "Inflammatory bowel disease: is it really just another break in the wall?," *Gut*, vol. 56, no. 1, pp. 6–8, 2007.

[47] A. Fasano, "Leaky gut and autoimmune diseases," *Clinical Reviews in Allergy & Immunology*, vol. 42, no. 1, pp. 71–78, 2012.

[48] Q. Mu, J. Kirby, C. M. Reilly, and X. M. Luo, "Leaky gut as a danger signal for autoimmune diseases," *Frontiers in Immunology*, vol. 8, p. 598, 2017.

[49] J. M. Cavaillon, "Exotoxins and endotoxins: inducers of inflammatory cytokines," *Toxicon*, vol. 149, pp. 45–53, 2018.

[50] A. Gonzalez-Sarrias, M. A. Nunez-Sanchez, M. A. Avila-Galvez et al., "Consumption of pomegranate decreases plasma lipopolysaccharide-binding protein levels, a marker of metabolic endotoxemia, in patients with newly diagnosed colorectal cancer: a randomized controlled clinical trial," *Food & Function*, vol. 9, no. 5, pp. 2617–2622, 2018.

[51] L. Zhao, L. Luo, W. Jia et al., "Serum diamine oxidase as a hemorrhagic shock biomarker in a rabbit model," *PLoS One*, vol. 9, no. 8, article e102285, 2014.

[52] S. W. Yee, L. Lin, M. Merski et al., "Prediction and validation of enzyme and transporter off-targets for metformin," *Journal of Pharmacokinetics and Pharmacodynamics*, vol. 42, no. 5, pp. 463–475, 2015.

[53] J. Miyoshi, H. Miyamoto, T. Goji et al., "Serum diamine oxidase activity as a predictor of gastrointestinal toxicity and malnutrition due to anticancer drugs," *Journal of Gastroenterology and Hepatology*, vol. 30, no. 11, pp. 1582–1590, 2015.

Hindawi
BioMed Research International
Volume 2024, Article ID 9820370, 1 page
https://doi.org/10.1155/2024/9820370

Retraction

Retracted: Component-Resolved Diagnostic Study of Egg Allergy in Northern Chinese Children

BioMed Research International

Received 12 March 2024; Accepted 12 March 2024; Published 20 March 2024

This article has been retracted by Hindawi following an investigation undertaken by the publisher [1]. This investigation has uncovered evidence of one or more of the following indicators of systematic manipulation of the publication process:

(1) Discrepancies in scope

(2) Discrepancies in the description of the research reported

(3) Discrepancies between the availability of data and the research described

(4) Inappropriate citations

(5) Incoherent, meaningless and/or irrelevant content included in the article

(6) Manipulated or compromised peer review

The presence of these indicators undermines our confidence in the integrity of the article's content and we cannot, therefore, vouch for its reliability. Please note that this notice is intended solely to alert readers that the content of this article is unreliable. We have not investigated whether authors were aware of or involved in the systematic manipulation of the publication process.

Wiley and Hindawi regrets that the usual quality checks did not identify these issues before publication and have since put additional measures in place to safeguard research integrity.

We wish to credit our own Research Integrity and Research Publishing teams and anonymous and named external researchers and research integrity experts for contributing to this investigation.

The corresponding author, as the representative of all authors, has been given the opportunity to register their agreement or disagreement to this retraction. We have kept a record of any response received.

References

[1] J. Zhang, Y. Shen, J. Li, H. Li, and P. Si, "Component-Resolved Diagnostic Study of Egg Allergy in Northern Chinese Children," *BioMed Research International*, vol. 2020, Article ID 3831087, 9 pages, 2020.

Hindawi
BioMed Research International
Volume 2020, Article ID 3831087, 9 pages
https://doi.org/10.1155/2020/3831087

Research Article

Component-Resolved Diagnostic Study of Egg Allergy in Northern Chinese Children

Jiayi Zhang,[1] **Yongming Shen**,[1] **Junpu Li**,[2] **Huiqiang Li**,[3] **and Ping Si**[1]

[1]*Department of Medical Laboratory, Tianjin Children's Hospital, Tianjin, China*
[2]*Department of Clinical Laboratory, Tianjin Chest Hospital, Tianjin, China*
[3]*School of Medical Laboratory, Tianjin Medical University, Tianjin, China*

Correspondence should be addressed to Ping Si; kangsiping@live.cn

Received 16 January 2020; Accepted 24 February 2020; Published 11 March 2020

Academic Editor: Gang Liu

Background. Egg component-specific IgE can be useful to evaluate and diagnose egg allergy, but their prevalence and clinical significance remain unclear in the local population. Previous studies have led to contradictory results regarding the value of specific IgG and specific IgG4 in sensitization. *Objective*. We aimed to determine the level of specific IgE, IgG, and IgG4 antibodies to the major egg allergens in egg-allergic children. *Methods*. Children from 6 months to 10 years of age were recruited. Egg allergy was confirmed by either a strong clinical history or an increased egg white-sIgE level. Other allergies were diagnosed by reactivity to other allergens but without egg-related symptoms and history. The serum sIgE, sIgG, and sIgG4 levels to major egg allergenic components (Gal d 1, Gal d 2, Gal d 3, Gal d 4, and Gal d 5), sIgE level to egg white, and tIgE level were determined by light-initiated chemiluminescent assay (LICA), ELISA, or ImmunoCAP. *Results*. Egg-allergic children had significantly higher levels of sIgE, sIgG, and sIgG4 to egg components than nonallergic children. Gal d 2 was the predominant allergen, and Gal d 2 sIgE level correlated with the egg white-sIgE level. Ratios of sIgE/sIgG4 to egg components were highest before 1 year of age and dropped gradually in the first decade of life. *Conclusion*. Patterns of sIgE to egg components could distinguish different forms of egg allergy. Ratios of sIgE/sIgG4 could be useful in predicting tolerance in egg-sensitive subjects, but this needs further evaluation and investigation using more accurate models.

1. Introduction

Egg is one of the earliest food resources introduced during childhood, and egg allergy (EA) has become one of the most common pediatric food allergy problems globally. EA may include IgE- and/or non-IgE-mediated reactions, and it is estimated to affect 0.5-2% infants and children [1, 2]. The high prevalence is partly due to immature immune responses; hence, most EA children will develop clinical tolerance by school age. However, a small proportion of EA children's symptoms will persist and not be resolved until adolescence [3, 4].

The function of specific IgE (sIgE) in EA pathogenesis has been well described as the majority of symptoms of EA are related to IgE-related type I hypersensitivity reactions. As a widely used *in vitro* test, immunoassay of serum sIgE to egg has been proven to be an effective method to evaluate potential EA patients and to predict clinical reactions to oral food challenges with less exposure risks and less likelihood of interference from prior treatments [5].

Component-resolved diagnostics (CRD) have introduced the application of sIgE to allergen components and thus extended the allergen repertoire to a more precise sensitization profile [6]. Egg allergens are composed of more than 20 types of proteins and glycoproteins, among which the most predominant ones are Gal d 1 (ovomucoid), Gal d 2 (ovalbumin), Gal d 3 (ovotransferrin, conalbumin), Gal d 4 (egg white lysozyme) from egg white, and Gal d 5 (alpha-livetin) from egg yolk [7]. Gal d 1 is associated with allergy to heated egg and persistent allergy due to its stability in the

Table 1: Characteristics of other allergy, egg-allergy, and nonallergic subjects.

	Group A Other allergies	Group EA Egg allergy	Group NA Control	p value
n	39	56	35	
Age (y), median (range)	2.7 (0.5-8)	3.2 (0.5-8)	3 (0.5-10)	0.219
Male subjects, no. (%)	24 (61.5)	37 (66.1)	20 (57.1)	0.689
Total IgE (kU/L), median (range)	75 (2-1006)	193 (9-2166)	42 (2-312)	<0.001**
Egg white-sIgE (kU_A/L), median (range)	<0.35	1.4 (0.37-100)	<0.35	<0.001**

p values were calculated by performing Student's t-test, chi-square test (frequencies), and Kruskal-Wallis test. The lower and upper limits of egg-sIgE detection assay are 0.35 and 100 kU_A/L. A: atopic; EA: egg allergy; NA: nonatopic; sIgE: specific IgE.

presence of heat and proteinases, whereas other allergens, such as Gal d 2, are related to uncooked rather than cooked egg allergy [4]. Although the allergenicity of individual allergens has been investigated based on their molecular structures and biological properties, there is limited information about the diagnostic value of sIgE to egg components [8].

There are still ongoing debates concerning the function of specific IgG (sIgG) and specific IgG4 (sIgG4) during the process of EA, although sIgG is reported to trigger anaphylaxis as well [9]. Egg sIgG and sIgG4 are found in both atopic and healthy children, so they are not considered as recommended markers of allergic status [10, 11]. However, recent studies proposed that the sIgG4 or sIgE/sIgG4 ratio to egg or egg proteins could be a marker of tolerance either naturally occurring or after immunotherapy [12–14].

The aim of this study is to evaluate the polyisotypic responses to egg components for CRD in children from northern China and to investigate potential markers of sensitization and resolution in EA patients.

2. Materials and Methods

2.1. Subjects. 130 children were included in this study, and all of whom were recruited from Tianjin Children's Hospital, China. The egg-allergic group included 56 children with typical symptoms (including cutaneous, respiratory, and gastrointestinal symptoms) and either a convincing history of clinical reaction after egg consumption ($n = 13$) or an increased egg-specific serum IgE level above 2 kU_A/L (ImmunoCAP, Phadia, Uppsala, Sweden) ($n = 43$) [15]. The atopic group consisted of 39 patients with other allergen reactivities but no egg-related clinical symptoms and history, while the control subjects comprised 35 patients recruited from a surgical department with neither symptoms nor history of allergy. Due to the limited funding of our research and vulnerable relationship between clinicians and patients, provoking tests, like oral food challenges or skin prick test (SPT), were not conducted in our study. No subjects included in this study had received immunotherapy, such as glucocorticoid or antihistamine therapy. All recruited subjects who had received immunotherapy were excluded. There were no significant differences between groups in terms of age, gender, or ethnicity. Sera of all groups were collected at the time of study entry. The study was approved by the Ethics Committee of Tianjin Children's Hospital, and informed consent was obtained.

Table 2: Summary of clinical manifestation of children in the egg-allergic group.

Symptoms	N	Frequency (%)
Eczema	14	25
Urticaria	10	17.9
Other skin symptoms	6	10.7
Asthma	3	5.4
Coughing	3	5.4
Diarrhea	3	5.4
Conjunctivitis	2	3.6

2.2. Determination of Total IgE and Egg-Specific IgE Levels. Total serum IgE and egg white-specific IgE levels were determined by using ImmunoCAP (Phadia, Uppsala, Sweden) and Phadia 250 system. Samples with sIgE to egg white $\geq$ 0.35 kU_A/L were defined as positive.

2.3. Determination of Egg Component-Specific Immunoglobulin Levels. Specific IgE and specific IgG4 to egg components Gal d 1, Gal d 2, Gal d 3, Gal d 4, and Gal d 5 were determined by light-initiated chemiluminescent assay (LICA): methodological details are described elsewhere [16, 17]. The results of sIgE and sIgG4 were calculated as relative light units (RLU). The relative prevalence of single component-sIgE was calculated by comparing sIgE levels in the EA group with the mean value of sIgE levels in the atopic and control groups. The cutoff value was defined as two standard deviations above mean values for both the atopic and control groups.

Specific IgG to egg components Gal d 1, Gal d 2, Gal d 3, Gal d 4, and Gal d 5 were determined by ELISA. Gal d 1 (cat# T2011), Gal d 2 (cat# A5503), Gal d 3 (cat# C0755), and Gal d 4 (cat# L6876) were purchased from Sigma-Aldrich, USA. Gal d 5 (cat# CSA62) was purchased from Equitech-Bio, Inc., USA. Allergen-coated wells were prepared by adding 100 μL phosphate-buffered saline- (PBS-) diluted (20 μg/mL) allergen to each well of 96-well plates and incubating at 4°C overnight. Then, the plates were washed 3 times with PBS containing 0.05% Tween 20 (PBST), before blocking at

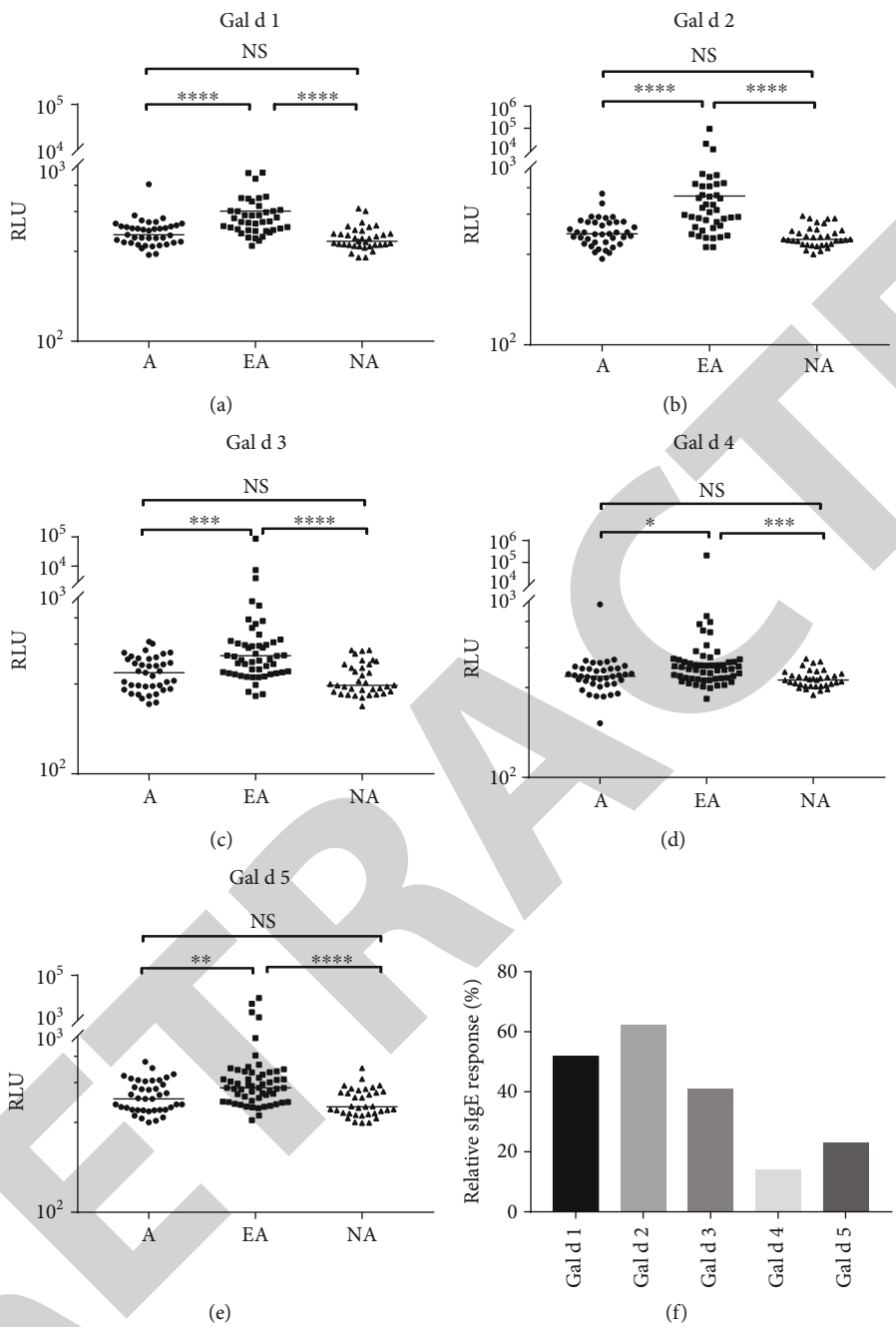

Figure 1: sIgE levels to 5 types of egg protein components (Gal d 1-Gal d 5) in all groups (a–e) and prevalence of sIgE response in the EA group (f). Levels of specific IgE (RLU) to 5 types of egg allergy protein were measured in all subjects, and relative sIgE response was determined by comparing the data from the egg allergy group to the other two groups. p values were calculated with the Kruskal-Wallis test and Mann-Whitney U test, when appropriate. sIgE: specific IgE; NA: nonatopic; EA: egg allergy; A: atopic; NS: not significant; RLU: relative light units; $^{*}p < 0.01$; $^{**}p < 0.001$; $^{***}p < 0.0001$; $^{****}p < 0.00001$.

37°C for an hour with 150 μL 3% bovine serum albumin (BSA). After that, 100 μL PBST-diluted sera (1 : 20) were added to the plates and incubated for an hour at 37°C. Subsequently, plates were washed with PBST again, and 100 μL horseradish peroxidase- (HRP-) conjugated anti-human IgG (purchased from Sigma-Aldrich, USA) (1 : 2000) diluted in PBST was added and incubated for 30 min at 37°C. 3,3′,5,5′-Tetramethylbenzidine (TMB) was added to develop the plates in the dark for 5 min, and 10% H_2SO_4 was added to terminate the reaction. OD values of the plates were measured at 450 nm immediately. The results of sIgG were calculated as the absorbance units (AU)/mL.

2.4. Statistical Analyses. Data and graphs were analyzed and generated by using GraphPad Prism 7 (GraphPad Software Inc., San Diego, CA, USA). Comparisons of general

characteristics between groups were determined using Student's t-test, chi-square test (frequencies), and Kruskal-Wallis test.

Comparisons of sIgE, sIgG, and sIgG4 levels between groups were determined using the Kruskal-Wallis test. Once significant differences were found, the Mann-Whitney U test was performed to further evaluate differences between every two groups. Correlations were calculated with Spearman's rank order correlation coefficient test. A p value of <0.05 was considered to be statistically significant.

3. Results

3.1. Participants and Clinical History. Children in the egg-allergic, atopic, and control groups were similar in terms of age and gender. Members of the egg-allergic and other allergic groups had significantly higher total IgE levels and wider ranges of total IgE compared with control subjects. As expected, children in the egg-allergic group had a higher level of egg white-sIgE, whereas subjects in the other two groups had no detectable egg white-specific IgE (Table 1).

The most typical symptoms in egg allergy patients were cutaneous reactions, including eczema, urticaria, and other symptoms, which were observed in 30 (54%) children in this group.

Only a small proportion of patients presented with respiratory symptoms (asthma), gastrointestinal symptoms (diarrhea), and oral allergy syndromes (coughing and conjunctivitis) in the egg atopic group (Table 2). Of 56 egg-allergic children, 13 (23%) had reported a reaction to egg or egg-related food, and 7 (12%) had a parental history of atopy.

3.2. Egg Protein-Specific IgE Levels. Levels of sIgE to individual egg proteins were measured in all groups, whereas the allergenicity (IgE binding activity) was only determined in egg atopic participants. Patients with egg allergy had a significantly higher sIgE response to all 5 egg components than other atopic and nonatopic children, but these sIgE levels showed no statistical difference between other atopic and nonatopic patients (Figures 1(a)–1(e)). The higher sIgE relative values of EA children compared to other groups tended to be more significant in Gal d 2 and Gal d 3 than in other components (Figures 1(b) and 1(c)). Among the allergens in our study, Gal d 2 and Gal d 1 were the most allergenic, with 62.5% EA patients and 51.8% EA patients, respectively, showing a detectable sIgE. Of 56 EA children, 41.1% had detectable sIgE responses to Gal d 3, which were also higher compared with 14.3% to Gal d 4 and 23.2% to Gal d 5 (Figure 1(f)).

We found that in the EA group, Gal d 2 sIgE had the highest frequency of response in almost all egg component-sIgE screening-positive subjects (35 of 38, 92.1%). By contrast, Gal d 4 sIgE was only found in 3 patients with 4-type sIgE positive and 5 patients were allergic to all 5 components. And all participants who had Gal d 4 sIgE had a combination of sIgE to Gal d 1, Gal d 2, and Gal d 3. About one-third of the egg-allergic children (18 of 56, 32.1%) showed no IgE reaction to any of the 5 egg components examined (Table 3).

Table 3: Patterns of sensitization to egg components in children with EA ($N = 56$).

Types of sIgE detected	Pattern of sIgE combination	N
0	NA	18
1	Gal d 1	1
	Gal d 2	5
	Gal d 3	1
	Gal d 5	1
2	Gal d 1+Gal d 2	7
	Gal d 1+Gal d 2+Gal d 3	8
3	Gal d 1+Gal d 2+Gal d 5	1
	Gal d 2+Gal d 3+Gal d 5	2
4	Gal d 1+Gal d 2+Gal d 3+Gal d 4	3
	Gal d 1+Gal d 2+Gal d 3+Gal d 5	4
5	Gal d 1+Gal d 2+Gal d 3+Gal d 4+Gal d 5	5

More than a half of the egg allergy patients (30 of 56, 53.6%) had more than one type of egg protein-specific IgE (Table 3), while only 8 children (14.3%) had one single detectable sIgE among the studied allergens (Figures 2(a) and 2(b)). Levels of egg white-sIgE correlated significantly with numbers of egg component-sIgE detected ($r = 0.4876$, $p = 0.0001$) and levels of Gal d 2 sIgE ($r = 0.4855$, $p = 0.0001$) in egg-atopic subjects (Figures 2(c) and 2(d)).

3.3. Egg Protein-Specific IgG and IgG4 Levels. Egg component protein-sIgG and sIgG4 levels were determined in all subjects. A significantly higher IgG response to allergens was seen among EA and atopic children versus nonatopic children. When compared with the atopic group, the EA group had a statistically higher sIgG level to all proteins except for Gal d 5 (Figure 3).

Children with EA had the highest levels of sIgG4 to Gal d 1 and Gal d 2 compared with the other two groups, and there is no statistical difference between other atopic and nonatopic subjects. For Gal d 3, Gal d 4, and Gal d 5, EA children had a higher sIgG4 response than nonatopic participants, whereas the difference between other atopic and egg-allergic subjects and between other atopic and nonatopic subjects was not significant (Figure 4).

3.4. Egg Protein-sIgE/sIgG4 Ratio among EA Children of Different Ages. In EA infants below 1 year old, sIgE/sIgG4 ratios to all egg components were similar in number (range: 3-9). After that, the sIgE/sIgG4 ratios of Gal d 1 and Gal d 2 dropped steeply in the early stage of childhood. Then, the trends began to decrease slowly until reaching a steady and low level (approximately 0.01) at around 6 years old.

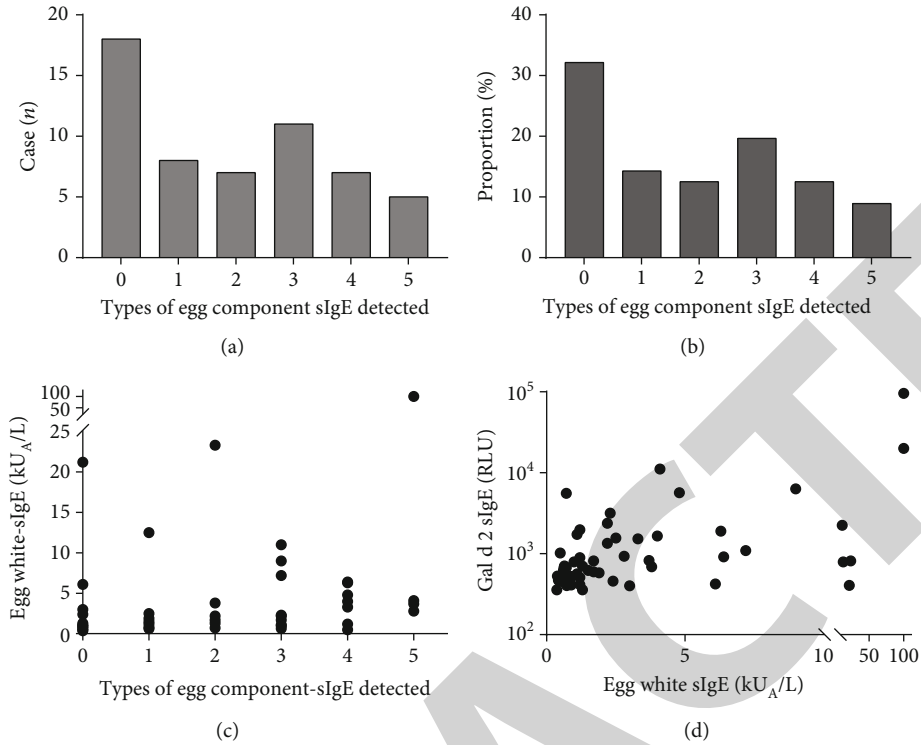

Figure 2: Prevalence of multicomponent-sIgE in children with egg allergy. The number of cases (a), proportion of cases (b), and egg white-sIgE (kU$_A$/L) levels (c) with multiple types of protein-sIgE detected in the EA group. Correlation of Gal d 2 sIgE (RLU) levels (d) and egg white-sIgE (kU$_A$/L) levels in EA patients. Correlations were calculated by using Spearman's rank order correlation coefficient test. sIgE: specific IgE; EA: egg allergy.

In contrast, the sIgE/sIgG4 ratios of components Gal d 3, Gal d 4, and Gal d 5 in EA children showed a slight drop before 4 years of age; then, the ratios remained steadily at about 0.3 for Gal d 3 and about 1 for Gal d 4 and Gal d 5. After 7 years old, Gal d 3, Gal d 4, and Gal d 5 sIgE/sIgG4 ratios began to decline to a lower level in EA patients (Figure 5).

4. Discussion

A bead-based light-initiated chemiluminescent assay (LICA) system was demonstrated in our previous studies to determine serum egg component-sIgE and sIgG4 profiles. LICA has been proven to have excellent analytical performances and a good correlation with Phadia ImmunoCAP tests in sIgE measurement [16, 17]. Yet, only a limited profile of allergy tests has been introduced in our country; LICA could be a reliable complement in allergy screening and diagnosis. The advent of component-resolved diagnostics (CRD) had eliminated the cross-reactivity of conventional allergen extract sIgE assays and brought more detailed perspectives in assessing sensitization [6]. By using LICA technology, specific immunoglobulin to allergenic egg proteins could be quantified to characterize immune responses in children with different sensitization statuses.

In our study, EA patients produced significantly more egg component-sIgE than other groups. The highest frequency of positive responses was seen in Gal d 1 and Gal d 2, while Gal d 4 sIgE was the least common in EA subjects. These results were comparable with other findings [18, 19]. A previous study has presented similar reactive rates to our results in egg-allergic patients [20], while another study showed more Gal d 1 sIgE cases than Gal d 2 [19]. This may be due to the different age ranges of the subjects, different cooking effects on egg allergenicity, timing of egg introduction, and racial differences. Another interesting finding of this study was that about a third of EA patients had no component-sIgE detected. The reasons for this might be that other egg components, not identified in our study, were involved, like ovomucin, prostaglandin D synthase, and cystatin from egg white or vitellenin (apovitellenin I) and apoprotein B (apovitellenin VI) from yolk [2]. Furthermore, this also indicates that although CRD can provide a more personalized sensitization pattern, it cannot yet substitute for allergen extracts-sIgE tests. Egg component-sIgG and sIgG4 were detected not only in EA subjects but also in the atopic group and the control group. This is consistent with findings from other studies [21]. Previous studies have proposed that levels of egg and Gal d 2 (ovalbumin) sIgG and sIgG4 had no significant difference in sensitive, tolerant, and control subjects [11, 22]. However, our results suggested that this might not necessarily be the case, as the EA group

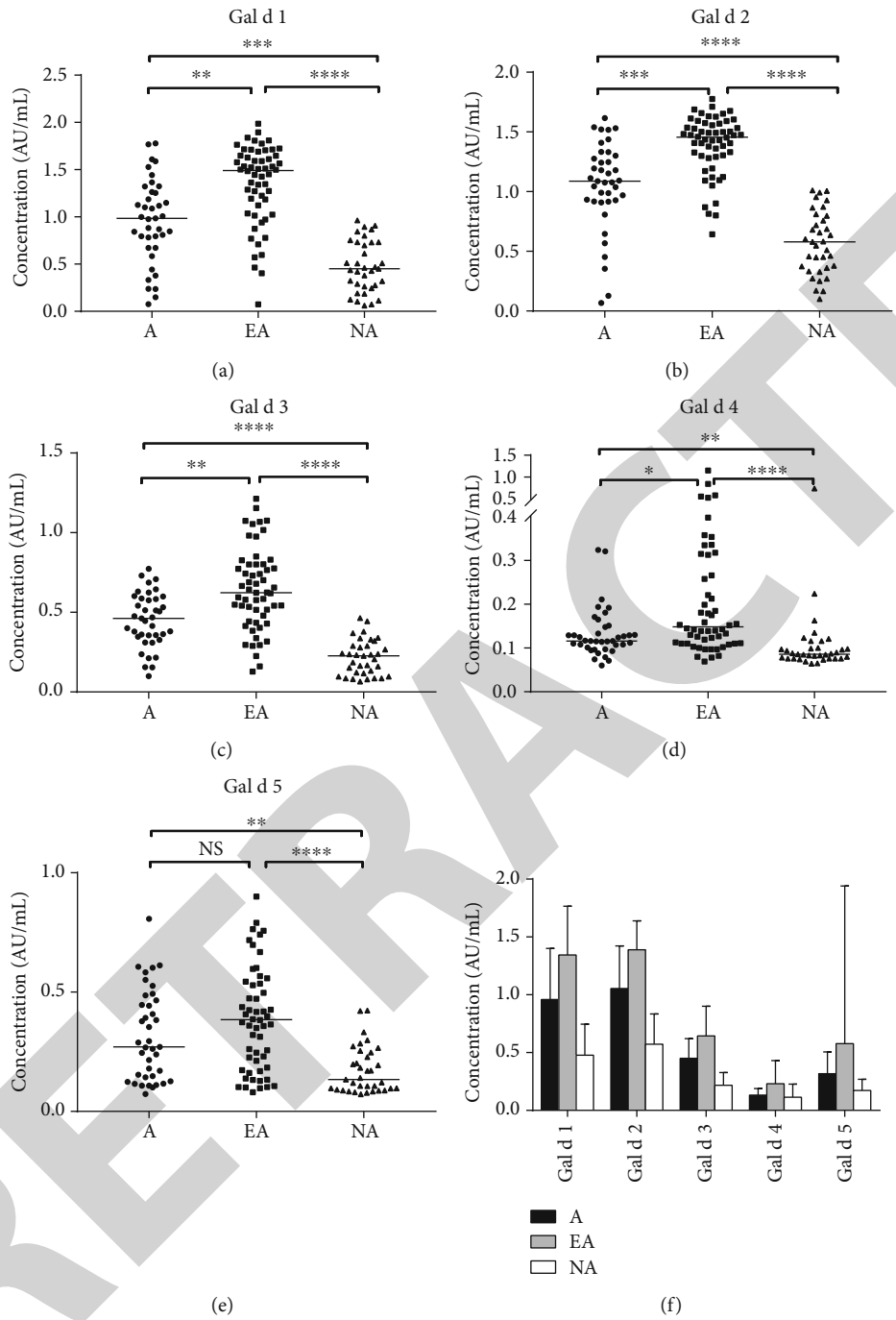

Figure 3: Egg protein components (Gal d 1-Gal d 5) sIgG levels in the A, EA, and NA groups (a–e) and comparison of antigenicity in all groups (f). Levels of specific IgG (AU/mL) to 5 types of egg allergy protein were determined and compared in all subjects. Boxes represent means and SDs of the values. p values were calculated by using the Kruskal-Wallis test and Mann-Whitney U test, when appropriate. sIgG: specific IgG; NA: nonatopic; EA: egg allergy; A: atopic; NS: not significant; $^{*}p < 0.01$; $^{**}p < 0.001$; $^{***}p < 0.0001$; $^{****}p < 0.00001$.

and the atopic group both had a higher component-sIgG level than nonatopic children. This is in line with the recent findings of IgE-sensitized children having more IgG responses due to induced gut permeability [10]. We further demonstrated that the EA group had higher egg protein-sIgG4 levels than the control group, which agreed with the work reported by Ruiter et al. [23]. Oral challenge tests were not performed in our study; thus, our EA patients might include allergic but tolerant individuals, and this could contribute to higher levels of sIgG4, which is regarded as an indicator of tolerance [12]. To identify the status of tolerance in egg-allergic children, egg protein-sIgE/sIgG4 ratios were investigated in previous studies [14, 24], and our study extended the findings to 5 egg

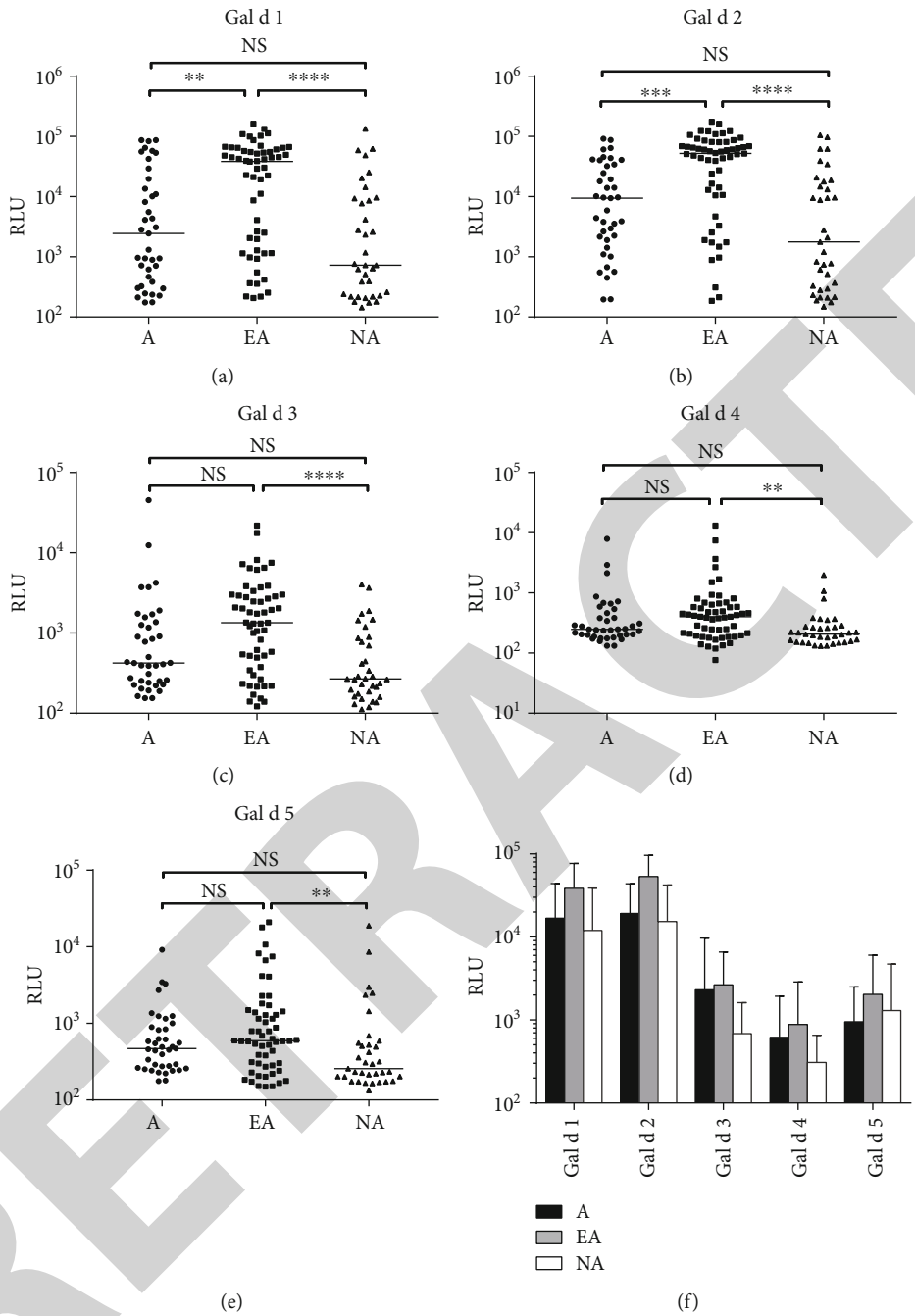

Figure 4: sIgG4 levels to 5 types of egg protein components (Gal d 1-Gal d 5) in all groups (a–e) and comparison of their relative values (f). Levels of specific IgG4 (RLU) to 5 types of egg components were determined and compared in all subjects. Boxes represent means and SDs of the values. p values were calculated using the Kruskal-Wallis test and Mann-Whitney U test, when appropriate. sIgG4: specific IgG4; NA: nonatopic; EA: egg allergy; A: atopic; RLU: relative light units; NS: not significant. $^{*}p < 0.01$; $^{**}p < 0.001$; $^{***}p < 0.0001$; $^{****}p < 0.00001$.

proteins. The trends of sIgE/sIgG4 ratios were found to have association with the resolution process of egg allergy [4]. Also, the Gal d 2 (ovalbumin) sIgE/sIgG4 ratio, along with the skin prick test, has been reported to perform better in distinguishing both cooked and uncooked egg tolerance [14]. Therefore, further work is required to assess the clinical value of egg protein-sIgE/sIgG4 ratios in the local population.

In summary, egg protein component-sIgE can be predictive in egg allergy diagnostics and the allergenicity varies widely in each component. Although sIgG levels to egg proteins were not necessarily associated with egg sensitization, we proposed that component-sIgE/sIgG4 ratios could be promisingly indicative for monitoring the status of tolerance in EA patients. Furthermore, CRD can provide evidence for more accurate desensitization, more personalized dietary

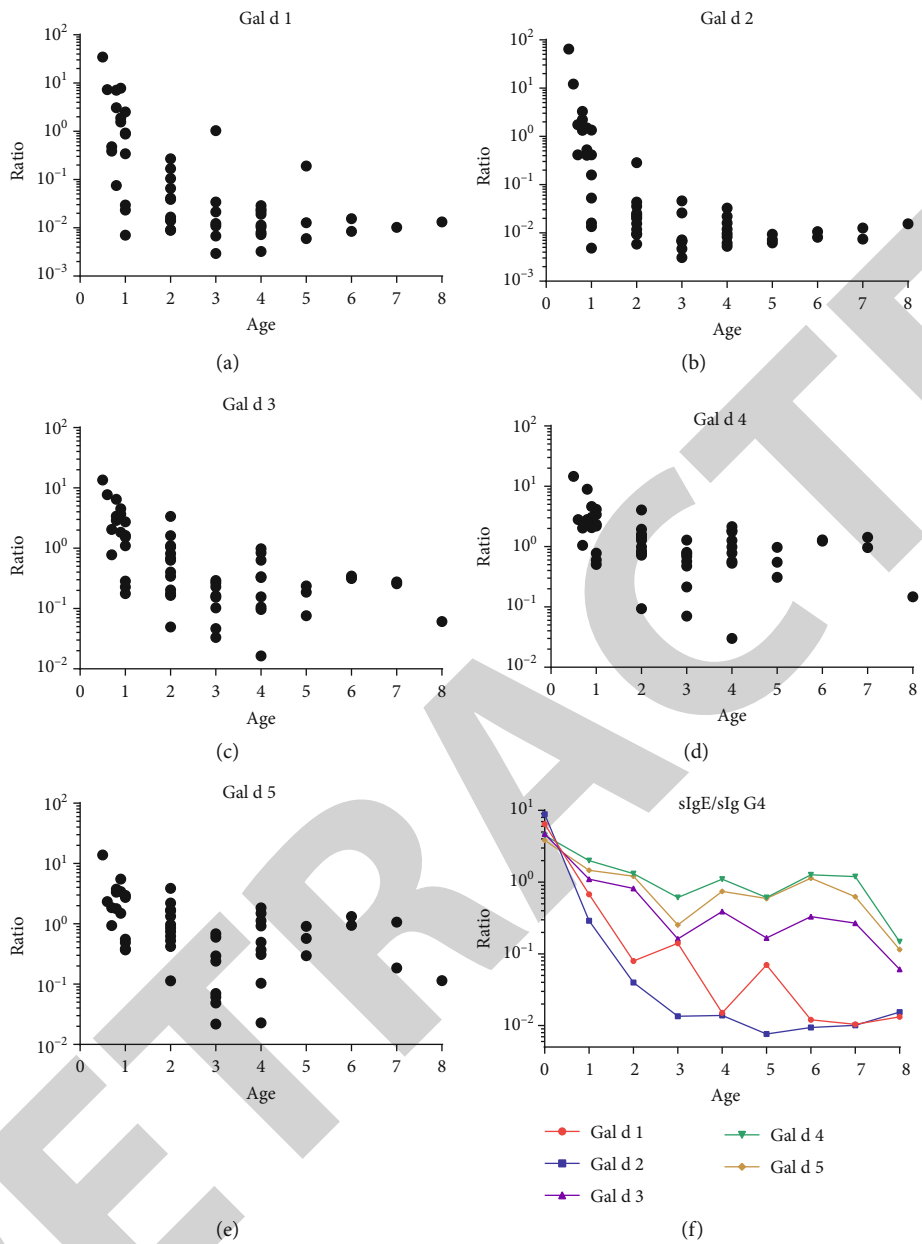

Figure 5: sIgE/sIgG4 ratios of single egg components in EA children (a–e) and comparison of means of sIgE/sIgG4 ratios in EA children (f) from 0 to 8 years of age. Ratios of reactions to 5 egg proteins were calculated by using paired data of sIgE and sIgG4 for each of the EA individuals and then plotted against their ages. Means and SD (not shown) of all 5 component ratios were determined in every age group and compared. Infants less than one year old were shown as age 0 in (f). sIgE: specific IgE; sIgG4: specific IgG4; EA: egg allergy; SD: standard deviation.

intervention and other patient-specific allergy management strategies. Future studies should be done to unveil key conformations of single allergens and to improve understanding about their allergenic mechanisms.

Abbreviations

AU: Absorbance units
CRD: Component-resolved diagnostics
EA: Egg allergy
NA: Nonatopic
LICA: Light-initiated chemiluminescent assay
RLU: Relative light units
sIgE: Specific IgE
sIgG: Specific IgG
sIgG4: Specific IgG4
SPT: Skin prick test.

Data Availability

The data to support this study are available at the correspondence author upon request.

Hindawi
BioMed Research International
Volume 2020, Article ID 6892961, 13 pages
https://doi.org/10.1155/2020/6892961

Review Article

The Antitumor Efficacy of β-Elemene by Changing Tumor Inflammatory Environment and Tumor Microenvironment

Qiang Xie,[1,2] **Fengzhou Li**,[1,2] **Lei Fang**,[1,2] **Wenzhi Liu**,[1,2] **and Chundong Gu**[1,2]

[1]*Department of Thoracic Surgery, The First Affiliated Hospital of Dalian Medical University, Dalian, Liaoning 116011, China*
[2]*Lung Cancer Diagnosis and Treatment Center of Dalian, The First Affiliated Hospital of Dalian Medical University, Dalian, Liaoning 116011, China*

Correspondence should be addressed to Chundong Gu; guchundong@dmu.edu.cn

Received 6 December 2019; Accepted 21 January 2020; Published 21 February 2020

Guest Editor: Hengjia Ni

Inflammatory mediators and inflammatory cells in the inflammatory microenvironment promote the transformation of normal cells to cancer cells in the early stage of cancer, promote the growth and development of cancer cells, and induce tumor immune escape. The monomeric active ingredient β-elemene is extracted from the traditional Chinese medicine *Curcuma wenyujin* and has been proven to have good anti-inflammatory and antitumor activities in clinical applications for more than 20 years in China. Recent studies have found that this traditional Chinese medicine plays a vital role in macrophage infiltration and M2 polarization, as well as in regulating immune disorders, and it even regulates the transcription factors NF-κB and STAT3 to alter inflammation, tumorigenesis, and development. In addition, β-elemene regulates not only different inflammatory factors (such as TNF-α, IFN, TGF-β, and IL-6/10) but also oxidative stress in vivo and in vitro. The excellent anti-inflammatory and antitumor effects of β-elemene and its ability to alter the inflammatory microenvironment of tumors have been gradually elaborated. Although the study of monomeric active ingredients in traditional Chinese medicines is insufficient in terms of quality and quantity, the pharmacological effects of more active ingredients of traditional Chinese medicines will be revealed after β-elemene.

1. Introduction

Curcuma wenyujin, a kind of traditional Chinese medicine that has been planted and used for thousands of years, belongs to Zingiberaceae and has an oval, long oval, or spindle shape [1]. The good cholagogic action and analgesic and bactericidal effects of *Curcuma wenyujin* have been recorded in the *Compendium of Materia Medica* [2, 3]. Current studies have shown that it also has antioxidant, antiproliferation, and antitumor effects [4, 5].

Elemene, a sesquiterpene compound extracted from *Curcuma wenyujin*, is composed of two essential elements, carbon and hydrogen [6]. The chemical formula of elemene is $C_{15}H_{24}$, and the molecular mass is 204.355. β-Elemene (1-methyl-1-vinyl-2,4-diisopropenyl-cyclohexane) is the main active ingredient among all three monomer forms of elemene: α, β, and δ [7] (Figure 1). It is a noncytotoxic class II antineoplastic drug that was developed in China with a new structure and has many outstanding advantages, such as broad antineoplastic effects, exact curative effects, low toxicity and side effects, and low resistance [6, 8, 9].

Research has found that β-elemene has direct antitumor effects, and its antitumor mechanisms include inducing apoptosis [10], arresting the cell cycle [11], inhibiting angiogenesis and cell migration [12], enhancing the immunogenicity of tumor cells [13], promoting erythrocyte immune function, and inhibiting cancer stem cell-like effects [14]. β-Elemene not only has direct antitumor effects but also reverses multidrug resistance by reducing mitochondrial membrane potential, activating the intracellular redox system, and inducing apoptosis of tumor cells [10, 15]. β-Elemene increases chemosensitivity by inducing tumor cell apoptosis and increases

(a) (b) (c)

Figure 1: (a) Curcuma wenyujin, a green plant of family Zingiberaceae, is the source of elemene. (b) The traditional Chinese medicine turmeric, taken from the roots of Curcuma wenyujin. (c) The molecular structure of effective monomer components of β-elemene.

the sensitivity to radiotherapy by inhibiting the P21-activated kinase1 (PAK1) signaling pathway [16, 17], inducing DNA damage, and restraining DNA damage repair [18].

Currently, β-elemene and its derivatives have been utilized to treat various tumors including lung cancer [10], liver cancer [11], brain cancer [19], breast cancer [20], ovarian cancer [21], stomach cancer [16], prostate cancer, and other tissues for over 20 years [22]. Their practical and effective medicinal value has been confirmed gradually.

A total of 120 patients with refractory/relapsed acute myeloid leukemia (AML) were treated with HAA (homoharringtonine, arabinosylcytosine, and aclacinomycin) combined with β-elemene. The total effective rate of the β-elemene emulsion plus HAA group was 80.8%, which was significantly better than that of the control group (52.9%). This result indicated that β-elemene had a synergistic effect on acute myelogenous leukemia [23].

In 2019, a meta-analysis of 15 randomized controlled trials (RCTs) in accordance with PRISMA guidelines recruited 1410 patients with stage III/IV non-small-cell lung cancer (NSCLC) and found that elemene improved clinical efficacy, enhanced cellular immune function, and reduced the toxicity of chemotherapy. It was confirmed that β-elemene was a safe and effective adjuvant therapy for platinum-based chemotherapy in stage III/IV NSCLC patients [24]. In 2018, Wang et al. pooled 46 controlled clinical trials with a total of 2992 patients. The results showed that β-elemene significantly increased the overall efficacy of controlling malignant pleural effusion without increasing the incidence of chest pain and fever [25].

In addition, Xu et al. [9], Wang et al. [26], Jiang et al. [27], and Xu et al. [28] also confirmed the efficacy and safety of β-elemene in clinical use over the past 20 years.

2. The Inflammatory Microenvironment and Tumorigenesis

2.1. Overview of Inflammation and Tumors. There is an abnormal relationship between the tumor parenchyma and its surrounding microenvironment [29]. The interstitial cells of the tumor are composed of two major types: cellular components and noncellular components [30]. The interstitium of the tumor participates in the interaction of the tumor parenchyma to determine the biological behavior of the tumor [31]. When a pathogen enters the host, it causes damage to the organism and activates the immune system [32, 33]. Moreover, a large number of inflammatory cells, such as tumor-related macrophages and dendritic cells, infiltrate and activate [34]. These cells also promote each other with tumor-related inflammatory cells, which results in a variety of tumorigenic factors in the tumor microenvironment [35]. These changes promote the growth of tumor parenchyma and the formation of the tumor interstitial blood vessels and destroy the immune system of the body, resulting in the transformation of the interstitium and the metastasis of tumors [31, 36, 37].

2.2. Changes in the Tumor Inflammatory Environment. When the body is infected or repairs wounds, it permanently activates and chemotactically accumulates a large number of white blood cells (such as macrophages, neutrophils, lymphocytes, and dendritic cells) at the site of injury by releasing cytokines/chemokines (such as interleukin-6/10 (IL-6/10) [38, 39] and tumor necrosis factor-α (TNF-α)) [40], growth factors (transforming growth factor-β (TGF-β)) [41], matrix metalloproteinases (MMPs) [42], vascular endothelial growth factor (VEGF) [43], reactive oxygen species (ROS) metabolites, and other substances [44]. These inflammatory cytokines not only recruit inflammatory cells to amplify inflammation at the tumor site [45] but also form a new environment [46], leading to the destruction and atrophy of normal tissues [47] and promoting mass production of the tumor matrix and blood vessels [48]. These factors play an essential role in the occurrence and development of tumors and promote the growth and metastasis of tumors. Inflammation leads to cell transformation, and the tumor cells and their surrounding interstitium secrete cytokines and chemical activators, forming a positive cycle between cancer and inflammation, which is conducive to the communication

between tumors and the host stroma, thus accelerating the progression of tumors [49, 50].

TNF-α is a special and multifunctional cytokine that plays a key role in immune regulation, the inflammatory response, and defense [51]. On the one hand, a high concentration of TNF-α destroys tumor blood vessels, causes cell necrosis, and also stimulates tumor-specific T cells, which have an antitumor effect. In vitro studies have shown that TNF-α directly kills various human tumor cells, such as melanoma, breast cancer, and cervical cancer cells [52]. On the other hand, the role of TNF-α in chronic inflammation and its tumor-promoting effect have also been proven [53]. In human tumors such as bladder cancer, prostate cancer, colon cancer, leukemia, and lymphoma, elevated TNF-α levels have been detected [54]. In the tumor microenvironment, TNF-α is secreted by macrophages and tumor cells. Continuous TNF-α stimulation promotes tumor angiogenesis, DNA damage, tumor epithelial-mesenchymal transition (EMT), and other mechanisms to promote tumor survival and metastasis [55], and its mechanism may be related to the activation of the nuclear factor kappa-B (NF-κB) signaling pathway [56]. TNF-α treatment of tumor cells that were then intravenously injected into nude mice significantly enhanced their tumorigenicity [57]; at 9 days after tail vein injection of cancer cells in nude mice, LPS stimulation not only significantly improved the level of TNF-α but also increased the number of lung metastases [58]. These studies show that TNF-α plays an important role in the inflammatory environment and tumor microenvironment. Moreover, we hypothesize that the tumor-promoting or anticancer response of TNF-α in the tumor microenvironment depends not only on the local concentration but also on its expression source in the tumor.

As an inflammatory cytokine, IL-6 is mainly derived from stromal cells such as macrophages and fibroblasts around the tumor, and it is not secreted or is rarely secreted by the tumor cells themselves [59, 60]. IL-6, similar to TNF-α, promotes the transformation of noncancer cells into cancer stem cells [61] while regulating the biological activity of tumor cells, leading to cell proliferation or distant metastasis [62]. In addition, IL-6 promotes tumor development by enhancing the T cell-mediated immune-inflammatory response, regulating gene expression, and inhibiting apoptosis in the cell through the JAK-STAT signaling pathway [63, 64].

2.3. Macrophages and Tumors. There are many inflammatory cells involved in the initiation, development, and metastasis of cancer, of which tumor-associated macrophages (TAMs) account for the largest proportion (50% of inflammatory cells) and play the most significant role [65, 66]. Macrophages secrete a variety of cytokines and cytotoxic mediators, including activator of transcription 3 (STAT3), colony-stimulating factor receptors (CSF-1), ROS, and MMP [67], which promote not only abnormal proliferation and apoptosis of early cells but also the formation and development of tumors and accelerate the infiltration and metastasis of tumor cells [68]. Studies have shown that M1 macrophages are the main type in the early stage of inflammation, and the M2-type macrophages are mainly found in the late stage [69]. In addition, M1 macrophages can transform into M2 macrophages, which have immunosuppressive functions to accelerate the malignant transformation of benign tumors [70]. Therefore, the previous understanding of the functions of M1 and M2 macrophages is not altogether true, but we can be sure that macrophages are crucial in the transformation of the tumor microenvironment and tumorigenesis.

2.4. Immune Function and Tumors. The immune characteristics of the tumor microenvironment have been listed as one of the ten characteristics of the tumor [71]. Studies have shown that the tumor is locally infiltrated with a variety of immune cell subsets. Macrophages, mast cells, dendritic cells (DCs), and myeloid-derived suppressor cells (MDSCs) are distributed in the central area and around the tumor. NK cells are mainly located in the tumor matrix. Immature DCs are mainly located in the central area of the tumor, while mature DCs and B cells are mostly found in secondary lymphoid tissue. In addition, $CD8^+$ T cells are mainly distributed at the edge of the tumor [72, 73].

The body's normal immune system is able to recognize and remove foreign cells or cancerous cells [74]. However, in the inflammatory microenvironment, dynamic changes in inflammation and immune abnormalities develop, which mainly manifest as inflammation-induced immunosuppression and immune escape [75]. Tumor cells also secrete a variety of immunosuppressive factors. The inhibitory effects of TGF-β1 and IL-10 are relatively strong [76, 77]. Immunosuppressive factors activate inflammatory mediators, such as macrophages, mast cells, and natural killer (NK) cells, to secrete IL-10, IL-6, and TNF-α [78]. The vicious cycle is formed in the inflammatory microenvironment, which induces tumor immunosuppression to some extent.

2.5. Oxidative Stress and Tumors. Infection or chronic inflammation contributes to the occurrence of cancer mainly by leukocytes and immune cells in inflammatory lesions, which are activated by inflammation and produce ROS and reactive nitrogen species (RNS) [79, 80]. ROS cause damage by oxidizing DNA (including point mutations, deletions, and gene reassortment), disrupting DNA repair, and post-translationally modifying cancer proteins [81]. DNA damage is increased by the secretion of MIF from macrophages and T lymphocytes [82]. When cells are exposed to persistent oxidative stress caused by chronic inflammation, the RNS nitric oxide (NO) induces gene mutation and inactivates key enzymes for DNA damage repair, thereby preventing or impairing DNA repair and exacerbating DNA damage [83, 84]. NO is an important inflammatory mediator that is associated with chronic inflammation and cancer and is produced endogenously through different isomerizations of nitric oxide synthase (NOS) during arginine metabolism [85, 86]. During inflammation, macrophages and epithelial cells induce iNOS expression. In the inflammatory microenvironment, local iNOS activity is induced for a short time, resulting in increased NO of more than 10^3 times the basal level [87]. The local increase in NO is easily oxidized by ROS to produce nitrogen peroxide (NOO), which is a RNS.

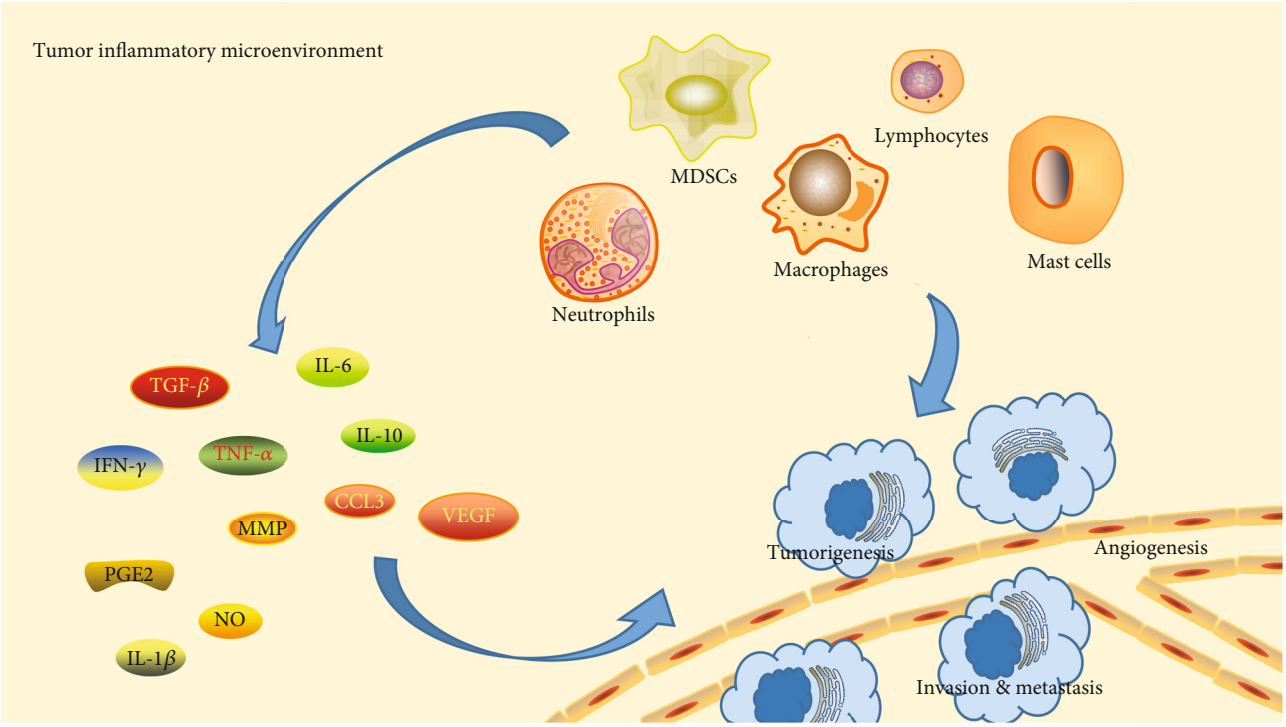

Figure 2: Effect of inflammatory factors and inflammatory cells on tumor development in the inflammatory microenvironment.

In the clinic, many precancerous lesions and cancers have elevated levels of iNOS and NO [85]. The endogenous NO produced by tumor cells and tumor vascular endothelial cells plays an important role in promoting tumor angiogenesis and ensuring the maximum blood supply of tumors. Tumor angiogenesis is the basis of tumor growth and metastasis [88].

In addition, there is a dual relationship between NO and tumors: an appropriate concentration of NO promotes tumor growth, while a high concentration of NO is not conducive to tumor growth and has an antitumor effect [89]. In general, the concentration of NO that has an antitumor effect is 10-100 times higher than the concentration that promotes tumor growth [90]. On the one hand, NO mediates the tumor-killing effect of macrophages. NO is more effective than TNF-α in mediating the killing of tumor cells by activated macrophages [91]. On the other hand, NO directly kills tumor cells: (1) NO acts on mitochondrial oxidoreductase, and tumor cells die due to energy metabolism disorders [92]; (2) NO combines with superoxide anion in cells to generate nitrogen/oxygen free radicals, resulting in genotoxicity and DNA damage [93]; (3) NO inhibits cell proliferation by inhibiting protein synthesis [94]; (4) NO activates the expression of p53 and induces apoptosis of tumor cells [94]; and (5) NO inhibits platelet aggregation and tumor metastasis [95]. In addition, a large number of studies have found that NO is also widely involved in the chemotherapy and immunotherapy of tumors, interacting with chemotherapy drugs and cytokines and affecting the efficacy of drugs against tumors [96].

2.6. Tumor-Promoting Pathways. The transcription factors NF-κB and STAT3 are involved in inflammation and tumorigenesis and regulate cell survival, growth, and proliferation [97]. Many cytokines involved in the inflammatory response, such as TNF and IL-1, are involved in the activation of the NF-κB signaling pathway [88]. Activation of the STAT3 pathway also primarily depends on the corresponding inflammatory cytokines, such as IL-6, IL-10, and VEGF [98, 99].

There are some crossovers and interactions between these two signaling pathways. After activating these two signaling pathways in inflammatory cells, cytokines, chemokines, and enzymes related to the synthesis of prostaglandins and inducible nitric oxide synthase are released to form an inflammatory microenvironment that is conducive to tumorigenesis [100, 101]. In malignant transformed cells, these two signaling pathways promote malignant proliferation, enhance adhesion and promote the expression of antiapoptotic genes such as Bcl-2 [102], and play a key role in the production, survival, epithelial-mesenchymal transition (EMT), invasion, and metastasis of cancer cells by inhibiting adaptive immunity and drug resistance [103]. These two signaling pathways play a crucial role in bridging tumor cells and peripheral inflammatory cells (Figure 2).

3. β-Elemene Alters Inflammation and the Tumor Microenvironment

3.1. Regulation of Inflammatory Factors by β-Elemene. TNF is a cytokine that directly kills tumor cells and has no obvious toxicity to normal cells, and it is one of the most potent

biologically active factors [52]. In many injury models, elevated expression of TNF-α is associated with tissue damage [54]. β-Elemene decreases the levels of endotoxin in plasma, TNF-α in serum, and CD14 in the liver of rats with liver fibrosis, preventing concurrent liver fibrosis induced by carbon tetrachloride (CCl_4) and reducing liver injury and inflammatory reactions [104, 105]. Elemene reduces not only macrophage infiltration in inflammation but also the production of TNF-α and IL-6 by macrophages to alleviate endothelial damage and delay atherosclerosis [106]. In lipopolysaccharide- (LPS-) stimulated RAW264.7 macrophages, β-elemene inhibited β-catenin in a dose-dependent manner and inhibited the upregulation of IL-6, TNF-α, and IL-1β under LPS stimulation, thereby confirming the importance of the Wnt/β-catenin signaling pathway in the anti-inflammatory activity of β-elemene [106]. The decrease in TNF-α, IL-1β, IL-6, IL-8, and other inflammatory factors was detected after treatment of LPS-stimulated macrophages and neutrophils with elemene, which shows that the anti-inflammatory activity of β-elemene is similar to that of dexamethasone and indicates that elemene has a strong inhibitory effect on the inflammatory response [107–109]. When evaluating the immunoregulatory activity of neutrophils stimulated by LPS in vitro, it was found that reducing the generation of MMP-9 and TNF-α protected tissues from the proteolytic activity of matrix-degrading enzymes released by neutrophils and inhibited neutrophil migration [108]. The reduction in MMP-9 affected the release of TGF-β1, neutrophil chemotaxis, and VEGF [110].

The biological functions of TGF-β were initially studied in inflammation, tissue repair, and embryonic development [111]. Recently, it has been found that TGF-β plays an important role in regulating cell growth, differentiation, and immune function [112, 113]. In contrast to the effects on normal human airway fibroblasts, β-elemene dose-dependently inhibits the release and expression of Wnt3a, inactive GSK-3β, β-catenin, α-SMA, TGF-β, and Col-1 in human airway granulation tissue fibroblasts and has the same effect on the expression and nuclear translocation of active β-catenin [114]. Therefore, the effect of β-elemene on primary human airway granulation tissue fibroblasts may occur through the downregulation of the classical Wnt/β-catenin and TGF-β/Smad pathways [115, 116]. These pathways may be promising targets for improving benign airway stenosis and inhibiting excessive proliferation of fibroblasts. TGF-β and Col-1 are two important molecules that are secreted by fibroblasts and also induce fibroblasts to promote inflammation and cancer. The TGF-β-induced upregulation of α-SMA and CD44 in LX-2 cells was blocked by β-elemene [117]. In addition to CD44, α-SMA is produced when fibroblasts are stimulated and is essential for cell movement, tumor development, and invasion [118, 119].

3.2. β-Elemene Protects Immune Disorders. Progressive growth and immune escape in most malignant tumors occur when tumor antigens cannot be effectively presented to T cells to induce antigen-specific immune response [120, 121]. When β-elemene is combined with immunotherapy, a large number of inflammatory cells infiltrate tumor tissue and enhance dendritic cell (DC) antigen presentation, which may be one of the mechanisms by which β-elemene exerts antitumor immunity and counteracts tumor immune escape [122, 123]. When bone marrow-derived dendritic cells (BM-DCs) modified with the murine IL-23 gene were used in combination with elemene in pancreatic cancer model mice, we found that the combination therapy significantly increased the inhibition of tumors and enhances the specific Th1 and cytotoxic T lymphocyte (CTL) responses [124, 125]. This combination treatment significantly promoted the secretion of interferon-γ (IFN-γ) and had antiviral, antitumor, and immunoregulatory effects, and IFN-c inhibited the expression of IL-4 in vitro and in vivo [122, 124]. This effect against immune escape and the antitumor synergy of β-elemene are the focus of our future studies.

Immune disorders in tumors are often seen in demyelinating diseases. β-Elemene regulates the immune balance through the blood-brain barrier [126], inhibits the downregulation of Treg cells and Th17 and Th1 polarization, and downregulates the expression of the proinflammatory factor IL-17, which has a substantial protective effect on optic nerve inflammation in experimental autoimmune encephalomyelitis [127]. In an experimental autoimmune encephalomyelitis mouse model, we observed that β-elemene selectively downregulated CD4+ T lymphocytes without affecting the activation of peripheral lymphoid tissue, significantly weakened the signs in the nervous system and the development of experimental autoimmune encephalomyelitis (EAE), inhibited the Th1 cell-mediated immune response, and upregulated the Treg cell response in vitro [128]. Improvement of EAE by β-elemene may depend on inhibition of IL-6-activated RORγt signal transduction, the STAT3 pathway, and promotion of Treg cell proliferation to inhibit the development and differentiation of Th17 cells [129]. Therefore, β-elemene control of inflammatory diseases mediated by Th17 cells and other cells and regulation of tumor immunity disorder are of great significance (Figure 3).

3.3. β-Elemene Regulates NF-κB/STAT3. There is a strong link between the long-term inflammatory response and cancer, and an important mediator of the inflammatory response and cancer is NF-κB. Inhibition of the NF-κB signaling pathway may be one of the important mechanisms by which β-elemene changes the inflammatory environment and tumor microenvironment. In LPS-stimulated macrophages, expression of NF-κB (p65) decreased in the β-elemene treatment group [106], which may be related to the elemene-mediated inhibition of the expression of Toll-like receptor 4 (TLR4), iNOS, cyclooxygenase-2 (COX-2), TNF-α, IL-1β, IL-6, and IL-12 [107]. β-Elemene not only reduces the expression of NF-κB but also inhibits its transport to the nucleus; together with inhibition of the RAC1/MLK3/p38 signaling pathway, this may be one of the mechanisms by which elemene alleviates septicemia-related encephalopathy (SAE) [109]. As a radiosensitizer of lung cancer, β-elemene effectively controls radiation- and hypoxia-induced activation of the Prx-1/NF-κB/HIF-1α pathway, inhibiting the expression of monocyte chemoattractant protein 1 (MCP-1) and the infiltration and polarization of M2 macrophages induced by radiation

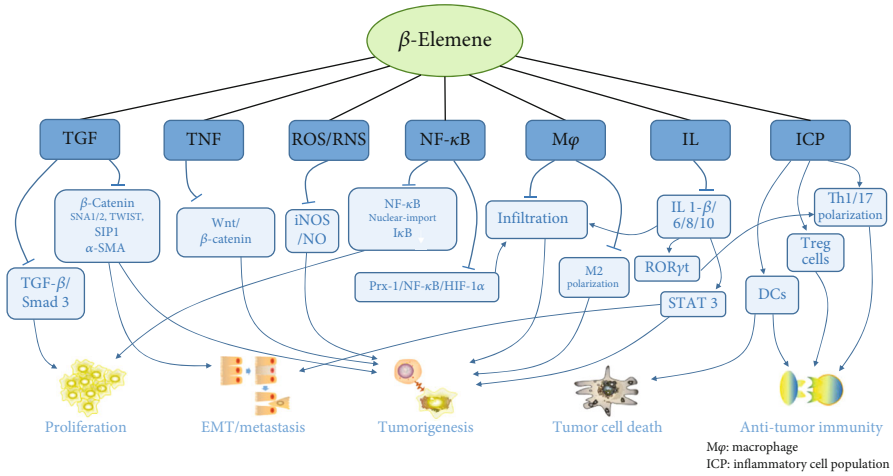

Figure 3: Overview of the mechanism by which β-elemene changes the inflammatory environment to regulate inflammatory processes and tumor development.

in vivo, which reduces the damage and improves the inflammatory environment of tumors [130]. Since β-elemene easily passes through the blood-brain barrier, the expression of inflammatory factors, TLR4 and Caspase-3, is significantly decreased, and the expression of IκB is upregulated when traumatic brain injury (TBI) is treated with β-elemene alone or in combination with hyperbaric oxygen (HO) [131], which exhibits an anti-inflammatory effect and neuroprotection by inhibiting the NF-κB signaling pathway. In the Th1 cell-mediated EAE animal model, β-elemene improves the course of EAE mice by inhibiting RORγt, which is activated by the IL-6 and STAT3 pathways [129]. The NF-κB and STAT3 pathways play key roles in the formation of the inflammatory environment, as well as in the development, invasion, and metastasis of tumors [97]. The inhibitory effect of β-elemene on these two pathways has shown good anti-inflammatory and anticancer applications, but this requires further research.

3.4. Effects of β-Elemene on Macrophages. Macrophages are the core participants in inflammation and the immune response and are involved in a variety of disease processes [65]. One of the most effective stimuli for macrophages is the bacterial endotoxin LPS [132]. When macrophages are exposed to LPS, TLR4 recognizes LPS and induces the production of many inflammatory cytokines, such as TNF-α, IL-6, and IL-1β. Treatment with β-elemene reduces the expression of TLR4, suggesting that elemene has anti-inflammatory activity in LPS-stimulated macrophages [107]. β-Elemene inhibits the LPS-induced expression of iNOS and IL-10 by inhibiting β-catenin and downregulating the Wnt/β-catenin signaling pathway [106]. β-Elemene effectively inhibits the synthesis of COX-2 and prostaglandin E2 (PGE2), and the concentrations of LPS-induced IL-1β, IL-6, TNF-α, and IL-12 also decrease with the downregulation of iNOS and NO [107], demonstrating the crucial role of β-elemene in the congenital and inflammatory responses of macrophages triggered by TLRs. In atherosclerotic lesions, macrophage foam cells contribute to the formation of fatty streaks, which is an essential event in the eventual formation of atherosclerotic plaques [133]. β-Elemene reduces macrophage infiltrations, inhibits the production of TNF-α and IL-6 in macrophages, and reduces serum total cholesterol (TC), triglycerides (TGs), and low-density lipoprotein (LDL-C) in vivo [105], regulating the level of blood lipids. Moreover, ROS are mainly produced by macrophages, and the decrease in macrophage infiltration also reduces endothelial oxidative stress injury and delays the progression of atherosclerosis [134].

Macrophages can be divided into two different phenotypes: the M1 phenotype, which is the classically activated phenotype that is involved in antitumor immunity, and the M2 phenotype, which is an alternatively activated phenotype with tumor-promoting properties [135]. A number of studies have found that TAMs are mostly M2-polarized, and it has been reported that these cells promote the growth and survival of tumors and may lead to resistance to cancer treatment [65]. β-Elemene not only decreases the proliferation, migration, and invasion and strengthens the radiosensitivity of lung cancer cells but also inhibits the promotion of migration, invasion, and EMT of lung cancer in M2 macrophage-conditioned medium, regulating the polarization of macrophages from M2 to M1 [136]. Research shows that tumor cells in the irradiated or hypoxic microenvironment recruit macrophages and induce MCP-1 secretion, which leads to nuclear accumulation of NF-κB and HIF-1α. β-Elemene significantly controls the infiltration and polarization of M2 macrophages and MCP-1 secretion induced by radiation and hypoxia by inhibiting the Prx-1/NF-κB/HIF-1α pathway [130]. MCP-1 is an important proinflammatory cytokine that is secreted by macrophages, monocytes, and fibroblasts during inflammation, and it has specific chemotactic effects on monocytes/macrophages [137]. β-Elemene inhibits macrophage infiltration in patients undergoing radiotherapy and increases the radiosensitivity of lung cancer cells by enhancing DNA damage, inhibiting DNA repair, or causing apoptosis of radiation cells, which is a promising strategy for chemotherapy or radiotherapy [10, 18]. β-Elemene participates in the defense against Leishmania through increased phagocytosis and lysosomal activity, which may be related

to the activation of M1 macrophages by β-elemene [138]. β-Elemene plays important anti-inflammatory and antitumor roles in inhibiting the activation and invasion of macrophages, and the effects of the inflammatory environment and tumor microenvironment on macrophages deserve further study.

3.5. β-Elemene Changes iNOS and NO Levels. iNOS, inducible nitric oxide synthase, is a catalytic enzyme that is produced by NOS active nitrogen free radicals in the body [86], and the level of iNOS may be an important indicator of the degree of inflammation in an organism [87]. In the inflammatory microenvironment, macrophages and epithelial cells induce the expression of iNOS, and then, the local iNOS activity in the inflammatory microenvironment is significantly increased quickly, leading to an increase in NO of more than 10^3 times the basal state [139]. NO participates in the regulation of physiological and pathophysiological processes such as vascular and nervous system functions and has cytotoxic effects at high concentrations [85]. Elemene treatment of NCI-H292 cells, a human lung adenocarcinoma cell line, increased the levels of p38 mitogen-activated protein kinase (MAPK) and iNOS, and so, a locally increased concentration of NO may be associated with elemene-induced apoptosis [140]. In a mouse model of experimental autoimmune encephalomyelitis, elemene restrained microglial activation and iNOS expression, which was associated with the inhibition of axonal demyelination and neuronal death during the development of the disease [128]. β-Elemene effectively downregulates iNOS expression and inhibits NO production; furthermore, inhibition of iNOS leads to a decrease in PGE2 synthesis and downregulation of COX-2 expression, which indicates that elemene has strong anti-inflammatory activity in LPS-stimulated macrophages [107, 141]. The inhibition of iNOS and IL-10 by β-elemene inhibits β-catenin activity in a dose-dependent manner and downregulates the Wnt/β-catenin signaling pathway [106]. β-Elemene increases the activity of T-AOC, SOD, CAT, and GSH-Px, suggesting that β-elemene enhances the removal of free radicals and protects cells from oxidative damage caused by free radicals [142]. By inhibiting the activation of the MAPK signaling pathway, β-elemene significantly inhibits the production of ROS and inhibits hydrogen peroxide-induced apoptosis of human umbilical vein endothelial cells (HUVECs), enhancing the viability of damaged cells [143, 144]. The potential value of β-elemene in effectively resisting oxidative stress associated with cardiovascular diseases deserves further study.

NO expression in endothelial cells exerts antiproliferative, anti-inflammatory, and antioxidative effects in the vascular wall. β-Elemene increases the production of nitric oxide (NO) in HUVECs by significantly improving plasma nitrite and nitrate levels and promotes the phosphorylation of eNOS (ser1177) and Akt in vitro to maintain endothelial function [145]. These data show that β-elemene acts through its antioxidant and anti-inflammatory characteristics to affect atherosclerosis and enhanced plaque stability. In mouse models of arterial injury, β-elemene effectively controls the proliferation and migration of VSMCs and inhibits neointimal formation in vivo [146]. These factors are associated with oxidative stress and VSMC dilation and reveal the potential clinical application of β-elemene in preventing vascular stenosis and remodeling. There is no obvious cytotoxicity of β-elemene or a series of its derivatives. These factors have the ability to increase superoxide dismutase activity and nitric oxide secretion in cells and simultaneously decrease malondialdehyde content and lactate dehydrogenase release in cells; these changes mediate antioxidant activity [147]. In addition, the regulation of biochemical substances (SOD, MDA, NO, and LDH) in HUVECs treated with hydrogen peroxide is better than that of the positive control vitamin [148], and so, β-elemene may be a potential treatment to effectively resist oxidative stress associated with cardiovascular disease. β-Elemene and some derivatives produce high levels of NO in vitro, and its antitumor activity in U87 cells was significantly attenuated by NO scavengers (hemoglobin or carboxyl-PTIO), and blocking activation of the PI3K/Akt pathway induced G2 arrest of the cell cycle and apoptosis in U87 cells, inhibiting tumor growth [149, 150].

3.6. The Relationship between β-Elemene and EMT. TGF-β is a potent inflammatory factor, as well as a strong activator of the EMT, which is involved in the progression and metastasis of cancer [151]. β-Elemene reduces the expression and phosphorylation of Smad3 to inhibit the expression of nuclear transcription factors (such as SNAI1, SNAI2, TWIST, and SIPI1) and block the EMT induced by TGF-β1 in the human breast cancer cell line MCF-7 [116]. TGF-β1 induces the upregulation of α-SMA in human hepatic stellate cells, and its expression and EMT phenotypic transformation can be blocked by β-elemene [117]. TLR4 induces the EMT and the production of antiapoptotic proteins and angiogenesis factors, promoting the survival of cancer cells and inducing immunosuppression [152]. The expression of TLR4 in the TBI rat model is significantly downregulated by β-elemene and changes the expression levels of Caspase-3 and IκB [131]. The combination of elemene and gefitinib profoundly impairs epithelial cell transformation to mesenchymal cells, in a large part due to the regulation of the enhancer of zeste homolog 2 (EZH2), a carcinogenic histone methyltransferase and gene transcription regulator, thereby modulating the subsequent effector molecule required for cancer progression [153]. β-Catenin may also be the target of β-elemene in reversing the malignant phenotype of tumor cells; moreover, notch1, sonic hedgehog, and the epithelial marker of E-cadherin are upregulated by β-elemene in human glioblastoma cells in vitro and in vivo [19]. β-Elemene-mediated blockade of the phenotype transition of type 3 EMT in metastatic malignant tumors under the continuous stimulation of inflammation may also be an important antitumor mechanism of β-elemene.

4. Conclusion

It is well known that inflammatory factors in the inflammatory microenvironment are closely related to the development of inflammatory cells and tumors, and the regulation

of the inflammatory microenvironment is also involved in the regulation of inflammation and tumor development. β-Elemene, an effective monomer extracted from the traditional Chinese medicine *Curcuma wenyujin*, has been applied clinically for more than 20 years in China and exhibits good antitumor and anti-inflammatory activities without obvious cytotoxicity or clinical side effects. The ability of β-elemene to regulate the inflammatory environment of tumors has also been demonstrated in recent research. β-Elemene regulates many important inflammatory factors (such as TNF-α, IFN, TGF-β, and IL-6/10), similar to dexamethasone, indicating that it has robust anti-inflammatory and regulatory abilities in the inflammatory environment of tumors. β-Elemene downregulates the levels of iNOS and NO, regulates oxidative stress in vivo and in vitro, alleviates tissue damage, and inhibits the formation of the microenvironment that promotes tumorigenesis. Under certain conditions, elemene also increases the ability of iNOS, which results in apoptosis induced by a locally increased NO concentration, but its specific mechanism needs to be further explored. The NF-κB and STAT3 pathways play key roles in the formation of the inflammatory environment and the occurrence, development, invasion, and metastasis of tumors. β-Elemene not only reduces the expression of NF-κB and inhibits its translocation to the nucleus but also upregulates the expression of IκB. However, beyond that, β-elemene influences the inflammatory microenvironment of tumors and inflammation and tumor progression by inhibiting the IL-6-induced RORγt and STAT3 pathways. The inhibitory effect of β-elemene on these two pathways shows good anti-inflammatory and anticancer application prospects. Immune escape is an important reason for the rapid growth and metastasis of tumors. Elemene plays an important role in inhibiting macrophage infiltration and M2 polarization, as well as in regulating immune disorders. The modern pharmacological mechanism of elemene as an antineoplastic drug and radiosensitizer is gradually becoming understood. We hope that more effective monomers of traditional Chinese medicine will gain attention and that more traditional Chinese medicines with thousands of years of application history will be verified by modern pharmacology.

Conflicts of Interest

The authors declare that they have no conflicts of interest.

Acknowledgments

The authors are thankful to Mr. Shilei Zhao and Mr. Tao Guo from The First Affiliated Hospital of Dalian Medical University and Mr. Zhuoshi Li from Dalian Medical University for revising the article. This study was supported by grants from the National Natural Science Foundation of China (Nos. 81173453, 81774078, and 81803886) and the Natural Science Foundation of Liaoning Province of China (Nos. 201602227 and 20170540300).

References

[1] W. Zang, H. Bian, X. Huang et al., "Traditional Chinese medicine (TCM) Astragalus membranaceus and Curcuma wenyujin promote vascular normalization in tumor-derived endothelial cells of human hepatocellular carcinoma," *Anticancer Research*, vol. 39, no. 6, pp. 2739–2747, 2019.

[2] H. Cao, Y. Sasaki, H. Fushimi, and K. Komatsu, "Molecular analysis of medicinally-used Chinese and Japanese Curcuma based on 18S rRNA gene and trnK gene sequences," *Biological & Pharmaceutical Bulletin*, vol. 24, no. 12, pp. 1389–1394, 2001.

[3] Y. Zhou, M. Xie, Y. Song et al., "Two traditional Chinese medicines Curcumae Radix and Curcumae Rhizoma: an ethnopharmacology, phytochemistry, and pharmacology review," *Evidence-based Complementary and Alternative Medicine*, vol. 2016, Article ID 4973128, 30 pages, 2016.

[4] G. P. Yin, L. C. Li, Q. Z. Zhang et al., "iNOS inhibitory activity of sesquiterpenoids and a monoterpenoid from the rhizomes of Curcuma wenyujin," *Journal of Natural Products*, vol. 77, no. 10, pp. 2161–2169, 2014.

[5] G. P. Yin, Q. Z. Zhang, Y. W. An, J. J. Zhu, and Z. M. Wang, "Advance in chemical constituents and pharmacological activity of Curcuma wenyujin," *Zhongguo Zhong Yao Za Zhi*, vol. 37, no. 22, pp. 3354–3360, 2012.

[6] Y. T. Guo, "Isolation and identification of elemene from the essential oil of Curcuma wenyujin," *Zhong Yao Tong Bao*, vol. 8, no. 3, p. 31, 1983.

[7] Z. Jiang, J. A. Jacob, D. S. Loganathachetti, P. Nainangu, and B. Chen, "β-Elemene: mechanistic studies on cancer cell interaction and its chemosensitization effect," *Frontiers in Pharmacology*, vol. 8, p. 105, 2017.

[8] G. N. Zhang, C. R. Ashby Jr., Y. K. Zhang, Z. S. Chen, and H. Guo, "The reversal of antineoplastic drug resistance in cancer cells by β-elemene," *Chinese Journal of Cancer*, vol. 34, no. 3, pp. 488–495, 2015.

[9] H. B. Xu, L. P. Zheng, L. Li, L. Z. Xu, and J. Fu, "Elemene, one ingredient of a Chinese herb, against malignant tumors: a literature-based meta-analysis," *Cancer Investigation*, vol. 31, no. 2, pp. 156–166, 2013.

[10] K. Zhou, L. Wang, R. Cheng, X. Liu, S. Mao, and Y. Yan, "WITHDRAWN: Elemene increases autophagic apoptosis and drug sensitivity in human cisplatin (DDP)-resistant lung cancer cell line SPC-A-1/DDP by inducing Beclin-1 expression," *Oncology Research*, 2017.

[11] Y. Mao, J. Zhang, L. Hou, and X. Cui, "The effect of beta-elemene on alpha-tubulin polymerization in human hepatoma HepG2 cells," *Chinese Journal of Cancer Research*, vol. 25, no. 6, pp. 770–776, 2013.

[12] W. Tan, J. Lu, M. Huang et al., "Anti-cancer natural products isolated from Chinese medicinal herbs," *Chinese Medicine*, vol. 6, no. 1, p. 27, 2011.

[13] W. Wu, K. Liu, and X. Tang, "Preliminary study on the antitumor immuno-protective mechanism of beta-elemene," *Zhonghua Zhong Liu Za Zhi*, vol. 21, no. 6, pp. 405–408, 1999.

[14] H. B. Feng, J. Wang, H. R. Jiang et al., "β-Elemene selectively inhibits the proliferation of glioma stem-like cells through the downregulation of Notch1," *Stem Cells Translational Medicine*, vol. 6, no. 3, pp. 830–839, 2017.

[15] C. Yao, J. Jiang, Y. Tu, S. Ye, H. Du, and Y. Zhang, "β-Elemene reverses the drug resistance of A549/DDP lung cancer

cells by activating intracellular redox system, decreasing mitochondrial membrane potential and P-glycoprotein expression, and inducing apoptosis," *Thoracic Cancer*, vol. 5, no. 4, pp. 304–312, 2014.

[16] J. S. Liu, X. M. Che, S. Chang et al., "β-Elemene enhances the radiosensitivity of gastric cancer cells by inhibiting Pak1 activation," *World Journal of Gastroenterology*, vol. 21, no. 34, pp. 9945–9956, 2015.

[17] Q. Q. Li, G. Wang, M. Zhang, C. F. Cuff, L. Huang, and E. Reed, "β-Elemene, a novel plant-derived antineoplastic agent, increases cisplatin chemosensitivity of lung tumor cells by triggering apoptosis," *Oncology Reports*, vol. 22, no. 1, pp. 161–170, 2009.

[18] L. J. Li, L. F. Zhong, L. P. Jiang, C. Y. Geng, and L. J. Zou, "β-Elemene radiosensitizes lung cancer A549 cells by enhancing DNA damage and inhibiting DNA repair," *Phytotherapy Research*, vol. 25, no. 7, pp. 1095–1097, 2011.

[19] T. Zhu, X. Li, L. Luo et al., "Reversion of malignant phenotypes of human glioblastoma cells by β-elemene through β-catenin-mediated regulation of stemness-, differentiation- and epithelial-to-mesenchymal transition-related molecules," *Journal of Translational Medicine*, vol. 13, no. 1, p. 356, 2015.

[20] J. Zhang, H. Zhang, L. Chen et al., "β-Elemene reverses chemoresistance of breast cancer via regulating MDR-related microRNA expression," *Cellular Physiology and Biochemistry*, vol. 34, no. 6, pp. 2027–2037, 2014.

[21] Q. Q. Li, R. X. Lee, H. Liang et al., "β-Elemene enhances susceptibility to cisplatin in resistant ovarian carcinoma cells via downregulation of ERCC-1 and XIAP and inactivation of JNK," *International Journal of Oncology*, vol. 43, no. 3, pp. 721–728, 2013.

[22] B. Zou, Q. Q. Li, J. Zhao, J. M. Li, C. F. Cuff, and E. Reed, "β-Elemene and taxanes synergistically induce cytotoxicity and inhibit proliferation in ovarian cancer and other tumor cells," *Anticancer Research*, vol. 33, no. 3, pp. 929–940, 2013.

[23] C. Zheng, X. Cai, S. Wu, Z. Liu, Y. Shi, and W. Zhou, "Enhancing effect of β-elemene emulsion on chemotherapy with harringtonine, aclacinomycin, and Ara-c in treatment of refractory/relapsed acute myeloid leukemia," *Pakistan Journal of Medical Sciences*, vol. 30, no. 6, pp. 1270–1272, 2014.

[24] X. Wang, Z. Liu, X. Sui, Q. Wu, J. Wang, and C. Xu, "Elemene injection as adjunctive treatment to platinum-based chemotherapy in patients with stage III/IV non-small cell lung cancer: a meta-analysis following the PRISMA guidelines," *Phytomedicine*, vol. 59, article 152787, 2019.

[25] Q. T. Wang, Z. L. Zhang, H. Xiong et al., "Evaluation of the efficacy and safety of elemene in treating malignant pleural effusion caused by tumors: a PRISMA guided meta-analysis," *Medicine (Baltimore)*, vol. 97, no. 44, article e12542, 2018.

[26] B. Wang, X. X. Peng, R. Sun et al., "Systematic review of β-elemene injection as adjunctive treatment for lung cancer," *Chinese Journal of Integrative Medicine*, vol. 18, no. 11, pp. 813–823, 2012.

[27] X. Jiang, T. H. Hidru, Z. Zhang, Y. Bai, L. Kong, and X. Li, "Evidence of elemene injection combined radiotherapy in lung cancer treatment among patients with brain metastases: a systematic review and meta-analysis," *Medicine*, vol. 96, no. 21, article e6963, 2017.

[28] X. W. Xu, Z. Z. Yuan, W. H. Hu, and X. K. Wang, "Meta-analysis on elemene injection combined with cisplatin chemotherapeutics in treatment of non-small cell lung cancer," *Zhongguo Zhong Yao Za Zhi*, vol. 38, no. 9, pp. 1430–1437, 2013.

[29] K. Fousek and N. Ahmed, "The evolution of T-cell therapies for solid malignancies," *Clinical Cancer Research*, vol. 21, no. 15, pp. 3384–3392, 2015.

[30] E. Cortez, P. Roswall, and K. Pietras, "Functional subsets of mesenchymal cell types in the tumor microenvironment," *Seminars in Cancer Biology*, vol. 25, pp. 3–9, 2014.

[31] T. L. Whiteside, E. Letessier, H. Hirabayashi et al., "Evidence for local and systemic activation of immune cells by peritumoral injections of interleukin 2 in patients with advanced squamous cell carcinoma of the head and neck," *Cancer Research*, vol. 53, no. 23, pp. 5654–5662, 1993.

[32] V. A. K. Rathinam, Y. Zhao, and F. Shao, "Innate immunity to intracellular LPS," *Nature Immunology*, vol. 20, no. 5, pp. 527–533, 2019.

[33] J. A. S. Quaresma, "Organization of the skin immune system and compartmentalized immune responses in infectious diseases," *Clinical Microbiology Reviews*, vol. 32, no. 4, 2019.

[34] J. M. Cicchese, S. Evans, C. Hult et al., "Dynamic balance of pro- and anti-inflammatory signals controls disease and limits pathology," *Immunological Reviews*, vol. 285, no. 1, pp. 147–167, 2018.

[35] M. L. Disis, "Immune regulation of cancer," *Journal of Clinical Oncology*, vol. 28, no. 29, pp. 4531–4538, 2010.

[36] A. Rhodes and T. Hillen, "A mathematical model for the immune-mediated theory of metastasis," *Journal of Theoretical Biology*, vol. 482, article 109999, 2019.

[37] A. El-Kenawi, K. Hänggi, and B. Ruffell, "The immune microenvironment and cancer metastasis," *Cold Spring Harbor Perspectives in Medicine*, no. article a037424, 2020.

[38] C. J. Pyle, F. I. Uwadiae, D. P. Swieboda, and J. A. Harker, "Early IL-6 signalling promotes IL-27 dependent maturation of regulatory T cells in the lungs and resolution of viral immunopathology," *PLoS Pathogens*, vol. 13, no. 9, article e1006640, 2017.

[39] D. Thompson, N. Morrice, L. Grant et al., "Myeloid protein tyrosine phosphatase 1B (PTP1B) deficiency protects against atherosclerotic plaque formation in the ApoE$^{-/-}$ mouse model of atherosclerosis with alterations in IL10/AMPKα pathway," *Molecular Metabolism*, vol. 6, no. 8, pp. 845–853, 2017.

[40] M. Yamamoto, M. Kim, H. Imai, Y. Itakura, and G. Ohtsuki, "Microglia-triggered plasticity of intrinsic excitability modulates psychomotor behaviors in acute cerebellar inflammation," *Cell Reports*, vol. 28, no. 11, pp. 2923–2938.e8, 2019.

[41] S. M. Stanford, G. R. Aleman Muench, B. Bartok et al., "TGFβ responsive tyrosine phosphatase promotes rheumatoid synovial fibroblast invasiveness," *Annals of the Rheumatic Diseases*, vol. 75, no. 1, pp. 295–302, 2016.

[42] J. Steenbrugge, K. Breyne, K. Demeyere et al., "Anti-inflammatory signaling by mammary tumor cells mediates prometastatic macrophage polarization in an innovative intraductal mouse model for triple-negative breast cancer," *Journal of Experimental & Clinical Cancer Research*, vol. 37, no. 1, p. 191, 2018.

[43] A. Sidibe, P. Ropraz, S. Jemelin et al., "Angiogenic factor-driven inflammation promotes extravasation of human proangiogenic monocytes to tumours," *Nature Communications*, vol. 9, no. 1, p. 355, 2018.

[44] Y. S. Ryu, K. A. Kang, M. J. Piao et al., "Particulate matter induces inflammatory cytokine production via activation of NFκB by TLR5-NOX4-ROS signaling in human skin keratinocyte and mouse skin," *Redox Biology*, vol. 21, article 101080, 2019.

[45] B. Zou, W. Jiang, H. Han et al., "Acyloxyacyl hydrolase promotes the resolution of lipopolysaccharide-induced acute lung injury," *PLoS Pathogens*, vol. 13, no. 6, article e1006436, 2017.

[46] M. F. Eissmann, C. Dijkstra, A. Jarnicki et al., "IL-33-mediated mast cell activation promotes gastric cancer through macrophage mobilization," *Nature Communications*, vol. 10, no. 1, p. 2735, 2019.

[47] S. L. Passey, S. Bozinovski, R. Vlahos, G. P. Anderson, and M. J. Hansen, "Serum amyloid A induces Toll-like receptor 2-dependent inflammatory cytokine expression and atrophy in C2C12 skeletal muscle myotubes," *PLoS One*, vol. 11, no. 1, article e0146882, 2016.

[48] G. Andrés, D. Leali, S. Mitola et al., "A pro-inflammatory signature mediates FGF2-induced angiogenesis," *Journal of Cellular and Molecular Medicine*, vol. 13, no. 8B, pp. 2083–2108, 2009.

[49] Y. Wu, L. Shen, X. Liang et al., "Helicobacter pylori-induced YAP1 nuclear translocation promotes gastric carcinogenesis by enhancing IL-1β expression," *Cancer Medicine*, vol. 8, no. 8, pp. 3965–3980, 2019.

[50] Q. Lv, K. Wu, F. Liu, W. Wu, Y. Chen, and W. Zhang, "Interleukin-17A and heparanase promote angiogenesis and cell proliferation and invasion in cervical cancer," *International Journal of Oncology*, vol. 53, no. 4, pp. 1809–1817, 2018.

[51] A. Amadou, A. Nawrocki, M. Best-Belpomme, C. Pavoine, and F. Pecker, "Arachidonic acid mediates dual effect of TNF-α on Ca^{2+} transients and contraction of adult rat cardiomyocytes," *American Journal of Physiology-Cell Physiology*, vol. 282, no. 6, pp. C1339–C1347, 2002.

[52] J. Pu, R. Wang, G. Zhang, and J. Wang, "FGF-7 facilitates the process of psoriasis by inducing TNF-α expression in HaCaT cells," *Acta Biochimica et Biophysica Sinica*, vol. 51, no. 10, pp. 1056–1063, 2019.

[53] S. C. Chang and W. V. Yang, "Hyperglycemia, tumorigenesis, and chronic inflammation," *Critical Reviews in Oncology/Hematology*, vol. 108, pp. 146–153, 2016.

[54] H. J. Patel and B. M. Patel, "TNF-α and cancer cachexia: molecular insights and clinical implications," *Life Sciences*, vol. 170, pp. 56–63, 2017.

[55] V. De Simone, E. Franzè, G. Ronchetti et al., "Th17-type cytokines, IL-6 and TNF-α synergistically activate STAT3 and NF-kB to promote colorectal cancer cell growth," *Oncogene*, vol. 34, no. 27, pp. 3493–3503, 2015.

[56] J. Hou, T. Ma, H. Cao et al., "TNF-α-induced NF-κB activation promotes myofibroblast differentiation of LR-MSCs and exacerbates bleomycin-induced pulmonary fibrosis," *Journal of Cellular Physiology*, vol. 233, no. 3, pp. 2409–2419, 2018.

[57] M. K. Choo, H. Sakurai, K. Koizumi, and I. Saiki, "Stimulation of cultured colon 26 cells with TNF-α promotes lung metastasis through the extracellular signal-regulated kinase pathway," *Cancer Letters*, vol. 230, no. 1, pp. 47–56, 2005.

[58] J. L. Luo, S. Maeda, L. C. Hsu, H. Yagita, and M. Karin, "Inhibition of NF-κB in cancer cells converts inflammation- induced tumor growth mediated by TNFα to TRAIL-mediated tumor regression," *Cancer Cell*, vol. 6, no. 3, pp. 297–305, 2004.

[59] L. Hu, Z. Chen, L. Li, Z. Jiang, and L. Zhu, "Resveratrol decreases $CD45^{+}CD206^{-}$ subtype macrophages in LPS-induced murine acute lung injury by SOCS3 signalling pathway," *Journal of Cellular and Molecular Medicine*, vol. 23, no. 12, pp. 8101–8113, 2019.

[60] Y. Cai, C. Jiang, J. Zhu et al., "miR-449a inhibits cell proliferation, migration, and inflammation by regulating high-mobility group box protein 1 and forms a mutual inhibition loop with Yin Yang 1 in rheumatoid arthritis fibroblast-like synoviocytes," *Arthritis Research & Therapy*, vol. 21, no. 1, p. 134, 2019.

[61] C. Xie, J. Zhu, Y. Jiang et al., "Sulforaphane inhibits the acquisition of tobacco smoke-induced lung cancer stem cell-like Propertiesviathe IL-6/ΔNp63α/Notch axis," *Theranostics*, vol. 9, no. 16, pp. 4827–4840, 2019.

[62] R. Y. Chen, C. J. Yen, Y. W. Liu et al., "CPAP promotes angiogenesis and metastasis by enhancing STAT3 activity," *Cell Death & Differentiation*, 2019.

[63] U. Billing, T. Jetka, L. Nortmann et al., "Robustness and information transfer within IL-6-induced JAK/STAT signalling," *Communications Biology*, vol. 2, no. 1, p. 27, 2019.

[64] M. A. Milillo, A. Trotta, A. Serafino et al., "Bacterial RNA contributes to the down-modulation of MHC-II expression on monocytes/macrophages diminishing CD4+ T cell responses," *Frontiers in Immunology*, vol. 10, article 2181, 2019.

[65] R. Sumitomo, T. Hirai, M. Fujita, H. Murakami, Y. Otake, and C. L. Huang, "PD-L1 expression on tumor-infiltrating immune cells is highly associated with M2 TAM and aggressive malignant potential in patients with resected non-small cell lung cancer," *Lung Cancer*, vol. 136, pp. 136–144, 2019.

[66] S. M. Ferrari, P. Fallahi, M. R. Galdiero et al., "Immune and inflammatory cells in thyroid cancer microenvironment," *International Journal of Molecular Sciences*, vol. 20, no. 18, p. 4413, 2019.

[67] L. Yang and J. L. Ding, "MEK1/2 inhibitors unlock the constrained interferon response in macrophages through IRF1 signaling," *Frontiers in Immunology*, vol. 10, article 2020, 2019.

[68] Z. Lv, Z. Wang, L. Luo et al., "Spliceosome protein Eftud2 promotes colitis-associated tumorigenesis by modulating inflammatory response of macrophage," *Mucosal Immunology*, vol. 12, no. 5, pp. 1164–1173, 2019.

[69] M. Locati, G. Curtale, and A. Mantovani, "Diversity, mechanisms, and significance of macrophage plasticity," *Annual Review of Pathology: Mechanisms of Disease*, vol. 15, no. 1, pp. 123–147, 2020.

[70] Y. S. Weng, H. Y. Tseng, Y. A. Chen et al., "MCT-1/miR-34a/IL-6/IL-6R signaling axis promotes EMT progression, cancer stemness and M2 macrophage polarization in triple-negative breast cancer," *Molecular Cancer*, vol. 18, no. 1, p. 42, 2019.

[71] D. Hanahan and R. A. Weinberg, "Hallmarks of cancer: the next generation," *Cell*, vol. 144, no. 5, pp. 646–674, 2011.

[72] P. Wu, D. Wu, L. Zhao et al., "Inverse role of distinct subsets and distribution of macrophage in lung cancer prognosis: a meta-analysis," *Oncotarget*, vol. 7, no. 26, pp. 40451–40460, 2016.

[73] W. H. Fridman, F. Pagès, C. Sautès-Fridman, and J. Galon, "The immune contexture in human tumours: impact on clinical outcome," *Nature Reviews Cancer*, vol. 12, no. 4, pp. 298–306, 2012.

[74] K. Franciszkiewicz, A. Boissonnas, M. Boutet, C. Combadière, and F. Mami-Chouaib, "Role of chemokines and chemokine receptors in shaping the effector phase of the antitumor immune response," *Cancer Research*, vol. 72, no. 24, pp. 6325–6332, 2012.

[75] L. Z. Liu, Z. Zhang, B. H. Zheng et al., "CCL15 recruits suppressive monocytes to facilitate immune escape and disease progression in hepatocellular carcinoma," *Hepatology*, vol. 69, no. 1, pp. 143–159, 2019.

[76] J. Chen, J. A. Gingold, and X. Su, "Immunomodulatory TGF-β signaling in hepatocellular carcinoma," *Trends in Molecular Medicine*, vol. 25, no. 11, pp. 1010–1023, 2019.

[77] Y. Han, Z. Chen, Y. Yang et al., "Human $CD14^+$ $CTLA\text{-}4^+$ regulatory dendritic cells suppress T-cell response by cytotoxic T-lymphocyte antigen-4-dependent IL-10 and indoleamine-2,3-dioxygenase production in hepatocellular carcinoma," *Hepatology*, vol. 59, no. 2, pp. 567–579, 2014.

[78] J. M. Taube, R. A. Anders, G. D. Young et al., "Colocalization of inflammatory response with B7-h1 expression in human melanocytic lesions supports an adaptive resistance mechanism of immune escape," *Science Translational Medicine*, vol. 4, no. 127, article 127ra37, 2012.

[79] M. A. Ansari, K. N. Roberts, and S. W. Scheff, "A time course of NADPH-oxidase up-regulation and endothelial nitric oxide synthase activation in the hippocampus following neurotrauma," *Free Radical Biology & Medicine*, vol. 77, pp. 21–29, 2014.

[80] R. L. Flaherty, M. Owen, A. Fagan-Murphy et al., "Glucocorticoids induce production of reactive oxygen species/reactive nitrogen species and DNA damage through an iNOS mediated pathway in breast cancer," *Breast Cancer Research*, vol. 19, no. 1, p. 35, 2017.

[81] U. S. Srinivas, B. W. Q. Tan, B. A. Vellayappan, and A. D. Jeyasekharan, "ROS and the DNA damage response in cancer," *Redox Biology*, vol. 25, article 101084, 2019.

[82] Y. Liu, L. Zhao, Y. Ju et al., "A novel androstenedione derivative induces ROS-mediated autophagy and attenuates drug resistance in osteosarcoma by inhibiting macrophage migration inhibitory factor (MIF)," *Cell Death & Disease*, vol. 5, no. 8, article e1361, 2014.

[83] S. Ohnishi, N. Ma, R. Thanan et al., "DNA damage in inflammation-related carcinogenesis and cancer stem cells," *Oxidative Medicine and Cellular Longevity*, vol. 2013, Article ID 387014, 9 pages, 2013.

[84] Y. Wu, S. Antony, J. L. Meitzler, and J. H. Doroshow, "Molecular mechanisms underlying chronic inflammation-associated cancers," *Cancer Letters*, vol. 345, no. 2, pp. 164–173, 2014.

[85] F. Vannini, K. Kashfi, and N. Nath, "The dual role of iNOS in cancer," *Redox Biology*, vol. 6, pp. 334–343, 2015.

[86] M. A. Cinelli, H. T. Do, G. P. Miley, and R. B. Silverman, "Inducible nitric oxide synthase: regulation, structure, and inhibition," *Medicinal Research Reviews*, vol. 40, no. 1, pp. 158–189, 2020.

[87] C. H. Lee, H. J. Kim, Y. S. Lee et al., "Hypothalamic macrophage inducible nitric oxide synthase mediates obesity- associated hypothalamic inflammation," *Cell Reports*, vol. 25, no. 4, pp. 934–946.e5, 2018.

[88] J. Liu, Z. Wu, D. Han et al., "Mesencephalic astrocyte-derived neurotrophic factor inhibits liver cancer through small ubiquitin-related modifier (SUMO)ylation-related suppression of NF-κB/Snail signaling pathway and epithelial-mesenchymal transition," *Hepatology*, 2020.

[89] J. M. Song, P. Upadhyaya, and F. Kassie, "Nitric oxide-donating aspirin (NO-aspirin) suppresses lung tumorigenesis in vitro and in vivo and these effects are associated with modulation of the EGFR signaling pathway," *Carcinogenesis*, vol. 39, no. 7, pp. 911–920, 2018.

[90] J. PeÑarando, E. Aranda, and A. RodrÍguez-Ariza, "Immunomodulatory roles of nitric oxide in cancer: tumor microenvironment says "NO" to antitumor immune response," *Translational Research*, vol. 210, pp. 99–108, 2019.

[91] R. Keller, R. Keist, P. Joller, and A. Mülsch, "Coordinate Up- and Down-Modulation of Inducible Nitric Oxide Synthase, Nitric Oxide Production, and Tumoricidal Activity in Rat Bone Marrow-Derived Mononuclear Phagocytes by Lipopolysaccharide and Gram-Negative Bacteria," *Biochemical and Biophysical Research Communications*, vol. 211, no. 1, pp. 183–189, 1995.

[92] D. Huang, L. Cui, P. Guo et al., "Nitric oxide mediates apoptosis and mitochondrial dysfunction and plays a role in growth hormone deficiency by nivalenol in GH3 cells," *Scientific Reports*, vol. 7, no. 1, p. 17079, 2017.

[93] C. Wang, G. Gong, A. Sheh et al., "Interleukin-22 drives nitric oxide-dependent DNA damage and dysplasia in a murine model of colitis-associated cancer," *Mucosal Immunology*, vol. 10, no. 6, pp. 1504–1517, 2017.

[94] H. J. Lee, D. Feliers, M. M. Mariappan et al., "Tadalafil integrates nitric oxide-hydrogen sulfide signaling to inhibit high glucose-induced matrix protein synthesis in podocytes," *The Journal of Biological Chemistry*, vol. 290, no. 19, pp. 12014–12026, 2015.

[95] Y. Zang, K. C. Popat, and M. M. Reynolds, "Nitric oxide-mediated fibrinogen deposition prevents platelet adhesion and activation," *Biointerphases*, vol. 13, no. 6, article 06E403, 2018.

[96] L. Hou, Y. Zhang, X. Yang et al., "Intracellular NO-generator based on enzyme trigger for localized tumor-cytoplasm rapid drug release and synergetic cancer therapy," *ACS Applied Materials & Interfaces*, vol. 11, no. 1, pp. 255–268, 2019.

[97] B. E. Callejas, M. G. Mendoza-Rodríguez, O. Villamar-Cruz et al., "Helminth-derived molecules inhibit colitis-associated colon cancer development through NF-κB and STAT3 regulation," *International Journal of Cancer*, vol. 145, no. 11, pp. 3126–3139, 2019.

[98] A. Yadav, B. Kumar, J. C. Lang, T. N. Teknos, and P. Kumar, "A muscle-specific protein 'myoferlin' modulates IL-6/STAT3 signaling by chaperoning activated STAT3 to nucleus," *Oncogene*, vol. 36, no. 46, pp. 6374–6382, 2017.

[99] E. Seki, Y. Kondo, Y. Iimuro et al., "Demonstration of cooperative contribution of MET- and EGFR-mediated STAT3 phosphorylation to liver regeneration by exogenous suppressor of cytokine signalings," *Journal of Hepatology*, vol. 48, no. 2, pp. 237–245, 2008.

[100] X. Ye, H. Wu, L. Sheng et al., "Oncogenic potential of truncated RXRα during colitis-associated colorectal tumorigenesis by promoting IL-6-STAT3 signaling," *Nature Communications*, vol. 10, no. 1, article 1463, 2019.

[101] H. Zhang, Y. Song, H. Yang et al., "Tumor cell-intrinsic Tim-3 promotes liver cancer via NF-κB/IL-6/STAT3 axis," *Oncogene*, vol. 37, no. 18, pp. 2456–2468, 2018.

[102] A. Bhardwaj, G. Sethi, S. Vadhan-Raj et al., "Resveratrol inhibits proliferation, induces apoptosis, and overcomes chemoresistance through down-regulation of STAT3 and nuclear factor-κB-regulated antiapoptotic and cell survival gene products in human multiple myeloma cells," *Blood*, vol. 109, no. 6, pp. 2293–2302, 2007.

[103] S. Nakada, S. Kuboki, H. Nojima et al., "Roles of Pin1 as a key molecule for EMT induction by activation of STAT3 and NF-κB in human gallbladder cancer," *Annals of Surgical Oncology*, vol. 26, no. 3, pp. 907–917, 2019.

[104] J. Liu, Z. Zhang, J. Gao, J. Xie, L. Yang, and S. Hu, "Downregulation effects of beta-elemene on the levels of plasma endotoxin, serum TNF-alpha, and hepatic CD14 expression in rats with liver fibrosis," *Frontiers in Medicine*, vol. 5, no. 1, pp. 101–105, 2011.

[105] Y. Zhong, J. Liu, W. M. Huo, W. L. Duan, X. Wang, and J. Shang, "β-Elemene reduces the progression of atherosclerosis in rabbits," *Chinese Journal of Natural Medicines*, vol. 13, no. 6, pp. 415–420, 2015.

[106] Y. Fang, Y. Kang, H. Zou et al., "β-Elemene attenuates macrophage activation and proinflammatory factor production via crosstalk with Wnt/β-catenin signaling pathway," *Fitoterapia*, vol. 124, pp. 92–102, 2018.

[107] S. Patra, M. S. Muthuraman, M. Meenu, P. Priya, and B. Pemaiah, "Anti-inflammatory effects of royal poinciana through inhibition of toll-like receptor 4 signaling pathway," *International Immunopharmacology*, vol. 34, pp. 199–211, 2016.

[108] E. Sieniawska, P. Michel, T. Mroczek, S. Granica, and K. Skalicka-Woźniak, "*Nigella damascena* L. essential oil and its main constituents, damascenine and β-elemene modulate inflammatory response of human neutrophils *ex vivo*," *Food and Chemical Toxicology*, vol. 125, pp. 161–169, 2019.

[109] C. Pan, Y. Si, Q. Meng et al., "Suppression of the RAC1/MLK3/p38 signaling pathway by β-elemene alleviates sepsis-associated encephalopathy in mice," *Frontiers in Neuroscience*, vol. 13, p. 358, 2019.

[110] H. Wang and J. A. Keiser, "Vascular endothelial growth factor upregulates the expression of matrix metalloproteinases in vascular smooth muscle cells: role of flt-1," *Circulation Research*, vol. 83, no. 8, pp. 832–840, 1998.

[111] A. Leask, "Potential therapeutic targets for cardiac fibrosis: TGFβ, angiotensin, endothelin, CCN2, and PDGF, partners in fibroblast activation," *Circulation Research*, vol. 106, no. 11, pp. 1675–1680, 2010.

[112] D. Newsted, S. Banerjee, K. Watt et al., "Blockade of TGF-β signaling with novel synthetic antibodies limits immune exclusion and improves chemotherapy response in metastatic ovarian cancer models," *Oncoimmunology*, vol. 8, no. 2, article e1539613, 2019.

[113] Q. Shi and Y. G. Chen, "ALK-mediated Tyr95 phosphorylation of Smad4 impairs its transcription activity and the tumor suppressive activity of TGF-β," *Science China Life Sciences*, vol. 62, no. 3, pp. 431-432, 2019.

[114] C. Xue, L. L. Hong, J. S. Lin et al., "β-Elemene inhibits the proliferation of primary human airway granulation fibroblasts by down-regulating canonical Wnt/β-catenin pathway," *Bioscience Reports*, vol. 38, no. 2, 2018.

[115] C. Xue, X. P. Lin, J. M. Zhang, Y. M. Zeng, and X. Y. Chen, "β-Elemene suppresses the proliferation of human airway granulation fibroblasts via attenuation of TGF-β/Smad signaling pathway," *Journal of Cellular Biochemistry*, vol. 120, no. 10, pp. 16553–16566, 2019.

[116] X. Zhang, Y. Li, Y. Zhang et al., "Beta-elemene blocks epithelial-mesenchymal transition in human breast cancer cell line MCF-7 through Smad3-mediated down-regulation of nuclear transcription factors," *PLoS One*, vol. 8, no. 3, article e58719, 2013.

[117] J. Zheng, L. T. Ma, Q. Y. Ren et al., "The influence of astragalus polysaccharide and β-elemene on LX-2 cell growth, apoptosis and activation," *BMC Gastroenterology*, vol. 14, no. 1, p. 224, 2014.

[118] Q. Chen, D. Yang, H. Zong et al., "Growth-induced stress enhances epithelial-mesenchymal transition induced by IL-6 in clear cell renal cell carcinoma via the Akt/GSK-3β/β-catenin signaling pathway," *Oncogene*, vol. 6, no. 8, article e375, 2017.

[119] Y. Wang, J. A. Mack, and E. V. Maytin, "CD44 inhibits α-SMA gene expression via a novel G-actin/MRTF-mediated pathway that intersects with TGFβR/p38MAPK signaling in murine skin fibroblasts," *The Journal of Biological Chemistry*, vol. 294, no. 34, pp. 12779–12794, 2019.

[120] A. F. Setiadi, K. Omilusik, M. D. David et al., "Epigenetic enhancement of antigen processing and presentation promotes immune recognition of tumors," *Cancer Research*, vol. 68, no. 23, pp. 9601–9607, 2008.

[121] Z. Zhao, X. Xiao, P. E. Saw et al., "Chimeric antigen receptor T cells in solid tumors: a war against the tumor microenvironment," *Science China Life Sciences*, vol. 63, no. 2, pp. 180–205, 2020.

[122] F. F. Ni, Y. J. Liu, H. Zhou et al., "Treatment of hepatic cancer in mice by beta-elemene combined DC/Dribble vaccine: an immune mechanism research," *Zhongguo Zhong Xi Yi Jie He Za Zhi*, vol. 33, no. 2, pp. 214–219, 2013.

[123] J. Y. Kao, M. Zhang, M. J. Miller et al., "*Helicobacter pylori* immune escape is mediated by dendritic cell -induced Treg Skewing and Th17 suppression in mice," *Gastroenterology*, vol. 138, no. 3, pp. 1046–1054, 2010.

[124] G. Tan, Z. Wang, L. Che, and S. Yin, "Immunotherapeutic effects on murine pancreatic carcinoma by β-elemene combined with dendritic cells modified with genes encoding interleukin-23," *Frontiers of Medicine in China*, vol. 1, no. 1, pp. 41–45, 2007.

[125] K. Hagihara, S. Chan, L. Zhang et al., "Neoadjuvant sipuleucel-T induces both Th1 activation and immune regulation in localized prostate cancer," *Oncoimmunology*, vol. 8, no. 1, article e1486953, 2019.

[126] X. S. Wu, T. Xie, J. Lin et al., "An investigation of the ability of elemene to pass through the blood-brain barrier and its effect on brain carcinomas," *The Journal of Pharmacy and Pharmacology*, vol. 61, no. 12, pp. 1653–1656, 2009.

[127] R. Zhang, A. Tian, X. Shi, H. Yu, and L. Chen, "Downregulation of IL-17 and IFN-γ in the optic nerve by β-elemene in experimental autoimmune encephalomyelitis," *International Immunopharmacology*, vol. 10, no. 7, pp. 738–743, 2010.

[128] T. B. Alberti, R. Marcon, M. A. Bicca, N. R. Raposo, J. B. Calixto, and R. C. Dutra, "Essential oil from Pterodon emarginatus seeds ameliorates experimental autoimmune encephalomyelitis by modulating Th1/Treg cell balance," *Journal of Ethnopharmacology*, vol. 155, no. 1, pp. 485–494, 2014.

[129] R. Zhang, A. Tian, H. Zhang, Z. Zhou, H. Yu, and L. Chen, "Amelioration of experimental autoimmune encephalomyelitis by β-elemene treatment is associated with Th17 and Treg cell balance," *Journal of Molecular Neuroscience*, vol. 44, no. 1, pp. 31–40, 2011.

[130] X. Yu, Z. Li, Y. Zhang et al., "β-elemene inhibits radiation and hypoxia-induced macrophages infiltration via Prx-1/NF-κB/HIF-1α signaling pathway," *OncoTargets and Therapy*, vol. 12, pp. 4203–4211, 2019.

[131] X. Meng, N. Li, Y. Zhang et al., "Beneficial effect of β-elemene alone and in combination with hyperbaric oxygen in traumatic brain injury by inflammatory pathway," *Translational Neuroscience*, vol. 9, no. 1, pp. 33–37, 2018.

[132] K. Y. Sun, D. H. Xu, C. Xie et al., "*Lactobacillus paracasei* modulates LPS-induced inflammatory cytokine release by monocyte-macrophages via the up-regulation of negative regulators of NF-kappaB signaling in a TLR2-dependent manner," *Cytokine*, vol. 92, pp. 1–11, 2017.

[133] S. A. Doodnauth, S. Grinstein, and M. E. Maxson, "Constitutive and stimulated macropinocytosis in macrophages: roles in immunity and in the pathogenesis of atherosclerosis," *Philosophical Transactions of the Royal Society of London Series B: Biological Sciences*, vol. 374, no. 1765, article 20180147, 2019.

[134] U. Förstermann, N. Xia, and H. Li, "Roles of vascular oxidative stress and nitric oxide in the pathogenesis of atherosclerosis," *Circulation Research*, vol. 120, no. 4, pp. 713–735, 2017.

[135] S. Arora, K. Dev, B. Agarwal, P. Das, and M. A. Syed, "Macrophages: their role, activation and polarization in pulmonary diseases," *Immunobiology*, vol. 223, no. 4-5, pp. 383–396, 2018.

[136] X. Yu, M. Xu, N. Li et al., "β-Elemene inhibits tumor-promoting effect of M2 macrophages in lung cancer," *Biochemical and Biophysical Research Communications*, vol. 490, no. 2, pp. 514–520, 2017.

[137] L. Xu, D. Sharkey, and L. G. Cantley, "Tubular GM-CSF promotes late MCP-1/CCR2-mediated fibrosis and inflammation after ischemia/reperfusion injury," *Journal of the American Society of Nephrology*, vol. 30, no. 10, pp. 1825–1840, 2019.

[138] K. A. da Franca Rodrigues, L. V. Amorim, J. M. G. de Oliveira et al., "Eugenia uniflora L. essential oil as a potential anti-Leishmania agent: effects on Leishmania amazonensis and possible mechanisms of action," *Evidence-Based Complementary and Alternative Medicine*, vol. 2013, Article ID 279726, 10 pages, 2013.

[139] M. Lind, A. Hayes, M. Caprnda et al., "Inducible nitric oxide synthase: good or bad?," *Biomedicine & Pharmacotherapy*, vol. 93, pp. 370–375, 2017.

[140] C. Y. Xie, W. Yang, J. Ying et al., "B-cell lymphoma-2 overexpression protects δ-elemene-induced apoptosis in human lung carcinoma mucoepidermoid cells via a nuclear factor kappa B-related pathway," *Biological & Pharmaceutical Bulletin*, vol. 34, no. 8, pp. 1279–1286, 2011.

[141] S. S. Lim, K. H. Shin, H. S. Ban et al., "Effect of the essential oil from the flowers of *Magnolia sieboldii* on the lipopolysaccharide-induced production of nitric oxide and prostaglandin E_2 by rat peritoneal macrophages," *Planta Medica*, vol. 68, no. 5, pp. 459–462, 2002.

[142] G. X. Wang, L. Y. Wu, S. T. Tang, and T. Y. Yin, "The protection of elemene on injured HUVECs induced by hydrogen peroxide," *Zhong Yao Cai*, vol. 30, no. 11, pp. 1407–1410, 2007.

[143] J. C. Chen, W. L. Duan, R. R. Bai et al., "Synthesis of 13-β-elemene ester derivatives and evaluation of their antioxidant activity in human umbilical vein endothelial cells," *Chinese Journal of Natural Medicines*, vol. 13, no. 8, pp. 618–627, 2015.

[144] J. Chen, W. Duan, R. Bai, H. Yao, J. Shang, and J. Xu, "Design, synthesis and antioxidant activity evaluation of novel β-elemene derivatives," *Bioorganic & Medicinal Chemistry Letters*, vol. 24, no. 15, pp. 3407–3411, 2014.

[145] M. Liu, X. Chen, J. Ma et al., "β-Elemene attenuates atherosclerosis in apolipoprotein E-deficient mice *via* restoring NO levels and alleviating oxidative stress," *Biomedicine & Pharmacotherapy*, vol. 95, pp. 1789–1798, 2017.

[146] W. Sun, Y. Huang, T. Yin et al., "Effects of elemene on inhibiting proliferation of vascular smooth muscle cells and promoting reendothelialization at the stent implantation site," *Biomaterials Science*, vol. 5, no. 6, pp. 1144–1155, 2017.

[147] K. A. Ahmad, H. Ze, J. Chen et al., "The protective effects of a novel synthetic β-elemene derivative on human umbilical vein endothelial cells against oxidative stress-induced injury: involvement of antioxidation and PI3k/Akt/eNOS/NO signaling pathways," *Biomedicine & Pharmacotherapy*, vol. 106, pp. 1734–1741, 2018.

[148] J. Chen, R. Wang, T. Wang et al., "Antioxidant properties of novel dimers derived from natural β-elemene through inhibiting H_2O_2-induced apoptosis," *ACS Medicinal Chemistry Letters*, vol. 8, no. 4, pp. 443–448, 2017.

[149] J. Chen, T. Wang, S. Xu et al., "Discovery of novel antitumor nitric oxide-donating β-elemene hybrids through inhibiting the PI3K/Akt pathway," *European Journal of Medicinal Chemistry*, vol. 135, pp. 414–423, 2017.

[150] F. Li, S. Zhao, T. Guo, J. Li, and C. Gu, "The nutritional cytokine leptin promotes NSCLC by activating the PI3K/AKT and MAPK/ERK pathways in NSCLC cells in a paracrine manner," *BioMed Research International*, vol. 2019, Article ID 2585743, 8 pages, 2019.

[151] C. J. David, Y. H. Huang, M. Chen et al., "TGF-β tumor suppression through a lethal EMT," *Cell*, vol. 164, no. 5, pp. 1015–1030, 2016.

[152] Y. Y. Jing, Z. P. Han, K. Sun et al., "Toll-like receptor 4 signaling promotes epithelial-mesenchymal transition in human hepatocellular carcinoma induced by lipopolysaccharide," *BMC Medicine*, vol. 10, no. 1, p. 98, 2012.

[153] H. Cheng, X. Ge, S. Zhuo et al., "β-Elemene synergizes with gefitinib to inhibit stem-like phenotypes and progression of lung cancer via down-regulating EZH2," *Frontiers in Pharmacology*, vol. 9, article 1413, 2018.

Hindawi
BioMed Research International
Volume 2024, Article ID 9753242, 1 page
https://doi.org/10.1155/2024/9753242

Retraction

Retracted: Bone Marrow Plasma Cytokine Signature Profiles in Severe Aplastic Anemia

BioMed Research International

Received 12 March 2024; Accepted 12 March 2024; Published 20 March 2024

This article has been retracted by Hindawi following an investigation undertaken by the publisher [1]. This investigation has uncovered evidence of one or more of the following indicators of systematic manipulation of the publication process:

(1) Discrepancies in scope

(2) Discrepancies in the description of the research reported

(3) Discrepancies between the availability of data and the research described

(4) Inappropriate citations

(5) Incoherent, meaningless and/or irrelevant content included in the article

(6) Manipulated or compromised peer review

The presence of these indicators undermines our confidence in the integrity of the article's content and we cannot, therefore, vouch for its reliability. Please note that this notice is intended solely to alert readers that the content of this article is unreliable. We have not investigated whether authors were aware of or involved in the systematic manipulation of the publication process.

Wiley and Hindawi regrets that the usual quality checks did not identify these issues before publication and have since put additional measures in place to safeguard research integrity.

We wish to credit our own Research Integrity and Research Publishing teams and anonymous and named external researchers and research integrity experts for contributing to this investigation.

The corresponding author, as the representative of all authors, has been given the opportunity to register their agreement or disagreement to this retraction. We have kept a record of any response received.

References

[1] B. Liu, Y. Shao, Z. Liu, C. Liu, T. Zhang, and R. Fu, "Bone Marrow Plasma Cytokine Signature Profiles in Severe Aplastic Anemia," *BioMed Research International*, vol. 2020, Article ID 8789275, 11 pages, 2020.

Hindawi
BioMed Research International
Volume 2020, Article ID 8789275, 11 pages
https://doi.org/10.1155/2020/8789275

Research Article

Bone Marrow Plasma Cytokine Signature Profiles in Severe Aplastic Anemia

Bingnan Liu, Yuanyuan Shao, Zixuan Liu, Chunyan Liu, Tian Zhang, and Rong Fu

Department of Hematology, Tianjin Medical University General Hospital, 154 Anshan Street, Heping District, Tianjin 300052, China

Correspondence should be addressed to Rong Fu; furong8369@tmu.edu.cn

Received 3 January 2020; Revised 25 January 2020; Accepted 28 January 2020; Published 18 February 2020

Guest Editor: Hengjia Ni

Objective. We studied bone marrow plasma (BMP) cytokines in severe aplastic anemia (SAA) patients and healthy volunteers to investigate differences in the cytokine profiles between them and propose a cytokine signature of SAA. *Methods*. A Bio-Plex suspension array system was used to measure 27 analytes in BMP samples from 47 SAA patients and 30 healthy donors. *Results*. Compared to healthy people, SAA patients had higher levels of tumor necrosis factor α (TNF-α), interferon-γ (IFN-γ), interleukin-2 (IL-2), monocyte chemoattractant protein 1 (MCP-1), and granulocyte colony-stimulating factor (G-CSF). They also had lower levels of interleukin-1 receptor antagonist (IL-1ra), interleukin-9 (IL-9), regulated upon activation normal T cell expressed and secreted (RANTES) factor, platelet-derived growth factor-BB (PDGF-BB), and macrophage inflammatory protein 1β (MIP-1β). Levels of interleukin-4 (IL-4), IL-1ra, macrophage inflammatory protein 1α (MIP-1α), and eotaxin were significantly higher in recovering SAA (RSAA) patients. Levels of IL-5, IL-6, IL-10, IL-12, IL-13, IL-15, granulocyte-macrophage colony-stimulating factor (GM-CSF), and vascular endothelial growth factor (VEGF) were undetectable. There were no significant differences in the levels of IL-1β, IL-4, IL-7, IL-8, IL-17, basic fibroblast growth factor (FGF-β), and IFN inducible protein-10 (IP-10) between patients and healthy controls (HCs). Eotaxin, IL-1ra, MCP-1, MIP-1β, and RANTES levels increased after IST, whereas IFN-γ, G-CSF, IL-2, IL-7, and TNF-α levels decreased after IST. *Conclusions*. The current study demonstrated distinct cytokine profiles among untreated SAA patients, recovering SAA (RSAA) patients, and healthy people. The cytokines of RSAA patients showed similar characteristics to those of untreated SAA patients and healthy people, respectively, which may reflect that the immune status of RSAA patients is in different stages of recovery after IST; thus, it may provide an important tool in diagnosing and evaluating or predicting curative effects in clinics.

1. Introduction

Severe aplastic anemia (SAA) is a severe disease characterized by bone marrow failure and a high fatality rate. Bone marrow failure in SAA is usually caused by an immunologic mechanism, and immunosuppressive therapy (IST) is effective in most SAA patients [1, 2]. Cytokines and chemokines play a key role in immune cell activation in the pathogenesis of SAA. Cytokines and chemokines are low-molecular-weight proteins that are secreted by immunocytes, activate other immune cells, and mediate inflammatory responses. Previous studies have shown that $CD8^+$T cells are aberrantly activated in SAA as myeloid dendritic cells (mDCs) and helper Th1 cells [2, 3]. Meanwhile, IFN-γ, TNF-α, and IL-2 levels have been shown to significantly increase in SAA [4, 5]. Although the immune pathogenesis of SAA has been widely studied, very little is known about the alternations of cytokines and chemokines in the bone marrow.

In the past, measurements of cytokines have been limited to two or three in SAA [6]. Due to the large number of proteins involved in the immune reaction, the detection of a single cytokine is not enough to evaluate the change in disease. Based on this, we conducted a comprehensive

Table 1: Clinical and demographic parameters of patients participating in the present study.

Diagnosis	Number	Age (years)	ANC (10^9/L)	Hb (g/L)	Plt(10^9/L)	Ret%	Ret (10^9/L)	Bone marrow karyotype	Therapy	Duration (months)
Untreated SAA	28	40 (11–78)	0.52 ± 0.82	74.39 ± 11.43	15.14 ± 10.44	0.68 ± 0.83	16.59 ± 19.89	Male 46, XY [9] Female 46, XX [9]	Not treated except for transfusions	2 (1–3)
Recovering SAA	19	26 (15–65)	4.65 ± 3.33	104.68 ± 37.32	77.42 ± 76.72	2.35 ± 1.16	68.42 ± 33.29	Male 46, XY [9] Female 46, XX [9]	Treated with a combination of ATG and CsA	32 (6–116)

Values are expressed as means ± SDs. Age and duration values are expressed as follows: mid (min–max). ANC: absolute neutrophil count; Hb: hemoglobin; Plt: platelet count; Ret: reticulocyte. Duration of untreated SAA: from the onset of disease to the time of cytokine measurement; duration of recovering SAA: from the onset of ATG therapy to the time of cytokine measurement.

testing of 27 cytokines and chemokines in the bone marrow plasma (BMP) of healthy volunteers, untreated SAA patients, and recovering SAA (RSAA) patients. We describe differences in the cytokine profiles between these groups and propose a cytokine signature that might help in exploring the pathogenesis of SAA.

2. Patients and Methods

2.1. Patients. Forty-seven patient samples and thirty healthy control (HC) samples were measured in the present study. This cohort of patients included 28 SAA patients who were previously untreated and 19 RSAA patients. SAA was diagnosed according to the criteria of the International Aplastic Anemia Study Group [7]. Participants who had paroxysmal nocturnal hemoglobinuria, myelodysplastic syndrome, tumors, infections, or congenital diseases were excluded. Patients with SAA were diagnosed in our department from March 2018 to August 2019. In six of the untreated SAA patients, serial analyses were performed before and three and six months after rabbit anti-human thymocyte immunoglobulin (rATG) and cyclosporine (CsA) treatment. RSAA patients were defined as SAA patients having experienced substantial improvement after therapy with rATG (Fresenius, Germany) and a decreasing dose of CsA [8]; all of these patients became completely transfusion-independent. The clinical characteristics of the patients are listed in Table 1. Healthy volunteers were recruited from the staff of our laboratory and health examination center. The 77 samples included samples from 36 males and 41 females, with ages ranging from 11 to 78 years and a median age of 36 years. The study procedures and informed written consent were approved by the Ethics Committee of Tianjin Medical University.

2.2. Cytokine and Chemokine Measurement. Plasma samples were obtained by centrifugation of heparinized bone marrow and stored at −80°C until examination. We analyzed 27 cytokines and chemokines in the BMP of the samples by applying Luminex-based multiplex bead technology. The Bio-Plex Pro Human Cytokine group I Panel 27-Plex was applied out as follows: IL-1β, IL-1ra, IL-2, IL-4, IL-5, IL-6, IL-7, IL-8 (CXCL-8), IL-9, IL-10, IL-12p70, IL-13, IL-15, IL-17, basic fibroblast growth factor (FGF-β), eotaxin (CCL-11), granulocyte colony-stimulating factor (G-CSF), granulocyte-macrophage colony-stimulating factor (GM-CSF), IFN-γ, IFN inducible protein-10 (IP-10; CXCL-10), MCP-1 (CCL-2), macrophage inflammatory protein 1α (MIP-1α; CCL-3), MIP-1β (CCL-4), platelet-derived growth factor-BB (PDGF-BB), RANTES (CCL-5), TNF-α, and vascular endothelial growth factor (VEGF; Bio-Rad Laboratories, Inc., Made in the USA). All Bio-Plex assays were conducted according to the manufacturer's instructions. The median fluorescence intensities (MFIs) of analytes were analyzed on a Luminex-100 instrument (Luminex, Bio-Rad) using Bio-Plex Manager software version 6.0 (Bio-Rad, USA). Each analyte was tested in duplicate, and the average value was recorded as the measured concentration. The acquired data was processed by applying Data Pro Manager 1.02 (Bio-Rad, USA) and Prism Software version 6.0.

2.3. Statistical Analysis. When the normality of the distribution was proven using a Kolmogorov-Smirnov test, an independent t-test was used to compare the means of the analyte concentrations; otherwise, a nonparametric test was applied. For the nonnormal distribution data, a Mann–Whitney U test was used to compare two groups of continuous variables and a Kruskal–Wallis one-way ANOVA was used to compare three groups. In drawing a cluster heat map, a log transformation was applied to the data to correct for nonnormal distribution. A Spearman's rank correlation test was used to test for correlated data; when significant results were found, the correlation coefficient (r) was reported. Quantitative data was expressed in the form of means ± SDs and medians, and significance was considered when $p < 0.05$. SPSS 19.0 software (IBM, USA) was used for statistical analyses.

3. Results

3.1. BMP Cytokine Concentration in SAA Patients and Healthy Controls. Cytokine Bio-Plex assays were conducted to measure the BMP cytokine concentrations in SAA patients and HCs. The median cytokine concentrations of the SAA

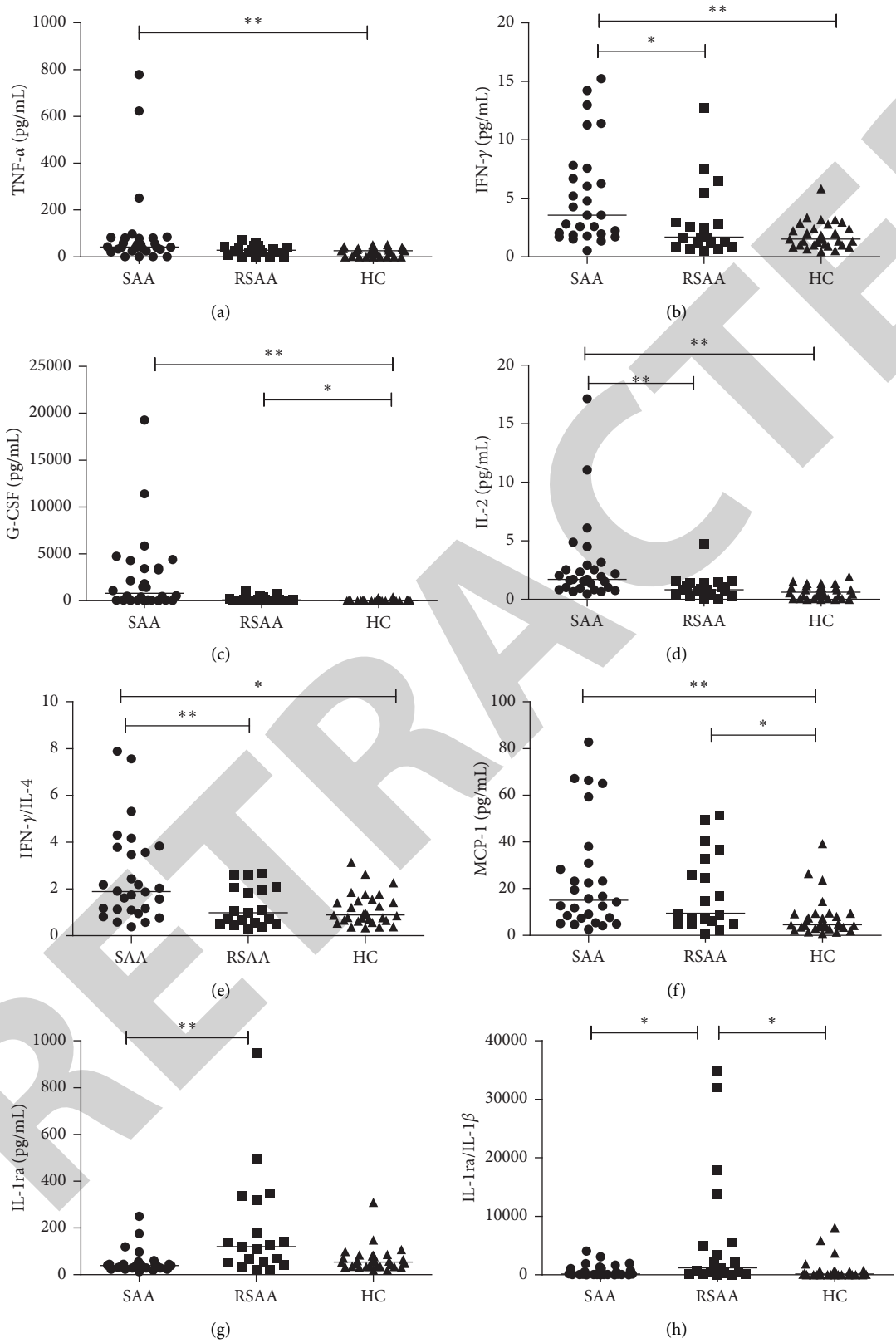

Figure 1: Continued.

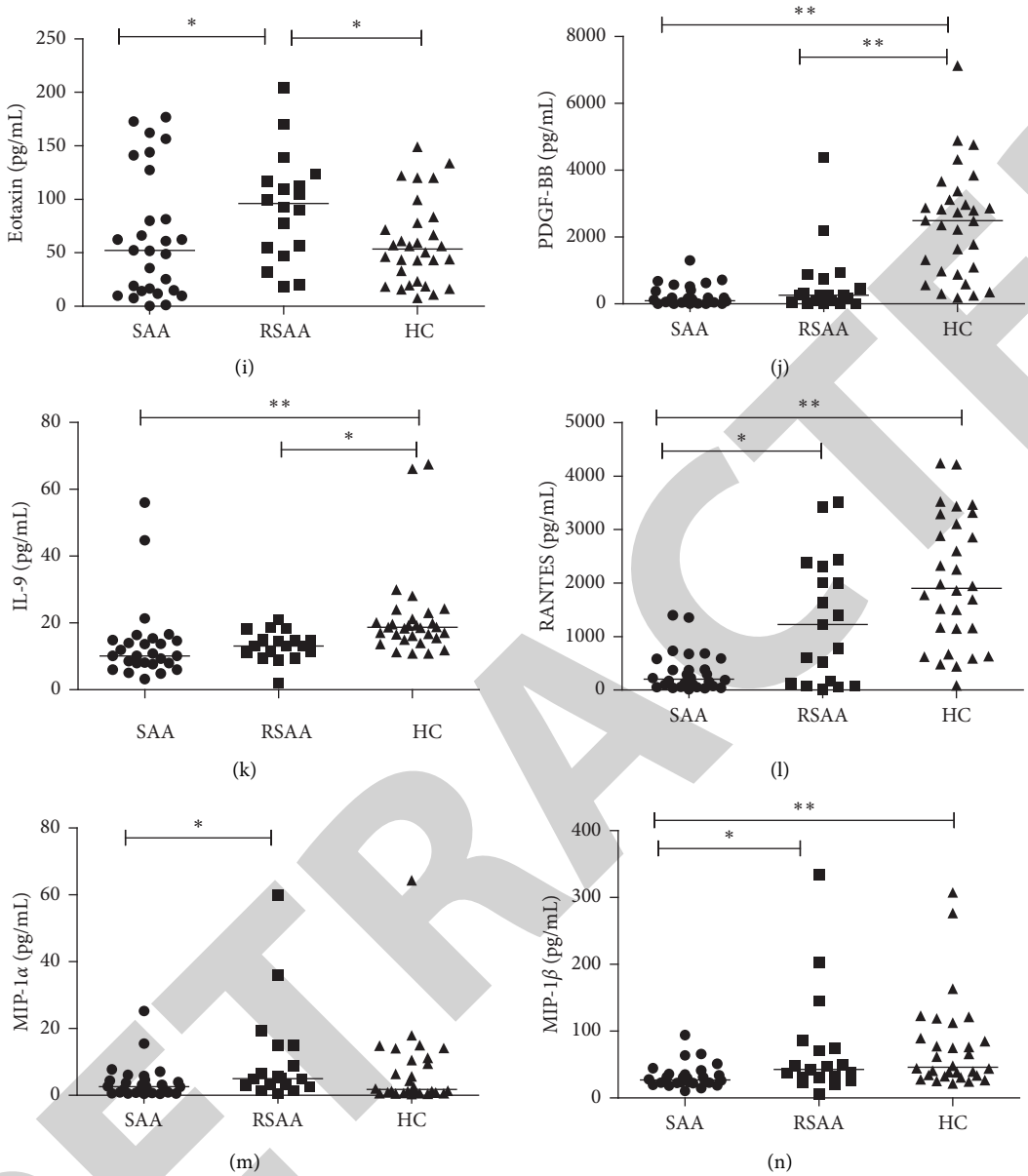

Figure 1: Levels of cytokines and growth factors in the BMP of SAA patients, RSAA patients, and HCs. The bars represent median values. A rank-based Kruskal-Wallis one-way analysis of variance (ANOVA) was performed to test for differences in the concentrations of cytokines among SAA patients, RSAA patients, and HCs. SAA: severe aplastic anemia; RSAA: recovering SAA; HC: healthy control; $^{**}p < 0.01$, $^{*}p < 0.05$.

patients, RSAA patients, and HCs are shown in Figure 1; the mean, standard deviation (SD) of the mean, and median values are presented in Table 2. As shown in Figure 1, higher levels of TNF-α, IFN-γ, G-CSF, IL-2, and MCP-1 (Figures 1(a)–1(f)) and lower levels of IL-1ra, PDGF-BB, IL-9, RANTES, and MIP-1β (Figures 1(g)–1(n)) were present in SAA patients compared to HCs. Additionally, levels of IL-1ra, eotaxin, and MIP-1α were significantly higher in RSAA patients than those in HCs (Figures 1(g), 1(i), and 1(m)). The median concentration of IFN-γ in untreated SAA patients was 3.56 ng/ml, which was higher than that found in recovery patients (1.69 ng/ml) and normal controls (1.51 ng/ml; $p < 0.001$; Figure 1(b)). The median concentration of RANTES in untreated SAA patients was 203.775 ng/ml, which was significantly lower than that found in RSAA patients (1222.56 ng/ml) and HCs (1903.03 ng/ml; $p < 0.001$; Figure 1(l)). The median concentrations of IL-1ra in SAA patients, RSAA patients, and HCs were 39.955 ng/ml, 120.72 ng/ml, and 54.55 ng/ml, respectively; the level of IL-1ra found in recovery patients was higher than that found in untreated patients ($p = 0.002$; Figure 1(g)). Levels of IL-5, IL-6, IL-10, IL-12p70, IL-13, IL-15, GM-CSF, and VEGF were undetectable. Additionally, there were no significant differences in IL-1β, IL-4, IL-7, IL-8, IL-17, FGF-β, and IP-10 levels between the SAA patients and the HCs.

Table 2: Statistical differences in the cytokine levels of SAA patients and HCs.

	SAA		RSAA		HC		p value
	Median	Mean ± SD	Median	Mean ± SD	Median	Mean ± SD	
IL-1β	0.25	0.60 ± 0.74	0.09	1.62 ± 6.04	0.40	1.19 ± 3.58	ns
IL-1ra	39.955	54.14 ± 50.87	120.72	190.63 ± 226.88	54.55	66.62 ± 54.05	0.002
IL-1ra/IL-1β	154.28	697.43 ± 1017.72	1211.00	6323.57 ± 10694.04	144.26	840.44 ± 1846.38	0.013
IL-2	1.69	2.85 ± 3.55	0.83	1.03 ± 1.02	0.605	0.63 ± 055	<0.001
IL-4	1.96	2.41 ± 1.85	2.31	2.46 ± 1.17	1.59	1.74 ± 0.63	ns
IL-7	20.17	19.99 ± 16.22	6.47	21.79 ± 47.52	10.22	15.65 ± 17.01	ns
IL-8	8.285	15.34 ± 13.80	11.46	79.21 ± 223.00	3.31	59.40 ± 182.72	ns
IL-9	10.53	19.17 ± 30.99	13.11	17.43 ± 18.61	18.69	21.50 ± 13.16	<0.001
IL-17	3.795	4.82 ± 3.26	6.84	7.15 ± 5.33	4.01	5.11 ± 2.58	ns
FGF-β	6.53	7.74 ± 4.83	5.94	7.06 ± 5.80	6.235	6.73 ± 2.61	ns
Eotaxin	52.125	64.78 ± 58.18	99.36	107.49 ± 80.50	53.415	59.07 ± 39.25	0.039
G-CSF	810.27	2518.84 ± 4163.51	84.32	191.90 ± 279.21	17.66	54.14 ± 94.76	<0.001
IFN-γ	3.56	5.19 ± 4.25	1.69	2.90 ± 3.12	1.51	1.84 ± 1.14	<0.001
IP-10	545.445	572.15 ± 356.15	442.08	460.00 ± 291.14	476.985	643.88 ± 515.86	ns
MCP-1	15.065	23.89 ± 23.02	9.47	18.36 ± 16.47	4.575	7.69 ± 8.39	<0.001
MIP-1α	2.635	3.96 ± 5.26	5.19	34.67 ± 104.49	2.31	27.57 ± 78.26	0.038
MIP-1β	26.895	32.58 ± 17.79	42.67	70.85 ± 79.20	46.32	76.94 ± 68.99	<0.001
PDGF-bb	96.85	236.80 ± 308.18	257.03	597.76 ± 1051.70	2492.395	2389.83 ± 1632.46	<0.001
RANTES	203.775	334.67 ± 366.43	1222.56	1299.58 ± 1162.78	1903.03	2027.68 ± 1201.01	<0.001
TNF-α	42.415	98.37 ± 178.04	27.96	28.16 ± 21.14	27.96	22.79 ± 17.69	0.003
IFN-γ/IL-4	1.89	2.50 ± 1.97	0.98	1.24 ± 0.84	0.885	1.13 ± 0.69	0.002

Data is presented in pg/ml; ns: not significant; SAA: severe aplastic anemia; RSAA: recovering SAA; HC: healthy control.

Compared to the RSAA patients and HCs, the SAA patients had higher levels of Type I lymphocyte factor secreted by T-helper cell 1 (Th1). IL-2, IFN-γ, and TNF-α levels were the highest among the SAA patients, with no differences between those of the RSAA patients and those of the HCs, and the IL-7 levels showed an increasing trend (p = 0.087) in the SAA patients (Figures 1(a), 1(b), and 1(d)). In contrast, we found an increasing trend of IL-4 levels (representative of Th2 cytokine) in the RSAA group, although this trend was not statistically significant (p = 0.098). The Th1/Th2 cytokine ratio of IFN-γ to IL-4 was significantly higher in the SAA group than that in the other groups (Figure 1(e)). Furthermore, MCP-1 (a Th2 cytokine) was the highest in the SAA patients ($p < 0.001$) but more elevated in the RSAA patients (p = 0.020) than in the HCs (Figure 1(f)). Among the cytokines that were the lowest in the SAA patients, IL-9 and PDGF-BB (Figures 1(j) and 1(k)) were also lower in the RSAA patients but MIP-1β and RANTES (Figures 1(l) and 1(n)) appeared to be higher in the RSAA patients and there were no statistic differences between RSAA and HC.

To classify cytokine patterns among the individuals, we performed a two-way hierarchical cluster analysis on log-transformed data from the SAA patients, RSAA patients, and HCs using OriginPro 2018 (Figure 2). The dendrogram above Figure 2 was categorized into three clusters, conforming to the corresponding groups for the majority of samples, which indicated that the SAA patients, RSAA patients, and HCs showed different cytokine patterns. Meanwhile, the overlaps of the three clusters implied that the cytokine pattern of some RSAA patients had not been recovered, while others had returned to normal. The dendrogram to the left of Figure 2 displayed the proximity between the different cytokines. The cluster heat map showed four groups of cytokines: (1) IL-7, TNF-α, MCP-1, IFN-γ, IL-2, and G-CSF; (2) IP-10, RANTES, PDGF-bb, and IL-9; (3) MIP-1β, MIP-1α, IL-8, and IL-1ra; and (4) eotaxin, IL-17, IL-4, FGF-β, and IL-1β. Cytokines in each of these groups may play proximate roles and/or share the same origin.

3.2. Correlation of BMP Cytokine Concentrations with Clinical Parameters. A Spearman correlation analysis was performed to investigate the correlation of BMP cytokines with blood cell levels in SAA and RSAA patients (Table 3). MIP-1α and RANTES levels correlated significantly with major blood cell types including absolute neutrophil count ($r = 0.481$, $p = 0.001$; $r = 0.291$, $p = 0.047$), hemoglobin ($r = 0.389$, $p = 0.007$; $r = 0.414$, $p = 0.004$), platelet count ($r = 0.360$, $p = 0.013$; $r = 0.442$, $p = 0.002$), proportion of reticulocytes ($r = 0.510$, $p < 0.001$; $r = 0.451$, $p = 0.001$), and absolute reticulocyte count ($r = 0.595$, $p < 0.001$; $r = 0.505$, $p < 0.001$). IL-1ra, eotaxin, G-CSF, and MIP-1β also significantly correlated with major blood cell types, except for hemoglobin, including absolute neutrophil count ($r = 0.481$, $p = 0.001$; $r = 0.291$, $p = 0.047$), platelet count ($r = 0.360$, $p = 0.013$; $r = 0.442$, $p = 0.002$), proportion of reticulocytes ($r = 0.510$, $p < 0.001$; $r = 0.451$, $p = 0.001$), and absolute reticulocyte count ($r = 0.595$, $p < 0.001$; $r = 0.505$, $p < 0.001$). Notably, IL-2, G-CSF, IFN-γ, and TNF-α negatively correlated with the aforementioned parameters, whereas the other cytokines correlated positively with these parameters. Among these cytokines, IFN-γ correlated more strongly with absolute neutrophil count ($r = -0.307$, $p < 0.001$) than did hemoglobin, platelet count, proportion of reticulocytes, or absolute reticulocyte count; TNF-α correlated more

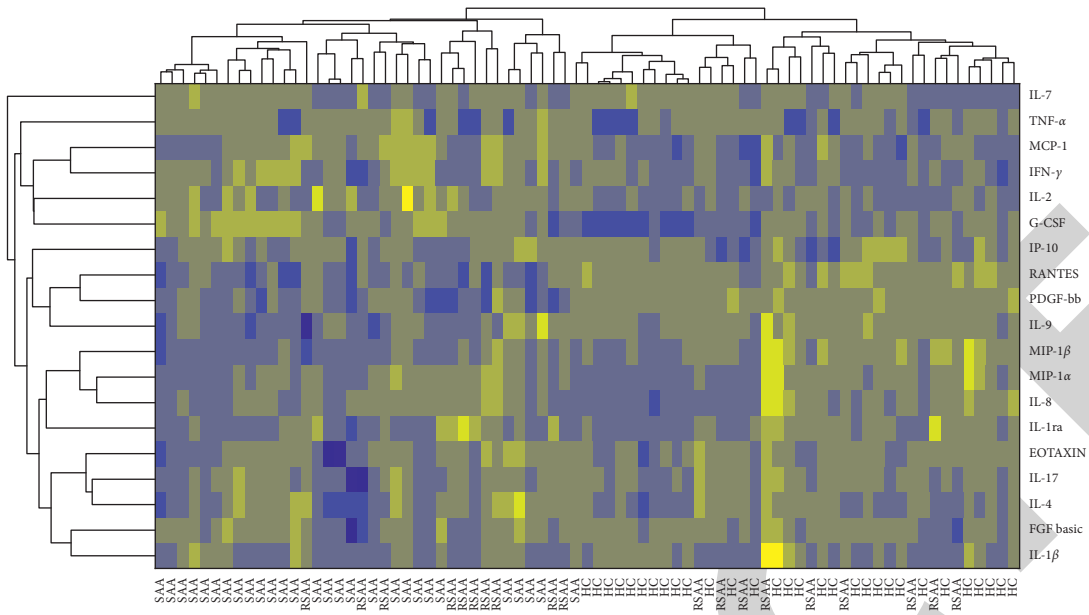

Figure 2: Different cytokine profiles of severe aplastic anemia (SAA) patients, recovering SAA (RSAA) patients, and healthy controls (HCs). A two-way hierarchical cluster analysis was performed on the log-transformed cytokine levels of SAA, RSAA, and HC samples using OriginPro 2018. Color scales represent cytokine levels (yellow indicates high levels; blue indicates low levels). The dendrogram above the figure was categorized into three clusters according to the cytokine profiles. The dendrogram to the left of the figure displays the proximities of the cytokines.

Table 3: Correlations of cytokines with blood cell counts in SAA and RSAA patients.

	ANC		Hb		Plt		Ret%		Ret	
IL-1ra	$r = 0.613$	$p < 0.001$	nc		$r = 0.448$	$p = 0.002$	$r = 0.323$	$p = 0.027$	$r = 0.457$	$p = 0.001$
IL-2	$r = -0.393$	$p = 0.006$	nc		$r = -0.355$	$p = 0.014$	nc		$r = -0.319$	$p = 0.029$
IL-9	nc		nc		$r = 0.456$	$p < 0.001$	$r = 0.343$	$p = 0.018$	$r = 0.302$	$p = 0.039$
IL-17	nc		nc		nc		nc		$r = 0.290$	$p = 0.048$
Eotaxin	$r = 0.381$	$p = 0.008$	nc		$r = 0.348$	$p = 0.017$	$r = 0.307$	$p = 0.036$	$r = 0.355$	$p = 0.014$
G-CSF	$r = -0.363$	$p = 0.012$	nc		$r = -0.416$	$p = 0.004$	$r = -0.521$	$p < 0.001$	$r = -0.498$	$p < 0.001$
IFN-γ	$r = -0.307$	$p < 0.001$	nc		nc		nc		nc	
MIP-1α	$r = 0.481$	$p = 0.001$	$r = 0.389$	$p = 0.007$	$r = 0.360$	$p = 0.013$	$r = 0.510$	$p < 0.001$	$r = 0.595$	$p < 0.001$
PDGF-bb	nc		nc		$r = 0.480$	$p = 0.001$	nc		$r = 0.338$	$p = 0.020$
MIP-1β	$r = 0.442$	$p = 0.002$	nc		$r = 0.424$	$p = 0.003$	$r = 0.440$	$p = 0.002$	$r = 0.500$	$p < 0.001$
RANTES	$r = 0.291$	$p = 0.047$	$r = 0.414$	$p = 0.004$	$r = 0.442$	$p = 0.002$	$r = 0.451$	$p = 0.001$	$r = 0.505$	$p < 0.001$
TNF-α	nc		nc		$r = -0.320$	$p = 0.028$	nc		nc	

ANC: absolute neutrophil count; Hb: hemoglobin; Plt: platelet count; Ret%: proportion of reticulocytes; Ret: absolute reticulocyte count; nc: no correlation.

strongly with platelet count ($r = -0.320$, $p = 0.028$) than did other cell types; and IL-2 correlated more strongly with absolute neutrophil count ($r = -0.393$, $p = 0.006$), platelet count ($r = -0.355$, $p = 0.014$), and absolute reticulocyte count ($r = -0.319$, $p = 0.029$) than did other cell types.

3.3. BMP Cytokine Concentration and Age/Gender. There were no significant differences in the levels of IL-1β, IL-4, IL-7, IL-8, IL-17, FGF-β, and IP-10 between the patients and the HCs. To explore what factors might have caused these cytokine levels to differ between individuals, we analyzed the correlations of age and gender with cytokine concentrations in all samples. We performed a Spearman test to explore the correlation of cytokine concentration with age. The results of this test showed that the levels of three cytokines were significantly and positively correlated with age: IL-8 ($r = 0.225$, $p = 0.049$), IP-10 ($r = 0.218$, $p = 0.049$), and FGF-β ($r = 0.278$, $p = 0.014$; Figures 3(a)–3(c)).

We conducted a Mann–Whitney test to evaluate the differences in cytokine concentrations between gender groups in all samples (36 males, 41 females). Only one BMP cytokine concentration was different between men and women: the median concentration of IL-17 was higher in men than in women (6.79 pg/mL versus 4.01 pg/mL; $p = 0.048$; Figure 3(d)).

3.4. BMP Cytokine Concentrations in SAA Patients before and after IST. In order to determine whether there were any changes in the cytokine levels of SAA patients after receiving IST, we detected the cytokine levels of six patients before and

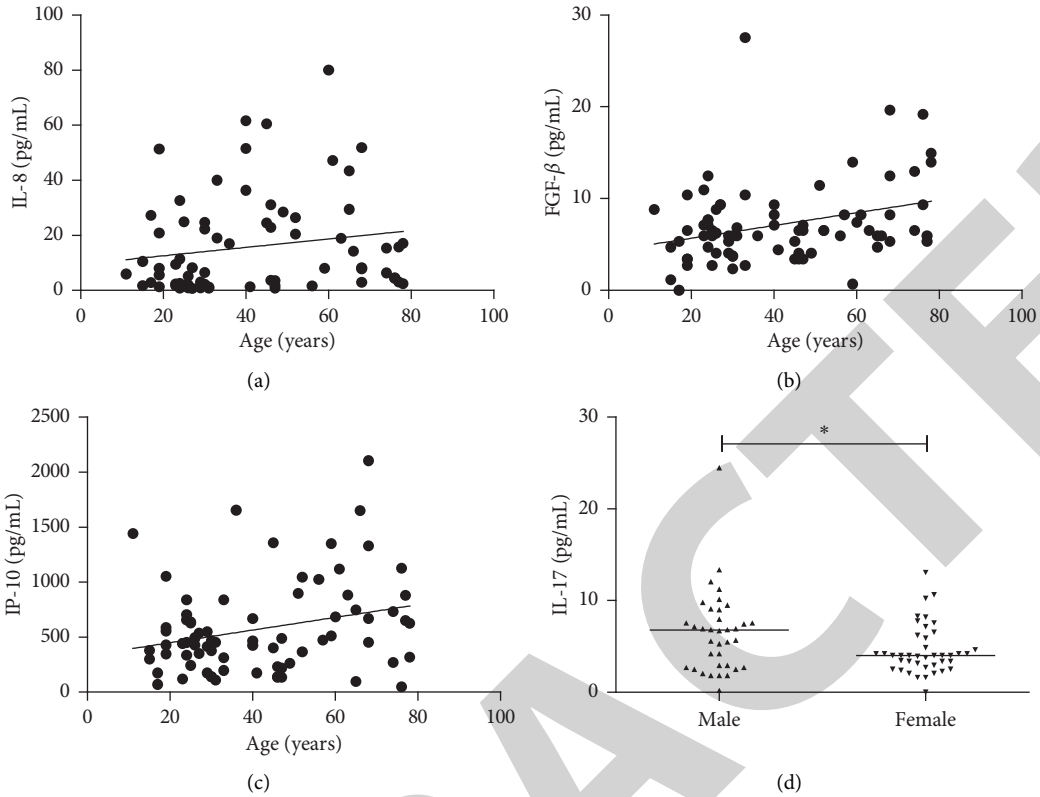

Figure 3: Correlation between cytokine concentration and age/gender. The 77 samples included samples from 36 males and 41 females, ranging in age from 11 to 78 years with a median age of 36 years.

three and six months after receiving ATG + CsA treatment (Figure 4). Statistically significant increases in eotaxin, IL-1ra, and MCP-1 had occurred by three months after IST. MIP-1β and RANTES levels had increased by six months after IST. IFN-γ and G-CSF concentrations, which were the highest in the untreated SAA patients, had decreased by three months after IST. Decreases in IL-2, IL-7, and TNF-α were observed by six months after IST.

4. Discussion

In the present study, increased levels of Type I lymphocyte factors IFN-γ, IL-2, and TNF-α were observed in the BMP of untreated SAA patients; these levels decreased after IST. These results are consistent with the theory of SAA immune pathogenesis, which suggests that SAA is an autoimmune disease that results from overactivation of the immune system, especially T lymphocytes [1, 2]. Cytokines are also excessively secreted by T cells, indicating that the pathogenesis of SAA is associated with the Th1 cell response [4, 5]. In addition, the immune pathogenesis of SAA also includes imbalance dendritic cell subsets (elevated mDC), enhanced dendritic cell function, insufficiency of Treg cells, and decreased proportion but enhanced function of NK cells [3, 10]. However, the IL-12 and GM-CSF involved in these immune processes were undetectable in all samples. A significant increase in G-CSF was also observed in SAA patients. The elevated concentrations of G-CSF in SAA patients may reflect a physiological negative feedback mechanism; this conclusion is consistent with those of previous studies [11]. Because Th2 cytokines showed an increasing trend in SAA and RSAA patients without statistically significant difference between the groups, we compared the Th1/Th2 cytokine ratio of IFN-γ to IL-4 between three groups, and the result of this comparison indicated that the SAA group had a significantly higher ratio of IFN-γ to IL-4 than did the RSAA and HC groups. Most Th2 cytokines, including IL-6, IL-5, IL-13, and IL-10, were undetectable in the present study. Monocyte chemoattractant protein-1 (CCL-2/MCP-1) is an important chemokine that regulates the migration and infiltration of macrophages/monocytes [12]. Although levels of MCP-1 (a Th2 cytokine) were significantly higher in SAA and RSAA patients than those in HCs, serial measurements before and after IST showed that MCP-1 concentrations increased after three months, indicating that both Th1 and Th2 cytokines increased in SAA patients but Th1 predominated.

Besides Th1/2 cytokines, there were a few studies about other cytokines in SAA. Our analysis revealed that the levels of PDGF-BB and IL-9 were significantly lower in both SAA and RSAA patients than those in HCs. Concentrations of RANTES and MIP-1β were significantly lower in SAA patients than those in RSAA patients and HCs; these concentrations also increased after IST.

Results concerning the functions of PDGF-BB in SAA were consistent with the results of studies concerning other

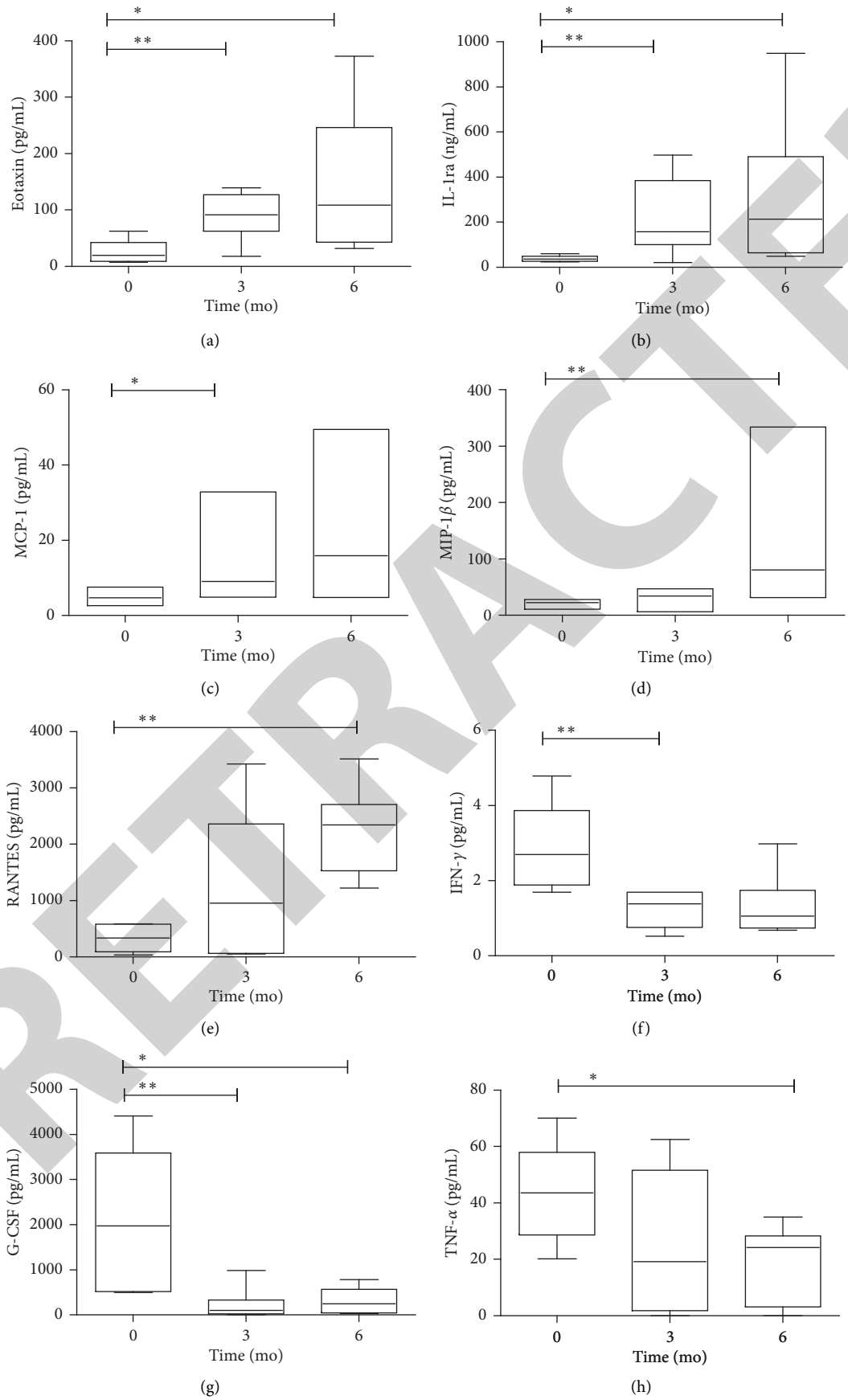

Figure 4: Continued.

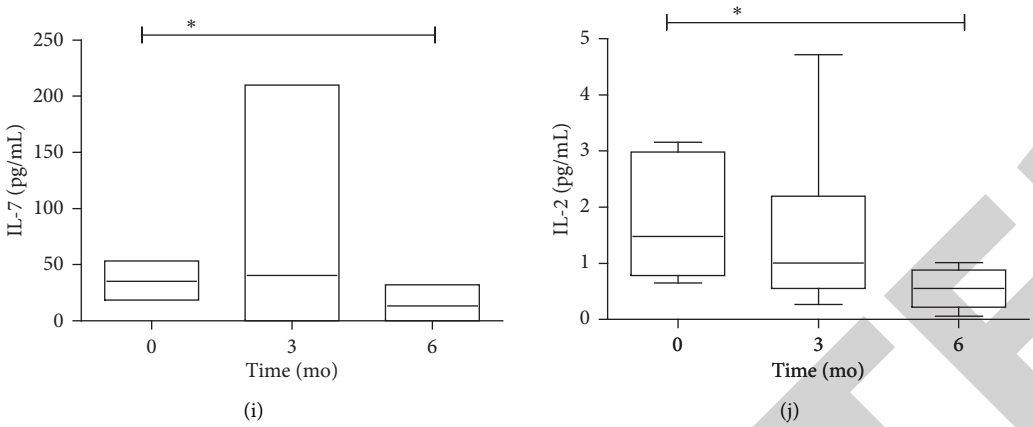

Figure 4: Alternations of cytokine levels in SAA patients after immunosuppressive therapy (IST). In six SAA patients who responded to rabbit ATG + cyclosporine, BMP cytokine concentrations were measured before and three and six months after IST. Differences in cytokine levels before IST versus three months and six months after IST were assessed using an independent *t*-test or a Mann–Whitney *U* test depending on the data distribution $^{**}p < 0.01$, $^{*}p < 0.05$.

diseases such as severe sepsis [13]. PDGF-BB is a cytokine that was found in this study to inhibit the activation of immunocytes and the production of cytokines *in vivo* and *in vitro*. PDGF-BB concentration was negatively correlated with proinflammatory cytokine (TNF-α, IL-1β, and IL-8) and chemokine (CXCL-1 and MCP-1) concentrations.

IL-9 levels have been reported to be higher in some tumors, such as multiple myeloma tumors, than those in the controls; however, IL-9 has complicated dual functions in different tumors [14]. IL-9 provokes an inflammatory environment promoting $CD8^+$ cytotoxic T lymphocyte activation in tumor tissues of melanoma models but is also involved in tumor immune tolerance in breast cancer [15]. Therefore, IL-9 has been proven to trigger physiological immune responses in terms of both innate and adaptive immunity but is not limited to any one function. In SAA, lower levels of IL-9 may indicate that the immune process is different from the way that in the tumor.

RANTES and MIP-1β were included in the CC family of chemokines. One study suggested that MIP-1α, MIP-1β, and RANTES are cosecreted to a large extent with IFN-γ by activated $CD4^+$ Th1, $CD8^+$T, and NK cells *in vitro* and in a model of murine listeriosis [16]. RANTES, MIP-1α, IFN-γ, and MIP-1β were considered together as a *functional unit* driving the Th1 immune response to certain pathogens by NK and $CD8^+$ T cells *in vivo* [16]. However, our data showed the opposite result in that RANTES and MIP-1β were significantly lower in SAA patients than those in RSAA patients and HCs. Besides the differences between *in vitro* and *in vivo* and between human and murine studies, it may be indicated that the antigens provoking immune progress were not a specific pathogen in SAA. In addition, a study with similar results to ours showed that elevated pre-antiretroviral-therapy MIP-1β levels identified long-term immunological nonresponse in HIV-infected patients, indicating that MIP-1β might be of use in the early identification of long-term immunological nonresponse [17]. MIP-1α levels were lower in SAA patients, although the RSAA group had significantly higher MIP-1α levels. This result was consistent with the results of a study on the expression of hematopoietic regulatory molecules in bone marrow mesenchymal stem cells induced by lipopolysaccharides in aplastic anemia patients [18]. Another study revealed that the endogenous MIP-1α promoter contains two consensus Runt-domain transcription factor (RUNX) sites in humans that are able to bind to an endogenous member of the mammalian family of RUNXs (RUNX1); this finding might indicate the possible pathogenesis of clonal hematopoiesis or myelodysplastic syndrome (MDS) upon marrow recovery [19]. There was no significant increase in MIP-1α after IST; this might have been due to the small sample size.

Eotaxin is also a CC chemokine and has been studied in bronchial asthma and many immune diseases [20]. An analysis of islet-infiltrating T cells in autoimmune diabetic syndrome demonstrated that the overexpression of pancreatic eotaxin, a typical Th2 chemokine, is associated with Th2-cell enrichment in insulitic lesions [9]. Of note, the RSAA patients experienced hyperfunction of the Th2 cytokines, which reversed their abnormally elevated Th1/Th2 ratios; eotaxin might play a similar role here. IL-1β and IL-1ra might play opposite roles and maintain the balance of the inflammatory response; therefore, the IL-1ra/IL-1β ratio is usually used in the study of other diseases such as coronary artery or central nervous system disease [21, 22]. In the present study, we found that IL-1ra levels and IL-1ra/IL-1β ratios were significantly higher in RSAA patients compared to HCs and SAA patients. Similarly, gene transfection of IL-1ra has been shown to inhibit degeneration and improve articular cartilage repair in osteoarthritis [23]. Recombinant human IL-1ra has also been observed to play a protective role in CCl4-induced acute liver injury in mice [24].

In correlation analysis, we observed that cytokine levels correlated with blood cell count in SAA and RSAA patients. Hemoglobin levels were only correlated with levels of MIP-1α and RANTES, possibly due to longer red blood cell life or erythrocyte transfusion in the early stage of SAA. Individual

cytokines showed different correlation patterns with different blood cell types. In particular, IFN-γ and TNF-α negatively correlated only with absolute neutrophil count and platelet count, respectively. Meanwhile, PDGF-BB positively correlated only with platelet count; this result might indicate the source of cytokines and provide an experimental foundation for treatment aimed at a certain linage of SAA *in vivo*.

We performed analyses of the linkages between age/gender and cytokine concentrations, which revealed no significant differences in these linkages between SAA patients and healthy people. IL-8, IP-10, and FGF-β concentrations were associated with increasing age, and median IL-17 concentrations were higher for males than for females. There have been few reports on the relationships between these cytokines/chemokines and age/gender except in several age-related diseases, such as exudative age-related macular degeneration and age-related vocal fold atrophy [25, 26]. We have no specific explanation as to why the four cytokines and chemokines were related to age/gender. We also performed analyses of the linkages between age/gender and all of the 19 detected cytokines, and the results of these analyses were consistent with those of previous studies of healthy people [27, 28] (data not shown).

Measurements of cytokine concentrations before and after IST showed that eotaxin, IL-1ra, and MCP-1 concentrations increased earlier than MIP-1β and RANTES concentrations, and IFN-γ and G-CSF concentrations decreased earlier than IL-7, TNF-α, and IL-2 concentrations. The results of the correlation analysis of cytokine concentration with blood cells' count showed that IFN-γ and G-CSF significantly correlated with early recovery of absolute neutrophil count. Meanwhile, the absolute neutrophil count also recovered at the earlier time after IST in SAA patients in clinical practice. Corresponding phenomena were always observed in IL-2 and TNF-α concentrations, which significantly correlated with platelet count. In addition, cytokines with increased concentrations in the early stage after IST might play a stronger or more effective protective role in the immune pathogenesis of SAA than that in the later period and should be studied as a potential treatment strategy.

In summary, we examined the BMP concentrations of 27 cytokines using a Bio-Rad 27-Plex Luminex kit to evaluate the differences in the cytokine profiles of SAA patients and healthy people. The test results confirmed that Th1 cytokine levels were significantly increased and dominated in untreated SAA patients, while both Th1 and Th2 cytokine levels were increased. More importantly, we focused on cytokines and chemokines that were significantly elevated in RSAA patients and/or healthy people, such as MCP-1, IL-1ra, MIP-1, RANTES, PDGF-BB, and eotaxin. Future studies focusing on these cytokines and chemokines could help to create new, relevant laboratory examinations and provide a potential diagnostic or evaluation tool in clinical practice. Examinations that involve standard assays (e.g., ELISAs) to target these cytokines could be used more widely for the diagnosis and efficacy evaluation or prediction in SAA cases.

Data Availability

All the data used to support this study are available from the corresponding author upon request.

Conflicts of Interest

The authors declare that they have no conflicts of interest.

Authors' Contributions

Bingnan Liu and Yuanyuan Shao contributed equally to this manuscript.

Acknowledgments

This work was supported by the National Natural Science Foundation of China (81770110, 81970115, 81800120, 81870101, 81800119, 81600093, 81700117, 81900125, and 81970116) and the Natural Science Foundation of Tianjin City (16JCZDJC35300, 17JCQNJC11500, 18JCYBJC91700, and 18ZXDBSY00140).

References

[1] N. S. Young, "Aplastic anemia," *New England Journal of Medicine*, vol. 379, no. 17, pp. 1643–1656, 2018.

[2] N. S. Young, "Current concepts in the pathophysiology and treatment of aplastic anemia," *Hematology*, vol. 2013, no. 1, pp. 76–81, 2013.

[3] S. Zonghong, T. Meifeng, W. Huaquan et al., "Circulating myeloid dendritic cells are increased in individuals with severe aplastic anemia," *International Journal of Hematology*, vol. 93, no. 2, pp. 156–162, 2011.

[4] S. Dubey, P. Shukla, and S. Nityanand, "Expression of interferon-γ and tumor necrosis factor-α in bone marrow T cells and their levels in bone marrow plasma in patients with aplastic anemia," *Annals of Hematology*, vol. 84, no. 9, pp. 572–577, 2005.

[5] T. Hara, K. Ando, H. Tsurumi, and H. Moriwaki, "Excessive production of tumor necrosis factor-alpha by bone marrow T lymphocytes is essential in causing bone marrow failure in patients with aplastic anemia," *European Journal of Haematology*, vol. 73, no. 1, pp. 10–16, 2004.

[6] Y. Gu, J. Zhang, J. Peng, X. Hu, and C. Xu, "Elevated expression of IL-12 and IL-23 in patients with aplastic anemia," *International Journal of Laboratory Hematology*, vol. 31, no. 2, pp. 207–214, 2009.

[7] S. B. Killick, N. Bown, J. Cavenagh et al., "Guidelines for the diagnosis and management of adult aplastic anaemia," *British Journal of Haematology*, vol. 172, no. 2, pp. 187–207, 2016.

[8] A. Bertrand, M. Philippe, Y. Bertrand, D. Plantaz, and N. Bleyzac, "Salvage therapy of refractory severe aplastic anemia by decreasing cyclosporine dose regimen," *European Journal of Haematology*, vol. 92, no. 2, pp. 172–176, 2014.

[9] G. Y. C. Chao, R. H. Wallis, L. Marandi et al., "Iddm30 controls pancreatic expression of Ccl11 (eotaxin) and the Th1/Th2 balance within the insulitic lesions," *The Journal of Immunology*, vol. 192, no. 8, pp. 3645–3653, 2014.

[10] C. Liu, Z. Li, W. Sheng et al., "Abnormalities of quantities and functions of natural killer cells in severe aplastic anemia," *Immunological Investigations*, vol. 43, no. 5, pp. 491–503, 2014.

Hindawi
BioMed Research International
Volume 2024, Article ID 9794810, 1 page
https://doi.org/10.1155/2024/9794810

Retraction

Retracted: Protective Effects of Hydrogen on Myocardial Mitochondrial Functions in Septic Mice

BioMed Research International

Received 12 March 2024; Accepted 12 March 2024; Published 20 March 2024

This article has been retracted by Hindawi following an investigation undertaken by the publisher [1]. This investigation has uncovered evidence of one or more of the following indicators of systematic manipulation of the publication process:

(1) Discrepancies in scope

(2) Discrepancies in the description of the research reported

(3) Discrepancies between the availability of data and the research described

(4) Inappropriate citations

(5) Incoherent, meaningless and/or irrelevant content included in the article

(6) Manipulated or compromised peer review

The presence of these indicators undermines our confidence in the integrity of the article's content and we cannot, therefore, vouch for its reliability. Please note that this notice is intended solely to alert readers that the content of this article is unreliable. We have not investigated whether authors were aware of or involved in the systematic manipulation of the publication process.

Wiley and Hindawi regrets that the usual quality checks did not identify these issues before publication and have since put additional measures in place to safeguard research integrity.

We wish to credit our own Research Integrity and Research Publishing teams and anonymous and named external researchers and research integrity experts for contributing to this investigation.

The corresponding author, as the representative of all authors, has been given the opportunity to register their agreement or disagreement to this retraction. We have kept a record of any response received.

References

[1] Y. Zhang, A. Dong, K. Xie, and Y. Yu, "Protective Effects of Hydrogen on Myocardial Mitochondrial Functions in Septic Mice," *BioMed Research International*, vol. 2020, Article ID 1568209, 7 pages, 2020.

Hindawi
BioMed Research International
Volume 2020, Article ID 1568209, 7 pages
https://doi.org/10.1155/2020/1568209

Research Article

Protective Effects of Hydrogen on Myocardial Mitochondrial Functions in Septic Mice

Yuanyuan Zhang, Aili Dong, Keliang Xie, and Yonghao Yu

Department of Anesthesiology, General Hospital of Tianjin Medical University, Tianjin, China

Correspondence should be addressed to Yuanyuan Zhang; yzhang10@tmu.edu.cn and Yonghao Yu; zyymzkzyy@126.com

Received 9 December 2019; Accepted 13 January 2020; Published 30 January 2020

Guest Editor: Hengjia Ni

Enhancement of mitochondrial physiological function prevents sepsis-induced dysfunction. The present study aimed to elucidate the mechanism by which hydrogen (H_2) affects mitochondrial function in a wild-type (WT) and homozygous nuclear factor erythroid 2-related factor 2 (Nrf2) knockout (KO, $Nrf2^{-/-}$) murine model of sepsis. In myocardial tissues with severe sepsis, H_2 gas treatment reduced mitochondrial dysfunction, whereas zinc protoporphyrin (ZnPPIX) negated these beneficial effects. H_2 treatment upregulated the protein expression of mitofusin-2 (Mfn2), peroxisome proliferator-activated receptor-gamma coactivator-1α (PGC-1α), and protein heme oxygenase-1 (HO-1) in WT mice with severe sepsis but not in their $Nrf2^{-/-}$ counterparts, and this upregulation was inhibited in the presence of ZnPPIX. In conclusion, the mechanism by which H_2 limits organ damage in mice with severe sepsis involves HO-1, whereas the mechanism that limits severe sepsis-related mitochondrial dysfunction involves both HO-1 and Nrf2.

1. Introduction

Systemic inflammation in response to infection can lead to sepsis, which, when severe, is characterized by multiple-organ dysfunction syndrome [1]. In 2007 and 2013, 200,535 and 279,530 sepsis cases, respectively, were reported, indicating an annual rate of increase of 5.7% [2]. Despite a decrease in sepsis-related mortality in recent years, average associated mortality rates remain significant (e.g., 31.3% in the U.S. and 32.3% in Europe) [3].

The pathophysiology of sepsis and septic shock is strongly associated with the cardiovascular system, in which cardiac function plays a fundamental role. Animal-based studies of sepsis have identified mitochondrial dysfunction in a variety of tissues, such as the heart, skeletal muscles, and liver [4]. Cardiac myocytes play a central role in the pathogenesis of sepsis, as the ability of these cells to use oxygen during sepsis is compromised because of mitochondrial dysfunction, which leads to cellular energy depletion [5]. Previous studies have reported the role of various factors in cardiac injury during sepsis, and the protein heme oxygenase-1 (HO-1), a rate-limiting microsomal enzyme in the catabolism of heme into carbon monoxide, free iron, and biliverdin, limited septic injury by suppressing interleukin-1β and nuclear factor-κB expression during the initial development of sepsis [6]. Furthermore, early inhibition of HO-1, also known as heat shock protein 32, during the development of an illness appeared to exacerbate septic damage. For example, treatment with zinc protoporphyrin IX (ZnPPIX) prior to cecal ligation and puncture (CLP) was associated with increased proinflammatory cytokine levels 6 h after the procedure [7]. In addition, nuclear factor erythroid 2-related factor 2 (Nrf2) is increasingly recognized as an important regulator of basal and induced expression of a range of antioxidant response element-dependent genes [8, 9]. Thus, Nrf2 regulates both physiological and pathophysiological responses to the presence of oxidants [10]. In the nucleus, the binding of Nrf2 to a DNA promoter under conditions of oxidative stress induced the transcription of antioxidant genes and subsequent translation of proteins, including HO-1 [11].

Hydrogen (H_2) has been identified as a potential antioxidant in the context of both preventive and therapeutic approaches, given its antioxidant, anti-inflammatory, and antiapoptotic properties [12]. A compelling body of evidence supports the positive biological impacts of H_2, which had positive therapeutic impacts in patients with more than 40 different illnesses and physiological conditions [13]. The fundamental mechanism underlying these positive effects has yet to be elucidated. A previous study found that H_2 enhanced the expression and activity of HO-1 both *in vivo* and *in vitro* [14, 15]. Another study demonstrated that inhalation of 2% H_2 could potentially alleviate intestinal damage caused by severe sepsis by regulating the release of HO-1 and high mobility group box 1 (HMGB1) [16]. Moreover, Nrf2 played a key role in the protective effect of H_2 against intestinal injury [17].

Our previous investigations demonstrated increased survival and reduced injury and dysfunction in different organs (e.g., lungs, liver, kidney, and intestinal tract) in various septic models treated with H_2 inhalation [17–19]. In the present study, using a CLP model, we investigated whether HO-1 mediated the positive effects of H_2 on myocardial injury in a murine model of sepsis.

2. Materials and Methods

2.1. Experimental Design. This work used murine models approved by the Institute for Cancer Research. All experimental procedures were conducted after receiving approval from the Animal Experimental Ethics Committee of Tianjin Medical University General Hospital, Tianjin, China. Wild-type (WT) and Nrf2 knockout (KO) male mice (body weight: 20–25 g; age: 6–8 wk) were supplied by the Better Biotechnology Company (Nanjing, China). The mice were housed in cages (five mice per cage) in an environmentally controlled environment (temperature: 22–25°C) under an automated 12-h/12-h light/dark cycle, with food, and water *ad libitum*.

First, 16 WT and 16 $Nrf2^{-/-}$ mice were arbitrarily divided into the following four groups, with eight mice in each group: (i) CLP, (ii) CLP + H_2, (iii) KO + CLP, and (iv) KO + CLP + H_2. Another 32 male WT mice were then arbitrarily divided into the following four groups ($n = 8$ in each): (i) CLP, (ii) CLP + H_2, (iii) CLP + ZNPPIX, and (iv) CLP + ZNPPIX + H_2. In both experiments, the mice were anaesthetized using 200 mg/kg of sodium pentobarbital 24 h after the commencement of CLP. Cardiac samples were collected from all mice.

CLP was used to induce sepsis according to previously described procedures [18]. ZNPPIX (40 mg/kg) was administered 1 h preoperatively via injection to mice in the CLP + ZNPPIX and CLP + ZNPPIX + H_2 groups. Prior to the surgical procedure, the mice were anaesthetized using a 50 mg/kg dose of sodium pentobarbital (Sigma-Aldrich, St. Louis, MO, USA) administered by an intraperitoneal injection. Subsequently, a midline incision was made, and the cecum was exposed, ligated 1 cm from the apex, and punctured twice (through-through) using a 20-gauge needle. To ascertain the success of the punctures, a small quantity of fecal material was gently squeezed from the cecum. Subsequently, the cecum was relocated, and the peritoneum and skin were closed using 4/0 sutures. The control mice were subjected to a mock operation involving only incision and cecum externalization. Immediately following the procedure, all mice received 1 ml of a saline solution administered intravenously and were provided with a standard laboratory diet and drinking water *ad libitum*. Mice subjected to both the mock and CLP procedures were monitored for 7 d to evaluate survival.

All mice assigned to receive the H_2 treatment were placed in a sealed plastic box fitted with inflow and outflow outlets [20]. These mice breathed a mixture of air and H_2 gas supplied at a rate of 4 L/min by a TF-1 gas flowmeter (YUTAKA Engineering Corp, Tokyo, Japan). An HY-ALERTA handheld detector (Model 500; H_2 Scan, Valencia, CA, USA) was used to continuously monitor the concentration of H_2 in the box. The concentration was maintained at 2% during the treatment period. The mice inhaled 2% H_2 for 60 min periods at the 1 h and 6 h time points after the CLP or mock procedure. The mice in the groups not treated with H_2 breathed normal air.

2.2. Isolation of Mitochondria. Complete mitochondria were isolated from harvested cardiac tissue using the differential centrifugation procedure described by Drew and Leeuwenburgh [21]. A Potter–Elvehjem glass-glass homogenizer was used to homogenize the cardiac tissue in a 1 : 10 wt/vol mixture of ice-cold water and buffer A consisting of mannitol (0.220 M), sucrose (0.070 M), EGTA (0.5 mM), HEPES (2 mM, pH 7.4), and fatty acid-free bovine serum albumin (0.1%). Homogenates of cardiac tissues were then centrifuged at 1,600 g and 4°C for 10 min in an Eppendorf 5810R device (Brinkmann Instruments, Laurel, MD, USA). The supernatants were subsequently isolated and subjected to centrifugation at 18,000g and 4°C for 10 min, and the resultant pellets were resuspended in buffer A prior to an additional 10 min centrifugation step at 18,000g and 4°C.

Samples obtained from the frontal cortex of the brain were similarly homogenized in a 1 : 10 wt/vol mixture of ice water and buffer B, which consisted of HEPES-KOH (20 mM, pH 7.5), KCl (10 mM), $MgCl_2$ (1.5 mM), EDTA (1 mM), EGTA (1 mM), DTT (1 mM), and PMSF (0.1 mM). After centrifugation of this homogenate at 750g and 4°C for 5 min, the supernatant was removed and subjected to centrifugation at 8,000g and 4°C for 20 min. After resuspending the pellets, the freshly separated mitochondria were immediately subjected to further analysis.

2.3. Measurements of the Mitochondrial Respiratory Control Ratio (RCR), Adenosine Triphosphate (ATP) Level, and Mitochondrial Membrane Potential (MMP). The respiratory control ratio (RCR), a measure of the stability and energy-conserving capability of the mitochondrial membrane, was evaluated according to the method of Silva et al. [19] as the ratio between state 3 and state 4 respiration rates. The total cellular ATP level was assessed using an ATP bioluminescence assay kit according to the manufacturer's protocol

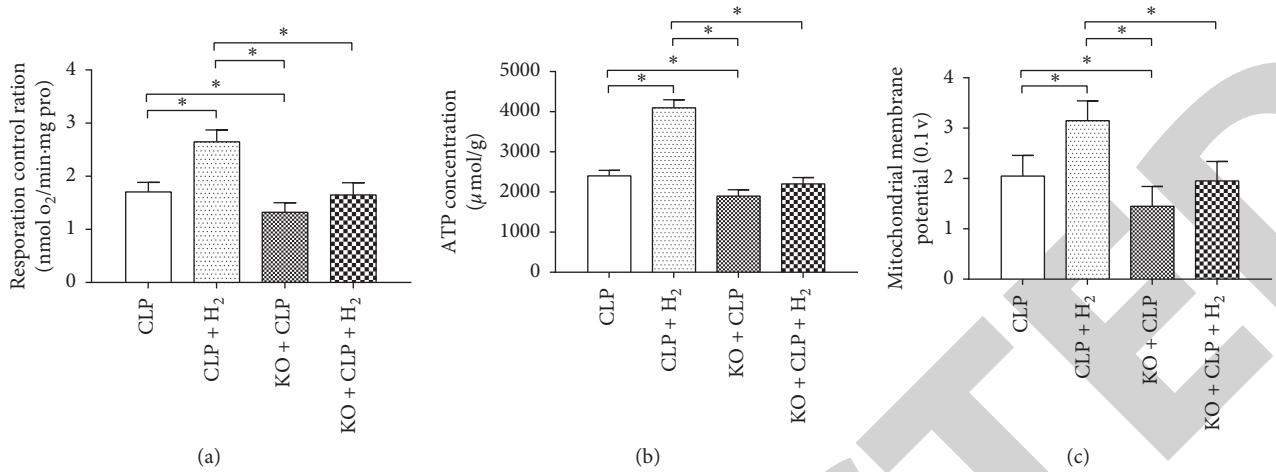

Figure 1: Effects of H_2 on mitochondrial function in a septic model of WT and $Nrf2^{-/-}$ mice. RCR, respiratory control ratio; MMP, mitochondrial membrane potential. $^*P < 0.05$ ($n = 8$).

(CLS II; Roche Applied Science, Mannheim, Germany). This protocol required collected cells to be counted using a Scepter cell counter (Millipore, Billerica, MA, USA). Subsequently, the cells were induced to release cellular ATP by adding the cell suspension to a boiling buffer consisting of Tris (100 mM) and EDTA (4 mM, pH 7.75) for 2 min. The bioluminescence signal was measured after diluting the reaction solution 1 : 1 (v/v) with luciferase reagent. ATP values were obtained by dividing the concentrations of ATP (determined using a standard curve) by the cell count [22]. The MMP was then assessed using an assay described by Sakamuru et al. [23].

2.4. Western Blotting. Twenty-four hours after both the CLP and mock operations, proteins were extracted from the harvested cardiac tissues and evaluated using a BCA protein assay kit (Pierce Biotechnology, Rockford, IL, US). Fifty-microgram aliquots of protein from each lysate were fractionated by 10% SDS-polyacrylamide gel electrophoresis and transferred to polyvinylidene difluoride membranes (Millipore, Billerica, MA, USA)), which were then blocked in a solution of 5% nonfat milk in phosphate-buffered saline-Tween-20 for 1 h at room temperature before blotting with the relevant primary antibody. Glyceraldehyde-3-phosphate dehydrogenase was detected as a loading control. The membranes were then washed four times with Tris-buffered saline and Tween-20, followed by incubation for 2 h with appropriate horseradish peroxidase-conjugated secondary antibodies (antirabbit or antimouse; Santa Cruz Biotechnology, Dallas, TX, USA). Quantity One software, version 4.5.2 (Bio-Rad, Hercules, CA, USA), was used to visualize the blots, and Gel-Pro analyzer (Media Cybernetics Inc., Rockville, MD, USA) was used to examine the integrated optical densities. For comparisons among experimental conditions, all changes in protein levels are presented relative to the control levels (i.e., the mock procedure).

2.5. Statistical Analysis. All statistical values are presented as means ± standard deviations. All analyses were performed using SPSS, version 20.0 (SPSS, Inc., Chicago, IL, USA). Differences between the mock procedure and CLP groups and those between the CLP + H_2 and CLP groups were examined using an unpaired t-test. The Mann–Whitney U test was used for nonnormally distributed values. P values of <0.05 were considered statistically significant.

3. Results

3.1. Effect of H_2 on Mitochondrial Physiological Function. To evaluate general mitochondrial function, we evaluated the RCR in the different groups of sepsis model mice. As shown in Figure 1, the RCR increased significantly in the CLP + H_2 group relative to that in the other groups ($P < 0.05$) but decreased significantly in the KO + CLP group relative to that in the CLP group ($P < 0.05$). We detected no significant differences in the RCR in a comparison of the KO + CLP + H_2 group with the CLP and KO + CLP groups (Figure 1(a)). Similarly, the ATP level (Figure 1(b)) and MMP (Figure 1(c)) increased significantly in the CLP + H_2 group relative to that in the other three groups ($P < 0.05$) but decreased significantly when compared with that in the CLP group ($P < 0.05$). We detected no significant differences in the ATP level and MMP in the KO + CLP + H_2 group compared with that in the CLP and KO + CLP groups.

When the mitochondrial status during the ZnPPIX treatment was evaluated, we observed the same trends in the RCR (Figure 2(a)), ATP level (Figure 2(b)), and MMP (Figure 2(c)) in the four groups. The RCR, ATP level, and MMP increased significantly in the CLP + H_2 group when compared with that in the other three groups ($P < 0.05$), whereas no significant differences in these parameters were observed among the CLP, CLP + ZnPPIX, and CLP + ZnPPIX + H_2 groups.

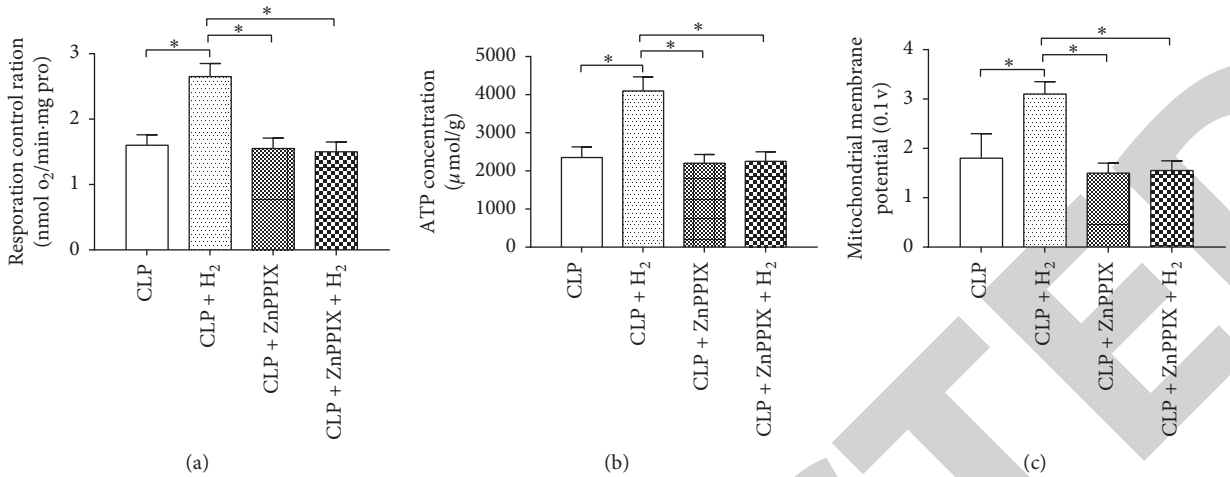

Figure 2: Effects of H_2 and ZnPPIX on mitochondrial function in a septic murine model. RCR, respiratory control ratio; MMP, mitochondrial membrane potential. $^*P < 0.05$ ($n = 8$).

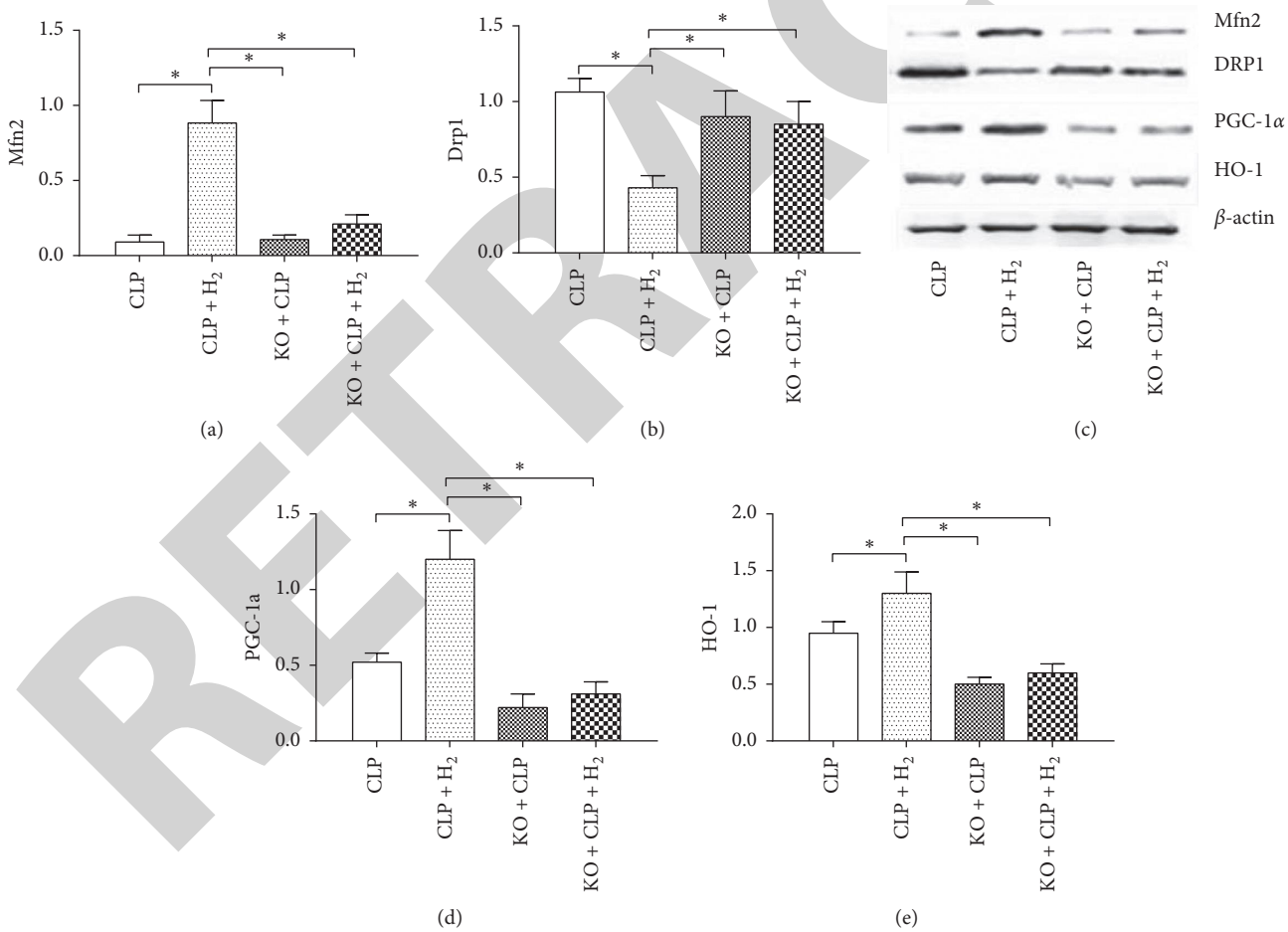

Figure 3: Effects of H_2 on mitochondrial protein expression in heart tissue of WT and $Nrf2^{-/-}$ mice. Mfn2, mitofusin-2; Drp1, dynamin-related protein 1; PGC-1α, peroxisome proliferator-activated receptor-gamma coactivator-1α; HO-1, heme oxygenase-1 HO-1. $^*P < 0.05$ ($n = 8$).

3.2. Effect of H_2 on the Nrf2/HO-1 Pathway in WT and $Nrf2^{-/-}$ Mice. We also measured the levels of several proteins. As shown in Figure 3, the levels of HO-1, mitofusin-2 (Mfn2), and peroxisome proliferator-activated receptor-gamma coactivator-1α (PGC-1α) increased significantly, and the level of dynamin-related protein 1 (Drp1) decreased

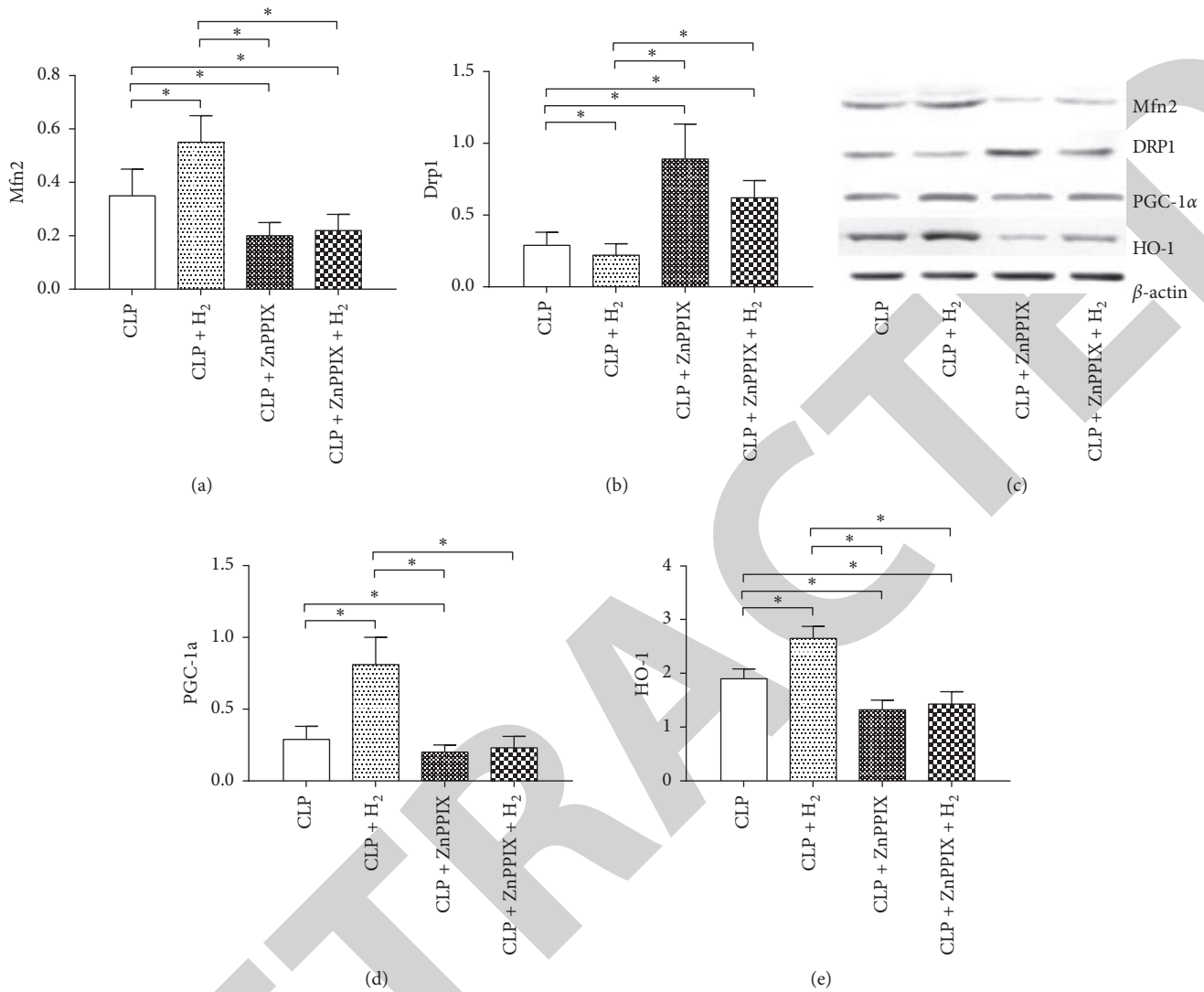

Figure 4: Effects of H_2 and ZnPPIX on mitochondrial protein expression in heart tissues. Mfn2, mitofusin-2; Drp1, dynamin-related protein 1; PGC-1α, peroxisome proliferator-activated receptor-gamma coactivator-1α; HO-1, heme oxygenase-1 (HO-1). $^*P < 0.05$ ($n = 8$).

significantly in the CLP + H_2 group relative to that in the other three groups ($P < 0.05$). However, we detected no differences in the expression of HO-1, Mfn2, PGC-1α, and Drp1 among the CLP, KO + CLP, and KO + CLP + H_2 groups.

Figure 4 shows the protein levels during the ZnPPIX treatment. The Drp1 level decreased significantly in the CLP + H_2 group relative to that in the other three groups ($P < 0.05$) but increased significantly in the CLP + ZnPPIX and CLP + ZnPPIX + H_2 groups as compared with that in the CLP group ($P < 0.05$). The CLP + H_2 group had significantly higher levels of Mfn2, HO-1, and PGC-1α when compared with those in the other three groups ($P < 0.05$), whereas the levels of Mfn2 and HO-1 in the CLP + ZnPPIX and CLP + ZnPPIX + H_2 groups were significantly lower than those in the CLP group ($P < 0.05$). Although the PGC-1α level in the CLP + ZnPPIX group was significantly lower than that in the CLP group ($P < 0.05$), no difference in the expression of this protein was observed in the CLP versus the CLP + ZnPPIX + H_2 groups.

4. Discussion

The CLP procedure is a well-established, clinically germane method for generating models used in sepsis research [8, 9]. Mice with severe CLP-induced sepsis exhibit increased damage, compared with nonseptic mice. Previous research reported that inhalation of H_2 gas at low concentrations (e.g., 2%) reduced the effects of sepsis and had therapeutic benefits in other illnesses [17]. In the present study, which included both WT and Nrf2$^{-/-}$ mice, we demonstrated beneficial effects of inhaled H_2 on mitochondrial function, as well as the central importance of Nrf2 and its downstream targets in this process.

Mitochondria are critical to the physiological processes of cells, and mitochondrial dysfunction has been linked to a wide range of illnesses, including cancer, cardiovascular diseases, diabetes, and neurodegenerative conditions [24–26]. The mitochondrion is often referred to as the powerhouse of the cell, as the eukaryotic cell derives almost

its entire energy balance from oxidative phosphorylation in this organelle. Within the mitochondrion, electrons are transferred from electron donors to electron acceptors (e.g., oxygen) via a sequence of redox reactions along the electron transport chain. This transfer yields an electrochemical gradient that drives the synthesis of ATP and provides a central criterion for the assessment of the MMP, a marker of mitochondrial function [15, 27]. The actions of noxious xenobiotic substances can directly or indirectly affect mitochondrial function, and such substances often disrupt various mitochondrial macromolecules and thus reduce the MMP, which in turn compromises several mitochondrial functions [15, 27].

Defects in mitochondrial dynamics involve changes in mitochondrial fission/fusion proteins, such as Drp1 and mitofusins (e.g., Mfn2) [28]. These dynamic changes are regulated by complex mechanisms that maintain mitochondrial function homeostasis. Mitochondrial fission begins with the induction of Drp1. Mitochondrial fusion is a complex physiological process that involves optic atrophy 1 in the outer membrane and Mfn2 in the inner membrane [29] and depends on the MMP and hydrolysis of guanosine-5′-triphosphate [30]. The present investigation demonstrated reduced cardiac mitochondrial function in septic $Nrf2^{-/-}$ mice as compared with that in their WT counterparts. Furthermore, the exacerbation of mitochondrial dysfunction observed in the $Nrf2^{-/-}$ mice were accompanied by notable upregulation in Drp1 levels and considerable reductions in Mfn2 and PGC-1α levels relative to corresponding levels in the CLP group. The observed significant enhancing effect of H_2 on mitochondrial function in septic mice involved Nrf2-mediated signaling in asepsis, as shown by the absence of any therapeutic benefit in the $Nrf2^{-/-}$ mice.

The Nrf2 transcription factor is a central regulator of relevant innate immune responses and a mediator of antioxidant and anti-inflammatory responses [31]. This protein is transported from the cytoplasm into the nucleus, where it can bind to the (antioxidant responsive element (ARE) gene and thus regulate the expression and activation of antioxidants (e.g., Superoxide dismutase, catalase) and phase II genes (e.g., glutathione S-transferase, NAD (P)H quinine oxidoreductase, and HO-1) [32, 33]. The downstream enzyme HO-1 can break down the proinflammatory molecule heme to generate anti-inflammatory carbon monoxide and bilirubin, thus potentially moderating the inflammatory response [34]. Previously, our research group demonstrated a notable increase in the levels of Nrf2 and HO-1 in septic cell models and septic organs (lung, intestine, brain, and kidney) from mice in the presence of 0.6 mmol/L of H_2-rich medium or the inhalation of 2% H_2 [17].

Numerous *in vivo* and *ex vivo* experimental models have used ZnPPIX and other metallic morpholines as standard HO-1 inhibitors [35]. In the present study, ZnPPIX completely negated the beneficial effects of H_2 treatment, including the observed increases in the RCR, MMP, ATP, and mitochondrial function-related protein expression. This finding further supports the ability of H_2 to provide protection against sepsis by upregulating the expression of HO-1. In our study, the H_2 treatment did not enhance the expression or activity of HO-1 or improve mitochondrial function and kinetics in the $Nrf2^{-/-}$ mice. In addition, the use of ZnPPIX to inhibit HO-1 further demonstrated that the protective effects of H_2 treatment for sepsis involved mitochondrial function and HO-1. Based on these findings, we conclude that H_2 enhances mitochondrial performance by controlling mitochondrial activity via the Nrf2/HO-1 pathway.

In conclusion, the present investigation indicates the therapeutic potential of 2% H_2 via inhalation for the management of mitochondrial dysfunction associated with severe sepsis. Furthermore, it suggests that these protective effects are mediated by a mechanism involving the regulation of HO-1 and Nrf2.

Data Availability

All data are available at Dr. Yuanyuan Zhang yzhang10@tmu.edu upon request.

Conflicts of Interest

The authors declare that there are no conflicts of interest regarding the publication of this article.

Authors' Contributions

Y. Z., A.D., and Y. Y. conceived the experiments. Y. Z., A. D., and K. X. conducted the experiments. Y. Z. and A. D. analysed the results. Y. Z. prepared the manuscript. All authors reviewed and approved the manuscript.

Acknowledgments

This work was supported by National Natural Science Foundation of China (81471842, 81772043, 81971879), Natural Science Foundation of Tianjin (17JCYBJC24800), and Science and Technology Support Key Program Affiliated to the Key Research and Development Plan of Tianjin Science and Technology Project Key Research and Development Plan (18YFZCSY00560).

References

[1] K. N. Iskander, M. F. Osuchowski, D. J. Stearns-Kurosawa et al., "Sepsis: multiple abnormalities, heterogeneous responses, and evolving understanding," *Physiological Reviews*, vol. 93, no. 3, pp. 1247–1288, 2013.

[2] C. Fleischmann, D. O. Thomas-Rueddel, M. Hartmann et al., "Hospital incidence and mortality rates of sepsis," *Deutsches Aerzteblatt Online*, vol. 113, no. 10, pp. 159–166, 2016.

[3] M. M. Levy, A. Artigas, G. S. Phillips et al., "Outcomes of the surviving sepsis campaign in intensive care units in the USA and Europe: a prospective cohort study," *The Lancet Infectious Diseases*, vol. 12, no. 12, pp. 919–924, 2012.

[4] H. Zhang, D. Liu, X. Wang et al., "Melatonin improved rat cardiac mitochondria and survival rate in septic heart injury," *Journal of Pineal Research*, vol. 55, no. 1, pp. 1–6, 2013.

[5] G. Landesberg, P. D. Levin, D. Gilon et al., "Myocardial dysfunction in severe sepsis and septic shock: no correlation

Hindawi
BioMed Research International
Volume 2024, Article ID 9791359, 1 page
https://doi.org/10.1155/2024/9791359

Retraction

Retracted: Glucosamine Supplementation in Premating Drinking Water Improves Within-Litter Birth Weight Uniformity of Rats Partly through Modulating Hormone Metabolism and Genes Involved in Implantation

BioMed Research International

Received 12 March 2024; Accepted 12 March 2024; Published 20 March 2024

This article has been retracted by Hindawi following an investigation undertaken by the publisher [1]. This investigation has uncovered evidence of one or more of the following indicators of systematic manipulation of the publication process:

(1) Discrepancies in scope

(2) Discrepancies in the description of the research reported

(3) Discrepancies between the availability of data and the research described

(4) Inappropriate citations

(5) Incoherent, meaningless and/or irrelevant content included in the article

(6) Manipulated or compromised peer review

The presence of these indicators undermines our confidence in the integrity of the article's content and we cannot, therefore, vouch for its reliability. Please note that this notice is intended solely to alert readers that the content of this article is unreliable. We have not investigated whether authors were aware of or involved in the systematic manipulation of the publication process.

Wiley and Hindawi regrets that the usual quality checks did not identify these issues before publication and have since put additional measures in place to safeguard research integrity.

We wish to credit our own Research Integrity and Research Publishing teams and anonymous and named external researchers and research integrity experts for contributing to this investigation.

The corresponding author, as the representative of all authors, has been given the opportunity to register their agreement or disagreement to this retraction. We have kept a record of any response received.

References

[1] C. Feng, T. Yuan, S. Wang et al., "Glucosamine Supplementation in Premating Drinking Water Improves Within-Litter Birth Weight Uniformity of Rats Partly through Modulating Hormone Metabolism and Genes Involved in Implantation," *BioMed Research International*, vol. 2020, Article ID 1630890, 9 pages, 2020.

Hindawi
BioMed Research International
Volume 2020, Article ID 1630890, 9 pages
https://doi.org/10.1155/2020/1630890

Research Article

Glucosamine Supplementation in Premating Drinking Water Improves Within-Litter Birth Weight Uniformity of Rats Partly through Modulating Hormone Metabolism and Genes Involved in Implantation

Cuiping Feng,[1] **Taolin Yuan**,[2] **Shilan Wang**,[2] **Ting Liu**,[2] **Shiyu Tao**,[2] **Dandan Han**,[2] **and Junjun Wang**[2]

[1]*Department of Obstetrics and Gynecology, China-Japan Friendship Hospital, Beijing 100029, China*
[2]*State Key Laboratory of Animal Nutrition, College of Animal Science and Technology, China Agricultural University, Beijing 100193, China*

Correspondence should be addressed to Cuiping Feng; bydfcp@hotmail.com

Received 21 October 2019; Accepted 23 November 2019; Published 8 January 2020

Guest Editor: Lei Sun

Within-litter birth weight variation in multiparous animals has become a big issue due to high incidence of low birth weight neonates, which gives rise to high preweaning mortality and morbidity. Foetus with various birth weights is the outcome of diverse embryos competence which is affected by oocyte quality. Glucosamine (GlcN) has been reported to be involved in oocyte maturation; however, its effect on pregnant outcomes remains unknown. The present study was conducted to investigate the effects of premating GlcN supplementation via drinking water on within-litter birth weight variation and its underlying mechanism. Fifty eight Sprague-Dawley female rats were randomly assigned to one of two groups with normal drinking water or drinking water supplemented with 0.5 mM GlcN from six to eight weeks old. Variation of within-litter birth weight in the GlcN group was 5.55%, significantly lower compared with 8.17% in the control group. Birth weight was significantly increased in the GlcN group (2.27 ± 0.06) compared with the control group (2.08 ± 0.04). Both absolute and relative weights of the ovary at the end of GlcN treatment were higher in the GlcN group than in the control group ($P < 0.05$). In the GlcN group, there were more successfully implanted blastocysts (13.38 ± 0.63 and 15.75 ± 0.59 in the control and treatment group, respectively) with more uniform distribution along the two uterine horns compared with the control group. Besides, gene expressions of Alk3 and Bmp2 were increased in the implantation sites, while IGF-1 and Mucin-1 were decreased significantly in rats administrated with GlcN. Maternal progesterone, estradiol, and IGF-1 concentrations on D 19.5 were significantly increased, while insulin and total cholesterol levels were significantly decreased in contrast with control dams. In summary, the administration of 0.5 mM GlcN solution before mating reduced within-litter birth weight variation, accompanied with increased fetal weight. Further investigation indicated that the improved outcome of pregnancy results at least partly from the increased ovary weights of the rats, the homogeneous embryo developmental competence, the enhanced receptivity of the uterine environment, and the adjusted maternal hormone levels.

1. Introduction

Poor postnatal survival and retarded growth performance induced by low birth weight and high within-litter birth weight variation in litter-bearing animals have been recognized for many decades [1, 2]. Birth weight variation can be influenced by many factors including breed, maternal physiology, and nutrition. The external environment of females before and during pregnancy, including nutrient intake, dietary behavior, temperature, and health condition, has a significant influence on oocyte and embryo development [3]. Changes in the amount and composition of food or

diet consumed before mating can affect oocyte maturation, blastocyst production, prenatal survival, and the number of surviving offspring [4].

In addition, maternal physiological conditions, especially lipid metabolism and hormones, play important roles in pregnancy results. During oocyte maturation or early embryonic development, diet-induced changes in maternal fatty acids may impact follicles and embryo quality [5]. Fatty acids are precursors of steroids and prostaglandins, and they are important for regular reproductive functions [6].

Exposed mouse cumulus-oocyte complexes to glucosamine (GlcN) during in vitro maturation severely perturbed blastocyst development [7]. Although the roles of GlcN on oocyte maturation and early embryo development have been studied *in vitro*, the effects of GlcN supplementation before mating on embryo implantation and reproductive results are poorly understood. The purpose of this paper was to investigate whether GlcN supplementation before mating improved within-litter birth weight uniformity related to the maternal metabolism and hormone concentration in serum and the expression of genes that target in implantation sites.

2. Materials and Methods

2.1. Animals, Diet, and Experimental Design. Sprague-Dawley (SD) dams ($n = 58$) were purchased from Sibeifu Inc. (Beijing, China). They were five weeks old and then acclimated for one week. The dams were housed individually at 23°C in a room with a 12 h light/12 h dark cycle and water and feed were provided ad libitum. This study was carried out in accordance with the recommendations of the guidelines for the Institutional Animal Care and Use Committee of China Agricultural University (AW11099102-1, Beijing, China).

The rats were fed a basal diet before mating and the pregnant rats were fed a reproductive diet during pregnancy, both of them mainly including corn, soybean meal, fish meal, flour, wheat bran, calcium ammonium phosphate salt, limestone powder, vitamin, microelements, and amino acids. Diet composition was supplied in the additional file (Table S1). The supplementation of GlcN (D-(+)-glucosamine, purity ≥99%, Sigma-Aldrich) was achieved via dissolving in drinking water. Rats ($n = 29$ per group) were allocated randomly to either 0.5 mM GlcN solution (the concentration was determined on the basis of a gradient experiment which additionally included 1.0 mM GlcN and the results are presented in Table S2) or drinking water as control. GlcN treatment lasted for two weeks when the dams were six to eight weeks old. After two-week GlcN administration, each dam was caged overnight with a male SD rat to mate. The presence of sperm in the vaginal smear the next morning was regarded as day 0.5 of pregnancy [8]. Unmated females were recaged with males and GlcN operations were continued until mating was completed, or mating attempts were made for up to 4 nights. Those that had not mated until the 4th night were excluded from the study, as described previously [8]. During GlcN treatment periods, rats were weighed individually at days 1, 5, 10, and 14 before mating. Feed and water consumption were monitored. Average daily gain (ADG), average daily feed intake (ADFI), and average daily drinking water intake (ADWI) were recorded to measure the growth performance of rats.

2.2. Sample Collection. The day before mating was regarded as day−1; 20 female rats (10 for Control and 10 for GlcN) were anesthetized by intraperitoneal injection of 1% sodium pentobarbital at 10 mg/100 g body weight and then sacrificed 5 minutes later. After weighed, ovaries and uteri were frozen in liquid nitrogen as soon as possible and then transformed to −80°C. The relative organ index = organ weight/body weight ∗ 100%. On the 6.5th day of pregnancy, when embryos started to contact the uterine endothelium, eight female rats per group were anaesthetized. Through intravenous injecting (0.1 mL/rat) Chicago Sky Blue dye solution (1% in saline, Sigma-Aldrich), implantation sites were observed according to previous studies [8, 9]. Rats were sacrificed 5 min later as described above, and then implantation sites were recorded and collected for further analysis. Pregnant rats ($n = 11$/group) were sacrificed as described above to investigate reproductive results on day 19.5 of gestation (gestation generally lasts 21–23 days) [8]. Coefficient of pup birth weight variation = standard deviation of litter birth weight/average litter birth weight. Maternal placental efficiency = fetal body weight/placental weight ratio [10]. The plasma of dams was collected in tubes containing anticoagulant from vena cava and then centrifuged at 3,000 rpm for 15 min and stored at −20°C for subsequent analysis.

2.3. RNA Extraction and Quantitative Real-Time PCR Analysis. Total RNA was isolated from implantation sites using Trizol reagent (CWBIO, China) according to the manufacturer's instructions, and RNA quality was determined with a Nano-Drop spectrophotometer (Thermo Scientific, USA). One microgram of RNA was reverse transcribed with RevertAid 1st Strand cDNA Synthesis Kit (Thermo, USA). The sequence of the primers is supplied in Table S3 [11–13], including specific genes ALK3, BMP2, insulin-like growth factor 1 (IGF-1), Mucin-1, iNOS, and β-actin. Gene expression of β-actin in each sample was quantified as a control. Complementary DNA (cDNA) was then used to amplify these primers by using SYBR Green (Takara, Japan) on an Applied Biosystems 7500 Real-Time PCR System (ABI, USA). The $2^{-\Delta\Delta ct}$ method was used to analyze gene expression levels as previously described [14].

2.4. Blood Test. To evaluate maternal metabolic state and body condition, total cholesterol (TC), low-density lipoprotein cholesterol (LDL-C), high-density lipoprotein cholesterol (HDL-C), and triglyceride (TG) in plasma were analyzed in duplicate using an Automatic Biochemistry Analyzer (Hitachi 7020, Japan). Estradiol, progesterone, insulin, and IGF-1 were analyzed by radioimmunoassay kits (Sino-UK Inc, China) [8].

2.5. Statistical Analysis. Data are presented as means ± SEM. The data were analyzed with Student's unpaired *t*-test (GraphPad Prism version 7.0). Statistical significance was detected at $P < 0.05$ and a trend at $0.05 < P < 0.1$. The unit in the statistical analysis individually is 11 dams per group for reproductive results, 8 dams per group for uniformity of implantation, and 10 for the organ index before mating.

3. Results

3.1. GlcN Supplementation before Mating Decreased Within-Litter Birth Weight Variation of Rats. In the present study, fetal weight refers to body weight in late pregnancy (day 19.5 of pregnancy), since colostrum intake could alter neonatal body weight and the variation of within-litter birth weight was indicated with a coefficient of variation for pup littermate birth weight. Coefficient of pup birth weight variation = standard deviation of litter birth weight/average litter birth weight. The pregnancy results are presented in Figure 1 and Table S2. Within-litter birth weight variation was statistically lower in the GlcN supplement group than in the control group (5.55% for 0.5 mM GlcN, 5.77% for control group, respectively), and average litter weight of live-born rats in the 0.5 mM GlcN-supplemented group (2.27 ± 0.06) was significantly higher than that from the control group (2.02 ± 0.04). In addition, maternal placental efficiency (fetal body weight to placental weight ratio) was significantly increased in the 0.5 mM GlcN group (3.61 ± 0.11) in comparison with the control group (3.28 ± 0.08). The litter size of the 0.5 mM GlcN and the control group, respectively, was 13.45 and 11.73, while there was no significant difference.

3.2. GlcN Supplementation before Mating Improved Ovary Weights of Rats. As shown in Table 1, both the absolute weight of ovary and relative weight of ovary in the GlcN supplementation group were higher than in the control group ($P < 0.05$) at the end of GlcN treatment (Table 1). Uterine weights were not statistically different between groups. There was no statistical difference in ADG, ADFI, and ADWI between the control and the GlcN groups (Table S4).

3.3. GlcN Supplementation before Mating Improved Uniformity of Implantation of Rats. Embryonic implantation was investigated on the 6.5th day of pregnancy when blastocysts establish contact with the uterine endometrium. Rat dams fed GlcN had more implantation sites (15.75 ± 0.59, Figure 2(b)) compared with control dams (13.38 ± 0.63, Figure 2(a)). In the aspect of embryos distribution, extreme differences indicated as the number of implantation sites in two uterine horns were mainly observed in the control group. Expression levels of uterine receptivity-related genes were evaluated by quantitative real-time PCR. GlcN increased Alk3 (Figure 2(d)) and Bmp2 (Figure 2(e)) expressions in implantation sites and decreased IGF-1 (Figure 2(f)) and Mucin-1 (Figure 2(g)) levels. There was a tendency for iNOS expression to decline in the GlcN group.

3.4. GlcN Supplementation before Mating Changed the Maternal Hormones. The concentration of maternal reproductive hormones in plasma and biochemical parameters on D 19.5 is presented in Figure 3. In the GlcN group, progesterone, estradiol, and IGF-1 concentrations were significantly increased, while insulin (INS) and total cholesterol levels were decreased significantly in contrast with control dams. While there was no statistical difference in LDL-C, HDL-C, and triglyceride levels (Data are not shown).

4. Discussion

Currently, special attention has been given to great within-litter birth weight variation in litter-bearing animals, which is characterized by a higher proportion of low birth weight littermates [15, 16]. Low birth weight can result in poor postnatal survival and growth performance subsequently [16, 17]. Glucosamine has been increasingly reported to play important roles in oocyte maturation and early stages of embryo development [18]. Limited studies have focused on the impacts of GlcN supplementation before mating on embryo implantation and pregnancy. In the present study, we demonstrated, for the first time, that 0.5 mM GlcN administration before mating decreased the within-litter birth weight variation, while the average litter weight of live-born rats was increased, which is partly because of improved implantation as well as development of ovary through affecting maternal plasma hormones concentrations and uterine receptivity related gene expressions.

As for the reproductive results, the within-litter birth weight variation was decreased, while the average litter weight was increased when 0.5 mM GlcN was supplemented before mating. Factors like ovulation rate, oocyte maturity, placental implantation ability, and placental transport efficiency could affect within-litter birth weight variation [15]. Glucosamine (GlcN) metabolism is closely related to oocyte maturation and early embryonic development through participating in the hexosamine biosynthesis pathway and activating the mTOR signal pathway [19]. GlcN is preferentially utilized as a substrate to form extracellular matrix hyaluronic acid, which is involved in the expansion of cumulus-oocyte complexes (COCs), mucification, and oocyte maturation *in vitro* [20–22]. The increased absolute and relative weight of the ovary indicated a better oocyte quality or more developed follicles in the GlcN group relative to controls [8]. Consistently, dams had a more efficient placenta (higher ratio of fetal body weight to placental weight) when administrated GlcN. Fetal development relies on the placenta to obtain nutrients and oxygen [23], especially during the rapid growth phase in the last third of gestation [24], and placental efficiency is related positively to reproductive performance [10]. In the present study, litter size did not markedly differ between the GlcN and the control groups. In contrast, several studies demonstrated an inhibitory effect of GlcN on litter size and embryo development. Tsai et al. [25] reported that litter size decreased when a sustained-release GlcN (15, 150 or 1500 μg) was implanted into uterine horn ten days before coitus and during pregnancy compared with that in the placebo-implanted control

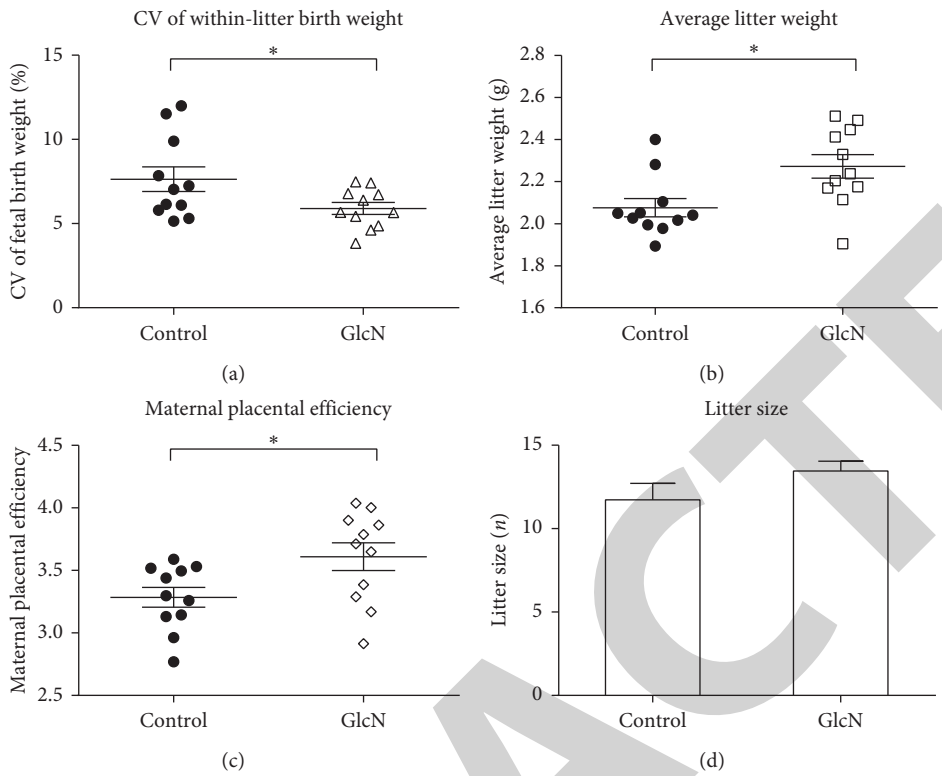

Figure 1: Glucosamine (GlcN) supplementation before mating improves reproductive outcomes on day 19.5 of pregnancy. Fetal weight indicated body weight in late gestation (day 19.5 of pregnancy). Each icon in the figure represents the index of a litter of rats ($n = 11$ dams per group). (a) Within-litter birth weight uniformity, coefficient of pup birth weight variation (CV) = standard deviation of litter birth weight/average litter birth weight. (b) Average litter weight of live-born rats and (c) maternal placental efficiency were improved in the GlcN group compared with the control group. (d) Litter size (number of live-born rats) did not have a significant difference between groups. All data were represented as mean ± SEM. *There were statistically significant differences between groups when P value <0.05.

Table 1: Organ index of rats at the end of GlcN treatment.

Items	Control	GlcN	P value
Absolute organ weight (g)			
Uterus	0.457 ± 0.073	0.431 ± 0.070	0.31
Ovary	0.145 ± 0.023	0.171 ± 0.026	0.01*
Relative organ index (%)			
Uterus	0.208 ± 0.007	0.195 ± 0.003	0.16
Ovary	0.066 ± 0.003	0.079 ± 0.003	0.01*

$n = 10$ dams per group. All data were presented as mean ± SEM. The relative organ index = organ weight/body weight ∗ 100%. *There were statistically significant differences between the two groups when P value <0.05.

group. Further, deteriorated implantation and reduced litter size on day 18 of gestation have been reported when 8-week-old mice were injected intraperitoneally with 20 or 400 mg/kg GlcN during periconception [26]. The difference between these observations and our results may be related to the much lower dose of GlcN used and different periods and route of administration.

There were significant differences between maternal plasma metabolites in the GlcN group and the control group, which partly explained the reproductive results. Higher concentrations of progesterone and IGF-1 were detected in rats treated with GlcN compared with control dams. Progesterone is necessary for the maintenance of pregnancy. Consistently, total plasma cholesterol concentration in GlcN the group was reduced, which could result from enhanced utilization of cholesterol to synthesis steroid hormones. This explanation is supported by the fact that the levels of progesterone and estradiol were increased while LDL-C and HDL-C concentrations did not differ in dams treated with GlcN compared with controls. Glucosamine supplementation increased IGF-1 concentration which is important for embryonic development. IGF-1 is a major regulator of the growth rate and development of fetal [27–29].

Interaction between blastocysts and endometrium during the process of embryo implantation is a critical stage, which requires the involvement of both blastocyst and endometrial receptivity [8, 30]. Different blastocyst development ability may reduce the success rate of implantation.

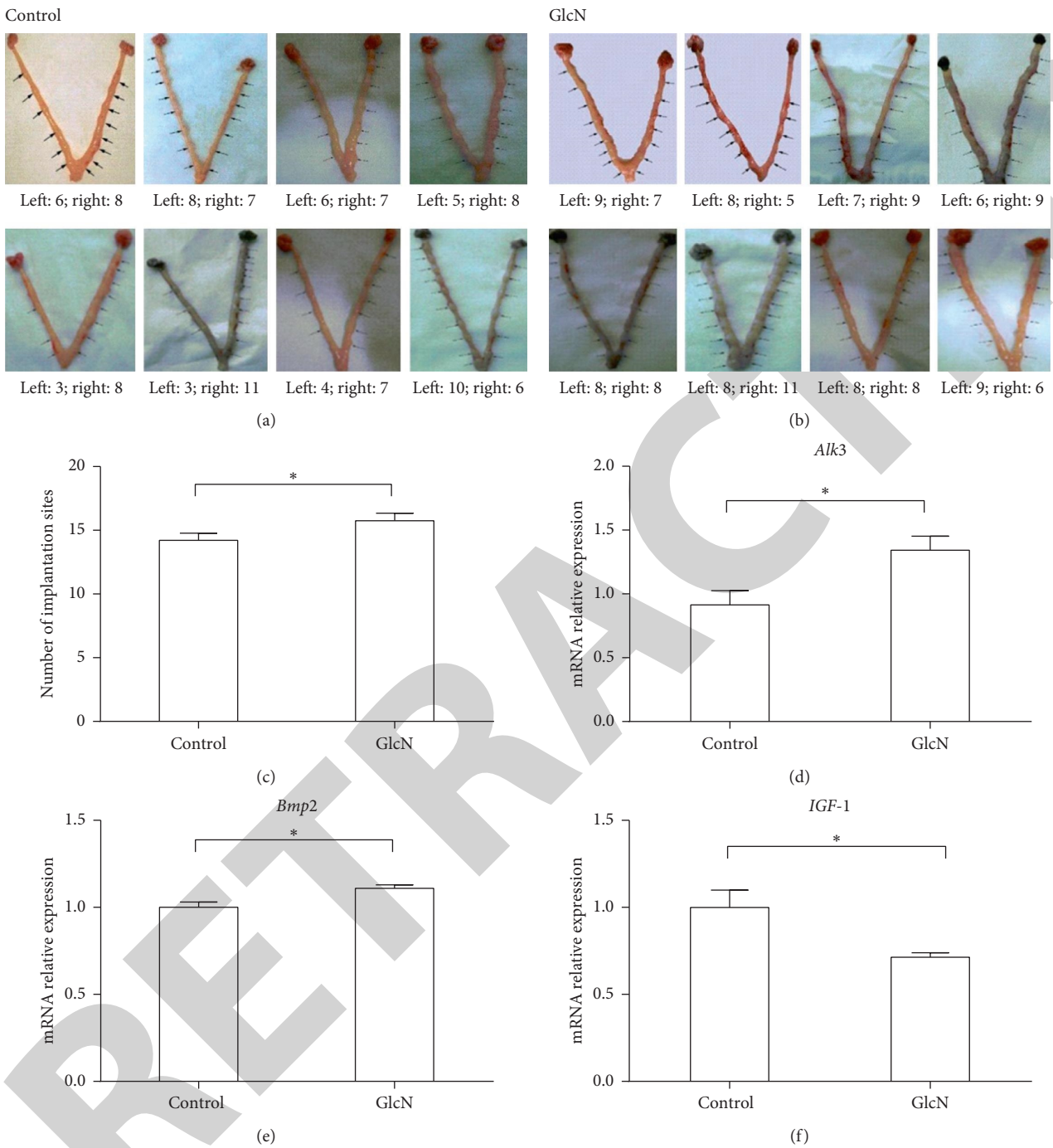

Figure 2: Continued.

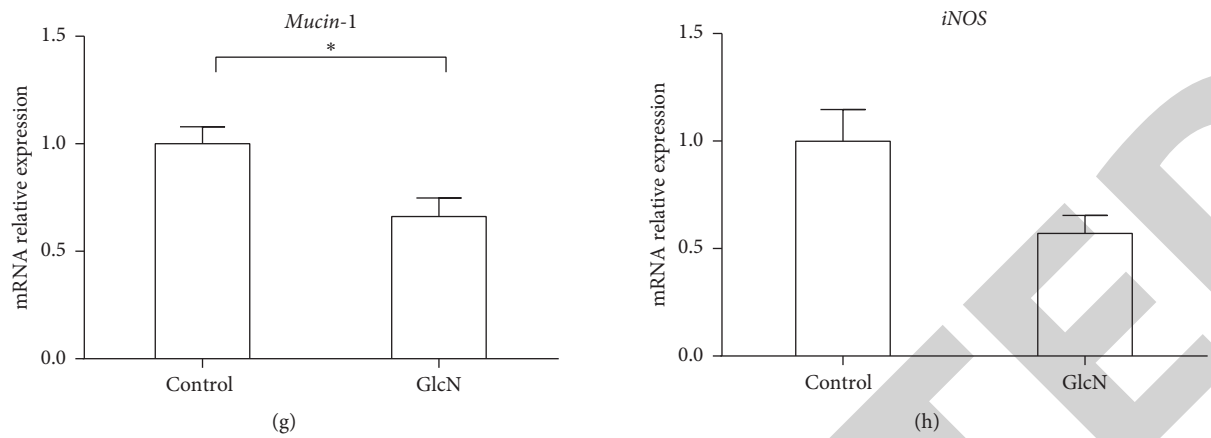

Figure 2: Effects of GlcN on implantation on day 6.5 of pregnancy. Distribution of implantation sites in the uterus in the control (a) and GlcN administration (b) groups. Implantation sites increased significantly in the GlcN groups compared with the control ones (c). The gene expression levels of Alk3 (d), Bmp2 (e), IGF-1 (f), Mucin-1 (g), and iNOS (h) in implantation sites were measured by quantitative real-time PCR. Data are expressed as mean ± SEM. *There were statistically significant differences between the two groups when P value <0.05.

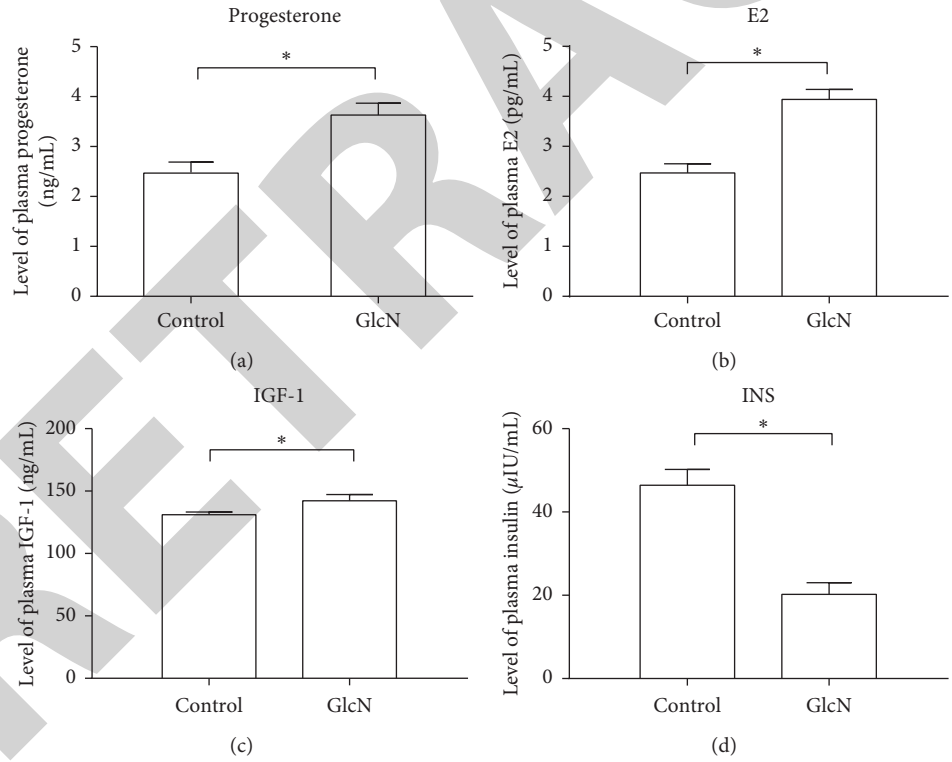

Figure 3: Continued.

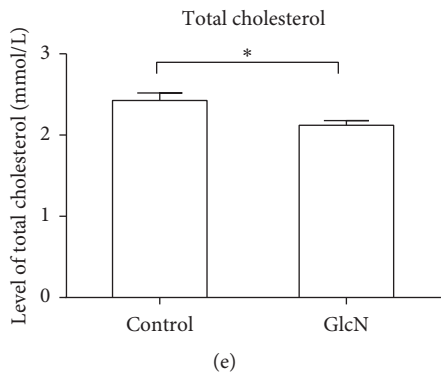

Figure 3: GlcN alters maternal plasma progesterone (a), E2 (b), IGF-1 (c), insulin (d), and total cholesterol (e) concentrations on day 19.5 of pregnancy ($n = 11$). *There were statistically significant differences between the two groups when P value <0.05.

A large number of embryos were lost during the implantation period [31]. Based on better pregnancy results in GlcN supplemented group, we further evaluated the effects of GlcN on embryonic implantation. The results showed that the number of implantation sites increased with the improved uterine environment in the GlcN group, which indicated better blastocyst and endometrial receptivity.

We further assessed gene expression that is closely relevant to placental implantation. Bmp plays important roles in endometrium stromal cell decidualization via Alk3 signal, and Alk3 has been demonstrated necessary for the transition of the uterus from nonreceptive to receptive stages by inhibiting uterine epithelial cell proliferation during the window of implantation [32–34]. In this study, the expression levels of Alk3 and Bmp2 genes in implantation sites of the GlcN group were increased, and the levels of IGF-1 and Mucin-1 were decreased, which indicated that the uterine receptivity was improved. Decreased IGF-1 inhibits endometrium proliferation [35], and Mucin-1 is an E2-mediated gene. The downregulation of Muc-1 may be due to the attenuated response of endometrium to E2; it is consistent with what uterine environment needs to be switched from E2-dominant to P4-dominant stage. As indicated, the distribution of embryos in bilateral uterine horns in the control group was seriously unequal. A reasonable explanation for improved uterine receptivity is that blastocyst competence is more uniform in rats treated with GlcN [8].

GlcN supplementation was conducted during the follicular phases of the estrous cycle, and its effects on within-litter variation and embryonic implantation seem to be closely related to the regulation of the ovaries development. Although several previous studies reported that the presence of glucosamine during maturation seriously interferes with the development of blastocysts *in vitro* [7], the relations between GlcN and oocyte maturation need further investigation *in vivo*.

5. Conclusions

Our study determined that GlcN supplementation before mating plays an important role in promoting the litter homogeneity, which is partly because of improved uterine receptivity. Our results provide a potential theoretical basis for formulating reasonable nutritional interventions to reduce the incidence of low birth weight animals, which will presumably improve the survival rate of newborns.

Data Availability

The data used to support the findings of this study are available from the corresponding author upon request.

Disclosure

Cuiping Feng and Taolin Yuan are co-first author.

Conflicts of Interest

The authors declare no conflicts of interest.

Acknowledgments

This research was funded by the Beijing Municipal Natural Science Foundation (S170001) and the National Natural Science Foundation of China (31272449, 31422052, and 31630074).

Supplementary Materials

The diet composition analysis is provided in Table S1. The concentration was determined on the basis of a gradient experiment which additionally included 1.0 mM GlcN and the results are presented in Table S2. A list of primer sequences is provided in Table S3. Growth performance during GlcN treatment periods is provided in Table S4. (*Supplementary Materials*)

References

[1] F. W. Bazer, W. W. Thatcher, F. Martinat-Botte, and M. Terqui, "Conceptus development in large white and prolific Chinese Meishan pigs," *Reproduction*, vol. 84, no. 1, pp. 37–42, 1988.

[2] W. F. Pope, M. H. Wilde, and S. Xie, "Effect of electrocautery of nonovulated day 1 follicles on subsequent morphological variation among day 11 porcine Embryos1," *Biology of Reproduction*, vol. 39, no. 4, pp. 882–887, 1988.

[3] P. Drbohlav, V. Bencko, J. Masata et al., "Detection of cadmium and zinc in the blood and follicular fluid in women in the IVF and ET program," *Ceska Gynekologie*, vol. 63, pp. 292–300, 1998.

[4] C. J. Ashworth, L. M. Toma, and M. G. Hunter, "Nutritional effects on oocyte and embryo development in mammals: implications for reproductive efficiency and environmental sustainability," *Philosophical Transactions of the Royal Society B: Biological Sciences*, vol. 364, no. 1534, pp. 3351–3361, 2009.

[5] N. Igosheva, A. Y. Abramov, L. Poston et al., "Maternal diet-induced obesity alters mitochondrial activity and redox status in mouse oocytes and zygotes," *PLoS One*, vol. 5, Article ID e10074, 2010.

[6] R. Mattos, C. R. Staples, and W. W. Thatcher, "Effects of dietary fatty acids on reproduction in ruminants," *Reviews of Reproduction*, vol. 5, no. 1, pp. 38–45, 2000.

[7] S. L. Wong, L. L. Wu, R. L. Robker, J. G. Thompson, and M. L. S. McDowall, "Hyperglycaemia and lipid differentially impair mouse oocyte developmental competence," *Reproduction, Fertility and Development*, vol. 27, no. 4, p. 583, 2015.

[8] T. Liu, B. Zuo, W. Wang, S. Wang, and J. Wang, "Dietary supplementation of leucine in premating diet improves the within-litter birth weight uniformity, antioxidative capability, and immune function of primiparous SD rats," *BioMed Research International*, vol. 2018, Article ID 1523147, 11 pages, 2018.

[9] M. Park, H.-R. Kim, Y. S. Kim et al., "Estrogen-induced transcription factor EGR1 regulates c-Kit transcription in the mouse uterus to maintain uterine receptivity for embryo implantation," *Molecular and Cellular Endocrinology*, vol. 470, pp. 75–83, 2018.

[10] K. Tanaka, K. Yamada, M. Matsushima et al., "Increased maternal insulin resistance promotes placental growth and decreases placental efficiency in pregnancies with obesity and gestational diabetes mellitus," *Journal of Obstetrics and Gynaecology Research*, vol. 44, no. 1, pp. 74–80, 2018.

[11] J. Silva, N. Ocarino, and R. Serakides, "Luteal activity of pregnant rats with hypo-and hyperthyroidism," *Journal of Ovarian Research*, vol. 7, no. 1, p. 75, 2014.

[12] D.-S. Lee, Y. Yanagimoto Ueta, X. Xuan et al., "Expression patterns of the implantation-associated genes in the uterus during the estrous cycle in mice," *Journal of Reproduction and Development*, vol. 51, no. 6, pp. 787–798, 2005.

[13] H. Shen, X. Hu, C. Liu et al., "Ethyl pyruvate protects against hypoxic-ischemic brain injury via anti-cell death and anti-inflammatory mechanisms," *Neurobiology of Disease*, vol. 37, no. 3, pp. 711–722, 2010.

[14] T. D. Schmittgen and K. j. Livak, "Analyzing real-time PCR data by the comparative C(T) method," *Nature Protocols*, vol. 3, no. 6, pp. 1101–1108, 2008.

[15] T- l. Yuan, Y. h. Zhu, M. Shi et al., "Within-litter variation in birth weight: impact of nutritional status in the sow," *Journal of Zhejiang University-SCIENCE B*, vol. 16, no. 6, pp. 417–435, 2015.

[16] T. van der Lende and D de Jager, "Death risk and preweaning growth rate of piglets in relation to the within-litter weight distribution at birth," *Livestock Production Science*, vol. 28, no. 1, pp. 73–84, 1991.

[17] N. Quiniou, J. Dagorn, and D. Gaudré, "Variation of piglets' birth weight and consequences on subsequent performance," *Livestock Production Science*, vol. 78, no. 1, pp. 63–70, 2002.

[18] L. A. Frank, M. L. Sutton-McDowall, D. L. Russell et al., "Effect of varying glucose and glucosamine concentration in vitro on mouse oocyte maturation and developmental competence," *Reproduction, Fertility and Development*, vol. 25, pp. 1095–1104, 2013.

[19] L. A. Frank, M. L. Sutton-McDowall, R. B. Gilchrist, and J. G. Thompson, "The effect of peri-conception hyperglycaemia and the involvement of the hexosamine biosynthesis pathway in mediating oocyte and embryo developmental competence," *Molecular Reproduction and Development*, vol. 81, no. 5, pp. 391–408, 2014.

[20] L. Chen, P. T. Russell, and W. j. Larsen, "Functional significance of cumulus expansion in the mouse: roles for the preovulatory synthesis of hyaluronic acid within the cumulus mass," *Molecular Reproduction and Development*, vol. 34, no. 1, pp. 87–93, 1993.

[21] M. L. Sutton-McDowall, R. B. Gilchrist, and J. G. Thompson, "Cumulus expansion and glucose utilisation by bovine cumulus-oocyte complexes during in vitro maturation: the influence of glucosamine and follicle-stimulating hormone," *Reproduction*, vol. 128, pp. 313–319, 2004.

[22] S. Tanghe, A. Van Soom, H. Nauwynck, M. Coryn, and A. de Kruif, "Minireview: functions of the cumulus oophorus during oocyte maturation, ovulation, and fertilization," *Molecular Reproduction and Development*, vol. 61, no. 3, pp. 414–424, 2002.

[23] E. Angiolini, A. Fowden, P. Coan et al., "Regulation of placental efficiency for nutrient transport by imprinted genes," *Placenta*, vol. 27, pp. S98–S102, 2006.

[24] E. Herrera, C. Muñoz, P. López-Luna, and P. Ramos, "Carbohydrate-lipid interactions during gestation and their control by insulin," *Brazilian Journal of Medical and Biological Research*, vol. 27, no. 11, pp. 2499–2519, 1994.

[25] J. h. Tsai, M. Schulte, K. O'Neill et al., "Glucosamine inhibits decidualization of human endometrial stromal cells and decreases litter sizes in mice," *Biology of Reproduction*, vol. 89, no. 1, p. 16, 2013.

[26] C. j. Schelbach, R. l. Robker, B. D. Bennett, A. G. Gauld, J. G. Thompson, and K. l. Kind, "Altered pregnancy outcomes in mice following treatment with the hyperglycaemia mimetic, glucosamine, during the periconception period," *Reproduction, Fertility and Development*, vol. 25, no. 2, pp. 405–416, 2013.

[27] J- P. Liu, J. Baker, A. S. Perkins, E. J. Robertson, and A. Efstratiadis, "Mice carrying null mutations of the genes encoding insulin-like growth factor I (Igf-1) and type 1 IGF receptor (Igf1r)," *Cell*, vol. 75, no. 1, pp. 59–72, 1993.

[28] J. Baker, J.-P. Liu, E. J. Robertson, and A. Efstratiadis, "Role of insulin-like growth factors in embryonic and postnatal growth," *Cell*, vol. 75, no. 1, pp. 73–82, 1993.

[29] A. Hellström, D. Ley, I. Hansen-Pupp et al., "Role of insulin like growth factor 1 in fetal development and in the early postnatal life of premature infants," *American Journal of Perinatology*, vol. 33, no. 11, pp. 1067–1071, 2016.

[30] A. Mihanfar, A. R. Sadigh, A. Fattahi et al., "Endothelins and their receptors in embryo implantation," *Journal of Cellular Biochemistry*, vol. 120, no. 9, pp. 14274–14284, 2019.

[31] Y. E. M. Koot, G. Teklenburg, M. S. Salker, J. J. Brosens, and N. S. Macklon, "Molecular aspects of implantation failure," *Biochimica et Biophysica Acta (BBA)—Molecular Basis of Disease*, vol. 1822, no. 12, pp. 1943–1950, 2012.

[32] D. Monsivais, C. Clementi, J. Peng et al., "Uterine ALK3 is essential during the window of implantation," *Proceedings of the National Academy of Sciences*, vol. 113, no. 3, pp. E387–E395, 2016.

Hindawi
BioMed Research International
Volume 2019, Article ID 6916189, 14 pages
https://doi.org/10.1155/2019/6916189

Review Article

What Is the Impact of Diet on Nutritional Diarrhea Associated with Gut Microbiota in Weaning Piglets: A System Review

Jing Gao,[1,2,3] **Jie Yin**,[1,2,3] **Kang Xu**,[1,2] **Tiejun Li**,[1,2] **and Yulong Yin**[1,2,3,4]

[1]*National Engineering Laboratory for Pollution Control and Waste Utilization in Livestock and Poultry Production, Institute of Subtropical Agriculture, The Chinese Academy of Sciences, Changsha, China*
[2]*Key Laboratory of Agro-Ecology, Institute of Subtropical Agriculture, The Chinese Academy of Sciences, Changsha, China*
[3]*University of Chinese Academy of Sciences, Beijing, China*
[4]*College of Life Science, Hunan Normal University, Changsha, Hunan, China*

Correspondence should be addressed to Tiejun Li; tjli@isa.ac.cn and Yulong Yin; yinyulong@isa.ac.cn

Received 11 October 2019; Revised 19 November 2019; Accepted 3 December 2019; Published 28 December 2019

Guest Editor: Deguang Song

Piglets experience severe growth challenges and diarrhea after weaning due to nutritional, social, psychological, environmental, and physiological changes. Among these changes, the nutritional factor plays a key role in postweaning health. Dietary protein, fibre, starch, and electrolyte levels are highly associated with postweaning nutrition diarrhea (PWND). In this review, we mainly discuss the high protein, fibre, resistant starch, and electrolyte imbalance in diets that induce PWND, with a focus on potential mechanisms in weaned piglets.

1. Introduction

Weaning is sudden and stressful and one of the most challenging periods in a pig's life [1]. Newly weaned pigs are usually stressed by nutritional, psychological, environmental, physiological, and social factors [2, 3]. Because of such stressors, piglets are often characterized with reduced growth performance and an increased prevalence of diarrhea after weaning [4, 5]. When undergoing the transition from a milk-based diet to a weaned diet, the piglets suffer a severe decrease in feed intake for a couple of days after weaning [6]. Furthermore, in order to adapt to the new environment, the composition of the gastrointestinal microbiota is also modified as a result of changes in feeding behavior and diet composition [6]. This period is often associated with a growth challenge because of a high incidence of gastrointestinal disorders, such as PWND [7].

Postweaning diarrhea is considered a major health problem and causes substantial morbidity and mortality in livestock [8, 9]. It is well established that postweaning diarrhea is a multifactorial gastrointestinal disease, and undernutrition has major etiological factors [10–12]. The gastrointestinal tract is a complex, balanced ecosystem [4, 13]. The dietary composition is a major factor influencing the intestinal microbial ecosystem [14, 15]. Hence, considering the balance between the intestinal microbial ecosystem and the composition of the diet, postweaning nutritional diarrhea (PWND) is a major problem during the postweaning period [11, 16].

The most efficient manner to alleviate the degree of PWND is to regulate the nutritional composition of the diet [15, 17]. Various nutritional approaches for improving the weaning transition and alleviating enteric diseases have been researched over the past several years [11, 18]. Evidence suggests that specific dietary interventions, such as the control of protein [19, 20], fibre [21], starch [22], electrolyte balance [23], and other constituents in the daily diet, could reduce the proliferation of certain PWND [11, 24, 25]. The purpose of the present review is to summarize several common kinds of PWND in order to better expound the role of nutrition in causing and modulating PWND in pigs.

2. High Protein Level Induces PWND

To decrease PWND, piglets are usually given antibiotics; however, antibiotics have been banned for use in livestock for human consumption. Thus, researchers have focused on finding a replacement for antibiotics in piglet feeding. One of the alternatives is the feeding of low-protein diets [26–28].

2.1. The Effect of Dietary Protein on Growth Performance and Digestibility of Nutrients of Weaned Piglets. The consumption of a low crude protein (CP) diet, which has direct effects on PWND, reduces the availability of substrates for bacterial fermentation and improves fecal consistency [29–31]. Dietary CP and individual AAs (amino acids) both affect the formation of metabolites during microbial fermentation [32]. However, high dietary CP concentration for early-weaned piglets could increase microbial fermentation of undigested protein and increase the proliferation of pathogenic bacteria in the gastrointestinal tract [3]. An excessive supply of dietary protein induces protein fermentation by intestinal microbiota in piglets [33]. Volatile fatty acids (VFAs) and potentially toxic compounds produced by bacterial fermentation of undigested protein substances, such as ammonia and amines, can reduce the growth performance of piglets [34, 35]. The increased production of amines has been found to increase the incidence of diarrhea at weaning in pigs [36, 37].

2.2. The Effect of Dietary Protein on the Gut Health of Weaned Piglets. It is well known that both exogenous and endogenous source proteins can be used by the gastrointestinal microbiota as a fermentable substrate [38, 39] and can be used for the production of diet proteins through degradation, including branched-chain fatty acids (BCFAs), ammonia, amines, phenols, and indoles [35, 39]. Bacteria, such as *Bacteroides* spp., *Propionibacterium* spp., *Streptococcus*, and *Clostridium* species, are associated with the formation of the substances listed above [20]. For example, BCFAs are produced by *Clostridia* [40]. Furthermore, intestinal concentrations of BCFAs possibly are used as indicators for the extent of protein fermentation [41].

Protein fermentation results in the production of metabolites that are in direct contact with the colonic mucosa and can directly interact with the mucosal cells. Undigested dietary protein and proteins of endogenous origin transfer to the large intestine for fermentation to toxic metabolites, such as ammonia, biogenic amines, and hydrogen sulfide. Most of these products can impair epithelial integrity and promote inflammatory reactions [34, 42]. Then, the metabolites or bacterial toxins may reduce the ability for fluid reabsorption and mask small intestinal hypersecretion [29]. An increased concentration of ammonia was found in parts of the intestinal tract of piglets fed high-protein diets [3]. Infusion of ammonium chloride from the isolated distal colon increased the proliferation of epithelial cells in rats, which may contribute to the development of gastrointestinal disorders [43]. Biogenic amine concentrations increased in the hindgut when feeding on highly fermentable protein, and bacterial putrescine played a role in the potential detrimental effects on gut health by decreasing the energy supply to the colonocytes [44]. Hydrogen sulfide impacts gut health by breaking down the mucus layer and by increasing the permeability of the mucus barrier [45]. According to several studies, high protein fermentation is associated with an increased risk of cancer [46].

2.3. The Effect of Dietary Protein on the Incidence of PWND. PWND is a gut disease induced by the stress of nutrition and is characterized by an increase in the microbial fermentation of supernumerary proteins [47]. Additionally, watery feces, decreased growth performance, high morbidity, and mortality have been noticed to occur with PWND [48]. However, the mechanism between protein fermentation and the gastrointestinal tract (GIT) is still unknown. Some studies showed that a high-protein diet led to a higher incidence of PWND [6, 35]. Interestingly, an increase in ammonia concentration has a detrimental effect on the health of the GIT and a negative effect on the growth and differentiation of intestinal epithelial cells [49, 50]. Additionally, BCFAs and ammonia are toxic metabolites for the intestinal mucosa and most likely trigger PWND and the poor performance in piglets [39, 51, 52]. More importantly, the upregulated expression of ammonia may induce a disorder of the intestinal microbial balance during weaning [20]. Additionally, the initially predominant lactobacilli decrease in number during weaning, leading to the downregulation of the GIT immunity and the formation of short chain fatty acids (SCFAs) [53]. More importantly, piglets fed a high-protein diet experience a high buffering capacity [54], an increase in the small intestinal pH [26], and a decrease in the expression of SCFAs, mainly butyrate, which probably permit a quick recovery of the intestinal epithelium, reducing the incidence and severity of PWND [55].

In summary, a high-protein diet increases the expression of BCFAs and ammonia, which can promote the growth of pathogenic bacteria, while a low-protein diet promises an increase in the expression of SCFAs, which may result in the establishment of beneficial microbes [56, 57]. Therefore, with a low-protein diet, beneficial bacteria rapidly proliferate and occupy the binding sites on the intestinal mucosa that could otherwise be occupied by pathogenic bacteria [58]. These differences between protein levels may reduce the incidence and severity of PWND and improve the growth performance of piglets [3]. Thus, it can be concluded that choosing a low-protein diet to feed postweaned piglets may be an effective way to decrease PWND incidence [3] (Figure 1).

3. The Effect of Dietary Fibre on PWND

Fermentable carbohydrates constitute the major energy source for microbial fermentation and therefore may act as a link between the piglet and its enteric commensal microbiota [59, 60]. Furthermore, dietary fibre may be beneficial for gut health and decreases diarrhea incidence in pigs [61, 62]. And significant effect on diarrhea incidence was observed in the

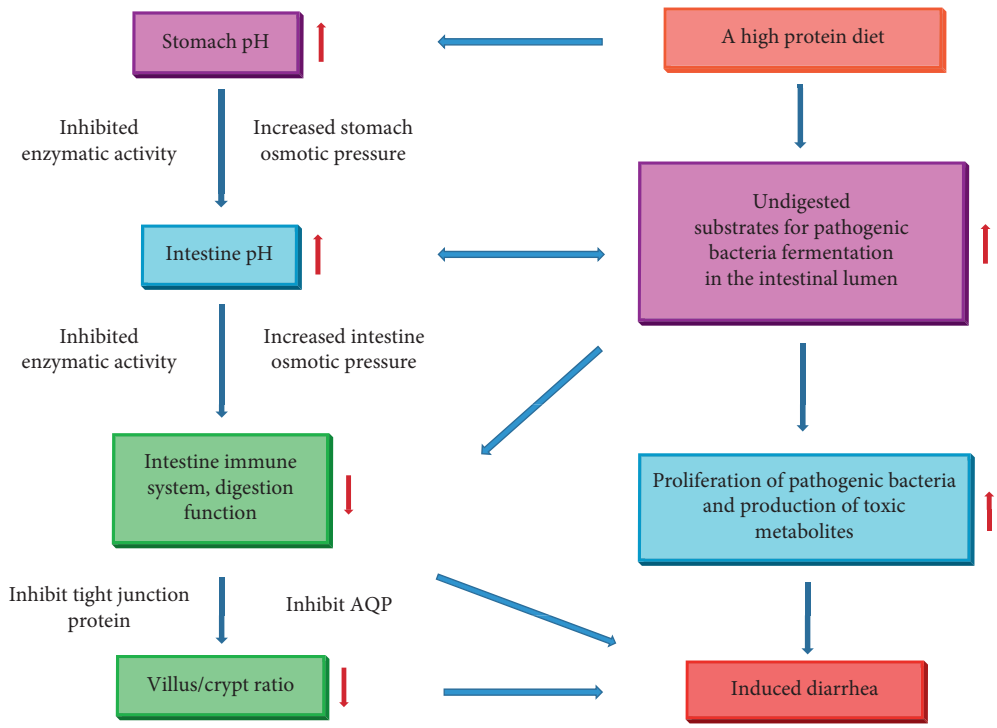

Figure 1: The possible mechanism of high protein diets induced postweaning nutritional diarrhea. AQP: aquaporin.

pigs fed the fibre source diet compared with the pigs fed the control diet [63, 64]. A difference in diarrhea incidence was observed among the different sources of fibre diets [60].

3.1. The Effect of Dietary Fibre on Growth Performance and Digestibility of Nutrients of Weaned Piglets. Adding fibre in the daily diet could improve the adaptation of the pigs during the weaning period [64]. Depending on the kinds of fibrous ingredients, the effects of feeding high-fibre diets on the performance of the piglets differed [62, 63]. The impact of dietary fibre on piglets' nutrition might be determined by the properties of fibre and/or fibre sources [65, 66]. For example, the fibre in the wheat bran diet was adapted by piglets and acted as prebiotics [60]. Wheat bran is a kind of insoluble fibre and when added to the weaned piglets' diet, it appears that it is related to a higher feed intake and development of the gastrointestinal tract [67, 68]. More research is necessary to clarify the effects of the dietary fibre composition on the growth performance of weaned piglets.

3.2. The Effect of Dietary Fibre on the Gut Health of Weaned Piglets. In consideration of intestinal bacteria, fibre diets influenced the health of piglets around the time of weaning [69, 70]. Previous studies showed that a lower villus height: crypt depth ratio is associated with microbial challenges and antigenic components of the feed [71, 72]. Moreover, a study of intestinal mucosal morphology was used to evaluate the surface area of the intestine undertaken for mucosal integrity [73, 74]. Adding wheat bran fibre to the daily feed elevated the ileal mucosal integrity by improving the ileum villus height and the villus height: crypt depth ratio, which is in agreement with previous findings that showed that feeding high-insoluble-fibre diets protected against pathogenic bacteria by increasing the villus length [75, 76]. Furthermore, research has shown that piglets fed soluble and insoluble dietary fibre had more goblet cells in the ileum than did fibre-free piglets [77, 78]. The goblet cells played an important role in the intestine by synthesizing and secreting several mediators, mainly found in the small and large intestine, that were resistant to proteolytic digestion and stimulated the repair process, such as mucin and peptide trefoil factors [24, 79]. Studies suggested that piglets fed a fibre diet had a higher TGF-α concentration in their colons than that of other fibre-free groups [80]. Altogether, a fibre diet could improve the intestinal barrier function by increasing the concentration of factors associated with intestinal barrier function. However, different dietary fibre compositions induce different changes in the intestinal bacteria [81, 82].

3.3. The Effect of Dietary Fibre on the Incidence of PWND. Dietary fibre has been reported to improve gut health and decrease the diarrhea incidence in pigs [61, 83]. A wheat bran diet has been shown to decrease the amount of pathogenic *E. coli* in the feces and reduce the incidence of PWND [61, 84]. It is reported that a pea fibre diet could improve the intestinal health in animals by reducing the adhesion and increasing the excretion of enterotoxigenic *E. coli*, and such a diet could reduce the incidence of PWND as well [85]. However, the effect of a fibre diet on the incidence of diarrhea was not observed between the piglets fed fibre diets and the control group. However, a difference in diarrhea incidence was observed among the fibre source diets

[64, 86]. The mechanism of the effects of the dietary fibre source on the incidence of diarrhea in weaned piglets may result from the inconsistent intestinal function in regulating intestinal bacteria [87]. Previous studies have shown that feeding weaned piglets high-insoluble-fibre diets might better protect them against pathogenic bacteria by increasing the villus length [85, 88]. The intestinal barrier integrity reflects the paracellular space between epithelial cells and may prevent the paracellular diffusion of intestinal bacteria across the epithelium [89]. Additionally, tight junction proteins play a key role in intestinal barrier integrity [90]. The probiotic *Lactobacillus* can increase occludin gene mRNA levels of Caco-2 cells, and *E. coli* decreases the levels of ZO-1, occludin, and claudin-1 tight junction complex in the epithelial cells, proving that bacteria affect the integrity of the intestinal barrier by regulating the gene expression level of tight junction proteins [91, 92]. The effect of fibre on tight junction proteins is associated with the number of bifidobacteria and lactobacilli [93]. Fibre in the diets has also promoted intestinal proinflammatory cytokine (IL-1 and TNF-α) mRNA levels as interference factors of the intestinal barrier [94, 95]. However, more research between PWND and intestinal bacteria alterations mediated by fibre in the diet must be done.

Complex fibre sources could affect the intestinal mucosal barrier function and regulate intestinal bacteria in weaning piglets. Additionally, fibre composition is considered to be an important factor affecting the intestinal barrier function in piglets and could induce the incidence of PWND (Figure 2).

4. The Effect of Dietary Electrolyte Balance on PWND

4.1. Dietary Electrolyte Absorption in the Intestine. The intestinal lumen accepts 8–10 L/day of fluid, containing ingested food and biological secretions. The small intestine absorbs the highest percentage of this fluid content, and the last 1.5–1.9 L of the fluid is absorbed by the large intestine [96]. Otherwise, <0.1–0.2 L/d of the fluid content is excreted in the feces in an abnormal condition [97]. However, piglets around the time of weaning suffer a significant reduction in the colon absorptive capacity, leading to diarrhea [98, 99].

Electroneutral sodium chloride in the intestine is absorbed by luminal Na^+/H^+ and Cl^-/HCO^- exchangers [100, 101]. The remaining absorption of sodium chloride is due to transcellular or paracellular absorption of Cl^- [102]. Na^+/H^+ and Cl^-/HCO^- exchangers in luminal brush-border membranes of the colonic epithelial cells are required to absorb sodium chloride [103]. This process is driven by the action of the Na^+-K^+-ATPase and is regulated by Na^+ depletion [104, 105].

The Na^+/H^+ exchangers play a key role in Na^+ and water absorption and the maintenance of intracellular pH and cell volume [106]. Eight types of Na^+/H^+ exchangers named NHE have been defined in the intestinal epithelium. In the intestine, NHE1 (SLC9A1), NHE2 (SLC9A2), NHE3 (SLC9A3), and NHE8 (SLC9A8) have been shown to be present in the intestinal epithelium [105, 107]. NHE1 (SLC9A1) is expressed in the basolateral membrane of the intestinal epithelial cells, is not affected by Na^+ depletion, and does not contribute to luminal ion and water absorption [108, 109]. NHE2 (SLC9A2) and NHE3 (SLC9A3) are both expressed in the intestinal epithelium, with a larger contribution of NHE3 (SLC9A3) to Na^+ absorption under control conditions [110]. Otherwise, NHE3 (SLC9A3) is reported as the main transporter for Na^+ absorption in the intestine [97, 111]. NHE3 (SLC9A3)-knockout mice had reduced intestinal Na^+ and water absorption and induced diarrhea [112, 113]. Na^+/H^+ exchange occurs in both surface and crypt epithelium and might be affected by CFTR Cl^- channels [114, 115]. However, the exact impact of CFTR Cl^- channels on the regulation of Na^+/H^+ exchange in the small intestine is not clear.

In mammalian intestinal epithelial cells, two types of SLC26 gene families, named DRA (SLC26A3) and PAT-1 (putative anion transporter, SLC26A6), have been identified as representing apical Cl^-/HCO_3^- exchangers [116, 117]. DRA is predominantly expressed in the colon and duodenum, whereas PAT-1 is mainly expressed in the jejunum and ileum [118, 119]. DRA mutations have been found to induce severe diarrhea, massive loss of Cl^- in stools, and metabolic alkalosis as well as serum electrolyte imbalance [120, 121]. PAT-1-knockout mice did not present this diarrhea phenotype [122]. In addition, similar to NHE3, a Cl^-/HCO_3^- exchange is also controlled by CFTR in the colonic epithelium [123, 124]. Taken together, the current studies indicate a regulation of both Na^+/H^+ and Cl^-/HCO_3^- exchangers by CFTR, which therefore play an important role in the electroneutral absorption of sodium chloride and regulation of cellular and mucosal pH in the animal gastrointestinal tract [117, 125, 126].

4.2. The Effect of Dietary Electrolyte Balance on the Growth Performance of Weaned Piglets. The animal industry is always concerned about minerals in feed, such as calcium (limestone), phosphorus (calcium phosphate), and sodium and chloride (salt and sodium bicarbonate) [127, 128]. Animal feed adds minerals not only to satisfy the mineral requirements but also to modify the dietary electrolyte balance (EB) [129]. The balance between cation (Na+) and anions (K^+/Cl^-) and the acid or alkaline load from the diet may strongly alter the acid-base status and growth performance of weaned piglets [130, 131]. It is reported that an excess of chloride ions induces a negative dietary EB and reduces the growth performance of weaned piglets [132–134]. In short, a dietary addition of minerals in postweaning diets, such as calcium chloride and sodium bicarbonate, could affect the EB and significantly alter the feeding behavior, apparent digestibility, and productive performance of postweaned piglets. Additionally, piglets showed a bias toward low-EB diets, which optimized their performance more so than that for high-EB diets [130, 135].

4.3. The Effect of Dietary Electrolyte Balance on the Incidence of PWND. Enteric pathogens have been proven to stimulate intestinal secretion of electrolytes and water [136, 137]. In

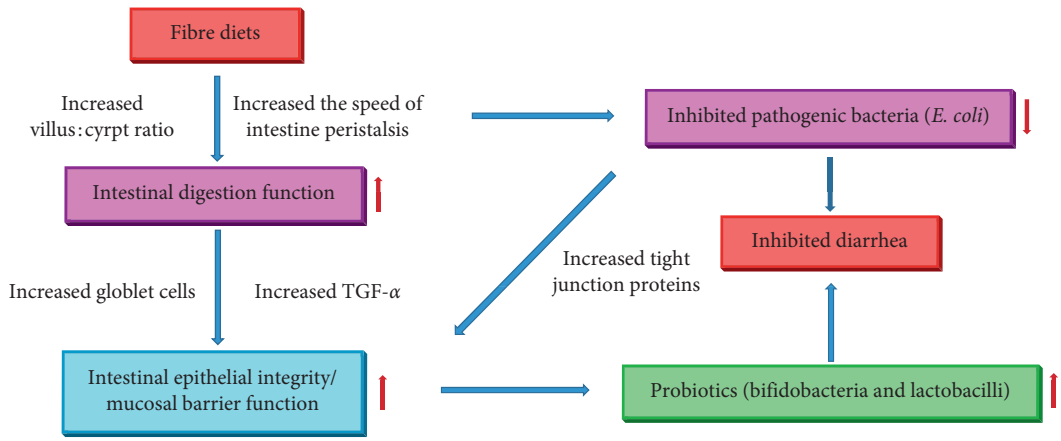

Figure 2: The possible mechanism of fibre diets regulated postweaning nutritional diarrhea. TGF-α: transforming growth factor-α.

most species, dietary electrolyte balance may be expressed as Na^+/H^+ and Cl^-/HCO_3^- and has been influenced by proportions of monovalent mineral cations and anions [138, 139]. Electrolyte balance plays a critical role in intestinal phenotype and function [140]. The disorder of daily electrolyte balance after weaning makes a large contribution to postweaning diarrhea, induces severe intestinal electrolyte turbulence, and negatively affects the piglets' growth performance after weaning through excessive loss of salt and water [130, 133]. The gastrointestinal tract exhibits segmental heterogeneity in the various ion transporters and channels in the postweaning period, which play a control role in conjunction and determine the electrolyte content and fluid volume in the lumen. In basic situation, the reason of PWND is the imbalance between the absorption and secretion of ions and solutes across the gut epithelium [141]. This imbalance of electrolytes in the digestive tract of piglets is induced by the presence of bacteria that could deliver toxins into the gut and disturb the development of the epithelium [142]. The enteric pathogens spread rapidly and cause infection in the piglets' intestines [143]. This situation results in the formation of watery feces, or PWND, in combination with reduced growth performance, morbidity, and even mortality of postweaning piglets.

In principle, the processes that result in induced PWND are proposed as follows. First, postweaning diets contain unabsorbed solutes that exert an osmotic force pulling water and electrolytes into the intestinal lumen [144, 145]. Second, the syndromes result in villus atrophy and crypt hypertrophy, thereby adversely altering the balance of absorption and secretion [146, 147]. Lastly, active secretion is stimulated by unabsorbed dihydroxy bile acid and fatty acid [148]. The altered bile acid and fatty acid transport themselves into the lipid phase of the plasma membrane [149, 150]. Then, the excess fecal water from the decreased intestinal absorption and the increased intestinal secretion is the reason for diarrhea [151, 152]. Generally, the electrolyte imbalance in postweaning diets exhibited alterations in motility, changes in paracellular permeability, loss of absorption surface, a change in electrolyte fluxes in postweaning piglets and, finally, induced PWND [153–155] (Figure 3).

5. The Effect of Dietary Starch Content on PWND

Starch is the main carbohydrate source of animal diets and the main energy source required for both animals and humans [156, 157]. It is composed of two types of a-glucan polymers: amylose and amylopectin [158, 159]. Starch has been proven to have a significant effect on the composition and activity of the intestinal microflora, through an improvement of the growth of beneficial bacteria and a reduction in the development of pathogenic bacteria in the intestines [160, 161]. Based on the digestible capacity, starches could be classified into rapidly digestible starch (RDS), slowly digestible starch (SDS), and resistant starch (RS) [162, 163]. RS cannot be absorbed in the small intestine, but it passes to the large bowel and beneficially modifies the gut microbial populations [164, 165].

5.1. The Effect of Resistant Starch Source on the Intestine Digestive Ability and Function of Postweaning Piglets. To ameliorate PWND and improve the gastrointestinal function of piglets, one useful alternative is to use a dietary prebiotic material, such as RS [166, 167]. The properties of prebiotics such as RS can act as indigestible carbohydrate substrates for cecal and colonic microbiota that influence the host gut health, as shown in animal and human studies [161, 166]. Starch digestion begins in the mouth. The enzyme α-amylase begins to digest starch to oligosaccharides and maltose. Starch does not digest in the stomach but is transported to the small intestine and broken down to glucose and maltose by pancreatic amylase [161, 168]. Then, the small intestine absorbs glucose by active transport, with the residual part being passively diffused through the villi [169, 170]. Starch digestion is influenced by many factors, such as the presence of lipids, proteins, and minerals, the amylose to amylopectin ratio, and digestion conditions [171, 172]. RS starts to be fermented in the large bowel by colonic microflora and then is digested into hydrogen, methane, and short-chain fatty acids (SCFAs), such as acetic, propionic, and butyric acid [173]. In addition, it is said that

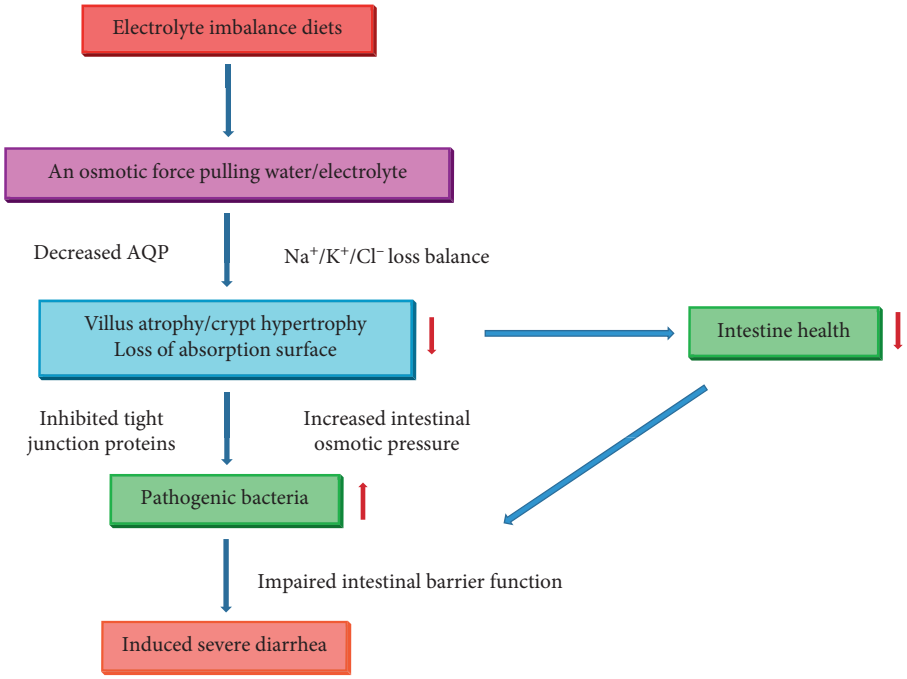

Figure 3: The possible mechanism of electrolyte imbalanced diets induced postweaning nutritional diarrhea. AQP: aquaporin.

the concentration of SCFAs is significantly increased in the large intestine after RS consumption [174, 175]. SCFAs play a positive role in colonic muscles and the absorption of calcium, magnesium, and water, and they also positively stimulate the colonic microflora [176, 177]. According to one experiment, a lower level of RS in the diet will decrease the growth challenge seen in postweaning piglets [178]. It is likely that piglets fed diets containing a higher level of RS (14%) exhibited more undigested starch in the ileum compared with that for piglets fed a diet without added RS [179]. It is reported that RS could be hydrolyzed by several Bifidobacterium strains, such as *B. adolescentis*, *B. bifidum*, *B. breve*, *B. infantis*, *B. lactis*, and *B. longum* [180]. In short, the beneficial effects of RS in the large bowel appear mainly because of the appearance of SCFAs formed by the previously mentioned bacterial fermentation [181]. Colonic bacteria ferment RS to SCFAs, mainly acetate, propionate, and butyrate, and benefit the large bowel of the postweaning piglet [166, 182].

5.2. The Effect of Resistant Starch Source on the Incidence of PWND. According to the existing research, a diet containing 7% resistant potato starch reduced the PWND incidence compared to that with a diet containing 14% resistant potato starch [178]. In addition, a diet containing 0.5 or 1.0% of resistant potato starch reduced the incidence of PWND and improved the growth performance in weaning piglets [169]. As we mentioned before, the concentration of SCFAs significantly increases in the large intestine after RS consumption [183]. In contrast, the molar proportion of BCFAs decreases. All of these results occurred because of the greater amounts of substrates available for carbohydrate-utilizing microbiota in the colons of pigs fed diets containing RS [184]. BCFAs are a harmful fermentation product and are a predisposing factor for PWND as well [185]. In addition, RS diets in piglets have a sharp reduction in ileal and cecal digesta pH [186]. According to what we know, bacteria ferment organic matter in the large intestine, including RS to SCFAs, and therefore reduce the pH in the GIT. There is a positive relationship between dietary intake of resistant starch and fecal output [187, 188]. Simply put, postweaning piglets fed a diet that includes a low level of RS leads to increases in the concentration of SCFAs, such as acetate, propionate, and butyrate, as well as the concentration of other terminal products, such as lactate, ethanol, succinate, carbon dioxide, hydrogen, and methane [165, 189]. The increasing SCFA levels decrease the gut pH; help raise gut motility; improve the absorption of nutrients, such as calcium, magnesium, and iron; and provide energy for the colonic epithelium and the host [190, 191]. Importantly, low-level RS diets decrease the concentrations of BCFAs, which are a harmful fermentation product as well as a predisposing factor for PWND [165, 192].

We learned that diets containing increased colonic fermentation associated with substrates such as RS also have striking effects on the composition of the gut microflora in order to increase the bacteria populations that are helpful to the bowel and decrease the bacteria populations that are harmful for a healthy large intestine [193, 194]. According to a previous study, lactobacilli and bifidobacteria are considered beneficial and were found to increase in abundance in the cecum with RS diets [195]. Furthermore, a trial that used a diet with lactobacilli strains added decreased the duration and incidence of diarrhea [196]. In short, supplementing weaned pigs' diets with at least 0.5% RS increased the populations of bacteria that are potentially good for the large intestines, such as lactobacilli and bifidobacteria

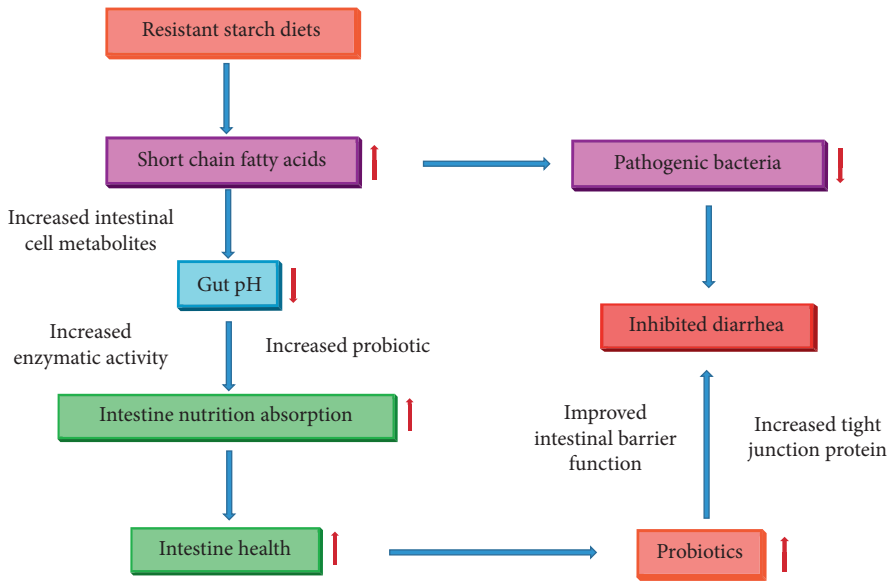

Figure 4: The possible mechanism of resistance starch diets induced postweaning nutritional diarrhea.

[197], which in turn decreased the amount of bacteria that are harmful for a healthy bowel. Finally, the increase in good bacteria populations and the decrease in harmful bacteria populations resulted in a decreased incidence of diarrhea [198, 199] (Figure 4).

6. Conclusion

Weaning is a grand challenge in the swine industry, which frequently induces severe intestinal disorders and gut diseases, raising serious economic and public health concerns. In addition, the gut microbiota derangement induced by changes in the diet of piglets around the time of weaning is the most direct reason of PWND. Despite the progress in modern pig farms during the last decade to prevent infectious diseases and improve global animal health, PWND is still an event that causes significant economic losses in the pig industry. However, we have now learned that the key component that leads to PWND is the composition of the daily diets for postweaning piglets. As described herein, the percentage of protein, fibre, and RS in the diet as well as the electrolyte balance could influence the fermentation products, thus altering the gastrointestinal microbiota composition and, as a result, inducing the incidence of PWND. Clearly, we require well-controlled studies to better understand the impact of nutrition on the growth of piglets around weaning. Controlling the nutrition in the diets is the most promising strategy for the prevention of PWND. The interaction of nutrition along the intestinal tract and the influence it has on the host still must be defined further in order to formulate appropriate "healthy" pig diets.

Conflicts of Interest

The authors declare that there are no conflicts of interest.

Authors' Contributions

All the authors contributed extensively to the work presented in this manuscript. JG mainly completed this review, performed the literature search, and wrote the manuscript. KX, JY, TL, and YY conceived the work and critically revised it. YY revised the manuscript.

Acknowledgments

This work was funded by the National Key R&D Program of China (2016YFD0501201), the Key Programs of Frontier Scientific Research of the Chinese Academy of Sciences (QYZDY-SSW-SMC008), the National Natural Science Foundation of China (31872371), the Key R&D Program of Hunan Province (2017NK2321), the Earmarked Fund for China Agriculture Research System (CARS-35), and the Hunan Provincial Science and Technology Department (2018TP1031).

References

[1] J. Yin, M. M. Wu, H. Xiao et al., "Development of an antioxidant system after early weaning in piglets," *Journal of Animal Science*, vol. 92, no. 2, pp. 612–619, 2014.

[2] T. M. Laine, T. Lyytikainen, M. Yliaho, and M. Anttila, "Risk factors for post-weaning diarrhoea on piglet producing farms in Finland," *Acta Veterinaria Scandinavica*, vol. 50, p. 21, 2008.

[3] J. M. Heo, J. C. Kim, J. Yoo, and J. R. Pluske, "A between-experiment analysis of relationships linking dietary protein intake and post-weaning diarrhea in weanling pigs under conditions of experimental infection with an enterotoxigenic strain of *Escherichia coli*," *Animal Science Journal*, vol. 86, no. 3, pp. 286–293, 2015.

[4] J. M. Campbell, J. D. Crenshaw, and J. Polo, "The biological stress of early weaned piglets," *Journal of Animal Science and Biotechnology*, vol. 4, no. 1, p. 19, 2013.

[5] J. M. Heo, F. O. Opapeju, J. R. Pluske, J. C. Kim, D. J. Hampson, and C. M. Nyachoti, "Gastrointestinal health and function in weaned pigs: a review of feeding strategies to control post-weaning diarrhoea without using in-feed antimicrobial compounds," *Journal of Animal Physiology and Animal Nutrition*, vol. 97, no. 2, pp. 207–237, 2013.

[6] J. Kluess, U. Schoenhusen, W. B. Souffrant, P. H. Jones, and B. G. Miller, "Impact of diet composition on ileal digestibility and small intestinal morphology in early-weaned pigs fitted with a T-cannula," *Animal*, vol. 4, no. 4, pp. 586–594, 2010.

[7] F. H. M. Aherne, E. T. Kornegay, G. C. Shurson et al., *Management and Nutrition of the Newly Weaned Pig*, National Pork Producers Council, Des Moines, IA, USA, 1992.

[8] W. Zhou, K. Ullman, V. Chowdry et al., "Molecular investigations on the prevalence and viral load of enteric viruses in pigs from five European countries," *Veterinary Microbiology*, vol. 182, pp. 75–81, 2016.

[9] G. Guan, S. Ding, Y. Yin, V. Duraipandiyan, NA. Al-Dhabi, and G. Liu, "Macleaya cordata extract alleviated oxidative stress and altered innate immune response in mice challenged with enterotoxigenic *Escherichia coli*," *Science China Life Sciences*, vol. 62, pp. 1019–1027, 2019.

[10] A. G. Atasever, P. E. Ozcan, K. Kasali, T. Abdullah, G. Orhun, and E. Senturk, "The frequency, risk factors, and complications of gastrointestinal dysfunction during enteral nutrition in critically ill patients," *Therapeutics and Clinical Risk Management*, vol. 14, pp. 385–391, 2018.

[11] J. R. Pluske, D. W. Pethick, D. E. Hopwood, and D. J. Hampson, "Nutritional influences on some major enteric bacterial diseases of pig," *Nutrition Research Reviews*, vol. 15, no. 2, pp. 333–371, 2002.

[12] J.-P. Lallès, P. Bosi, H. Smidt, and C. R. Stokes, "Nutritional management of gut health in pigs around weaning," *Proceedings of the Nutrition Society*, vol. 66, no. 2, pp. 260–268, 2007.

[13] X. Ma, P. Fan, L. S. Li, S. Y. Qiao, G. L. Zhang, and D. F. Li, "Butyrate promotes the recovering of intestinal wound healing through its positive effect on the tight junctions1," *Journal of Animal Science*, vol. 90, no. 4, pp. 266–268, 2012.

[14] B. Jayaraman and C. M. Nyachoti, "Husbandry practices and gut health outcomes in weaned piglets: a review," *Animal Nutrition*, vol. 3, no. 3, pp. 205–211, 2017.

[15] T. D. Leser, J. Z. Amenuvor, T. K. Jensen, R. H. Lindecrona, M. Boye, and K. Moller, "Culture-independent analysis of gut bacteria: the pig gastrointestinal tract microbiota revisited," *Applied and Environmental Microbiology*, vol. 68, no. 2, pp. 673–690, 2002.

[16] J. Gao, K. Xu, H. Liu et al., "Impact of the gut microbiota on intestinal immunity mediated by tryptophan metabolism," *Frontiers in Cellular and Infection Microbiology*, vol. 8, p. 13, 2018.

[17] M. R. A. J. Bedford, *Microbial Interactions in the Response to Exogenous Enzyme Utilization*, Wallingford, UK, 2001.

[18] E. Bauer, B. A. Williams, H. Smidt, R. Mosenthin, and M. W. A. Verstegen, "Influence of dietary components on development of the microbiota in single-stomached species," *Nutrition Research Reviews*, vol. 19, no. 1, pp. 63–78, 2006.

[19] G. Wu, "Dietary protein intake and human health," *Food and Function*, vol. 7, no. 3, pp. 1251–1265, 2016.

[20] V. T. S. Rist, E. Weiss, N. Sauer, R. Mosenthin, and M. Eklund, "Effect of dietary protein supply originating from soybean meal or casein on the intestinal microbiota of piglets," *Anaerobe*, vol. 25, pp. 72–79, 2014.

[21] C. Mu, L. Zhang, X. He, H. Smidt, and W. Zhu, "Dietary fibres modulate the composition and activity of butyrate-producing bacteria in the large intestine of suckling piglets," *Antonie Van Leeuwenhoek*, vol. 110, no. 5, pp. 687–696, 2017.

[22] G.-Q. Han, Z.-T. Xiang, B. Yu et al., "Effects of different starch sources on Bacillus spp. in intestinal tract and expression of intestinal development related genes of weanling piglets," *Molecular Biology Reports*, vol. 39, no. 2, pp. 1869–1876, 2012.

[23] H. A. Merchant, E. L. McConnell, F. Liu et al., "Assessment of gastrointestinal pH, fluid and lymphoid tissue in the Guinea pig, rabbit and pig, and implications for their use in drug development," *European Journal of Pharmaceutical Sciences*, vol. 42, no. 1-2, pp. 3–10, 2011.

[24] B. Deplancke and H. R. Gaskins, "Microbial modulation of innate defense: goblet cells and the intestinal mucus layer," *The American Journal of Clinical Nutrition*, vol. 73, no. 6, pp. 1131S–1141S, 2001.

[25] Y. Ji, X. Kong, H. Li, Q. Zhu, Q. Guo, and Y. Yin, "Effects of dietary nutrient levels on microbial community composition and diversity in the ileal contents of pregnant Huanjiang mini-pigs," *PLoS One*, vol. 12, no. 2, Article ID e0172086, 2017.

[26] J. K. Htoo, B. A. Araiza, W. C. Sauer et al., "Effect of dietary protein content on ileal amino acid digestibility, growth performance, and formation of microbial metabolites in ileal and cecal digesta of early-weaned pigs," *Journal of Animal Science*, vol. 85, no. 12, pp. 3303–3312, 2007.

[27] I. J. Wellock, P. D. Fortomaris, J. G. Houdijk, and I. Kyriazakis, "Effects of dietary protein supply, weaning age and experimental enterotoxigenic *Escherichia coli* infection on newly weaned pigs: health," *Animal*, vol. 2, pp. 834–842, 2008.

[28] F. O. Opapeju, D. O. Krause, R. L. Payne, M. Rademacher, and C. M. Nyachoti, "Effect of dietary protein level on growth performance, indicators of enteric health, and gastrointestinal microbial ecology of weaned pigs induced with postweaning colibacillosis1,2," *Journal of Animal Science*, vol. 87, no. 8, pp. 2635–2643, 2009.

[29] R. Pieper, C. Villodre Tudela, M. Taciak, J. Bindelle, J. F. Pérez, and J. Zentek, "Health relevance of intestinal protein fermentation in young pigs," *Animal Health Research Reviews*, vol. 17, no. 2, pp. 137–147, 2016.

[30] K. Qiu, X. Zhang, N. Jiao et al., "Dietary protein level affects nutrient digestibility and ileal microbiota structure in growing pigs," *Animal Science Journal*, vol. 89, no. 3, pp. 537–546, 2018.

[31] J. Yin, W. Ren, X. Huang, T. Li, and Y. Yin, "Protein restriction and cancer," *Biochimica et Biophysica Acta (BBA)-Reviews on Cancer*, vol. 1869, no. 2, pp. 256–262, 2018.

[32] G. Wu, F. W. Bazer, Z. Dai, D. Li, J. Wang, and Z. Wu, "Amino acid nutrition in animals: protein synthesis and beyond," *Annual Review of Animal Biosciences*, vol. 2, no. 1, pp. 387–417, 2014.

[33] R. Gresse, F. Chaucheyras-Durand, M. A. Fleury, T. Van de Wiele, E. Forano, and S. Blanquet-Diot, "Gut microbiota dysbiosis in postweaning piglets: understanding the keys to health," *Trends in Microbiology*, vol. 25, no. 10, pp. 851–873, 2017.

[34] V. T. S. Rist, E. Weiss, M. Eklund, and R. Mosenthin, "Impact of dietary protein on microbiota composition and activity in the gastrointestinal tract of piglets in relation to gut health: a review," *Animal*, vol. 7, no. 7, pp. 1067–1078, 2013.

[35] P. Bikker, A. Dirkzwager, J. Fledderus et al., "The effect of dietary protein and fermentable carbohydrates levels on growth performance and intestinal characteristics in newly weaned piglets1," *Journal of Animal Science*, vol. 84, no. 12, pp. 3337–3345, 2006.

[36] P. Porter and R. Kenworthy, "A study of intestinal and urinary amines in pigs in relation to weaning," *Research in Veterinary Science*, vol. 10, no. 5, pp. 440–447, 1969.

[37] M. S. Riaz Rajoka, J. Shi, H. M. Mehwish et al., "Interaction between diet composition and gut microbiota and its impact on gastrointestinal tract health," *Food Science and Human Wellness*, vol. 6, no. 3, p. 10, 2017.

[38] J. Zhao, X. Zhang, H. Liu, M. A. Brown, and S. Qiao, "Dietary protein and Gut microbiome composition and function," *Current Protein and Peptide Science*, vol. 20, no. 2, pp. 145–154, 2019.

[39] B. A. Williams, M. W. Bosch, A. Awati et al., "In vitro assessment of gastrointestinal tract (GIT) fermentation in pigs: fermentable substrates and microbial activity," *Animal Research*, vol. 54, no. 3, pp. 191–201, 2005.

[40] G. T. MSaM, *Proteolysis and Amino Acid Fermentation*, CRC Press, Boca Raton, FL, USA, 1995.

[41] G. Macfarlane, E. Beatty, and J. H. Cummings, "Estimation of short-chain fatty acid production from protein by human intestinal bacteria based on branched-chain fatty acid measurements," *FEMS Microbiology Letters*, vol. 101, no. 2, pp. 81–88, 1992.

[42] H. M. Hamer, V. De Preter, K. Windey, and K. Verbeke, "Functional analysis of colonic bacterial metabolism: relevant to health?," *American Journal of Physiology-Gastrointestinal and Liver Physiology*, vol. 302, no. 1, pp. G1–G9, 2012.

[43] H. Ichikawa and T. Sakata, "Stimulation of epithelial cell proliferation of isolated distal colon of rats by continuous colonic infusion of ammonia or short-chain fatty acids is nonadditive," *The Journal of Nutrition*, vol. 128, no. 5, pp. 843–847, 1998.

[44] R. Pieper, S. Kröger, J. F. Richter et al., "Fermentable fiber ameliorates fermentable protein-induced changes in microbial ecology, but not the mucosal response, in the colon of piglets," *The Journal of Nutrition*, vol. 142, no. 4, pp. 661–667, 2012.

[45] N. Ijssennagger, C. Belzer, G. J. Hooiveld et al., "Gut microbiota facilitates dietary heme-induced epithelial hyperproliferation by opening the mucus barrier in colon," *Proceedings of the National Academy of Sciences*, vol. 112, no. 32, pp. 10038–10043, 2015.

[46] C. D. Davis and J. A. Milner, "Gastrointestinal microflora, food components and colon cancer prevention," *The Journal of Nutritional Biochemistry*, vol. 20, no. 10, pp. 743–752, 2009.

[47] Y. Wu, Z. Jiang, C. Zheng et al., "Effects of protein sources and levels in antibiotic-free diets on diarrhea, intestinal morphology, and expression of tight junctions in weaned piglets," *Animal Nutrition*, vol. 1, no. 3, pp. 170–176, 2015.

[48] I. J. Wellock, P. D. Fortomaris, J. G. Houdijk, and I. Kyriazakis, "Effects of dietary protein supply, weaning age and experimental enterotoxigenic *Escherichia coli* infection on newly weaned pigs: performance," *Animal*, vol. 2, pp. 825–833, 2008.

[49] H. R. Gaskins, *Intestinal Bacteria and Their Influence on Swine Growth*, CRC Press LLC, Boca Raton, FL, USA, 2001.

[50] M. Ni Lochlainn, R. C. E. Bowyer, and C. J. Steves, "Dietary protein and muscle in aging people: the potential role of the gut microbiome," *Nutrients*, vol. 10, 2018.

[51] R. G. Hermes, F. Molist, M. Ywazaki et al., "Effect of dietary level of protein and fiber on the productive performance and health status of piglets1," *Journal of Animal Science*, vol. 87, no. 11, pp. 3569–3577, 2009.

[52] K. E. García, T. C. R. de Souza, G. M. Landín, A. A. Barreyro, M. G. B. Santos, and J. G. G. Soto, "Microbial fermentation patterns, diarrhea incidence, and performance in weaned piglets fed a low protein diet supplemented with probiotics," *Food and Nutrition Sciences*, vol. 5, no. 18, pp. 1776–1786, 2014.

[53] B. Jensen, "The impact of feed additives on the microbial ecology of the gut in young pigs," *Journal of Animal and Feed Sciences*, vol. 7, pp. 45–64, 1998.

[54] K. H. Partanen and Z. Mroz, "Organic acids for performance enhancement in pig diets," *Nutrition Research Reviews*, vol. 12, no. 1, pp. 117–145, 1999.

[55] D. G. Burrin, Y. Petersen, B. Stoll, and P. Sangild, "Glucagon-like peptide 2: a nutrient-responsive gut growth factor," *The Journal of Nutrition*, vol. 131, no. 3, pp. 709–712, 2001.

[56] B. A. Williams, M. W. A. Verstegen, and S. Tamminga, "Fermentation in the large intestine of single-stomached animals and its relationship to animal health," *Nutrition Research Reviews*, vol. 14, no. 2, pp. 207–227, 2001.

[57] N. Ma, Y. Tian, Y. Wu, and X. Ma, "Contributions of the interaction between dietary protein and gut microbiota to intestinal health," *Current Protein and Peptide Science*, vol. 18, pp. 795–808, 2017.

[58] T. Anthony, T. Rajesh, N. Kayalvizhi, and P. Gunasekaran, "Influence of medium components and fermentation conditions on the production of bacteriocin(s) by Bacillus licheniformis AnBa9," *Bioresource Technology*, vol. 100, no. 2, pp. 872–877, 2009.

[59] L. Zhang, C. Mu, X. He et al., "Effects of dietary fibre source on microbiota composition in the large intestine of suckling piglets," *FEMS Microbiology Letters*, vol. 363, no. 14, 2016.

[60] H. Chen, X. Mao, J. He et al., "Dietary fibre affects intestinal mucosal barrier function and regulates intestinal bacteria in weaning piglets," *British Journal of Nutrition*, vol. 110, no. 10, pp. 1837–1848, 2013.

[61] F. Molist, A. G. de Segura, J. Gasa et al., "Effects of the insoluble and soluble dietary fibre on the physicochemical properties of digesta and the microbial activity in early weaned piglets," *Animal Feed Science and Technology*, vol. 149, no. 3-4, pp. 346–353, 2009.

[62] F. Molist, M. van Oostrum, J. F. Pérez, G. G. Mateos, C. M. Nyachoti, and P. J. van der Aar, "Relevance of functional properties of dietary fibre in diets for weanling pigs," *Animal Feed Science and Technology*, vol. 189, pp. 1–10, 2014.

[63] C. Yu, S. Zhang, Q. Yang et al., "Effect of high fibre diets formulated with different fibrous ingredients on performance, nutrient digestibility and faecal microbiota of weaned piglets," *Archives of Animal Nutrition*, vol. 70, no. 4, pp. 263–277, 2016.

[64] P. Superchi, R. Saleri, P. Borghetti et al., "Effects of a dietary crude fibre concentrate on growth in weaned piglets," *Animal*, vol. 11, no. 11, pp. 1905–1912, 2017.

[65] J. E. Lindberg, "Fiber effects in nutrition and gut health in pigs," *Journal of Animal Science and Biotechnology*, vol. 5, p. 15, 2014.

[66] R. Jha and J. D. Berrocoso, "Review: dietary fiber utilization and its effects on physiological functions and gut health of swine," *Animal*, vol. 9, no. 9, pp. 1441–1452, 2015.

[67] H. Chen, W. Wang, J. Degroote et al., "Arabinoxylan in wheat is more responsible than cellulose for promoting intestinal barrier function in weaned male piglets," *The Journal of Nutrition*, vol. 145, no. 1, pp. 51–58, 2015.

[68] H. D. Holscher, "Dietary fiber and prebiotics and the gastrointestinal microbiota," *Gut Microbes*, vol. 8, no. 2, pp. 172–184, 2017.

[69] K. Schedle, C. Plitzner, T. Ettle, L. Zhao, K. J. Domig, and W. Windisch, "Effects of insoluble dietary fibre differing in lignin on performance, gut microbiology, and digestibility in weanling piglets," *Archives of Animal Nutrition*, vol. 62, no. 2, pp. 141–151, 2008.

[70] T. S. Nielsen, H. Jørgensen, K. E. B. Knudsen, and H. N. Lærke, "The microbial fermentation characteristics depend on both carbohydrate source and heat processing: a model experiment with ileo-cannulated pigs," *International Journal of Food Sciences and Nutrition*, vol. 68, no. 7, pp. 811–820, 2017.

[71] C. W. Huang, T. T. Lee, Y. C. Shih, and B. Yu, "Effects of dietary supplementation of Chinese medicinal herbs on polymorphonuclear neutrophil immune activity and small intestinal morphology in weanling pigs," *Journal of Animal Physiology and Animal Nutrition*, vol. 96, no. 2, pp. 285–294, 2012.

[72] W. Ren, P. Wang, J. Yan et al., "Melatonin alleviates weanling stress in mice: involvement of intestinal microbiota," *Journal of Pineal Research*, vol. 64, no. 2, Article ID e12448, 2018.

[73] J. Wang, L. Zeng, B. Tan et al., "Developmental changes in intercellular junctions and Kv channels in the intestine of piglets during the suckling and post-weaning periods," *Journal of Animal Science and Biotechnology*, vol. 7, no. 1, 2016.

[74] L. Montagne, G. Boudry, C. Favier, I. L. Huërou-Luron, J.-P. Lallès, and B. Sève, "Main intestinal markers associated with the changes in gut architecture and function in piglets after weaning," *British Journal of Nutrition*, vol. 97, no. 1, pp. 45–57, 2007.

[75] M. S. Hedemann, M. Eskildsen, H. N. Lærke et al., "Intestinal morphology and enzymatic activity in newly weaned pigs fed contrasting fiber concentrations and fiber properties1," *Journal of Animal Science*, vol. 84, no. 6, pp. 1375–1386, 2006.

[76] T. Fukunaga, M. Sasaki, Y. Araki et al., "Effects of the soluble fibre pectin on intestinal cell proliferation, fecal short chain fatty acid production and microbial population," *Digestion*, vol. 67, no. 1-2, pp. 42–49, 2003.

[77] S. B. J. A. KirkR. Mohammad et al., "Modulation of intestinal goblet cell function during infection by an attaching and effacing bacterial pathogen," *Infection and Immunity*, vol. 76, no. 2, pp. 796–811, 2008.

[78] H. N. T. ShingoS. Kei et al., "Small intestinal goblet cell proliferation induced by ingestion of soluble and insoluble dietary fiber is characterized by an increase in sialylated mucins in rats," *The Journal of Nutrition*, vol. 142, pp. 1429–1436, 2012.

[79] J. P. Raymond, S. Ghosh, and A. Mahmood, "Growth factors and trefoil peptides in gastrointestinal health and disease," *Current Opinion in Pharmacology*, vol. 4, no. 6, pp. 567–571, 2004.

[80] T. M. Holling, E. Schooten, and P. J. van Den Elsen, "Function and regulation of MHC class II molecules in T-lymphocytes: of mice and men," *Human Immunology*, vol. 65, no. 4, pp. 282–290, 2004.

[81] B. U. Metzler-Zebeli, S. Hooda, R. Pieper et al., "Nonstarch polysaccharides modulate bacterial microbiota, pathways for butyrate production, and abundance of pathogenic *Escherichia coli* in the pig gastrointestinal tract," *Applied and Environmental Microbiology*, vol. 76, no. 11, pp. 3692–3701, 2010.

[82] H. Chen, D. Chen, J. Michiels, and S. De Smet, "Dietary fiber affects intestinal mucosal barrier function by regulating intestinal bacteria in weaning piglets," *Communications in Agricultural and Applied Biological Sciences*, vol. 78, pp. 71–78, 2013.

[83] I. J. Wellock, P. D. Fortomaris, J. G. M. Houdijk, J. Wiseman, and I. Kyriazakis, "The consequences of non-starch polysaccharide solubility and inclusion level on the health and performance of weaned pigs challenged with enterotoxigenic *Escherichia coli*," *British Journal of Nutrition*, vol. 99, no. 3, pp. 520–530, 2008.

[84] H. L. Simpson and B. J. Campbell, "Review article: dietary fibre-microbiota interactions," *Alimentary Pharmacology & Therapeutics*, vol. 42, no. 2, pp. 158–179, 2015.

[85] P. M. W. P. BeckerA. J. Jansman et al., "Pea dietary fiber for adhesion and excretion of enterotoxigenic *E. coli* K88 to prevent intestinal colonization," *Journal of Animal Science*, vol. 87, pp. 172–189, 2009.

[86] R. Zhao, Y. Wang, Y. Huang et al., "Effects of fiber and probiotics on diarrhea associated with enteral nutrition in gastric cancer patients," *Medicine*, vol. 96, no. 43, p. e8418, 2017.

[87] A. Seidu, C. Dongsheng, Q. Guixin, J. Hailong, R. Han, and C. Tlotliso Sello, "Interactions of dietary fiber with nutritional components on gut microbial composition, function, and health in monogastrics," *Current Protein and Peptide Science*, vol. 19, no. 10, pp. 1011–1023, 2018.

[88] J. W. McRorie Jr. and N. M. McKeown, "Understanding the physics of functional fibers in the gastrointestinal tract: an evidence-based approach to resolving enduring misconceptions about insoluble and soluble fiber," *Journal of the Academy of Nutrition and Dietetics*, vol. 117, no. 2, pp. 251–264, 2017.

[89] K. Zhang, M. W. Hornef, and A. Dupont, "The intestinal epithelium as guardian of gut barrier integrity," *Cellular Microbiology*, vol. 17, no. 11, pp. 1561–1569, 2015.

[90] S. M. Curry, K. J. Schwartz, K. J. Yoon, N. K. Gabler, and E. R. Burrough, "Effects of porcine epidemic diarrhea virus infection on nursery pig intestinal function and barrier integrity," *Veterinary Microbiology*, vol. 211, pp. 58–66, 2017.

[91] B. P. Blackwood, C. Y. Yuan, D. R. Wood et al., "Integrity in experimental necrotizing enterocolitis," *Journal of Probiotics and Health*, vol. 5, 2017.

[92] M. C. Valenzano, K. DiGuilio, J. Mercado et al., "Remodeling of tight junctions and enhancement of barrier integrity of the CACO-2 intestinal epithelial cell layer by micronutrients," *PLoS One*, vol. 10, Article ID e0133926, 2015.

[93] R. C. Anderson, A. L. Cookson, W. C. McNabb et al., "Lactobacillus plantarum MB452 enhances the function of the intestinal barrier by increasing the expression levels of genes involved in tight junction formation," *BMC Microbiology*, vol. 10, no. 1, p. 316, 2010.

[94] M. Ogata, T. Ogita, H. Tari, T. Arakawa, and T. Suzuki, "Supplemental psyllium fibre regulates the intestinal barrier and inflammation in normal and colitic mice," *British Journal of Nutrition*, vol. 118, no. 9, pp. 661–672, 2017.

[95] T. Chen, C. Y. Kim, A. Kaur et al., "Dietary fibre-based SCFA mixtures promote both protection and repair of intestinal epithelial barrier function in a Caco-2 cell model," *Food and Function*, vol. 8, no. 3, pp. 1166–1173, 2017.

[96] H. J. Binder, "Mechanisms of diarrhea in inflammatory bowel diseases," *Annals of the New York Academy of Sciences*, vol. 1165, no. 1, pp. 285–293, 2009.

[97] R. D. Gill, *Mechanisms and Regulation of NaCl Absorption in the Human Intestine*, Research Signpost, Thiruvananthapuram, India, 2003.

[98] S. Priyamvada, R. Gomes, R. K. Gill, S. Saksena, W. A. Alrefai, and P. K. Dudeja, "Mechanisms underlying dysregulation of electrolyte absorption in inflammatory bowel disease-associated diarrhea," *Inflammatory Bowel Diseases*, vol. 21, no. 12, pp. 2926–2935, 2015.

[99] C. M. Surawicz, "Mechanisms of diarrhea," *Current Gastroenterology Reports*, vol. 12, no. 4, pp. 236–241, 2010.

[100] H. H. Wenzl, "Diarrhea in chronic inflammatory bowel diseases," *Gastroenterology Clinics of North America*, vol. 41, no. 3, pp. 651–675, 2012.

[101] K. M. Hoque, S. Chakraborty, I. A. Sheikh, and O. M. Woodward, "New advances in the pathophysiology of intestinal ion transport and barrier function in diarrhea and the impact on therapy," *Expert Review of Anti-infective Therapy*, vol. 10, no. 6, pp. 687–699, 2012.

[102] F. K. Ghishan and P. R. Kiela, "Small intestinal ion transport," *Current Opinion in Gastroenterology*, vol. 28, no. 2, pp. 130–134, 2012.

[103] J. Foulke-Abel, J. In, J. Yin et al., "Human enteroids as a model of upper small intestinal ion transport physiology and pathophysiology," *Gastroenterology*, vol. 150, no. 3, pp. 638–649e8, 2016.

[104] J. P. Geibel, V. M. Rajendran, and H. J. Binder, "Na+-dependent fluid absorption in intact perfused rat colonic crypts," *Gastroenterology*, vol. 120, no. 1, pp. 144–150, 2001.

[105] M. Donowitz, C. Ming Tse, and D. Fuster, "SLC9/NHE gene family, a plasma membrane and organellar family of Na^+/H^+ exchangers," *Molecular Aspects of Medicine*, vol. 34, no. 2-3, pp. 236–251, 2013.

[106] A. Kato and M. F. Romero, "Regulation of electroneutral NaCl absorption by the small intestine," *Annual Review of Physiology*, vol. 73, no. 1, pp. 261–281, 2011.

[107] P. R. Kiela, H. Xu, and F. K. Ghishan, "Apical NA^+/H^+ exchangers in the mammalian gastrointestinal tract," *Journal of Physiology and Pharmacology*, vol. 57, no. 7, pp. 51–79, 2006.

[108] M. D. Parker, E. J. Myers, and J. R. Schelling, "Na+-H+ exchanger-1 (NHE1) regulation in kidney proximal tubule," *Cellular and Molecular Life Sciences*, vol. 72, no. 11, pp. 2061–2074, 2015.

[109] P. G. Vallés, V. Bocanegra, A. Gil Lorenzo, and V. V. Costantino, "Physiological functions and regulation of the Na," *Kidney and Blood Pressure Research*, vol. 40, no. 5, pp. 452–466, 2015.

[110] A. Shawki, M. A. Engevik, R. S. Kim et al., "Intestinal brush-border Na+/H+ exchanger-3 drives H+-coupled iron absorption in the mouse," *American Journal of Physiology-Gastrointestinal and Liver Physiology*, vol. 311, pp. G423–G430, 2016.

[111] P. He, L. Zhao, L. Zhu et al., "Restoration of Na^+/H^+ exchanger NHE3-containing macrocomplexes ameliorates diabetes-associated fluid loss," *Journal of Clinical Investigation*, vol. 125, pp. 3519–3531, 2015.

[112] C. B. Larmonier, D. Laubitz, F. M. Hill et al., "Reduced colonic microbial diversity is associated with colitis in NHE3-deficient mice," *American Journal of Physiology-Gastrointestinal and Liver Physiology*, vol. 305, no. 10, pp. G667–G677, 2013.

[113] A. Kumar, P. Malhotra, H. Coffing et al., "Epigenetic modulation of intestinal Na(+)/H(+) exchanger-3 expression," *American Journal of Physiology-Gastrointestinal and Liver Physiology*, vol. 314, pp. G309–G318, 2018.

[114] R. L. Jakab, A. M. Collaco, and N. A. Ameen, "Characterization of CFTR high expresser cells in the intestine," *American Journal of Physiology-Gastrointestinal and Liver Physiology*, vol. 305, pp. G453–G465, 2013.

[115] K. Gholami, S. Muniandy, and N. Salleh, "In-vivo functional study on the involvement of CFTR, SLC26A6, NHE-1 and CA isoenzymes II and XII in uterine fluid pH, volume and electrolyte regulation in rats under different sex-steroid influence," *International Journal of Medical Sciences*, vol. 10, no. 9, pp. 1121–1134, 2013.

[116] W. Xia, Q. Yu, B. Riederer et al., "The distinct roles of anion transporters Slc26a3 (DRA) and Slc26a6 (PAT-1) in fluid and electrolyte absorption in the murine small intestine," *Pflügers Archiv: European Journal of Physiology*, vol. 466, pp. 1541–1556, 2014.

[117] J. Malakooti, S. Saksena, R. K. Gill, and P. K. Dudeja, "Transcriptional regulation of the intestinal luminal Na(+) and Cl(–) transporters," *Biochemical Journal*, vol. 435, pp. 313–325, 2011.

[118] S. L. Alper and A. K. Sharma, "The SLC26 gene family of anion transporters and channels," *Molecular Aspects of Medicine*, vol. 34, no. 2-3, pp. 494–515, 2013.

[119] Q. Xie, R. Welch, A. Mercado, M. F. Romero, and D. B. Mount, "Molecular characterization of the murine Slc26a6 anion exchanger: functional comparison with Slc26a1," *American Journal of Physiology-Renal Physiology*, vol. 283, pp. F826–F838, 2002.

[120] S. Wedenoja, E. Pekansaari, P. Hoglund, S. Makela, C. Holmberg, and J. Kere, "Update on SLC26A3 mutations in congenital chloride diarrhea," *Human Mutation*, vol. 32, no. 7, pp. 715–722, 2011.

[121] C. W. Schweinfest, D. D. Spyropoulos, K. W. Henderson et al., "slc26a3 (dra)-deficient mice display chloride-losing diarrhea, enhanced colonic proliferation, and distinct up-regulation of ion transporters in the colon," *Journal of Biological Chemistry*, vol. 281, no. 49, pp. 37962–37971, 2006.

[122] M. N. Chernova, L. Jiang, B. E. Shmukler et al., "Acute regulation of the SLC26A3 congenital chloride diarrhoea anion exchanger (DRA) expressed in *Xenopus* oocytes," *The Journal of Physiology*, vol. 549, no. 1, pp. 3–19, 2003.

[123] K. Gholami, S. Muniandy, and N. Salleh, "Progesterone downregulates oestrogen-induced expression of CFTR and SLC26A6 proteins and mRNA in rats' uteri," *Journal of Biomedicine and Biotechnology*, vol. 2012, p. 596084, 2012.

[124] M. W. Musch, D. L. Arvans, G. D. Wu, and E. B. Chang, "Functional coupling of the downregulated in adenoma Cl-/base exchanger DRA and the apical Na^+/H^+ exchangers NHE2 and NHE3," *American Journal of Physiology-Gastrointestinal and Liver Physiology*, vol. 296, pp. G202–G210, 2009.

[125] X. F. Wang, M. K. Yu, S. Y. Lam et al., "Expression, immunolocalization, and functional activity of Na^+/H^+ exchanger isoforms in mouse endometrial epithelium," *Biology of Reproduction*, vol. 68, pp. 302–308, 2003.

[126] V. J. Wheat, H. Shumaker, C. Burnham, G. E. Shull, J. R. Yankaskas, and M. Soleimani, "CFTR induces the expression of DRA along with Cl(–)/HCO(3)(–) exchange activity in tracheal epithelial cells," *American Journal of Physiology-Cell Physiology*, vol. 279, no. 1, pp. C62–C71, 2000.

[127] E. J. Joy, E. L. Ander, S. D. Young et al., "Dietary mineral supplies in Africa," *Physiologia Plantarum*, vol. 151, no. 3, pp. 208–229, 2014.

[128] Y. Liu, Y. L. Ma, J. M. Zhao, M. Vazquez-Anon, and H. H. Stein, "Digestibility and retention of zinc, copper, manganese, iron, calcium, and phosphorus in pigs fed diets containing inorganic or organic minerals," *Journal of Animal Science*, vol. 92, no. 8, pp. 3407–3415, 2014.

[129] R. A. Budde and T. D. Crenshaw, "Chronic metabolic acid load induced by changes in dietary electrolyte balance increased chloride retention but did not compromise bone in growing swine," *Journal of Animal Science*, vol. 81, no. 1, pp. 197–208, 2003.

[130] S. A. Guzman-Pino, D. Sola-Oriol, R. Davin, E. G. Manzanilla, and J. F. Perez, "Influence of dietary electrolyte balance on feed preference and growth performance of postweaned piglets," *Journal of Animal Science*, vol. 93, no. 6, pp. 2840–2848, 2015.

[131] Y. Dersjant-Li, M. W. Verstegen, A. Jansman, H. Schulze, J. W. Schrama, and J. A. Verreth, "Changes in oxygen content and acid-base balance in arterial and portal blood in response to the dietary electrolyte balance in pigs during a 9-h period after a meal," *Journal of Animal Science*, vol. 80, no. 5, pp. 1233–1239, 2002.

[132] L. N. Edwards, T. E. Engle, M. A. Paradis, J. A. Correa, and D. B. Anderson, "Persistence of blood changes associated with alteration of the dietary electrolyte balance in commercial pigs after feed withdrawal, transportation, and lairage, and the effects on performance and carcass quality," *Journal of Animal Science*, vol. 88, no. 12, pp. 4068–4077, 2010.

[133] J. F. Patience, R. E. Austic, and R. D. Boyd, "Effect of dietary electrolyte balance on growth and acid-base status in swine," *Journal of Animal Science*, vol. 64, no. 2, pp. 457–466, 1987.

[134] Y. Dersjant-Li, H. Schulze, J. W. Schrama, J. A. Verreth, and M. W. Verstegen, "Feed intake, growth, digestibility of dry matter and nitrogen in young pigs as affected by dietary cation-anion difference and supplementation of xylanase," *Journal of Animal Physiology and Animal Nutrition*, vol. 85, no. 3-4, pp. 101–109, 2001.

[135] P. G. Lawlor, P. B. Lynch, P. J. Caffrey, J. J. O'Reilly, and M. K. O'Connell, "Measurements of the acid-binding capacity of ingredients used in pig diets," *Irish Veterinary Journal*, vol. 58, pp. 447–452, 2005.

[136] T. Suzuki, "Regulation of intestinal epithelial permeability by tight junctions," *Cellular and Molecular Life Sciences*, vol. 70, no. 4, pp. 631–659, 2013.

[137] V. K. Viswanathan, K. Hodges, and G. Hecht, "Enteric infection meets intestinal function: how bacterial pathogens cause diarrhoea," *Nature Reviews Microbiology*, vol. 7, no. 2, pp. 110–119, 2009.

[138] M. H. Farahat, E. I. Hassanein, W. M. Abdel-Razik, and S. L. Noll, "Effect of dietary corn dried distillers grains with solubles, canola meal, and chloride on electrolyte balance, growth performance, and litter moisture of growing turkeys," *Poultry Science*, vol. 92, no. 5, pp. 1254–1265, 2013.

[139] L. J. Magnoni, E. Salas-Leiton, M. J. Peixoto et al., "Dietary electrolyte balance affects growth performance, amylase activity and metabolic response in the meagre (Argyrosomus regius)," *Comparative Biochemistry and Physiology Part B: Biochemistry and Molecular Biology*, vol. 211, pp. 8–15, 2017.

[140] S. Wedenoja, P. Hoglund, and C. Holmberg, "Review article: the clinical management of congenital chloride diarrhoea," *Alimentary Pharmacology and Therapeutics*, vol. 31, no. 4, pp. 477–485, 2010.

[141] D. S. Merrell, S. M. Butler, F. Qadri et al., "Host-induced epidemic spread of the cholera bacterium," *Nature*, vol. 417, pp. 642–645, 2002.

[142] S. M. Butler, E. J. Nelson, N. Chowdhury, S. M. Faruque, S. B. Calderwood, and A. Camilli, "Cholera stool bacteria repress chemotaxis to increase infectivity," *Molecular Microbiology*, vol. 60, no. 2, pp. 417–426, 2006.

[143] J. A. S. Guttman, F. N. Samji, Y. Li, W. Deng, A. Lin, and B. Brett Finlay, "Aquaporins contribute to diarrhoea caused by attaching and effacing bacterial pathogens," *Cellular Microbiology*, vol. 9, pp. 131–141, 2007.

[144] R. K. Buddington, P. T. Sangild, B. Hance, E. Y. Huang, and D. D. Black, "Prenatal gastrointestinal development in the pig and responses after preterm birth," *Journal of Animal Science*, vol. 90, no. 4, pp. 290–298, 2012.

[145] G. Boudry, E. S. David, V. Douard, I. M. Monteiro, I. Le Huerou-Luron, and R. P. Ferraris, "Role of intestinal transporters in neonatal nutrition: carbohydrates, proteins, lipids, minerals, and vitamins," *Journal of Pediatric Gastroenterology and Nutrition*, vol. 51, no. 4, pp. 380–401, 2010.

[146] W. F. Stenson, "Postnatal growth in the intestine," *Current Opinion in Gastroenterology*, vol. 29, no. 2, pp. 107–111, 2013.

[147] O. Adeola and D. E. King, "Developmental changes in morphometry of the small intestine and jejunal sucrase activity during the first nine weeks of postnatal growth in pigs," *Journal of Animal Science*, vol. 84, no. 1, pp. 112–118, 2006.

[148] A. F. Hofmann, V. Loening-Baucke, J. E. Lavine et al., "Altered bile acid metabolism in childhood functional constipation: inactivation of secretory bile acids by sulfation in a subset of patients," *Journal of Pediatric Gastroenterology and Nutrition*, vol. 47, no. 5, pp. 598–606, 2008.

[149] M. Kim, L. Friesen, J. Park, H. M. Kim, and C. H. Kim, "Microbial metabolites, short-chain fatty acids, restrain tissue bacterial load, chronic inflammation, and associated cancer in the colon of mice," *European Journal of Immunology*, vol. 48, no. 7, pp. 1235–1247, 2018.

[150] E. Prince and G. J. Fuchs, "1.3.6 Fluid and electrolytes. 1.3 Nutritional needs," *World Review of Nutrition and Dietetics*, vol. 113, pp. 56–61, 2015.

[151] R. N. Appleby and J. R. Walters, "The role of bile acids in functional GI disorders," *Neurogastroenterology and Motility*, vol. 26, no. 8, pp. 1057–1069, 2014.

[152] J. M. Ridlon, D. J. Kang, P. B. Hylemon, and J. S. Bajaj, "Gut microbiota, cirrhosis, and alcohol regulate bile acid metabolism in the gut," *Digestive Diseases*, vol. 33, no. 3, pp. 338–345, 2015.

[153] L. Bishop, "Nutritional tips for managing electrolyte imbalances in post-renal transplant patients," *Journal of Renal Nutrition*, vol. 22, no. 4, pp. e37–e38, 2012.

[154] S. Saravanan, I. Geurden, Z. G. Orozco, S. J. Kaushik, J. A. Verreth, and J. W. Schrama, "Dietary electrolyte balance affects the nutrient digestibility and maintenance energy expenditure of Nile tilapia," *British Journal of Nutrition*, vol. 110, no. 11, pp. 1948–1957, 2013.

[155] C. Fusch and F. Jochum, "Water, sodium, potassium and chloride," in *World Rev Nutr Diet*, vol. 110, pp. 99–120, 2014.

[156] J. Wiseman, "Variations in starch digestibility in non-ruminants," *Animal Feed Science and Technology*, vol. 130, no. 1-2, pp. 66–77, 2006.

[157] C. Souza da Silva, D. Haenen, S. J. Koopmans et al., "Effects of resistant starch on behaviour, satiety-related hormones

and metabolites in growing pigs," *Animal*, vol. 8, pp. 1402–1411, 2014.

[158] Y. Li, A. R. Zhang, H. F. Luo et al., "In vitro and in vivo digestibility of corn starch for weaned pigs: effects of amylose:amylopectin ratio, extrusion, storage duration, and enzyme supplementation," *Journal of Animal Science*, vol. 93, no. 7, pp. 3512–3520, 2015.

[159] Y. M. Lim, P. Hoobin, D. Ying, I. Burgar, P. R. Gooley, and M. A. Augustin, "Physical characterisation of high amylose maize starch and acylated high amylose maize starches," *Carbohydrate Polymers*, vol. 117, pp. 279–285, 2015.

[160] S. Liu, F. Ren, L. Zhao et al., "Starch and starch hydrolysates are favorable carbon sources for bifidobacteria in the human gut," *BMC Microbiology*, vol. 15, no. 1, p. 54, 2015.

[161] Z. Zhou, Y. Zhang, P. Zheng, X. Chen, and Y. Yang, "Starch structure modulates metabolic activity and gut microbiota profile," *Anaerobe*, vol. 24, pp. 71–78, 2013.

[162] M. Miao, B. Jiang, S. W. Cui, T. Zhang, and Z. Jin, "Slowly digestible starch–a review," *Critical Reviews in Food Science and Nutrition*, vol. 55, no. 12, pp. 1642–1657, 2015.

[163] S. Y. You, S. K. Oh, H. S. Kim, and H. J. Chung, "Influence of molecular structure on physicochemical properties and digestibility of normal rice starches," *International Journal of Biological Macromolecules*, vol. 77, pp. 375–382, 2015.

[164] L. B. Bindels, J. Walter, and A. E. Ramer-Tait, "Resistant starches for the management of metabolic diseases," *Current Opinion in Clinical Nutrition and Metabolic Care*, vol. 18, no. 6, pp. 559–565, 2015.

[165] M. J. Keenan, J. Zhou, M. Hegsted et al., "Role of resistant starch in improving gut health, adiposity, and insulin resistance," *Advances in Nutrition*, vol. 6, no. 2, pp. 198–205, 2015.

[166] S. A. Zaman and S. R. Sarbini, "The potential of resistant starch as a prebiotic," *Critical Reviews in Biotechnology*, vol. 36, pp. 578–584, 2016.

[167] D. F. Birt, T. Boylston, S. Hendrich et al., "Resistant starch: promise for improving human health," *Advances in Nutrition*, vol. 4, no. 6, pp. 587–601, 2013.

[168] B. Svihus, "Starch digestion capacity of poultry," *Poultry Science*, vol. 93, no. 9, pp. 2394–2399, 2014.

[169] S. K. Bhandari, C. M. Nyachoti, and D. O. Krause, "Raw potato starch in weaned pig diets and its influence on postweaning scours and the molecular microbial ecology of the digestive tract," *Journal of Animal Science*, vol. 87, no. 3, pp. 984–993, 2009.

[170] A. M. V. Perera and R. T. Tyler, "Resistant starch: a review of analytical protocols for determining resistant starch and of factors affecting the resistant starch content of foods," *Food Research International*, vol. 43, no. 8, pp. 1959–1974, 2010.

[171] J. S. Al-Rabadi, R. G. Gilbert, and M. J. Gidley, "Effect of particle size on kinetics of starch digestion in milled barley and sorghum grains by porcine alpha-amyla-se," *Journal of Cereal Science*, vol. 50, no. 2, pp. 198–204, 2009.

[172] M. K. M. Leeman, A. C. Eliasson, and I. Bjorck, "Resistant starch formation in temperature treated potato starches varying in amylose/amylopectin ratio," *Carbohydrate Polymers*, vol. 65, no. 3, pp. 306–313, 2006.

[173] A. A. Alsaffar, "Effect of thermal processing and storage on digestibility of starch in whole wheat grains," *Journal of Cereal Science*, vol. 52, no. 3, pp. 480–485, 2010.

[174] K. Lange, F. Hugenholtz, M. C. Jonathan et al., "Comparison of the effects of five dietary fibers on mucosal transcriptional profiles, and luminal microbiota composition and SCFA concentrations in murine colon," *Molecular Nutrition and Food Research*, vol. 59, pp. 1590–1602, 2015.

[175] D. Haenen, J. Zhang, C. Souza da Silva et al., "A diet high in resistant starch modulates microbiota composition, SCFA concentrations, and gene expression in pig intestine," *The Journal of Nutrition*, vol. 143, no. 3, pp. 274–283, 2013.

[176] E. Puertollano, S. Kolida, and P. Yaqoob, "Biological significance of short-chain fatty acid metabolism by the intestinal microbiome," *Current Opinion in Clinical Nutrition and Metabolic Care*, vol. 17, no. 2, pp. 139–144, 2014.

[177] C. S. Byrne, E. S. Chambers, D. J. Morrison, and G. Frost, "The role of short chain fatty acids in appetite regulation and energy homeostasis," *International Journal of Obesity*, vol. 39, no. 9, pp. 1331–1338, 2015.

[178] T. C. Rideout, Q. Liu, P. Wood, and M. Z. Fan, "Nutrient utilisation and intestinal fermentation are differentially affected by the consumption of resistant starch varieties and conventional fibres in pigs," *British Journal of Nutrition*, vol. 99, no. 5, pp. 984–992, 2008.

[179] O. C. Umu, J. A. Frank, J. U. Fangel et al., "Resistant starch diet induces change in the swine microbiome and a predominance of beneficial bacterial populations," *Microbiome*, vol. 3, no. 1, p. 16, 2015.

[180] R. G. Crittenden, L. F. Morris, M. L. Harvey, L. T. Tran, H. L. Mitchell, and M. J. Playne, "Selection of a Bifidobacterium strain to complement resistant starch in a synbiotic yoghurt," *Journal of Applied Microbiology*, vol. 90, no. 2, pp. 268–278, 2001.

[181] I. Figueroa-Gonzalez, G. Quijano, G. Ramirez, and A. Cruz-Guerrero, "Probiotics and prebiotics–perspectives and challenges," *Journal of the Science of Food and Agriculture*, vol. 91, no. 8, pp. 1341–1348, 2011.

[182] A. R. Bird, M. A. Conlon, C. T. Christophersen, and D. L. Topping, "Resistant starch, large bowel fermentation and a broader perspective of prebiotics and probiotics," *Beneficial Microbes*, vol. 1, no. 4, pp. 423–431, 2010.

[183] W. Wu, J. Xie, and H. Zhang, "Dietary fibers influence the intestinal SCFAs and plasma metabolites profiling in growing pigs," *Food and Function*, vol. 7, no. 11, pp. 4644–4654, 2016.

[184] J. M. Heo, A. K. Agyekum, Y. L. Yin, T. C. Rideout, and C. M. Nyachoti, "Feeding a diet containing resistant potato starch influences gastrointestinal tract traits and growth performance of weaned pigs," *Journal of Animal Science*, vol. 92, no. 9, pp. 3906–3913, 2014.

[185] E. G. Manzanilla, M. Nofrarias, M. Anguita et al., "Effects of butyrate, avilamycin, and a plant extract combination on the intestinal equilibrium of early-weaned pigs," *Journal of Animal Science*, vol. 84, no. 10, pp. 2743–2751, 2006.

[186] E. Hijova and A. Chmelarova, "Short chain fatty acids and colonic health," *Bratisl Lek Listy*, vol. 108, pp. 354–358, 2007.

[187] D. L. Topping and P. M. Clifton, "Short-chain fatty acids and human colonic function: roles of resistant starch and non-starch polysaccharides," *Physiological Reviews*, vol. 81, no. 3, pp. 1031–1064, 2001.

[188] T. S. Nielsen, P. K. Theil, S. Purup, N. P. Norskov, and K. E. Bach knudsen, "Effects of resistant starch and arabinoxylan on parameters related to large intestinal and metabolic health in pigs fed fat-rich diets," *Journal of Agricultural and Food Chemistry*, vol. 63, no. 48, pp. 10418–10430, 2015.

[189] J. L. Slavin, "Carbohydrates, dietary fiber, and resistant starch in white vegetables: links to health outcomes," *Advances in Nutrition*, vol. 4, no. 3, pp. 351S–355S, 2013.

[190] D. Subaric, D. Ackar, J. Babic, and B. Milicevic, "Starch for health," *Medicinski Glasnik*, vol. 9, pp. 17–22, 2012.

[191] J. M. Wong, R. de Souza, C. W. Kendall, A. Emam, and D. J. Jenkins, "Colonic health: fermentation and short chain fatty acids," *Journal of Clinical Gastroenterology*, vol. 40, no. 3, pp. 235–243, 2006.

[192] R. L. Ordonio and M. Matsuoka, "Increasing resistant starch content in rice for better consumer health," *Proceedings of the National Academy of Sciences*, vol. 113, no. 45, pp. 12616–12618, 2016.

[193] X. He, W. Sun, T. Ge, C. Mu, and W. Zhu, "An increase in corn resistant starch decreases protein fermentation and modulates gut microbiota during in vitro cultivation of pig large intestinal inocula," *Animal Nutrition*, vol. 3, no. 3, pp. 219–224, 2017.

[194] H. Yan, R. Potu, H. Lu et al., "Dietary fat content and fiber type modulate hind gut microbial community and metabolic markers in the pig," *PLoS One*, vol. 8, Article ID e59581, 2013.

[195] X. Zhao, Y. Xian, C. Li et al., "Feeding Lactobacillus plantarum and Lactobacillus casei increased microbial diversity and short chain fatty acids production in the gut-intestinal tract of weaning piglets," *Wei Sheng Wu Xue Bao*, vol. 56, pp. 1291–1300, 2016.

[196] V. Rosenfeldt, K. F. Michaelsen, M. Jakobsen et al., "Effect of probiotic Lactobacillus strains in young children hospitalized with acute diarrhea," *The Pediatric Infectious Disease Journal*, vol. 21, no. 5, pp. 411–416, 2002.

[197] P. Janczyk, R. Pieper, H. Smidt, and W. B. Souffrant, "Changes in the diversity of pig ileal lactobacilli around weaning determined by means of 16S rRNA gene amplification and denaturing gradient gel electrophoresis," *FEMS Microbiology Ecology*, vol. 61, no. 1, pp. 132–140, 2007.

[198] J. A. Higgins, "Resistant starch and energy balance: impact on weight loss and maintenance," *Critical Reviews in Food Science and Nutrition*, vol. 54, no. 9, pp. 1158–1166, 2014.

[199] L. A. Bello-Perez, P. C. Flores-Silva, E. Agama-Acevedo, and J. Tovar, "Starch digestibility: past, present, and future," *Journal of the Science of Food and Agriculture*, 2018.

Hindawi
BioMed Research International
Volume 2019, Article ID 8348430, 8 pages
https://doi.org/10.1155/2019/8348430

Research Article

The Protective Effect of Bosentan against Atherosclerosis in Apolipoprotein E-Deficient Mice Is Mediated by miRNA-21

Xiaona Xu, Zhiqiang Zhao, and Guangping Li

Tianjin Key Laboratory of Ionic-Molecular Function of Caidiovascular Disease, Department of Cardiology, Tianjin Instiute of Cardiology, The Second Hospital of Tianjin Medical University, Tianjin 300211, China

Correspondence should be addressed to Guangping Li; tic_tjcardiol@126.com

Received 1 October 2019; Accepted 19 November 2019; Published 5 December 2019

Guest Editor: Deguang Song

Vascular calcification is an independent risk factor for plaque instability and is associated with endothelial cell function. Here, we investigated the role of endothelial cell function in the calcification of atherosclerotic plaques. We hypothesized that atherosclerosis would be associated with endothelial dysfunction and that bosentan (Tracleer®), a dual endothelin-receptor antagonist, would preserve endothelial cell function in an apolipoprotein E-deficient ($ApoE^{-/-}$) mouse model of atherosclerosis. Accordingly, 4–6-week-old $ApoE^{-/-}$ mice were fed a high-fat diet and treated with bosentan, and the effects of this treatment on body weight and blood lipid concentrations was evaluated. Endothelial damage in the aortic arch was assessed immunohistochemically to detect the proapoptotic proteins PDCD4, caspase-3, and Bax and the antiapoptotic protein Bcl-2. Notably, bosentan treatment was associated with decreased concentrations of these proteins and of blood lipids in $ApoE^{-/-}$ mice. Consistent with these findings, we observed increased concentrations of miRNA-21 and PDCD4 mRNA expression in the aortic arch endothelium after bosentan treatment. We conclude that bosentan can prevent endothelial cell death and protect against atherosclerosis in ApoE-deficient mice by upregulating miRNA-21.

1. Introduction

The pathobiology of atherosclerosis is characterized by the failure or malfunction of endothelial cells [1, 2], particularly in lesion-prone areas of the endothelial lining of the arterial vasculature. This lining interacts with the circulating blood and acts as an important transducer of mechanical and humoral signals [3–5]. In response to these signals [2, 6], vascular endothelial cells maintain vascular homeostasis via paracrine and autocrine mechanisms [7]. These interactions create a pathological risk of atherosclerosis, as phenotypic changes in the endothelium can lead to dysfunction. Moreover, the development of new drugs and treatments for atherosclerosis requires a more in-depth understanding of the endothelial biology of atherosclerosis [8].

MicroRNAs (miRNAs) comprise a broad class of small noncoding RNAs that modulate the expression of complementary target genes [9–13]. Dysfunction of miRNAs is associated with multiple pathological processes, including atherosclerotic vascular disease [14, 15]. Recent studies have confirmed that miRNA-21 is expressed in endothelial cells, macrophages, and smooth muscle cells [1, 16–18] and have identified a crucial role of this miRNA in the progression of diseases such as cancer and cardiovascular diseases [2, 16]. Furthermore, the importance of endothelial cells to atherosclerosis suggests that the expression of miRNA-21 in these cells may also contribute to the progression of disease. However, few previous studies have analyzed miRNA-21 expression patterns in atherosclerosis-related tissues.

Programmed cell death 4 (PDCD4) was recently identified as an important functional target of miRNA-21 [19, 20]. According to previous work, this protein acts as a tumor suppressor [21] and is upregulated during apoptosis. However, it remains unclear how miRNA-21 [22] regulates the specific and potentially pathological activities of PDCD4, such as proliferation and apoptosis. Therefore, clarification of the role of miRNA-21 (and other miRNAs) and its target PDCD4 in atherosclerosis is urgently needed. In this study,

we generated an animal model of atherosclerosis by raising apolipoprotein E-deficient ($ApoE^{-/-}$) mice on a high-fat diet and investigated the expression of miRNA-21 and its target PDCD4 during the progression of atherosclerosis in these animals.

2. Materials and Methods

2.1. Animals. All animal experiments were approved by and conducted according to the guidelines of the Animal Care and Use Committee of the Second Hospital. Wild-type C57BL/6J mice were purchased from the Jackson Laboratory (Beijing, China). All animals were housed in plastic cages (four mice/cage) under a 12 h light/dark cycle with free access to water and food. Bosentan was purchased from Sigma-Aldrich (St. Louis, MO, USA). Mice were randomly divided into two experimental groups, $ApoE^{-/-}$ and $ApoE^{-/-}$ + bosentan, and one control group ($n = 10$/group). All mice were treated with a one-week period of adaptive feeding before the start of the experiment. Subsequently, the control group was fed a basal diet (Fukang Biotechnology Co., Ltd. Beijing, China), while the two experimental groups were fed a high-fat diet containing 10% lard, 8% egg yolk powder, 2% cholesterol, 0.2% bile salt, and 80% basal diet (Fukang Biotechnology Co., Ltd.). Mice in the $ApoE^{-/-}$ + bosentan group were administered with daily intragastric doses of bosentan (100 mg/kg body weight). Mice in the control and $ApoE^{-/-}$ groups were administered with daily doses of normal saline via intragastric administration. All mice were sacrificed by cervical dislocation at week 12 of the experiment.

2.2. Collection of Samples and Determination of Hematological Parameters. Mice from different groups were anesthetized with ether and sacrificed by cervical dislocation. Blood samples were collected and stored at −80°C for subsequent biochemical studies. The blood concentrations of triglycerides (TG), high-density lipoprotein cholesterol (HDL), low-density lipoprotein cholesterol (LDL), and total cholesterol (TC) were measured using an Auto Hematology analyzer (Olympus Corporation, Tokyo, Japan).

2.3. Histological and Immunohistochemical Staining. To prepare specimens for microscopic imaging, aortic sinus tissues were dehydrated in a series of increasing concentrations of alcohol and xylene and subsequently embedded in paraffin. Next, 8 μm-thick sections were cut from the central segments of the fixed tissues using a rotating microtome (Leica® RM 2145, Wetzlar, Germany) and mounted on SuperFrost Plus slides (ThermoFisher Scientific, Waltham, MA, USA). The aortic sinus sections were subjected to dewaxing and rehydration via consecutive immersion in xylene and graded ethanol solutions. Hematoxylin and eosin staining of the sections was performed according to standard methods. Immunohistochemical staining was performed as described by Kato et al. [23].

2.4. RNA Isolation and Quantitation. Total RNA was extracted from the aortic tissues and purified using TRIzol reagent (Invitrogen, Carlsbad, CA, USA). One microgram of total RNA per sample was then used in a quantitative polymerase chain reaction (qPCR) analysis. Reverse transcription was performed using the M-MLV Reverse Transcription system (Takara Co. Ltd., Dalian, China) under the following conditions: 42°C for 2 min, 95°C for 5 s, and 37°C for 15 min. The resulting cDNA was subjected to qPCR using the SYBR Green reagent (Takara Co. Ltd.) and an ABI 7500 quantitative PCR instrument (Applied Biosystems, Inc., Foster City, CA, USA) under the following conditions: pre-denaturation at 95°C for 10 min, followed by 35 cycles of denaturation at 95°C for 15 s, annealing at 60°C for 25 s, and extension at 72°C for 30 s. Three independent reactions were run per sample. The relative mRNA concentrations were calculated after normalization to the concentration of GAPDH mRNA expression (internal control). The following primers were used: mmu-miR-21-Fwd: 5′-GTCAGGC TAGCTTATCAGA-3′; U6-Fwd: 5′-CTCGCTTCGGCAGCACA-3′, U6-Reverse: 5′-GTATCCAGTGCAGGGTCCGAGGT-3′; PDCD4-Fwd: 5′-AGGTCGTCTTAAACCAGAGAG-3′, PDCD4-Reverse: 5′-ATGTCAGAAATGCCTTGTACC-3′, GAPDH-Fwd: 5′- TCAAGAAGGTGGTGAAGCA-3′, GAPDH-Reverse: 5′-GTCAAAGGTGGAGGAGTGG-3′.

2.5. Statistical Analysis. All statistical analyses were performed using Prism 8 software (GraphPad, Inc., La Jolla, CA, USA). All results are expressed as mean values ± standard deviations. A P value of <0.05 was considered to indicate statistical significance, and clear statistical differences are commonly indicated by asterisks in figures (e.g., $^{*}P < 0.05$). Student's t-test was used for comparisons of two groups. A one-way ANOVA and the Bonferroni posttest were used for comparisons of more than two groups.

3. Results

3.1. Histopathological Analysis of Atherosclerosis in $ApoE^{-/-}$ Mice Fed a High-Fat Diet. At week 12, mice from the control group and $ApoE^{-/-}$ groups were sacrificed, and the aortic sinus tissues were collected. The successful inclusion of atherosclerosis was shown in the $ApoE^{-/-}$ group. The $ApoE^{-/-}$ mice presented with features of typical atherosclerosis, such as a thin fibrous cap and the presence of foam cells and cholesterol crystals within the atherosclerotic plaque (Figure 1).

3.2. Bosentan Treatment Did Not Affect Blood Lipid Concentrations in $ApoE^{-/-}$ Mice. Mice in the $ApoE^{-/-}$ and bosentan-treated groups exhibited significantly larger gains in body weight relative to mice in the control group (Figure 1). Moreover, $ApoE^{-/-}$ mice exhibited a significantly greater weight gain than those in the bosentan-treated group (Table 1).

As shown in Table 2, a hematological analysis revealed lower concentrations of TG, HDL, LDL, and TC in the control group relative to the $ApoE^{-/-}$ group. These indices

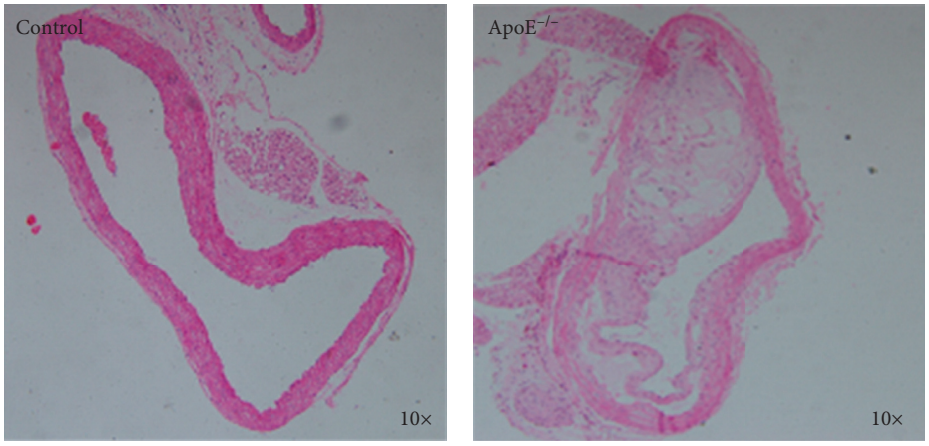

(a) (b)

Figure 1: Key histological features of tissue from an ApoE$^{-/-}$ mouse. Histological sections of aortic sinus tissues from control and ApoE$^{-/-}$ mice were stained with hematoxylin-eosin. ApoE$^{-/-}$ mice developed typical atherosclerosis of the aortic arteries in response to a high-fat diet.

Table 1: The body weights of mice in the control, ApoE$^{-/-}$, and bosentan groups at baseline and after 12 weeks of treatment.

Group	Number of animals	Body weight (g) At week 6	Body weight (g) At week 12
Control	10	15.98 ± 0.19	28.20 ± 0.82
ApoE$^{-/-}$	10	15.95 ± 0.29	33.62 ± 0.57*
ApoE$^{-/-}$ + bosentan	10	15.99 ± 0.20	32.04 ± 0.72$^{*\#}$

$^{*}P < 0.05$ vs. control group; $^{\#}P > 0.05$ vs. ApoE$^{-/-}$, group; $n = 10$/group.

Table 2: Effect of bosentan on the blood lipid concentrations in mice.

Group	n	Blood lipid concentrations (mmol/L)			
		TG	TC	HDL	LDL
Control	10	0.556 ± 0.033	1.740 ± 0.071	1.242 ± 0.057	0.164 ± 0.018
ApoE$^{-/-}$	10	1.210 ± 0.129*	19.36 ± 1.892*	2.760 ± 0.246*	5.310 ± 0.560*
ApoE$^{-/-}$ + bosentan	10	1.520 ± 0.338$^{*\#}$	16.44 ± 1.032$^{*\#}$	2.554 ± 0.292$^{*\#}$	4.882 ± 0.329$^{*\#}$

$^{*}P < 0.05$, compared with the control group; $^{\#}P > 0.05$, compared with the ApoE$^{-/-}$ group; $n = 10$/group. TG, triglycerides; TC, total cholesterol; HDL, high-density lipoprotein; LDL, low-density lipoprotein.

differed significantly between the control group and bosentan group but not between the ApoE$^{-/-}$ and bosentan groups.

3.3. Histopathological Analysis of Atherosclerosis in ApoE$^{-/-}$ Mice Treated with Bosentan. At week 12, mice from the control, ApoE$^{-/-}$, and bosentan groups were sacrificed, and the aortic sinuses were collected. As noted above, HE staining revealed characteristic features of atherosclerosis in the aortic sinuses of ApoE$^{-/-}$ mice. Notably, although typical atherosclerosis was observed in the bosentan group, these mice had significantly smaller atherosclerotic plaques than those observed in the ApoE$^{-/-}$ mice (Figure 2). The observations suggested that bosentan played a protective role against atherosclerosis in ApoE$^{-/-}$ mice raised on a high-fat diet.

3.4. Bosentan Treatment Reduced the Population of PDCD4-Positive Cells in ApoE$^{-/-}$ Mice. We further investigated the expression of PDCD4, a proapoptotic protein, in aortic sinus sections from the three groups of mice. Immunohistochemistry staining of the aortic sinus sections for PDCD4 revealed a significantly larger population of PDCD4-positive cells in ApoE$^{-/-}$ mice compared to the control group (Figure 3). Interestingly, although more PDCD4-positive cells were observed in the bosentan-treated group relative to the control group, this cell population was significantly smaller in the bosentan-treated group relative to the ApoE$^{-/-}$ group (Figure 3). Accordingly, it appeared that bosentan might have reversed the endothelial cell death induced by a high-fat diet in ApoE$^{-/-}$ mice.

3.5. Bosentan Treatment Reduced Caspase-3 and Bax Expression and Increased Bcl-2 Expression in the Aortic Sinuses of ApoE$^{-/-}$ Mice. To further confirm the antiapoptotic role of bosentan in the vascular endothelial cells of ApoE$^{-/-}$ mice fed a high-fat diet, we performed immunohistochemistry staining to detect caspase-3 (a downstream effector of Bcl proteins in

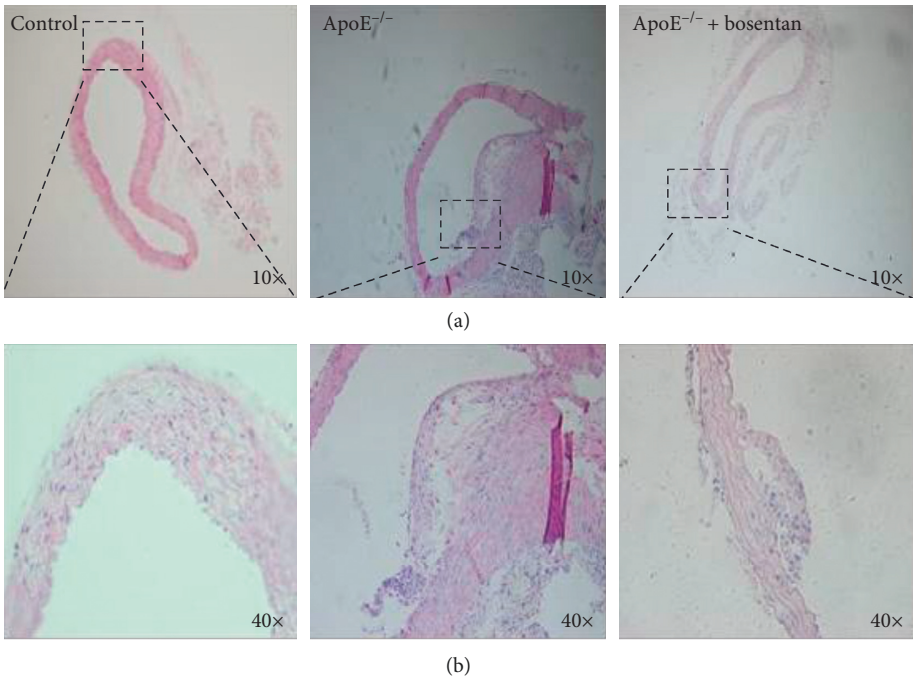

Figure 2: Treatment with bosentan reduced atherosclerotic plaque formation in ApoE$^{-/-}$ mice. (a) Hematoxylin-eosin staining of atherosclerotic plaques in bosentan-treated ApoE$^{-/-}$ mice. T atherosclerotic plaques contained fewer foam cells and cholesterol crystals than those from untreated mice (magnification: 10X). (b) Enlarged sectional areas of plaques in the control, ApoE$^{-/-}$, and bosentan groups (magnification: 40X).

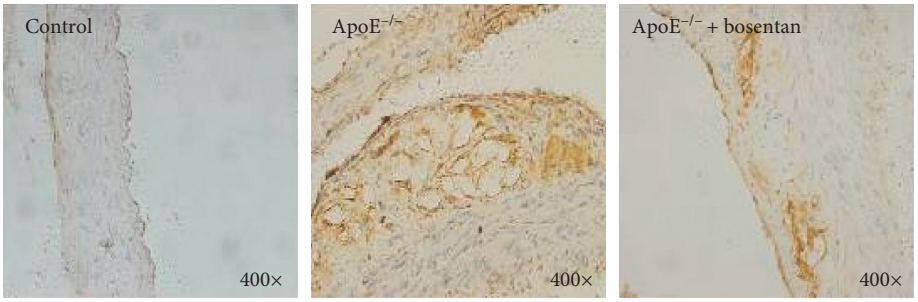

Figure 3: Bosentan treatment reduced PDCD4 expression in aortic sinus tissues from ApoE$^{-/-}$ mice. Immunohistochemistry staining for PDCD4 in atherosclerotic plaques from the indicated groups of mice.

the apoptotic cascade), Bax (a proapoptotic Bcl family member), and Bcl-2 (an antiapoptotic Bcl family member) in the aortic sinus tissues. As expected, we observed increases in caspase-3 and Bax positivity in the aortic sinuses from the ApoE$^{-/-}$ group relative to the control group. In contrast, bosentan treatment significantly reduced the concentrations of caspase-3 and Bax in the atherosclerotic plaques of ApoE$^{-/-}$ mice (Figures 4 and 5). More importantly, mice in the ApoE$^{-/-}$ group exhibited higher Bcl-2 concentrations in the aortic sinus when compared with control mice, whereas bosentan treatment significantly increased the expression of Bcl-2 in the atherosclerotic plaques (Figure 6).

3.6. Bosentan Treatment Enhanced miRNA-21 Expression and Decreased PDCD4 mRNA Expression in ApoE$^{-/-}$ Mice. MiRNA-21 targets the gene encoding PDCD4. Therefore, we next investigated the expression of miRNA-21 and PDCD4 mRNA in the aortic sinus. As shown in Figure 7, we observed a decreased concentration of miRNA-21 expression in the ApoE$^{-/-}$ group relative to the control group, whereas bosentan treatment significantly increased the expression and resultant concentration of miRNA-21. Consistent with the immunohistochemistry data, we also observed a significant increase in the expression of PDCD4 mRNA in the ApoE$^{-/-}$ group relative to the control group, whereas bosentan treatment induced a dramatic decrease in PDCD4 expression (Figure 8). Our data suggest that the anti-apoptotic effect of bosentan on endothelial cells may be mediated by miRNA-21.

4. Discussion

The Tampere Vascular Study [24] recently completed a series of miRNA expression profiles in human tissues. This study

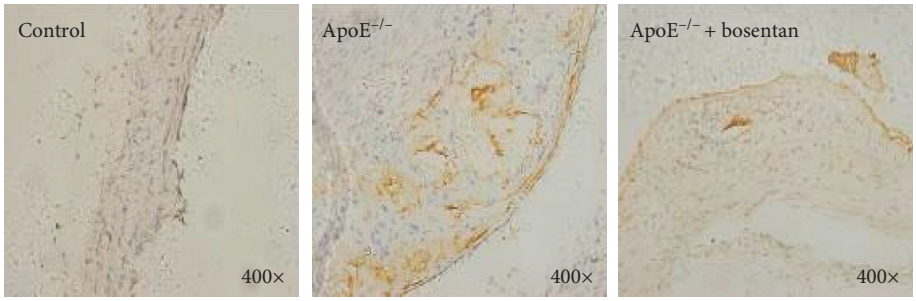

Figure 4: Bosentan reduced caspase-3 expression in the aortic sinuses of ApoE$^{-/-}$ mice. Immunohistochemistry staining for caspase-3 in atherosclerotic plaques from the indicated groups of mice.

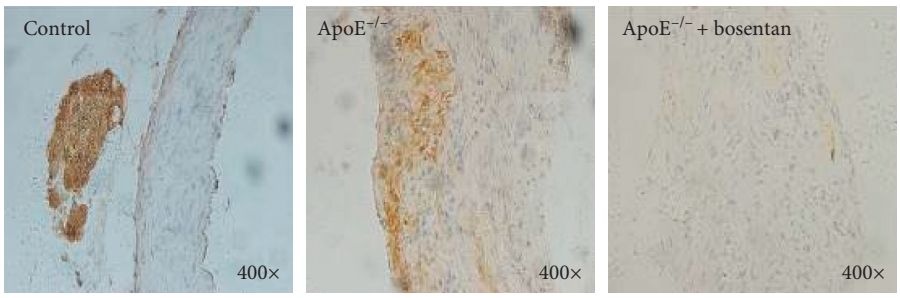

Figure 5: Bosentan reduced Bax expression in the aortic sinuses of ApoE$^{-/-}$ mice. Immunohistochemistry staining for Bax in atherosclerotic plaques from the indicated groups of mice.

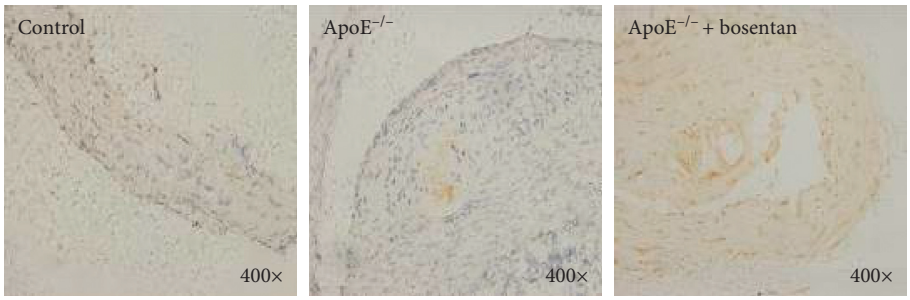

Figure 6: Bosentan increased Bcl-2 expression in the aortic sinuses of ApoE$^{-/-}$ mice. Immunohistochemistry staining for Bcl-2 in atherosclerotic plaques from the indicated groups of mice.

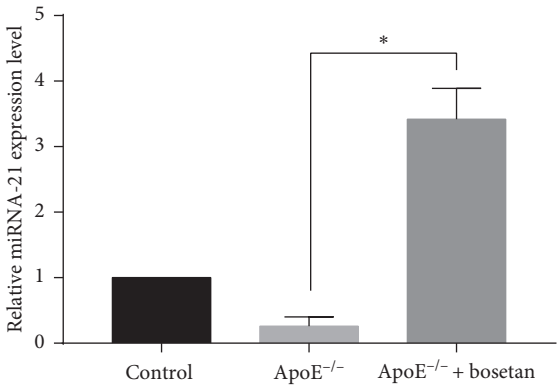

Figure 7: Bosentan enhanced the expression of miRNA-21 in ApoE$^{-/-}$ mice. A real-time qPCR analysis of miRNA-21 expression in atherosclerotic plaque from the indicated groups of mice. The miRNA abundance in each group was normalized to U6 RNA (internal control).

of femoral atherosclerotic, aortic, and carotid arteries acquired 12 atherosclerotic plaques and determined that miRNA-21 was the most strongly detected miRNA in the femoral artery samples. Notably, significant increases in miRNAs-21, -34a, and -210 were observed in the carotid artery samples relative to the control. The atherosclerosis-related functions of miRNA-21 are known to be associated with the inhibition of matrix metalloproteinases (MMPs) and the proliferation of vascular smooth muscle cells (VSMCs) [25]. Previous reports described the prominent role of miRNA-21 in VSMC proliferation [26, 27]. Moreover, the genetic and pharmacological inhibition of miRNA-21 expression was shown to significantly reduce the incidence of balloon-induced neointimal carotid artery injuries [20]. These findings have stimulated research exploring the manipulation of miRNA-21 expression as a possible local therapeutic strategy. However, the molecular mechanism by which bosentan regulates miRNA-21 remains

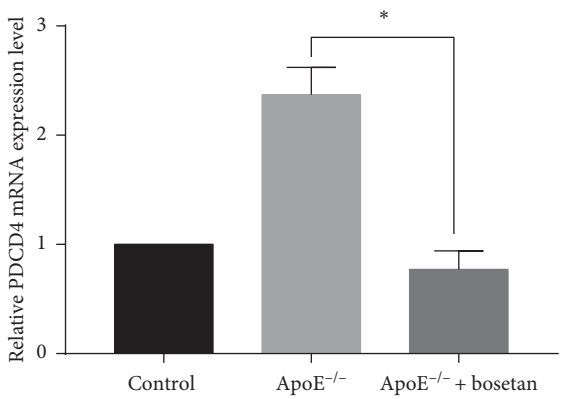

Figure 8: Bosentan reduced the expression of PDCD4 mRNA in ApoE$^{-/-}$ mice. A real-time qPCR analysis of PDCD4 mRNA expression in atherosclerotic plaques from the indicated groups of mice.

unclear and requires further investigation. In this study, we demonstrated that bosentan may be an effective treatment in patients with atherosclerosis, particularly as this drug led to major reductions in the atherosclerosis plaques of ApoE-deficient mice *in vivo*. This effect was likely attributable to the miRNA-21-mediated upregulation of antiapoptotic Bcl-2 and the downregulation of PDCD4 and the downstream proapoptotic effectors caspase-3 and Bax, resulting in a net antiapoptotic outcome.

Atherosclerosis, a major risk factor for coronary heart disease, is caused by the accumulation of cholesterol, macrophages, and cellular waste products (e.g., calcium and fatty materials) on artery walls. These deposits increase the thickness of the affected artery wall and can radically restrict blood flow [28, 29]. These physiological changes are associated with the pathology of atherosclerosis [30], wherein lipoproteins transport lipids in the blood and deposit these substances on arterial walls. Notably, we observed significant increases in the concentrations of TC, TG, and non-HDL-C and in the sizes of atherosclerotic lesion areas in ApoE$^{-/-}$ mice fed a high-fat diet, compared to mice fed a basal chow diet [28]. These phenomena indicated that dysregulation occurs in the sphingolipid and glycerophospholipid metabolic pathways during atherosclerotic dyslipidemia [31]. Moreover, we observed significant increases in the serum TG, TC, LDL, and HDL concentrations in both the bosentan and ApoE$^{-/-}$ groups relative to the control group. These data strongly suggested that certain dietary factors, such as high-fat diets, can enhance the development of atherosclerosis.

PDCD4 has been associated with biological processes such as inflammation and apoptosis [32, 33]. Notably, endothelial damage and dysfunction are the primary factors underlying atherosclerotic changes. In a previous study, PDCD4 deficiency greatly enhanced the ability of oxidized LDL to impair the autophagy efflux, which prevented the differentiation of macrophages to foam cells [34]. Another study determined that the downregulation of PDCD4 expression in the diseased vascular wall could cause an imbalance between VSMC apoptosis and proliferation, suggesting that PDCD4 may be a therapeutic target for proliferative vascular disease [35]. In atherosclerosis, PDCD4, as a target of miR-16, may inhibit the activation of inflammatory macrophages via the mitogen-activated protein kinase (MAPK) and NF-κB and signaling pathways, suggesting that PDCD4 could be a focus of atherosclerosis therapy [36].

The apoptosis-related protease caspase-4 has been identified in atherosclerotic plaques [37], whereas active caspase-3 was not detected in the neointima of normolipidemic animals after arterial injury [38]. In another study of caspase-3 expression, overexpression of the miRNA has-let-7 g was identified as key to the negative regulation of apoptosis in EAhy926 endothelial cells [39]. In apoptotic cells, morphological features such as DNA cleavage, nuclear condensation, and plasma membrane blebbing are blocked directly by Bcl-2, a negative regulator of cell death [40]. Bcl-2 is involved in cell survival and inhibits cell death in response to chemotherapeutic agents and stimuli such as ethanol and heat shock. In our study, we observed fewer PDCD4–, caspase-3–, and Bax-positive cells and more Bcl-2-positive cells in bosentan-treated mice relative to ApoE$^{-/-}$ mice.

Significant recent findings have revealed the important roles of endogenous inhibitors of gene expression in cardiovascular diseases, including atherosclerosis. Most previous reports have described the roles of these inhibitors in cancer, with some of these inhibitors being miRNAs, i.e., small (~22 nt) RNA sequences that regulate and alter gene expression at the posttranscriptional level [41, 42]. The functions of macrophages, endothelial cells, and VSMCs are controlled by miRNAs, which thereby regulate the progression of atherosclerosis [43]. Smooth muscle cell differentiation is controlled by the downregulation of miRNA-145, and this process also promotes the formation of lesions [44]. Furthermore, the transfer of miRNA-126 from apoptotic endothelial cells to microbubbles signals a need for cellular repair [45]. Atherosclerotic lesions and inflammatory macrophages signify the presence of increased concentrations of miR-155 [45]. A previous study identified miR-145 as the most abundant miRNA in differentiated VSMCs. However, this miRNA is rapidly downregulated in subcultured dedifferentiated VSMCs, although its expression in these cells can be stimulated by exposure to platelet-derived growth factor [46]. In our study, we observed a decrease in the expression of PDCD4 miRNA and an increase in the expression of miRNA-21 in aortic tissues from mice treated with bosentan.

In conclusion, we investigated the expression of miRNA-21 and its target PDCD4 during disease progression in an ApoE$^{-/-}$ mouse model of atherosclerosis induced by a high-fat diet. Notably, bosentan alleviated the adverse aortic effects of the high-fat diet, such as intimal thickening and deposition. Bosentan also decreased the expression of PDCD4, caspase 3, and Bax and increased the expression of Bcl-2 in aortic tissues, increased the expression of miRNA-21, and decreased the expression of PDCD4 mRNA. Our results thus indicated that the protective effect of bosentan against atherosclerosis in ApoE-deficient mice is mediated by miRNA-21.

Data Availability

The data used to support the findings of this study are available from the corresponding author upon request.

Conflicts of Interest

The authors declare there are no conflicts of interest to report.

Acknowledgments

This study was supported by the National Natural Science Foundation of China (Nos. 81700304 and 81370300), Tianjin Science and Technology Committee (18JCYBJC92200), Tianjin Natural Science Foundation Project (17JCQNJC11400), and Key Laboratory Science Foundation of Second Hospital of Tianjin Medical University (2017ZDSYS05).

References

[1] M. A. Gimbrone Jr. and G. García-Cardeña, "Endothelial cell dysfunction and the pathobiology of atherosclerosis," *Circulation Research*, vol. 118, no. 4, pp. 620–636, 2016.

[2] K. Theodorou and R. A. Boon, "Endothelial cell metabolism in atherosclerosis," *Frontiers in Cell and Developmental Biology*, vol. 6, p. 82, 2018.

[3] I. Tabas, G. García-Cardeña, and G. K. Owens, "Recent insights into the cellular biology of atherosclerosis," *The Journal of Cell Biology*, vol. 209, no. 1, pp. 13–22, 2015.

[4] P.-Y. Chen and M. Simons, "Fibroblast growth factor-transforming growth factor beta dialogues, endothelial cell to mesenchymal transition, and atherosclerosis," *Current Opinion in Lipidology*, vol. 29, no. 5, pp. 397–403, 2018.

[5] S. Paone, A. A. Baxter, M. D. Hulett, and I. K. H. Poon, "Endothelial cell apoptosis and the role of endothelial cell-derived extracellular vesicles in the progression of atherosclerosis," *Cellular and Molecular Life Sciences*, vol. 76, no. 6, pp. 1093–1106, 2019.

[6] M. N. Li, M. Qian, K. Kyler, and J. Xu, "Endothelial-vascular smooth muscle cells interactions in atherosclerosis," *Frontiers in Cardiovascular Medicine*, vol. 5, 2018.

[7] F. Gao, J. Chen, and H. Zhu, "A potential strategy for treating atherosclerosis: improving endothelial function via AMP-activated protein kinase," *Science China Life Sciences*, vol. 61, no. 9, pp. 1024–1029, 2018.

[8] W. Yao, Y. Gao, and Z. Wan, "Serum metabolomics profiling to identify biomarkers for unstable Angina," *BioMed Research International*, vol. 2017, p. 7657306, 2017.

[9] V. Ambros, "The functions of animal microRNAs," *Nature*, vol. 431, no. 7006, pp. 350–355, 2004.

[10] C. Chen, Y. Zhou, J. Wang, Y. Yan, L. Peng, and W. Qiu, "Dysregulated MicroRNA involvement in multiple sclerosis by induction of T helper 17 cell differentiation," *Frontiers in Immunology*, vol. 9, p. 1256, 2018.

[11] L. Cruz, J. A. A. Romero, R. P. Iglesia, and M. H. Lopes, "Extracellular vesicles: decoding a new language for cellular communication in early embryonic development," *Frontiers in Cell and Developmental Biology*, vol. 6, p. 94, 2018.

[12] P. Jessop and M. Toledo-Rodriguez, "Hippocampal TET1 and TET2 expression and DNA hydroxymethylation are affected by physical exercise in aged mice," *Frontiers in Cell and Developmental Biology*, vol. 6, p. 45, 2018.

[13] S. Ding, G. Liu, H. Jiang, and J. Fang, "MicroRNA determines the fate of intestinal epithelial cell differentiation and regulates intestinal diseases," *Current Protein & Peptide Science*, vol. 20, no. 7, pp. 666–673, 2019.

[14] A. Schober and M. Hristov, "MicroRNAs in the pathogenesis and therapy of atherosclerotic vascular disease," in *Atherosclerosis: Treatment and Prevention*, pp. 341–363, CRC Press, Boca Raton, FL, USA, 2012.

[15] W. P. Kloosterman and R. H. A. Plasterk, "The diverse functions of microRNAs in animal development and disease," *Developmental Cell*, vol. 11, no. 4, pp. 441–450, 2006.

[16] R. Kumarswamy, I. Volkmann, and T. Thum, "Regulation and function of miRNA-21 in health and disease," *RNA Biology*, vol. 8, no. 5, pp. 706–713, 2011.

[17] T. Bejerano, S. Etzion, S. Elyagon, Y. Etzion, and S. Cohen, "Nanoparticle delivery of miRNA-21 mimic to cardiac macrophages improves myocardial remodeling after myocardial infarction," *Nano Letters*, vol. 18, no. 9, pp. 5885–5891, 2018.

[18] J. Gu, X. Zhu, Y. Li et al., "miRNA-21 regulates arsenic-induced anti-leukemia activity in myelogenous cell lines," *Medical Oncology*, vol. 28, no. 1, pp. 211–218, 2011.

[19] Y. Jiang, Q. Gao, L. Y. Wang et al., "Deficiency of programmed cell death 4 affects the balance of T cell subsets in hyperlipidemic mice," *Molecular Immunology*, vol. 112, pp. 387–393, 2019.

[20] Y. Song, C. Zhang, J. Zhang et al., "Localized injection of miRNA-21-enriched extracellular vesicles effectively restores cardiac function after myocardial infarction," *Theranostics*, vol. 9, no. 8, pp. 2346–2360, 2019.

[21] J. L. Cmarik, H. Min, G. Hegamyer et al., "Differentially expressed protein Pdcd4 inhibits tumor promoter-induced neoplastic transformation," *Proceedings of the National Academy of Sciences*, vol. 96, no. 24, pp. 14037–14042, 1999.

[22] Z. Lu, M. Liu, V. Stribinskis et al., "MicroRNA-21 promotes cell transformation by targeting the programmed cell death 4 gene," *Oncogene*, vol. 27, no. 31, pp. 4373–4379, 2008.

[23] R. Kato, M. Hayashi, T. Aiuchi, N. Sawada, T. Obama, and H. Itabe, "Temporal and spatial changes of peroxiredoxin 2 levels in aortic media at very early stages of atherosclerotic lesion formation in ApoE-knockout mice," *Free Radical Biology and Medicine*, vol. 130, pp. 348–360, 2019.

[24] E. Raitoharju, L.-P. Lyytikäinen, M. Levula et al., "miR-21, miR-210, miR-34a, and miR-146a/b are up-regulated in human atherosclerotic plaques in the tampere vascular study," *Atherosclerosis*, vol. 219, no. 1, pp. 211–217, 2011.

[25] J. Hu, S. Ni, Y. Cao et al., "The angiogenic effect of microRNA-21 targeting TIMP3 through the regulation of MMP2 and MMP9," *PLoS One*, vol. 11, no. 2, Article ID e0149537, 2016.

[26] F. P. Li, D. Q. Lin, and L. Y. Gao, "LncRNA TUG1 promotes proliferation of vascular smooth muscle cell and atherosclerosis through regulating miRNA-21/PTEN axis," *European Review for Medical and Pharmacological Sciences*, vol. 22, no. 21, pp. 7439–7447, 2018.

[27] Q. Jiang, Y. Han, H. Gao, R. Tian, P. Li, and C. Wang, "Ursolic acid induced anti-proliferation effects in rat primary vascular smooth muscle cells is associated with inhibition of microRNA-21 and subsequent PTEN/PI3K," *European Journal of Pharmacology*, vol. 781, pp. 69–75, 2016.

[28] J. Zheng, B. Liu, Q. Lun et al., "Longxuetongluo capsule inhibits atherosclerosis progression in high-fat diet-induced

ApoE$^{-/-}$ mice by improving endothelial dysfunction," *Atherosclerosis*, vol. 255, pp. 156–163, 2016.

[29] Y. Zhao, L. Xiang, Y. Liu, M. Niu, J. Yuan, and H. Chen, "Atherosclerosis induced by a high-cholesterol and high-fat diet in the inbred strain of the wuzhishan miniature pig," *Animal Biotechnology*, vol. 29, no. 2, pp. 110–118, 2018.

[30] F. R. Maxfield and I. Tabas, "Role of cholesterol and lipid organization in disease," *Nature*, vol. 438, no. 7068, pp. 612–621, 2005.

[31] Y. Chen, S. Wen, M. Jiang et al., "Atherosclerotic dyslipidemia revealed by plasma lipidomics on ApoE$^{-/-}$ mice fed a high-fat diet," *Atherosclerosis*, vol. 262, pp. 78–86, 2017.

[32] J. Davignon and P. Ganz, "Role of endothelial dysfunction in atherosclerosis," *Circulation*, vol. 109, no. 23, pp. 3–27, 2004.

[33] K. Meehan and L. J. Vella, "The contribution of tumour-derived exosomes to the hallmarks of cancer," *Critical Reviews in Clinical Laboratory Sciences*, vol. 53, no. 2, pp. 121–131, 2016.

[34] L. Wang, Y. Jiang, X. Song et al., "Pdcd4 deficiency enhances macrophage lipoautophagy and attenuates foam cell formation and atherosclerosis in mice," *Cell Death & Disease*, vol. 7, Article ID e2055, 2016.

[35] X. Liu, Y. Cheng, J. Yang, T. J. Krall, Y. Huo, and C. Zhang, "An essential role of PDCD4 in vascular smooth muscle cell apoptosis and proliferation: implications for vascular disease," *American Journal of Physiology-Cell Physiology*, vol. 298, no. 6, pp. C1481–C1488, 2010.

[36] X. Liang, Z. Xu, M. Yuan et al., "MicroRNA-16 suppresses the activation of inflammatory macrophages in atherosclerosis by targeting PDCD4," *International Journal of Molecular Medicine*, vol. 37, no. 4, pp. 967–975, 2016.

[37] S. Matulevicius, A. Rohatgi, A. Khera et al., "The association between plasma caspase-3, atherosclerosis, and vascular function in the Dallas heart study," *Apoptosis*, vol. 13, no. 10, pp. 1281–1289, 2008.

[38] R. Hutter, C. Valdiviezo, B. V. Sauter et al., "Caspase-3 and tissue factor expression in lipid-rich plaque macrophages: evidence for apoptosis as link between inflammation and atherothrombosis," *Circulation*, vol. 109, no. 16, pp. 2001–2008, 2008.

[39] Y. Zhang, N. Chen, J. Zhang, and Y. Tong, "Hsa-let-7 g miRNA targets caspase-3 and inhibits the apoptosis induced by ox-LDL in endothelial cells," *International Journal of Molecular Sciences*, vol. 14, no. 11, pp. 22708–22720, 2013.

[40] M. S. Ola, M. Nawaz, and H. Ahsan, "Role of Bcl-2 family proteins and caspases in the regulation of apoptosis," *Molecular and Cellular Biochemistry*, vol. 351, no. 1-2, pp. 41–58, 2011.

[41] K. J. Moore, K. J. Rayner, Y. Suárez, and C. Fernández-Hernando, "microRNAs and cholesterol metabolism," *Trends in Endocrinology & Metabolism*, vol. 21, no. 12, pp. 699–706, 2010.

[42] F. Huang, J. Du, Z. Liang et al., "Large-scale analysis of small RNAs derived from traditional Chinese herbs in human tissues," *Science China Life Sciences*, vol. 62, no. 3, pp. 321–332, 2019.

[43] J. Madrigalmatute, N. Rotllan, J. F. Aranda, and C. Fernándezhernando, "MicroRNAs and atherosclerosis," *Current Atherosclerosis Reports*, vol. 15, no. 5, p. 322, 2013.

[44] M. Chandy, M. Ishida, E. A. Shikatani et al., "c-Myb regulates transcriptional activation of miR-143/145 in vascular smooth muscle cells," *PLoS One*, vol. 13, no. 8, Article ID e0202778, 2018.

[45] Y. Wei, M. Nazari-Jahantigh, P. Neth, C. Weber, and A. Schober, "MicroRNA-126, -145, and -155: a therapeutic triad in atherosclerosis?," *Arteriosclerosis, Thrombosis, and Vascular Biology*, vol. 33, no. 3, pp. 449–454, 2013.

[46] Y. Cheng, X. Liu, J. Yang et al., "MicroRNA-145, a novel smooth muscle cell phenotypic marker and modulator, controls vascular neointimal lesion formation," *Circulation Research*, vol. 105, no. 2, pp. 158–166, 2009.

Hindawi
BioMed Research International
Volume 2024, Article ID 9836273, 1 page
https://doi.org/10.1155/2024/9836273

Retraction

Retracted: MicroRNA-205-5p Targets HMGB1 to Suppress Inflammatory Responses during Lung Injury after Hip Fracture

BioMed Research International

Received 12 March 2024; Accepted 12 March 2024; Published 20 March 2024

This article has been retracted by Hindawi following an investigation undertaken by the publisher [1]. This investigation has uncovered evidence of one or more of the following indicators of systematic manipulation of the publication process:

(1) Discrepancies in scope

(2) Discrepancies in the description of the research reported

(3) Discrepancies between the availability of data and the research described

(4) Inappropriate citations

(5) Incoherent, meaningless and/or irrelevant content included in the article

(6) Manipulated or compromised peer review

The presence of these indicators undermines our confidence in the integrity of the article's content and we cannot, therefore, vouch for its reliability. Please note that this notice is intended solely to alert readers that the content of this article is unreliable. We have not investigated whether authors were aware of or involved in the systematic manipulation of the publication process.

Wiley and Hindawi regrets that the usual quality checks did not identify these issues before publication and have since put additional measures in place to safeguard research integrity.

We wish to credit our own Research Integrity and Research Publishing teams and anonymous and named external researchers and research integrity experts for contributing to this investigation.

The corresponding author, as the representative of all authors, has been given the opportunity to register their agreement or disagreement to this retraction. We have kept a record of any response received.

References

[1] X. Yu, X. Chen, and T. Sun, "MicroRNA-205-5p Targets HMGB1 to Suppress Inflammatory Responses during Lung Injury after Hip Fracture," *BioMed Research International*, vol. 2019, Article ID 7304895, 13 pages, 2019.

Hindawi
BioMed Research International
Volume 2019, Article ID 7304895, 13 pages
https://doi.org/10.1155/2019/7304895

Research Article

MicroRNA-205-5p Targets HMGB1 to Suppress Inflammatory Responses during Lung Injury after Hip Fracture

Xiaojie Yu,[1] **Xiaobin Chen**,[2] **and Tiansheng Sun**[1,2]

[1]*Department of Orthopaedics, The Second School of Clinical Medicine, Southern Medical University, Guangzhou, Guangdong 510515, China*
[2]*Chinese PLA General Hospital, Medical Center 7, Department of Orthopedic Surgery, Beijing 100700, China*

Correspondence should be addressed to Tiansheng Sun; suntiansheng-@163.com

Received 3 October 2019; Accepted 5 November 2019; Published 28 November 2019

Guest Editor: Hengjia Ni

Hip fracture is the most common type of injury in elderly people and is associated with a high incidence of complications and risk of mortality. In these patients, subsequent pulmonary infection can contribute to the development of an acute lung injury, a consequence of the systemic inflammatory response induced by hip fracture. Although the crucial role of microRNAs (miRNAs) in inflammatory responses has been established, the functions of miRNAs in the inflammatory responses associated with lung injury after hip fracture remain poorly understood. In this study, we explored the potential role of miR-205-5p in lung injury after hip fracture in an *in vivo* hip fracture model and *in vitro* cultures of human pulmonary alveolar epithelial cells (HPAEpiC). An analysis of clinical serum samples revealed increased levels of miR-205-5p and high mobility group box 1 (HMGB1) after hip fracture. A bioinformatics analysis and dual-luciferase reporter assay identified *HMGB1* as a potential target of miR-205-5p. The overexpression of miR-205-5p clearly reduced the expression of HMGB1 and inhibited NF-κB signaling, apoptosis, and proinflammatory cytokine production while enabling continued cell proliferation. Our results demonstrate that the upregulation of miR-205-5p suppresses inflammatory responses and promotes cell viability and proliferation by selectively targeting HMGB1 in the context of lung injury after hip fracture. Therefore, miR-205-5p may be an alternative target of therapeutic strategies for lung injury after hip fracture.

1. Introduction

Hip fracture is a common type of bone fracture in the elderly and is associated with high rates of mortality and a high incidence of complications that mainly result from immune disorders (e.g., rapid inflammatory response) [1]. Lung infection is the most severe of these complications, and previous studies have demonstrated that a hip fracture may subsequently contribute to a potentially fatal lung infection [2, 3]. For instance, hip fracture can affect the release of mitochondrial DNA release and induce lung injury via the TLR9/NF-kappa B (NF-κB) pathway [4]. Moreover, the trauma associated with surgery, which is the current standard treatment strategy for hip fracture, could induce posttraumatic systemic inflammation and subsequent remote organ damage. For example, lung infection is the most common postoperative complication and has been associated with high hospitalization and mortality rates [5–8]. Although improvements in surgical techniques and hospital care and advanced prevention strategies have led to reductions in the incidence of complications after hip fracture, the risk of infectious and inflammatory lung injury after hip fracture remains very high [9]. Therefore, a detailed exploration of the molecular mechanisms involved in the progression of lung injury after hip fracture and the identification of a critical mediator as a potential therapeutic target in such cases are highly important.

Recent research has identified potentially crucial roles of microRNAs (miRNAs) in multiple pathological conditions, including cancers, cardiovascular diseases, and neurodegenerative diseases [10]. miRNAs regulate gene expression by directly targeting the 3′-untranslated region (3′-UTR)

and inhibiting protein translation. Therefore, miRNAs contribute to most physiological and pathological processes by targeting the major molecular regulators. Studies have revealed that miRNAs may also play regulatory roles in remote organ damage caused by infection and inflammation [11–13]. For example, miR-146a was shown to act as a repressor of the inflammatory response during lipopolysaccharide- (LPS-) induced acute lung injury by inhibiting the expression of interleukin-1 receptor-associated kinase 1 (IRAK1) and tumor necrosis factor (TNF) receptor-associated factor 6 (TRAF6) [11, 12]. Another study demonstrated that human miR-921 mediates lung injury by targeting interleukin-37 (IL-37) expression [13]. miR-205-5p has been identified as a regulatory factor in several pathological conditions, including colon cancer [14], breast cancer [15], sepsis [16], and liver cancer [17].

Despite the above findings, the roles of miRNAs in the development of lung injury after hip fracture have not been well investigated. Therefore, we sought to identify the key miRNA in this process, as well as its potential target, with the aim of providing new insights into the underlying mechanism and identifying therapeutic strategies to treat lung injury after hip fracture. In this study, we explored the potential contribution of miR-205-5p to the progression of lung injury after hip fracture using both *in vivo* and *in vitro* models. We also investigated the expression of miR-205-5p and its regulatory effect on the inflammatory mediator HMGB1. Our results may provide new insights to inform the development of advanced therapeutic treatment and prevention strategies for lung injury after hip fracture.

2. Materials and Methods

2.1. Patients and Samples Collection. The clinical characteristics of patients with hip fracture who were included in this study are shown in Table 1. Serum samples were collected from all patients. Bone biopsies were conducted in accordance with the Updated Banff 07 Classification. The human experimental protocol was approved by the ethics committee of joint surgery of Zhuzhou Central Hospital (Hunan, China). The study protocol adhered strictly to the Code of Ethics of the World Medical Association (i.e., Declaration of Helsinki). All patients and their families participated voluntarily in the study and provided signed informed consent.

2.2. Experimental Animals. The animal experimental protocol was approved by the Animal Ethics Review Committee of Nanfang Hospital, Southern Medical University. Twenty male Sprague-Dawley (SD) rats were housed with unlimited access to food and water. After an acclimation period of >1 week, all of the animals were randomly assigned to one of two groups: control and fracture groups. The hip fracture model was established as described previously [18–20]. Briefly, the SD rats in the fracture group were anesthetized with sodium pentobarbital (60 mg/kg, intraperitoneally (i.p.)) and laid on the base of a blunt guillotine ramming apparatus. After identifying and marking the proximal femur, hip fracture was induced by dropping a blunt guillotine (weight: 500 g) from a height of 15 cm.

Table 1: Clinicopathological characteristics of patients included in the study sample.

	Hip fracture	Control
Variable	20	5
Sex		
Male	10	1
Female	10	4
Age		
60–69 years	6	1
70–79 years	6	3
80–89 years	6	1
90–99 years	2	0
Type of hip fracture		
Left femoral intertrochanteric fracture	9	
Right femoral intertrochanteric fracture	11	
Comorbid conditions		
Type II diabetes	9	
Hypertension	9	
Stroke complications	7	
Chronic lung diseases	2	

X-ray imaging was performed on Days 0 and 28 after hip fracture, and blood was collected at 0 h, at 8 h, and on Days 1, 7, 14, and 28. Lung tissues were collected on Day 28 after hip fracture. Changes in the statuses of the model animals were monitored by experienced technicians to avoid potential side effects such as peritonitis. At the end of the experiment (Day 28), the rats were anesthetized using 3% sodium pentobarbital i.p. and sacrificed by bleeding through the abdominal aorta. A postmortem examination was conducted to identify signs of peritonitis before further study.

2.3. Histomorphology Analysis. A section of lung tissue was treated with a fixative solution (4% formaldehyde and 1% glutaraldehyde in PBS, pH 7.4) and embedded in paraffin. A Leica SM2010R microtome (Leica, Shanghai, China) was used to cut the embedded tissue into 5-micrometer-thick slices, which were subjected to ethanol gradient dehydration and hematoxylin and eosin (H&E) staining. Finally, the slices were observed under a light microscope (Eclipse E100, Nikon, Japan; 40x magnification).

2.4. Immunohistochemical Staining. For immunohistochemical staining, fixed sections of lung tissue were blocked and then incubated with a primary antibody specific for HMGB1 (1 : 4000 dilution; ab79823, Abcam, UK) in 10% rabbit serum overnight at 4°C. The sections were then treated with a secondary antibody conjugated to horseradish peroxidase (1 : 10000 dilution; ab7090, Abcam). After the colorimetric reaction was completed, the sections were observed under a light microscope (Eclipse E100, Nikon; 40x magnification).

2.5. TUNEL Assay. Apoptosis was confirmed and quantified in tissue sections using the TUNEL assay. Tissue sections

were stained with fluorescein-conjugated TUNEL (Click-iT™ TUNEL Alexa Fluor™ 594 Imaging Assay, Thermo Fisher Scientific, USA) according to the manufacturer's instructions [21]. The number of TUNEL-positive cells was counted in 30 sections per slide.

2.6. Cell Culture. Human pulmonary alveolar epithelial cells (HPAEpiC; BNCC337714, BeNa Culture Collection, Beijing, China) were cultured in Dulbecco's modified Eagle's medium (DMEM, 10566024, Gibco, USA) supplemented with 10% (*v*/*v*) fetal bovine serum (FBS, 10099-141, Gibco), 100 U/mL penicillin, 100 mg/mL streptomycin, and 2 mM glutamine. The cells were cultured at 37°C in an atmosphere of 5% CO_2 and were passaged once they reached 70–80% confluency. HPAEpiC cells in the HMGB1-treated group were exposed to 15 μg/mL HMGB1 [22]. Cells were cultured in DMEM medium containing 1% FBS and subjected to the following biochemistry analysis.

2.7. Cell Proliferation Assay. Cell proliferation was determined using Cell Counting Kit 8 (CCK-8) and an ethynyl-2-deoxyuridine incorporation assay (EdU Apollo DNA *in vitro* kit, RIBOBIO, Guangzhou, China) according to the manufacturer's instructions. For the CCK-8 assay, the cells were cultured at a density of 5×10^4 per well in a 96-well plate. After a 24 h incubation to enable adherence, the cells were treated with CCK-8 solution for 2 h at 37°C. Subsequently, the absorbance at 450 nm was measured in each well using a multiwell plate reader (Multiskan MK3, Thermo Fisher Scientific).

For the EdU assay, the cells were treated with 100 μL of EdU (50 μM) for 2 h at 37°C at the end of each time point, then fixed in 100 μL of 4% polyformaldehyde for 30 min at room temperature, treated with 50 μL of glycine (2 mg/mL) for 5 min, and washed with 100 μL of phosphate-buffered saline (PBS). After permeabilization with 0.5% Triton X, the cells were incubated in 1× Apollo solution for 30 min, in 100 μL of 1× Hoechst 33342 solution (Cat. No. C10327, RiboBio, Shanghai, China) for another 30 min at room temperature in the dark, and washed with 100 μL of PBS.

2.8. Apoptosis Analysis by Flow Cytometry and Hoechst 33258 Staining. Apoptosis was measured by the double staining of cells with Annexin V and propidium iodide (PI). After treating the culture plates with trypsin-EDTA, the detached cells were washed twice with PBS and resuspended in binding buffer (10 mM HEPES pH7.4, 150 mM NaCl, 5 mM KCl, 1 mM $MgCl_2$, and 1.8 mM $CaCl_2$) containing FITC-Annexin V (1 g/mL) for 20 min. PI (10 g/mL) was then added to the cell suspension. The cells were analyzed via flow cytometry, using the 488 nm and 575 nm wavelength channels to detect FITC and PI, respectively.

After the cells were transfected, 50 mL of cell stationary fluid (PBS containing 4% paraformaldehyde) was added. After 30-minute incubation at room temperature, the fluid was discarded and the samples were rinsed twice in PBS for 3 min per rinse. Next, a Hoechst 33258 staining solution (C1011, Beyotime, Beijing, China; final concentration: 20 μM) was added for coverage at room temperature for 5 min. The dye solution was then discarded, and the samples were rinsed twice with PBS. Fluorescence microscopy was conducted at a wavelength of 460 nm.

2.9. Cell Cycle Analysis via Flow Cytometry. Cells were collected, washed with cold PBS buffer, and fixed in 70% ethanol at −20°C overnight. Subsequently, the cells were labeled with a staining solution containing 10 μg/mL RNase A and 50 μg/mL PI at 37°C for 30 min in the dark and then carefully washed with cold PBS. The cell cycle distribution was analyzed via flow cytometry with Cell Quest software (BD Biosciences, USA).

2.10. Analysis of RNA Expression by Real-Time PCR. The total RNA was isolated from cells using TRIzol (Invitrogen, USA). First-strand cDNA was then synthesized via reverse transcription and used in real-time PCR reactions, which were performed on an ABI 7500 Real-Time PCR System (Applied Biosciences, USA). Each assay was performed in triplicate. The following primer sequences were used: HMGB1, 5′-GTGCAAACTTGTCGGGAG-3′ (forward) and 5′-CGATACTCAGAGCAGAAGAGG-3′ (reverse); miR-205-5p, 5′-TCCTTCATTCCACCGGAGTCTG-3′ (forward) and 5′-CTCAACTGGTGTCGTGGAGTCGGCAATTCAGTTGAGCAGACTC-3′ (reverse); GAPDH, 5′-TGTTCGTCATGGGTGTGAAC-3′ (forward) and 5′-ATGGCATGGACTGTGGTCAT-3′ (reverse); and U6, 5′-CTCGCTTCGGCAGCACA-3′ (forward) and 5′-AACGCTTCACGAATTTGCGT-3′ (reverse). The relative expression levels of miR-205-5p and HMGB1 were calculated using the a $2^{-\Delta\Delta Ct}$ method. GAPDH and U6 were set as the internal controls, respectively.

2.11. In Silico Prediction and Dual-Luciferase Reporter Assay. The putative targets of miR-205-5p were predicted using Target Scan Release 7.2. Reporter vectors under the control of the wild-type and mutant human HMGB1 3′UTR were constructed using the pmirGLO vector backbone. A dual-luciferase assay reporter kit was used to detect firefly luciferase and *Renilla* luciferase signals.

2.12. Immunofluorescent Staining. Prior to immunofluorescent staining, the cells were fixed with 4% paraformaldehyde for 10 min and blocked with 5% FBS containing 0.5% Triton X-100 for 5 min. Subsequently, the cells were incubated at 4°C overnight in a solution containing primary antibodies specific for HMGB1 (1 : 4000 dilution, ab79823, Abcam) and NF-κB p65 (1 : 1000, ab16502, Abcam). Subsequently, the cells were stained with an Alexa Fluor 488-conjugated anti-rabbit antibody and Alexa Fluor-564-conjugated anti-rabbit antibody. The cells were mounted on slides with mounting buffer containing DAPI. Immunofluorescence was detected using a fluorescence microscope.

2.13. Transfection of miR-205-5p Mimics and Inhibitor. miR-205-5p mimics and inhibitory and scramble (mock) miRNA were synthesized by GenePharma (Suzhou, China). HPAEpiC cells that had reached 80% confluency were transfected with miRNA via Lipofectamine 3000 reagent (Invitrogen, USA) according to the manufacturer's instructions.

2.14. Small Interfering RNA (siRNA) and Transfection Assays. *HMGB1*-specific siRNA was synthesized chemically, along with scramble siRNA as a negative control (NC). The siRNAs were transfected into cells using Lipofectamine 2000 reagent (Invitrogen) according to the manufacturer's instructions.

2.15. Western Blot Analysis. The samples were lysed with a protein lysis buffer containing 1% proteinase inhibitor and homogenized with an ultrasound homogenizer. After centrifugation for 10 min at 1200 g and 4°C, the supernatant was discarded and the total protein concentration in each sample was detected using a bicinchoninic acid (BCA) kit (PIERCE). Equal concentrations of protein per sample were prepared in 20 μL of loading buffer and separated via sodium dodecyl sulfate-polyacrylamide gel electrophoresis (SDS-PAGE) at a constant voltage of 80 V. The separated proteins were then transferred to a polyvinylidene fluoride (PVDF) membrane (IPVH00010, Millipore, USA) at a constant voltage of 100 V for 90 min and then blocked in a 5% skim milk solution for 2 h. Then the band was cut according to the size of target band and incubated with primary rabbit antibodies specific for RAGE (1 : 1000, ab228861, Abcam), HMGB1 (1 : 4000, ab79823, Abcam), p65 (1 : 1000, ab16502, Abcam), and p-IkBα/IKBα (1 : 1000, ab133462/ab32518, Abcam) in Tris-buffered saline containing Tween-20 (TBS-T) overnight at 4°C. Next, the membranes were washed in TBS-T three times (10 min each) and incubated with a secondary antibody-linked HRP (1 : 10 000, ab7090, Abcam, UK). After adding an electrochemiluminescent solution, the membrane was imaged using a fluorescence imaging technique.

2.16. Cytokine and Chemokine ELISA Analysis. The concentrations of proinflammatory cytokines and chemokines in cell culture supernatants were evaluated using enzyme-linked immunosorbent assays (ELISAs) at 48 h after transfection. The supernatants were collected by centrifugation at 13000 g and 4°C for 10 min, and the total protein concentrations were measured using a DC protein assay (Bio-Rad, Hercules, CA, USA). The concentrations of HMGB1, IL-6, and TNF-α were then quantified by ELISA.

2.17. Data Analysis. Statistical calculations were performed using Prism 7 (GraphPad Software, Inc., USA). Data are presented as means ± standard deviations. Student's *t*-test was used for intergroup comparisons. Continuous data from multiple groups were analyzed using a one-way ANOVA, followed by Tukey's post hoc test. A Pearson correlation analysis was used to assess correlations between the expression of miR-205-5p and that of HMGB1 in human serum samples. Differences with P values <0.05 were considered statistically significant.

3. Results

3.1. Determination of Hip Fractures in SD Rats. X-ray images of rats in the control and hip fracture groups on Days 0 and 28 confirmed the successful establishment of the hip fracture model (Figure 1(a)). H&E staining of lung tissue sections revealed the main histologic differences in the hip fracture group relative to control group, including neutrophil marginalization around the lobules and cellulose-like necrosis in the arteries. Immunohistochemistry analysis revealed a remarkable increase in the HMGB1 level in the hip fracture group relative to the control group (Figure 1(b)). A TUNEL apoptosis assay indicated an increase in apoptosis in the hip fracture group relative to the control group (Figure 1(c)).

To explore the inflammatory responses in the SD rat model of hip fracture, we examined the concentrations of IL-6 and HMGB1 in serum samples via ELISA. Notably, we observed significant increases in HMGB1 in the fracture group at 8 h ($P < 0.001$) and on Days 1 ($P < 0.001$), 7 ($P < 0.001$), 14 ($P < 0.001$), and 28 ($P < 0.001$) after model induction. Similarly, we observed significant increases in IL-6 in the fracture group at 8 h ($P < 0.001$) and on Days 1 ($P < 0.001$), 7 ($P < 0.01$), and 14 ($P < 0.01$) after hip fracture. The serum level of miR-205-5p also increased at 8 h ($P < 0.001$) and on Days 1 ($P < 0.001$), 7 ($P < 0.001$), and 14 ($P < 0.05$) after hip fracture (Figure 1(d)). A Western blot analysis of lung tissue confirmed the dramatic increase in the level of HMGB1, as well as increases in NF-κB p65, p-IkBα/IKBα, and RAGE in the hip fracture group relative to the control group (Figure 1(e)).

3.2. HMGB1 as a Target of miR-205-5p. Next, we determined the serum levels of miR-205-5p in lung injury after hip fracture patients against control group using quantitative real-time PCR (qPCR). Notably, miR-205-5p was upregulated in the sera of patients with lung injury ($P < 0.01$) after hip fracture relative to the controls. We also observed a significantly higher serum level of HMGB1 in patients with lung injury after hip fracture ($P < 0.001$) relative to controls (Figure 1(f)) and determined a positive correlation between the levels of miR-205-5p and HMGB1 in human serum ($R = 0.684$, Figure 1(g)).

Next, we conducted an *in silico* prediction analysis (miRBase, TargetScan, PicTar, and MiRanda) to identify the potential sites of binding between *HMGB1* mRNA and miR-205-5p. We determined that the 3′UTR of *HMGB1* mRNA includes a miR-205-5p-binding site that is conserved in mammals (Figure 1(h)). We then evaluated the effect of miR-205-5p on *HMGB1* expression using a luciferase reporter assay. Notably, an increase in miR-205-5p led to a significant decrease in luciferase activity under the control of the wild-type *HMGB1* 3′UTR relative to negative control. However, no significant difference from the control was

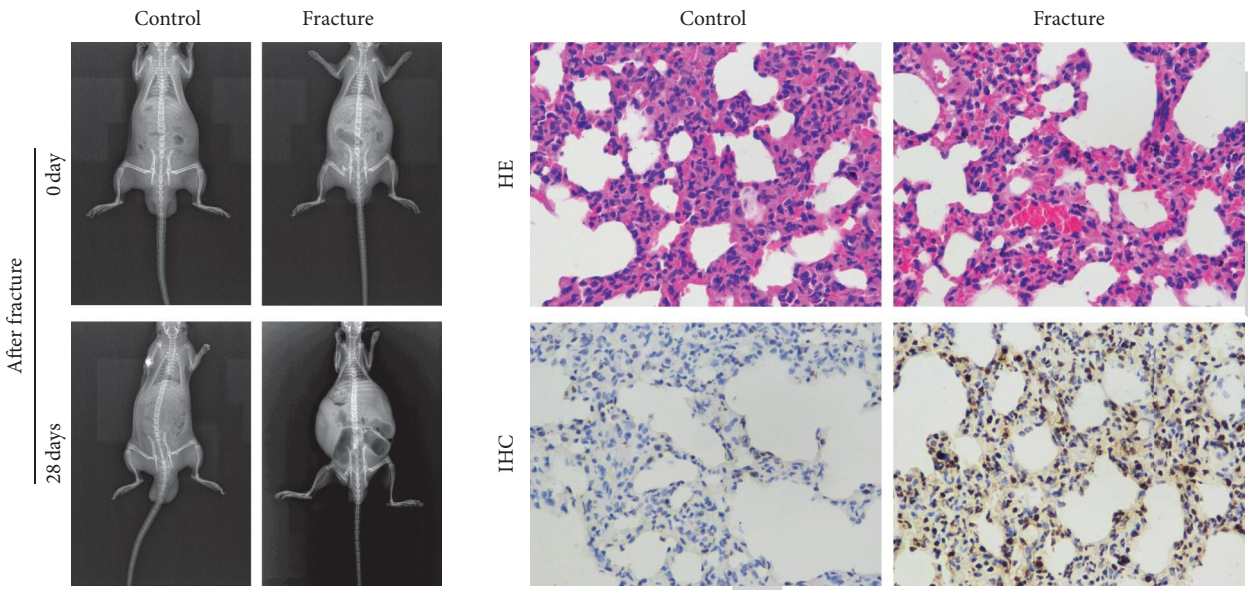

(a)

(b)

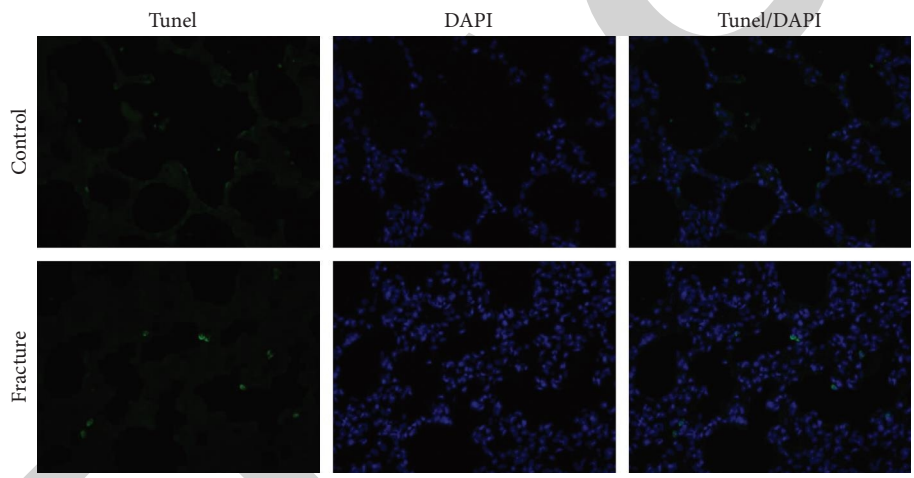

(c)

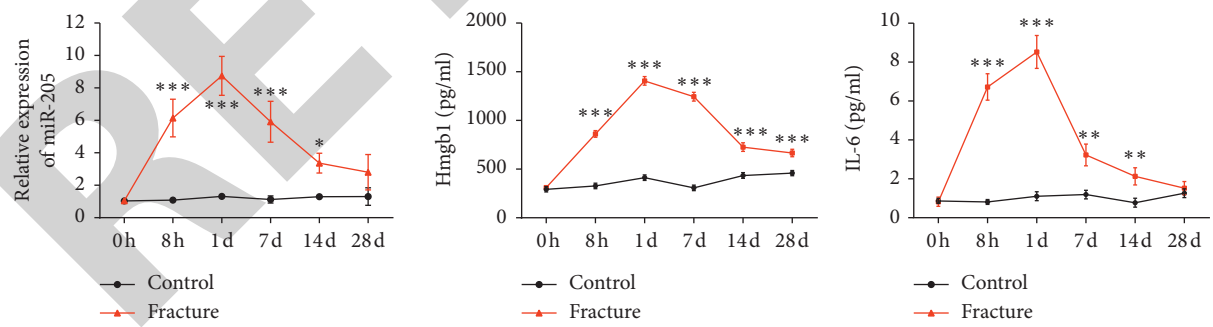

(d)

Figure 1: Continued.

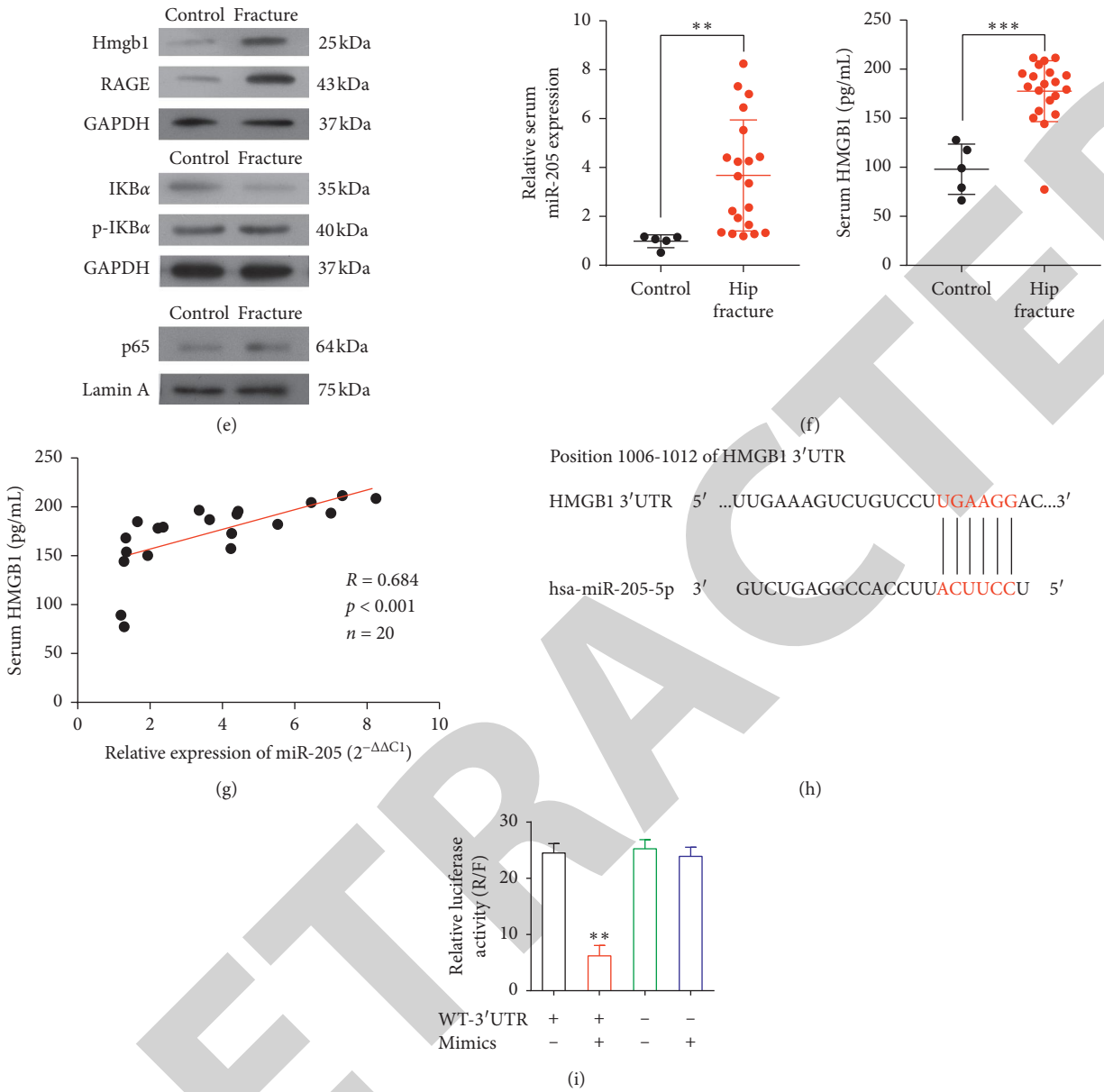

Figure 1: Determination of successful hip fracture in a Sprague-Dawley (SD) rat and of HMGB1 as the target of miR-205-5p. (a) Representative X-ray image of a SD rat model of hip fracture and control (1 : 1). (b) Representative hematoxylin and eosin-stained lung tissue sections and representative tissue sections stained immunohistochemically to detect HMGB1 are shown in the top and bottom panels, respectively (magnification, 40×). (c) Representative fluorescent images of tissues subjected to the TUNEL assay. Green and blue areas represent apoptotic cells and cell nuclei, respectively (magnification, 40×). (d) The relative expression levels of miR-205-5p and HMGB1 and IL-6 mRNA in the hip fracture and control groups were determined using qPCR. $^{*}P < 0.05$, $^{**}P < 0.01$, and $^{***}P < 0.001$ vs. the control. (e) Western blot analysis of the levels of HMGB1, p65, p-IkBα/IkBα, and RAGE. Equal protein loading was verified using GAPDH or Lamin A as an internal control. (f) Relative levels of miR-205-5p and HMGB1 in serum samples from human patients relative to controls. $^{**}P < 0.01$; $^{***}P < 0.001$. (g) Correlation analysis between the levels of miR-205-5p and HMGB1 in human serum samples. (h) Predicted conserved miR-205-5p binding sites in HMGB1 mRNA. (i) Luciferase activity analysis of cells transfected with constructs encoding wild-type or mutated HMGB1 in the presence of miR-205-5p or NC. WT-3′UTR (+) indicates wild-type HMGB 3′UTR. WT-3′UTR (-) indicates mutant-3′UTR HMGB1. Mimics indicates miR-205-5p mimics. $^{**}P < 0.01$ vs. the control.

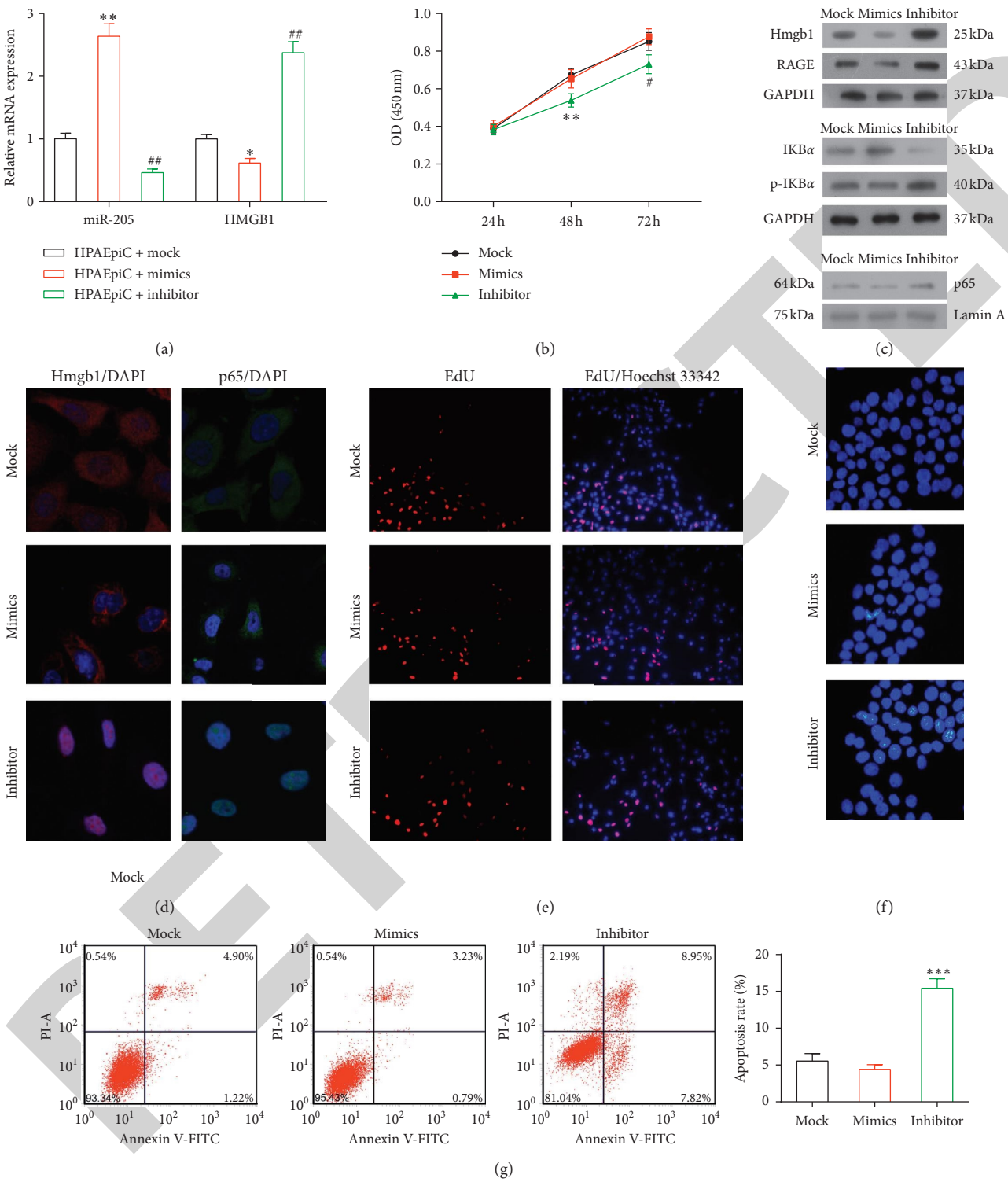

Figure 2: Continued.

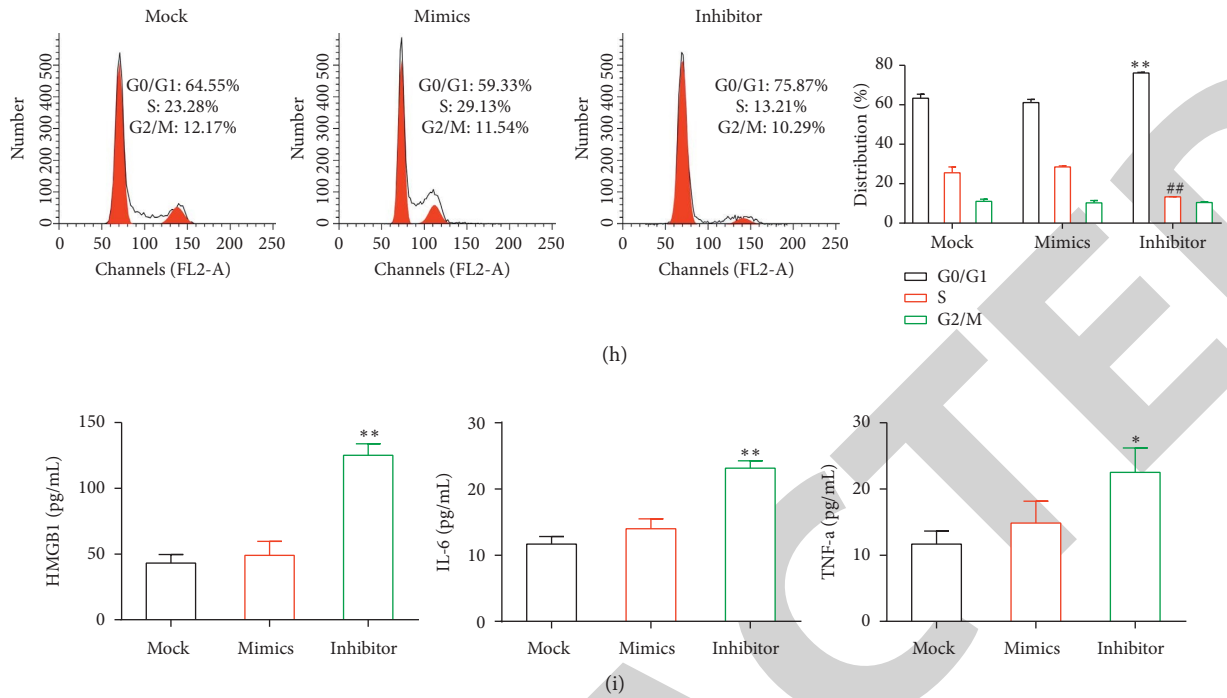

Figure 2: Effects of a transfected miR-205-5p mimic or inhibitor in HPAEpiC cells. (a) The relative expression levels of miR-205-5p and HMGB1 were determined by qPCR. $^{*}P < 0.05$, $^{**}P < 0.01$, $^{\#\#}P < 0.01$ and vs. the other two groups. (b) CCK8 assay of cell proliferation. The results represent the means of three independent experiments. $^{**}P < 0.01$ and $^{\#}P < 0.05$ vs. the other two groups. (c) Western blot analysis of the levels of HMGB1, p65, p-IkBα/IkBα, and RAGE. Equal protein loading was verified using GAPDH or Lamin A as internal controls. (d) The levels of HMGB1 and p65 were determined via immunofluorescence analysis (magnification, LSM 120×). (e) Representative micrographs of EdU-labeled samples from three groups (magnification, 10×) and (f) corresponding fluorescence images of samples stained with Hoechst 33258 (magnification, 20×). (g) Flow cytometric detection of apoptotic cells in samples double-stained with Annexin V-FITC and PI. $^{***}P < 0.001$ vs. the other groups. (h) Images of a cell cycle analysis as determined by PI staining and flow cytometry. $^{**}P < 0.01$ vs. the other groups. (i) The concentrations of HMGB1, IL-6, and TNF-α in cell supernatants were determined by ELISA. $^{*}P < 0.05$, $^{**}P < 0.01$, and $^{***}P < 0.001$ vs. the other groups.

observed when the predicted miR-205-5p-binding site in *HMGB1* mRNA was mutated (Figure 1(i)).

3.3. Effect of a miR-205-5p Mimic or Inhibitor in HPAEpiC Cells. To determine the effect of miR-205-5p on lung injury, miR-205-5p mimics or inhibitors (or mock) were transfected into HPAEpiC cells. We then evaluated the expression of miR-205-5p using qPCR, using U6 RNA as an internal control. miR-205-5p mimics significantly enhanced the expression of miR-205-5p ($P < 0.01$), while the miR-205-5p inhibitor dramatically decreased the expression of endogenous miR-205-5p ($P < 0.01$) relative to the controls. Moreover, the miR-205-5p mimic reduced the expression of *HMGB1* ($P < 0.05$), whereas the miR-205-5p inhibitor dramatically increased the expression of *HMGB1* ($P < 0.001$) by more than twofold (Figure 2(a)).

The CCK8 and EdU proliferation assays demonstrated that the transfection of the miR-205-5p mimic maintained cell proliferation, in contrast with the transfection of the miR-205-5p inhibitor (Figures 2(b) and 2(e)). Western blotting revealed significantly lower levels of HMGB1, NF-κB p65, p-IkBα, and RAGE in the miR-205-5p mimic group and significantly higher levels of all four proteins in the miR-205-5p inhibitor group, relative to the miR-205-5p mock group (Figure 2(c)). Immunofluorescence staining of HMGB1 and p65 yielded similar results (Figure 2(d)).

Our apoptosis analysis revealed a significantly higher apoptosis rate in the miR-205-5p inhibitor group ($P < 0.001$; Figures 2(f) and 2(g)). Notably, transfection of the miR-205-5p inhibitor also disrupted the cell cycle distribution, with an increased percentage of cells in the G0/G1 phase ($P < 0.01$) and a corresponding decrease in the percentage of cells in the S phase ($P < 0.01$; Figure 2(h)). Furthermore, ELISA analyses revealed significant increases in the concentrations of HMGB1 ($P < 0.01$), IL-6 ($P < 0.01$), and TNF-α ($P < 0.05$) in the supernatants of cells in the miR-205-5p inhibitor group relative to the other two groups (Figure 2(i)).

3.4. The Effect of HMGB1 Administration and HMGB1 siRNA Transfection in HPAEpiC Cells. We validated the ability of HMGB1 siRNA to downregulate the expression of *HMGB1* using qPCR and western blotting. This RNA interference strategy significantly reduced the level of HMGB1 ($P < 0.01$) in the treated cells relative to the negative control cells (Figure 3(a)). Cell proliferation and apoptosis analyses revealed that the administration of HMGB1 significantly inhibited cell proliferation ($P < 0.05$) and promoted cell apoptosis ($P < 0.01$). However, transfection with siHMGB1

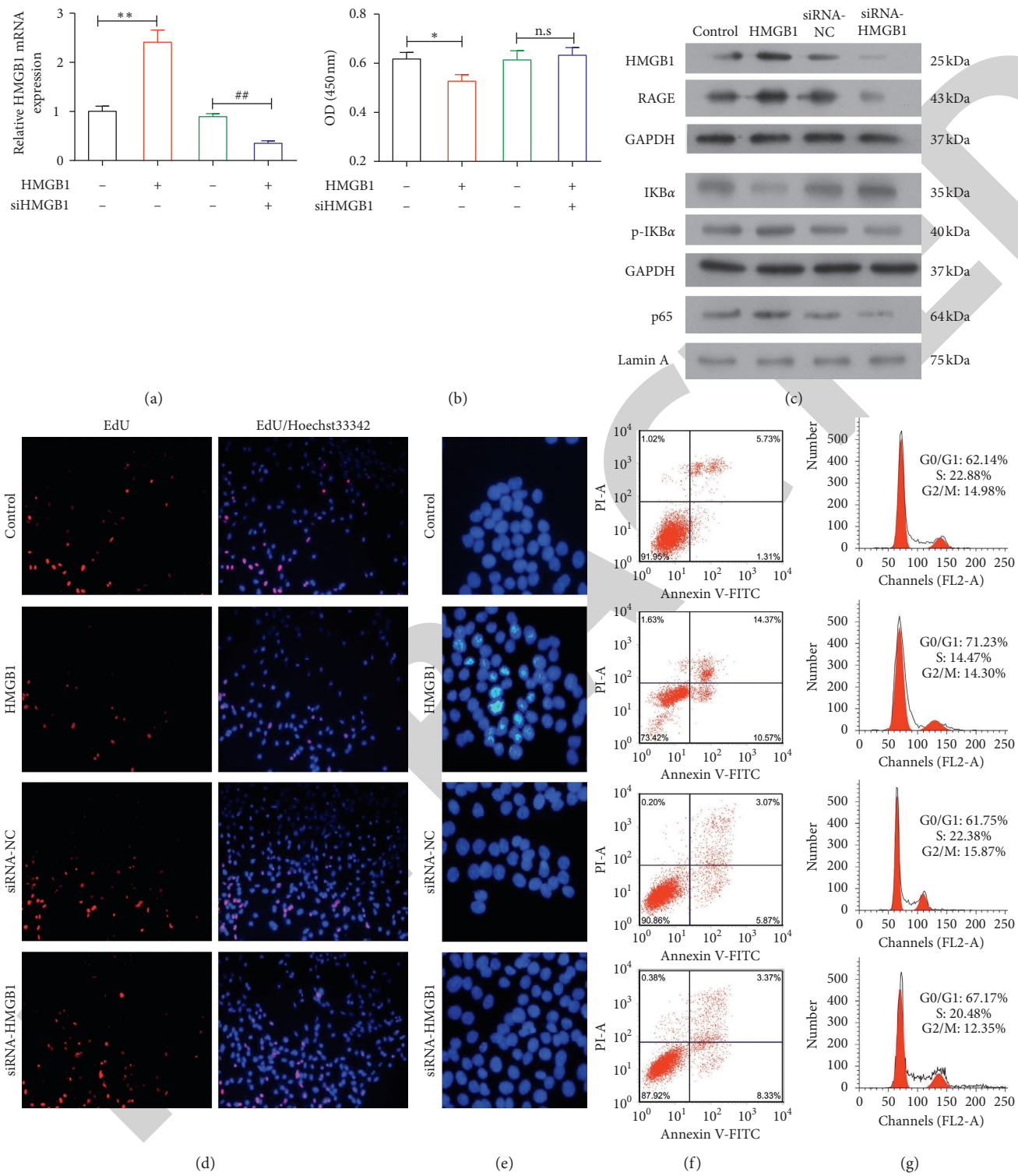

Figure 3: Continued.

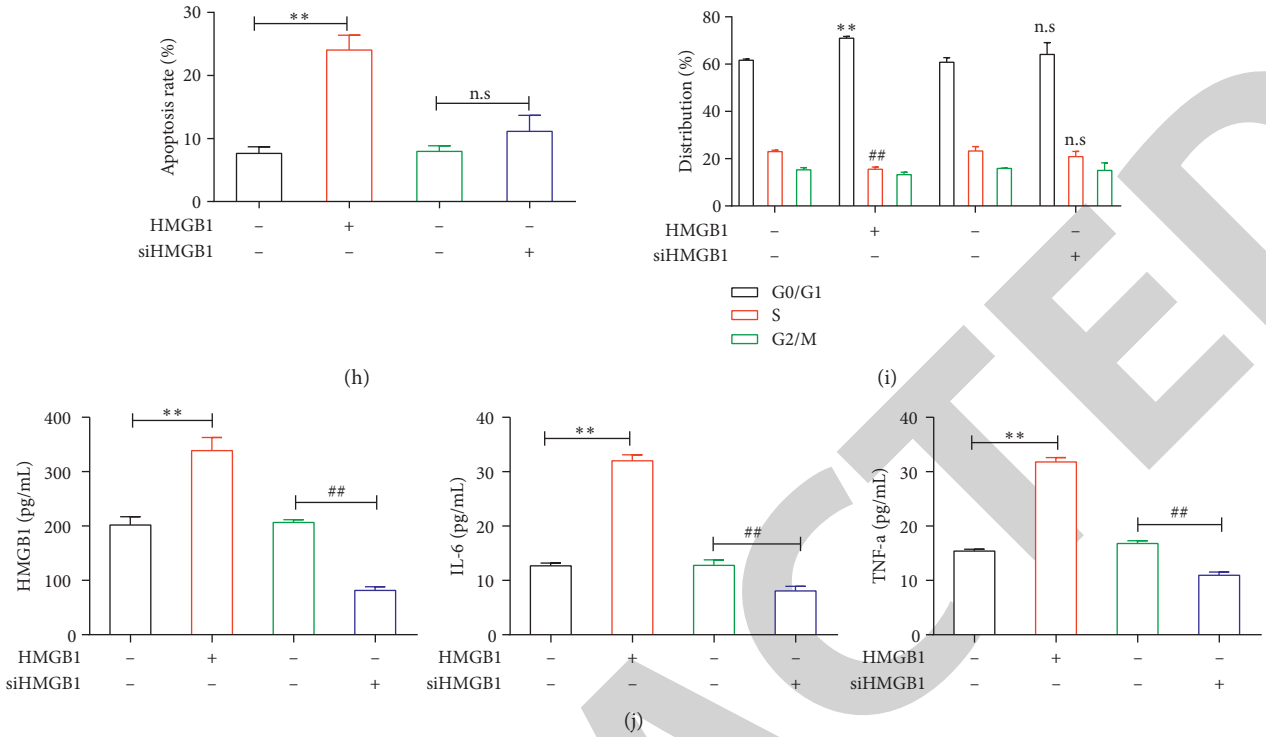

Figure 3: Effects of HMGB1 administration and siRNA-mediated inhibition in HPAEpiC cells. (a) The relative expression levels of miR-205-5p and HMGB1 were determined by qPCR. The control and siRNA control (siRNA-NC) groups are indicated by black and green bars, respectively. (b) Results of a CCK8 proliferation assay. The results are presented as the means of three independent experiments. $^{**}P < 0.05$ and $^{\#\#}P < 0.05$ vs. the other groups. (c) Western blot analysis of the levels of HMGB1, p65, p-IkBα/IkBα, and RAGE. Equivalent protein loading was verified using GAPDH or Lamin A as internal controls. (d) Representative micrographs of EdU-labeled samples from four groups and (e) corresponding fluorescence images of samples stained with Hoechst 33258. (f, h) Apoptotic cells were detected by flow cytometry and double-staining with Annexin V-FITC and PI. $^{**}P < 0.01$ vs. the other groups. (g, i) Images of a flow cytometry-based cell cycle analysis of PI-labeled cells. $^{**}P < 0.01$ and $^{\#\#}P < 0.01$ vs. the other groups. (j) ELISA analysis of the levels of HMGB1, IL-6, and TNF-α in culture supernatants. $^{*}P < 0.05$, $^{**}P < 0.01$, and $^{\#\#}P < 0.01$ vs. the other groups.

had no significant effect on either proliferation or apoptosis (Figures 3(b) and 3(d)–3(i)). Treatment with HMGB1 led to remarkable increases in the levels of p65, p-IkBα/IKBα, and RAGE relative to the control group, whereas decreased levels of all three proteins were observed in cells transfected with siHMGB1 (Figure 3(c)). An ELISA analysis confirmed significant increases in the levels of HMGB1 ($P < 0.01$), IL-6 ($P < 0.01$), and TNF-α ($P < 0.01$) in the supernatants of cells treated with HMGB1 group relative to the control, whereas the siRNA-mediated knockdown of HMGB1 significantly suppressed the expression of HMGB1 as expected ($P < 0.01$), as well as of IL-6 ($P < 0.01$) and TNF-α ($P < 0.01$; Figure 3(j)).

3.5. Effects of a miR-205-5p Mimic and HMGB1 Administration in HPAEpiC Cells. HPAEpiC cells transfected with a miR-205-5p mimic were subsequently treated with HMGB1, which led to a decrease in cell proliferation ($P < 0.01$) and an increase in apoptosis ($P < 0.05$) as indicated by flow cytometry and Hoechst 33258 staining analyses (Figures 4(a)–4(c)). Western blotting revealed decreased levels of HMGB1, NF-κB p65, p-IkBα/IKBα, and RAGE in the miR-205-5p mimic + HMGB1 group relative to the HMGB1 group (Figure 4(d)). An ELISA analysis indicated significantly lower levels of HMGB1 ($P < 0.01$), IL-6 ($P < 0.01$), and TNF-α ($P < 0.05$) in the supernatants of miR-205-5p mimic + HMGB1 cells relative to the HMGB1 cells (Figure 4(e)).

4. Discussion

Recently, investigators have increasingly expressed interest in miRNAs, which selectively inhibit the expression of critical molecular compounds and thus contribute to the regulation of fundamental biological and physiopathological processes [23]. miRNAs also play modulatory roles in various cancers (e.g., breast, colon, liver, and cervical cancer), cardiovascular diseases (e.g., cardiac hypertrophy, hypertension, stroke, and arrhythmias), and neurodegenerative diseases (e.g., Alzheimer's disease, Huntington's disease, and Parkinson's disease) [24]. These pathological conditions are at least partially mediated by several miRNAs, suggesting that these elements may be useful as biomarkers or therapeutic targets. However, studies of the roles of miRNAs in inflammatory responses have been overshadowed by reports of the regulatory roles of miRNAs in cancers. To address this research gap, we investigated the

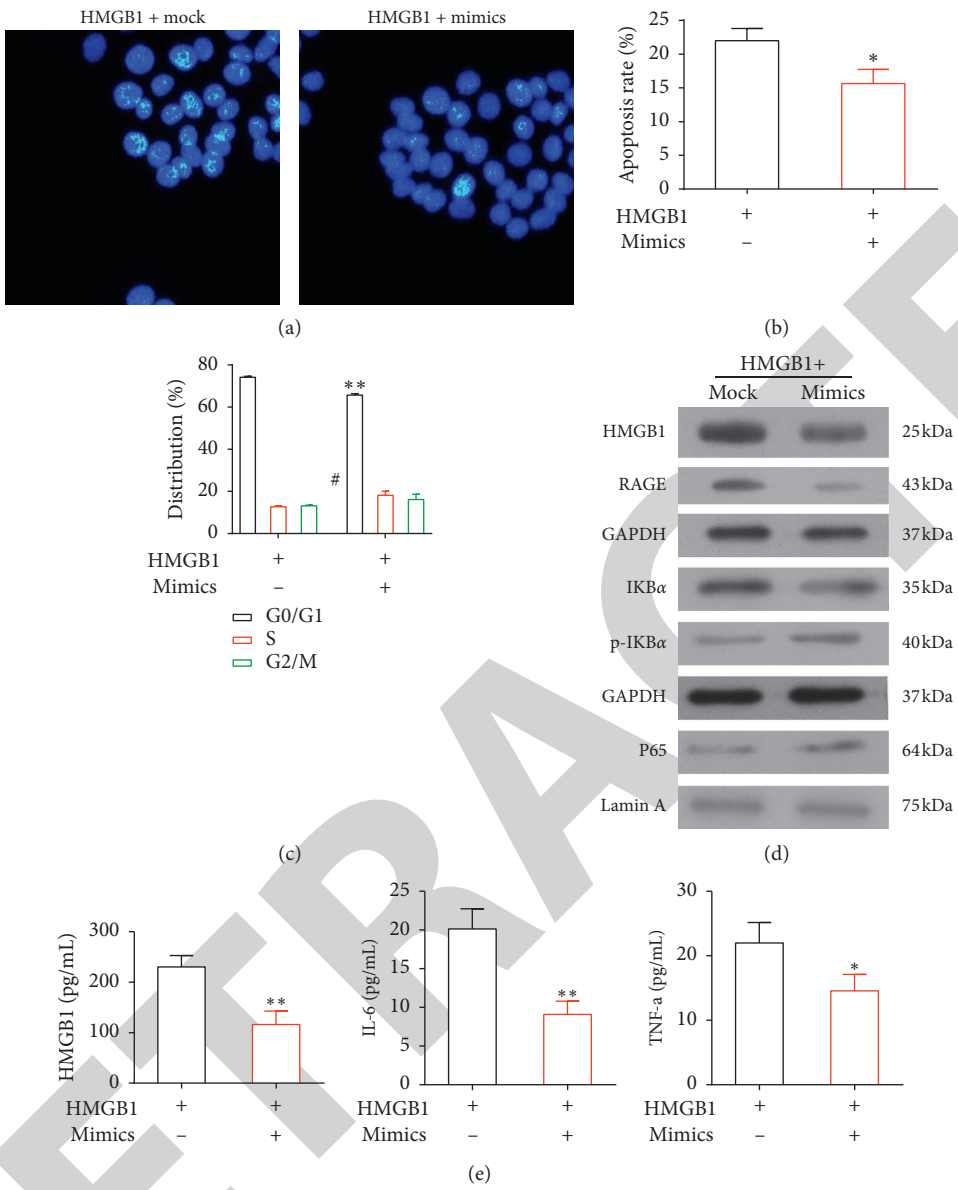

Figure 4: Effects of a transfected miR-205-5p mimic and HMGB1 treatment in HPAEpiC cells. (a) Fluorescence images of cells labeled with Hoechst 33258. (b) Apoptotic cells were detected by flow cytometry after double-staining with Annexin V-FITC and PI. $^{*}P < 0.05$ vs. the other groups. (c) Images of a flow cytometric cell cycle analysis of PI-labeled cells. $^{**}P < 0.01$ and $^{\#}P < 0.05$ vs. the other groups. (d) Western blot analysis of the levels of HMGB1, p65, p-IkBα/IkBα, and RAGE in cultured cells. (e) ELISA analysis of the concentrations of HMGB1, IL-6, and TNF-α in the culture supernatants. $^{*}P < 0.05$ and $^{**}P < 0.01$ vs. the other groups.

functional role of a specific miRNA in the progression of the inflammatory response during lung injury after hip fracture.

Previous work established the ability of miRNAs to function as delay switches in the negative feedback regulation of inflammatory responses. For instance, miR-21 retards the inhibition of programmed cell death 4 (PDCD4) by activating NF-κB [25]. Other studies have identified miR-146a as a modulator of immune suppression and miR-155 as a promoter of inflammatory responses [26–29]. In our study, we focused on the effect of miR-205-5p in inflammatory responses during lung injury after hip fracture, using clinical patient samples and cell culture experiments, as well as an *in vivo* rat model. Notably, we observed the upregulation of miR-205-5p in serum samples from patients and determined that the overexpression of miR-205-5p *in vitro* protected HPAEpiC cells from NF-κB-mediated inflammatory responses induced by targeting HMGB1.

HMGB1 is produced and secreted by immune cells, such as macrophages and monocytes, and functions as a cytokine mediator in inflammatory responses. This protein exhibits multiple functions that depend on its subcellular location and may play a critical role in various pathological conditions [30, 31]. HMGB1 binds to Toll-like receptors (TLRs) and the receptor for advanced glycation end-products (RAGE) and thus activates NF-κB signaling, which induces a variety of inflammatory responses. HMGB1 has been

implicated to the progression of cancer, and one study described the ability of miR-200a to regulate liver cancer progression by targeting HMGB1 [32]. Moreover, Yao et al. demonstrated that miR-325 regulates HMGB1 in lung cancer [33].

In addition to the roles of other miRNAs, studies have demonstrated the involvement of miR-205-5p in the regulation of various proteins under different pathophysiological conditions [34–37]. In this study, we determined that the onset of inflammation due to hip fracture led to an increased level of HMGB1 and the upregulation of miR-205-5p. We subsequently identified HMGB1 as a direct target of miR-205-5p and observed that the overexpression of this miRNA reduced the levels of the NF-κB signaling indicator p65, p-IkBα, RAGE, and the cytokines IL-6 and TNF-α in HPAEpiC cells, whereas the inhibition of miR-205-5p yielded the opposite effects. These results suggest that the miR-205-5p-mediated inhibition of HMGB1 led to the attenuation of NF-κB signaling and subsequent inflammatory responses in HPAEpiC cells. We further observed that miR-205-5p affected apoptosis and cell proliferation in HPAEpiC cells. However, as these processes were not affected by siHMGB1, we cannot rule out the potential involvement of other pathways in this regulation. We plan to elucidate the exact mechanism in a future study. We note that treatment with HMGB1 enhanced NF-κB signaling-induced inflammatory responses and apoptosis in HPAEpiC cells, thus supporting a direct relationship between miR-205-5p and HMGB1 in the suppression of inflammatory responses during lung injury after hip fracture. Our western blotting analysis revealed that treatment with miR-205 mimics remarkably reduced the level of HMGB1 in the cells. However, an ELISA analysis of protein levels in cell culture supernatants revealed no significant difference in the HMGB1 concentrations of the control and mimic-treated cultures. These findings further emphasize that the clinical effects of miR-205-5p and potential underlying mechanism will require further evaluation. Potentially, the application of a miR-205 mimic, miR-205 inhibitor, and siHMGB1 to a model of lung injury *in vivo* will elucidate this mechanism.

In conclusion, we have demonstrated that miR-205-5p attenuates the inflammatory responses and apoptosis induced by NF-κB signaling and maintains the cell proliferative ability in the context of lung injury after hip fracture. The identification of HMGB1 as a specific target of miR-205-5 in this context provides a new direction for the development of small RNA-based therapies for lung injury after hip fracture.

Abbreviations

CCK8: Cell counting kit 8
ELISA: Enzyme-linked immunosorbent assay
H&E: Hematoxylin and eosin
HMGB1: High mobility group box 1
HPAEpiC: Human pulmonary alveolar epithelial cells
PDCD4: Programmed cell death 4
PI: Propidium iodide
RAGE: Receptor for advanced glycation end-products
SD: Sprague Dawley
siRNA: Small interfering RNA
TLRs: Toll-like receptors.

Data Availability

The raw data of this study were available at the corresponding author upon reasonable request.

Conflicts of Interest

The authors declare that they have no conflicts of interest.

Authors' Contributions

Xiaojie Yu, Xiaobin Chen, and Tiansheng Sun contributed to the conception and design of the study, data collection, interpretation, and final approval of the manuscript for submission.

Acknowledgments

This work was financially supported by the National Natural Science Foundation of China (81341119).

References

[1] M. von Friesendorff, F. E. McGuigan, A. Wizert et al., "Hip fracture, mortality risk, and cause of death over two decades," *Osteoporosis International*, vol. 27, no. 10, pp. 2945–2953, 2016.

[2] J. C. Lin and W. M. Liang, "Mortality, readmission, and reoperation after hip fracture in nonagenarians," *BMC Musculoskeletal Disorders*, vol. 18, no. 1, p. 144, 2017.

[3] J. Z. Zhang, J. Wang, W. C. Qu et al., "Plasma mitochondrial DNA levels were independently associated with lung injury in elderly hip fracture patients," *Injury*, vol. 48, no. 2, pp. 454–459, 2017.

[4] L. Gan, X. Chen, T. Sun et al., "Significance of serum mtDNA concentration in lung injury induced by hip fracture," *Shock*, vol. 44, no. 1, pp. 52–57, 2015.

[5] J. Panula, H. Pihlajamaki, V. M. Mattila et al., "Mortality and cause of death in hip fracture patients aged 65 or older: a population-based study," *BMC Musculoskeletal Disorders*, vol. 12, no. 1, p. 105, 2011.

[6] J. J. Roche, R. T. Wenn, O. Sahota, and C. G. Moran, "Effect of comorbidities and postoperative complications on mortality after hip fracture in elderly people: prospective observational cohort study," *BMJ*, vol. 331, no. 7529, p. 1374, 2005.

[7] I. L. Lo, C. W. Siu, H. F. Tse, T. W. Lau, F. Leung, and M. Wong, "Pre-operative pulmonary assessment for patients with hip fracture," *Osteoporosis International*, vol. 21, no. S4, pp. S579–S586, 2010.

[8] Z. Hao, S. Tiansheng, L. Zhi, Z. Jianzheng, W. Xiaowei, and L. Jia, "Hip fracture aggravates systemic inflammation and lung injury in aged chronic cigarette smoke exposed rats," *Journal of Orthopaedic Research*, vol. 32, no. 1, pp. 24–30, 2014.

[9] S. Haleem, L. Lutchman, R. Mayahi, J. E. Grice, and M. J. Parker, "Mortality following hip fracture: trends and geographical variations over the last 40 years," *Injury*, vol. 39, no. 10, pp. 1157–1163, 2008.